UNIVERSITÀ
DEGLI STUDI
FIRENZE

DOTTORATO DI RICERCA TOSCANO IN NEUROSCIENZE

CICLO XXXIII

COORDINATORE Prof.ssa Felicita Pedata

New insight into the role of adenosine and acetylcholine receptors on neuronal excitability and oligodendrogliogenesis: an *in vitro* study

Settore Scientifico Disciplinare BIO/14

Dottorando
Dott.ssa *Cherchi Federica*

Tutore principale
Prof.ssa *Felicita Pedata*

Tutore supervisore
Prof.ssa *Anna Maria Pugliese*

Coordinatore
Prof.ssa *Felicita Pedata*

Anni 2017/2020

Introduction.

Chapter I - Ionic channels in excitable cells

The plasma membrane is a double layer of lipids and proteins that have several functions, most importantly communication (receptors and ion channels), structure (cytoskeletal anchors) and cellular homeostasis (e.g. ionic pumps, enzymes). In addition, plasma membrane surrounds the cell and separates cytoplasm from the external environment, therefore resulting in two spaces (intracellular and extracellular) with different ionic concentration. The number of positively charged ions outside the cell is usually greater than the cytoplasm, and this causes a voltage difference across the membrane, known as membrane potential (V_m). However, ions can cross the cell membrane through open channels, generating a movement driven by electrical (voltage) or chemical (concentration) gradients, that could change the membrane potential, that represent a signal and are essentials to neuronal communication. In addition, ionic currents change the intracellular concentration of a particular ion and could trigger an event (e.g. throughout intracellular Ca^{2+}) (Hammond, 2008).

These mechanisms underlie cell-to-cell communication in excitable tissue, i.e. brain and muscles, as well as numerous functions of non-excitable cells, i.e. secretion or migration.

Ion channels open and close either spontaneously or in response to a specific stimulus, such as the binding of a small molecule to the channel protein (ligand-gated ion channels) or voltage changes across the membrane (voltage-gated ion channels). Voltage difference is sensed by charged domains of the channel protein. In addition, most ion channels are selective, allowing only certain ions to pass through. Some channels conduct only one type of ion (e.g. K^+), whereas other channels exhibit relative selectivity (e.g. positively charged cations).

Cells in higher organisms may express more than 300 different types of ion channels, each with different selectivity and distinct gating properties and

functions. Ion channels may be classified based on their gating properties (i.e. activated by changing in V_m or a ligand), the species of ions passing (i.e. K^+ channels), the number of gates (i.e. two pores channels) and localization of proteins.

In this thesis we focus on voltage-gated channels in central and peripheral nervous system (CNS and PNS), that are principal players in regulating the electrical signals in neurons. In addition, these families represent an important target for the development of future treatments for psychiatric and neurologic disorders.

Ion channels play a key role both in basic functions and more complex functions, as cell-to-cell communication. During the evolution, several natural toxins have been developed that target ion channels. Examples include the voltage-gated Na^+ channel blocker tetrodotoxin, which is produced by bacteria resident in puffers (blowfish) and several other organisms, as honeybees and scorpions. In addition, pharmacologists developed many therapeutic drugs, including local anaesthetics, benzodiazepines, and sulfonylurea derivatives, acting directly or indirectly to modulate ion channel activity. On the other hand, inherited mutations in ion channel genes or genes encoding proteins that regulate ion channel activity have been implicated in a number of diseases, including ataxia (the inability to coordinate voluntary muscle movements), diabetes mellitus, certain types of epilepsy, and cardiac arrhythmias. For example, genetic variations in Na^+ or K^+ channels, or in their associated regulatory subunits, underlie some forms of long-QT syndrome. These genetic and autoimmune disorders of the ion channels cause channelopathies.

1. Voltage-gated channels

Each channel has an ability to select one or more specific ions, as mentioned above, that depends on sophisticated design of protein domains. The best-known member of this family is represented by Na^+ channels. The principal α subunit consists of four internally homologous domains, each consisting of six

membrane-spanning α helices, that surround a central pore. A similar structure is shared by other voltage-gated channels, for example Ca^{2+} channels (Fig. 1). It is known that four of these subunits multimerize in the plasma membrane to form a channel that is similar in structure to the Na^{+} and Ca^{2+} channels. Several other families of ion channels (KCa, CNG, HCN, and TRP) also present this tetrameric structure (Nestler et al., 2002)

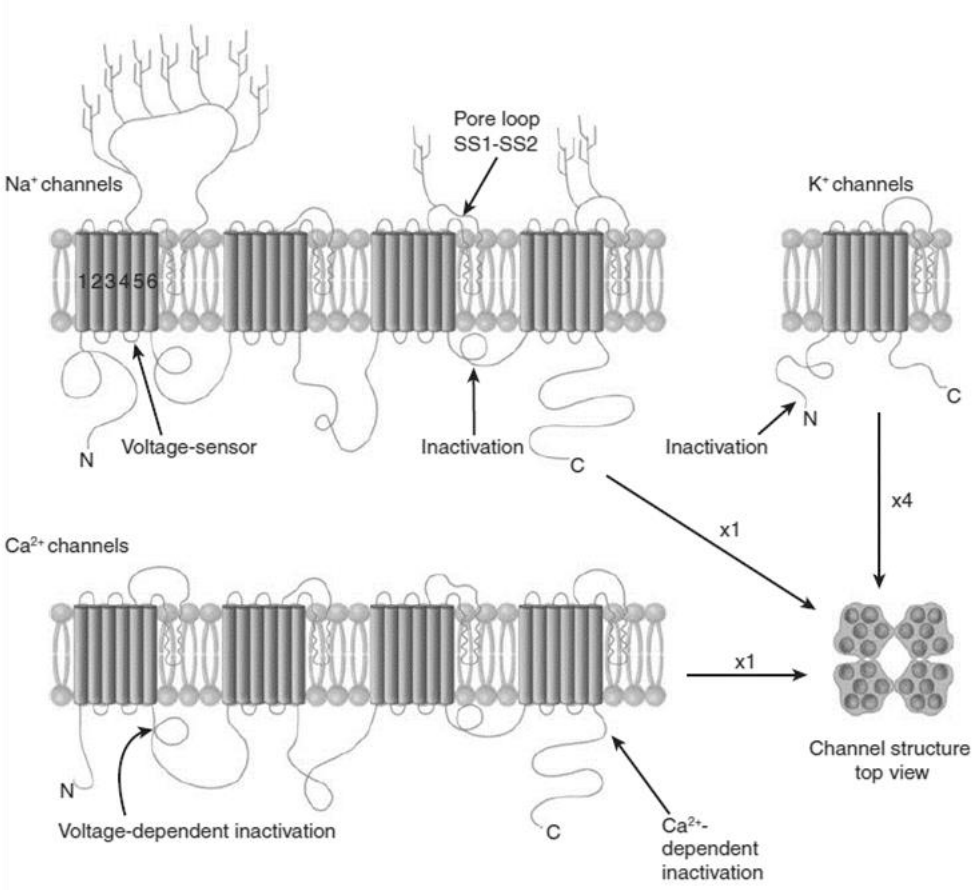

Figure 1. ***Structural similarities shared by voltage-gated Na^{+}, Ca^{2+} and K^{+} channels.*** (modified from: Nestler et al., 2002).

Voltage-activated ion channels display a gating charge that produces a shift in the distribution of charged aminoacids across the membrane. This shift allows channel activation and is believed to result from the movement of a putative voltage sensor within the ion channel itself (Nestler et al., 2002). When the change in membrane voltage subsides, the channel undergoes another conformational change to return in its resting conformation (*deactivation*). In some cases, the channel closes immediately after its activation even in the presence of sustained depolarization. This phenomenon, called *inactivation*, is

typical of Na^+ channels and is present also in some Ca^{2+} (T-type) and K^+ channels (I_A) channels. Several toxins (scorpion toxin) and drugs (antiepileptic compounds) modulate channel inactivation, for examples to maintain Na+ channels open or to stabilize their inactivated state.

1.1. Voltage-gated Na^+ channels

The expression of voltage-gated Na^+ channels (NaVs) is a key feature for initiation and conduction of action potentials (APs) in excitable tissues and cells such as myocytes and neurons. Sodium currents were first recorded by Hodgkin and Huxley, who used voltage clamp techniques to demonstrate the three key features that characterize the Na^+ channel: (i) voltage-dependent activation (about -10 mV), (Hodgkin and Huxley, 1952a); (ii) rapid inactivation (1-2 ms), required for repetitive firing of APs in neural circuits and for control of excitability in nerve and muscle cells (Catterall, 2017); (iii) selective ion conductance, controlled by a set of four residues (DEKA) that control selectivity for Na^+ vs. Ca^{2+} (Heinemann et al., 1992b).

All Na^+ channels studied to date share similar permeation properties and are therefore expected to have similar selectivity filters. Of note, cardiac Na^+ channels bind tetrodotoxin with 200-fold lower affinity, as a result of a change of a tyrosine or phenylalanine, in domain I, to cysteine in the cardiac Na^+ channel (Heinemann et al., 1992a). A serine in this position causes even larger decreases in tetrodotoxin binding affinity, making it become TTX-insensitive Na_V (Na_V 1.8, 1.9), typical of some peripheral nervous tissues (Sivilotti et al., 1997). Since cadmium interacts with the cysteine residue of domain I, it's a high-affinity blocker of cardiac Na^+ channels, but not of brain or skeletal muscle Na^+ channels (Backx et al., 1992). Typically, TTX-insensitive Na_V show smaller single-channel conductance, slower kinetics, and a more positive current-voltage relation than TTX-sensitive ones (Savio-Galimberti et al.,

2012). However there are peptides of drosotoxin that can block the activity of both TTX-insensitive and TTX-sensitive channels (Li and Zhu, 2011).

Natural toxins, as α-scorpion and sea anemone toxins, uncouple channel activation from inactivation by binding to a receptor site at the extracellular end of the S4 segment of IV domain and preventing its normal gating movement, probably trapping it in a position that is permissive for activation but not for fast inactivation (Catterall, 2000). Sodium channels are also blocked by drugs used clinically as local anaesthetics (lidocaine), antiarrhythmics (quinidine) and antiepileptics (carbamazepine) (Catterall, 1987).

Biochemical studies have shown that purified Na^+ channels are phosphorylated by the cAMP-dependent protein kinase A (PKA) at multiple sites in the intracellular loop between domains I and II (Cantrell and Catterall, 2001). Consistent with the biochemical studies, phosphorylation of these sites reduces peak Na^+ currents in brain neurons and in cells expressing cloned Na^+ channels without substantially altering the voltage dependence of activation and inactivation (Li et al., 1992). For examples, it has been well-described that dopamine modifies the firing properties and the input-output properties of medium spiny neurons in the ventral and dorsal striatum through the activation of D1-like dopamine receptors. Activation of the G_s protein coupled to D1 and, consequently, cAMP increase activates PKA thus reducing Na^+ currents and the generation of APs (Yu and Catterall, 2003). Sodium channels are also rapidly phosphorylated by protein kinase C (PKC) (Costa and Catterall, 1984), and PKC activation by diacylglycerols or by acetylcholine acting through muscarinic receptors slows Na^+ channel inactivation and reduces peak Na^+ currents (Numann et al., 1991). The slowing of Na^+ channel inactivation results from phosphorylation of a site in the inactivation gate (West et al., 1991), while the reduction in peak Na^+ current requires phosphorylation of sites in the intracellular loop between domains I and II, as observed for PKA modulation (Cantrell and Catterall, 2001).

Direct interaction of Na^+ channels with tenascin and receptor protein tyrosine phosphatase β, which are implicated in neuronal development, axonal pathfinding, and synapse formation, suggests that Na^+ channels and other molecules involved in neuronal signal generation and propagation may also participate directly in the protein–protein interactions that determine neuronal development and cell connectivity (Catterall, 2000).

In addition to the differences in cellular and tissue expression, mammalian Na^+ channels also have differential expression profiles during development and different subcellular localizations, consistent with a distinct role for each channel subtype in mammalian physiology. Nav1.1 and Nav1.3 are localized to the soma of neurons, where they may control neuronal excitability through the integration of synaptic impulses to set the threshold for AP initiation and propagation to the dendritic and axonal compartments. Evidence from immunocytochemical experiments indicates that Nav1.2 is expressed in unmyelinated axons, where it propagates the AP (Westenbroek et al., 1989; Yu and Catterall, 2003). During development, however, Nav1.6 has been shown to replace Nav1.2 in maturing nodes of Ranvier, the gaps between myelin sheaths along myelinated axons where saltatory AP conduction takes place (Kaplan et al., 2001).

A number of painful and painless neuropathies have been linked to mutations on genes that encode for the Na_V channels (especially Na_V 1.7, 1.8, 1.9), in particular in regions that control opening, closing or channel inactivation and produce changes to the biophysical properties of the channel (Lampert et al., 2014). Nav1.1, and Nav1.6 are also significantly expressed in the peripheral nervous system (PNS), but the most abundant Na^+ channels expressed in the PNS are the three isoforms that have been cloned from sympathetic and dorsal root ganglion neurons, namely Nav1.7, Nav1.8 and Nav1.9. Among these, Nav1.7 is broadly expressed in the PNS and appears to be localized to axons, where it may function to initiate and conduct the AP (Toledo-Aral et al., 1997). Differently, Nav1.8 and Nav1.9 are expressed in small sensory neurons of the

dorsal root and trigeminal ganglia, where they have a key role in the perception of pain (Akopian et al., 1999). Finally, Nav1.4 and Nav1.5 are muscle Na^+ channels that control the excitability of the skeletal and cardiac myocytes, respectively. Nav1.5 is transiently expressed in developing skeletal muscle but is replaced by Nav1.4 in the adult (Goldin, 2001).

A large number of genetic diseases are caused by mutations of Na^+ channels, including inherited forms of periodic paralysis, cardiac arrhythmia, epilepsy, and chronic pain (Catterall et al., 2008; Lehmann-Horn and Jurkat-Rott, 1999).

Channel	Tissue expression	Channel distribution	TTX EC_{50} (nm)	Examples of human channelophaties
$Na_v1.1$	CNS, PNS	Soma	6	Epilepsy, Dravet syndrome, Doose syndrome
$Na_v1.2$	CNS, PNS	Unmyelinated and premyelinated axons	18	Inherited febrile seizures and epilepsy
$Na_v1.3$	CNS, PNS	Soma	4	Potential contributor to peripheral neuropathic pain after spinal cord injury
$Na_v1.4$	Skeletal muscle	Skeletal Myocytes	25	Muscle Na^+ channelopathies
$Na_v1.5$	Heart	Cardiac myocytes, developing skeletal muscle	5'700	Congenital long QT syndrome, Brugada syndrome
$Na_v1.6$	CNS, PNS	Maturing nodes of Ranvier	6	Cerebellar ataxia in jolting mice, motor end-plate disease
$Na_v1.7$	PNS	DRG neuron axons	25	Congenital insensitivity to pain, familial primary erythromelalgia, paroxysmal extreme pain disorder
$Na_v1.8$	PNS	Small DRG neurons	60'000	Peripheral pain syndromes
$Na_v1.9$	PNS	Small DRG neurons	40'000	Potential role in nociception and hyperalgesic syndromes
Na_x	Glia	DRG neurons,	unknown	Potential role in temporal lobe epilepsy

Table 1. Tissue expression of voltage-gated Na^+ channel family (modified from: Bagal et al., 2015; Lee and Ruben, 2009; Savio-Galimberti et al., 2012).

1.2. Voltage-gated Ca^{2+} channels

Voltage-gated Ca^{2+} channels (Ca_Vs), as mentioned above, present an amino acid sequence and a predicted transmembrane structure like Na_Vs (Fig. 1), with four domains, containing six transmembrane segments. The α_1-subunit incorporates the conduction pore (pore loop between S5 and S6 segments), the voltage sensor (S4 segment) and gating apparatus, and its arrangement determines the pharmacological and electrophysiological diversity of Ca_Vs (Hofmann et al., 1994). Three families of Cav have been distinguished, based on structure and function: Ca_V1, 2 and 3, where the number indicates the gene subfamily (Catterall et al., 2005). Unlike other ions, Ca^{2+} does not have a merely electrogenic role, but it is also important as intracellular messenger. Indeed, the intracellular Ca^{2+} concentration (about 100 nM) is maintained very low by Ca^{2+}-buffering molecules and sequestration into intracellular stores (Clapham, 2007). Therefore, when Ca_Vs open, Ca^{2+} influx along the electrochemical gradient leads to a rise of its concentration to the micromolar range (Wadel et al., 2007). This event triggers several intracellular Ca^{2+}-dependent mechanisms, as gene transcription, neurotransmitters release, Ca^{2+} spikes-APs, neurite outgrowth or activation of specific enzymes (Clapham, 2007). However, prolonged elevation of intracellular Ca^{2+} levels are cytotoxic (Stanika et al., 2012). For this reason, it is essential to finely regulate its levels. On these basis, it is easy to understand that dysregulation or alteration in Ca^{2+} channels could be linked to several neurological disorders, as epilepsy or chronic pain (Cain and Snutch, 2011). Hence, these channels represent an important pharmacological target.

Voltage-gated Ca^{2+} channels have been initially classified by their voltage dependence: high voltage-activated (HVA) and low voltage-activated (LVA). Then, a more accurate classification was performed, to consider the different kinetic and/or pharmacological properties of various Cav subtypes. Accordingly, they are classified in:

♦ **L-type** (*long-lasting* current): these channels are activated by large depolarization (HVA) and give rise to sustained currents throughout the period of depolarization, with negligible inactivating (Lipscombe et al., 2004). Furthermore, they are the only Ca_Vs sensitive to dihydropyridines (DHPs; e.g., nifedipine), that bind to a specific site on the α_1-subunit of L-type (Holz IV et al., 1988). Moreover, their activation by depolarization induces direct phosphorylation of channel by PKA, therefore the activity of L-type channels is modulated by the activation of adenylate cyclase (Gao et al., 1997; Hall et al., 2007; Kamp and Hell, 2000). Thus, it is clear that neurotransmitters and hormones can modulate L-type Ca^{2+} currents. Clinically, these channels are important targets for antianginal and antihypertensive drugs. In particular, organic L-type Ca^{2+} channel blockers, phenylalkylamines (e.g., verapamil), DHPs, and benzothiazepines (e.g., diltiazem), decrease myocardial contractile force and thereby reduce myocardial oxygen requirements, or reduce smooth muscle contractility and thereby decrease arterial and intraventricular pressure (Catterall et al., 2005; Striessnig et al., 2015). In the CNS, L-type Ca^{2+} channels are located primarily on the cell bodies and proximal dendrites of neurons (Ahlijanian et al., 1990),allowing Ca^{2+} to enter in the cell body during periods of strong depolarization, this influx causing second messenger activation and changes in gene transcription (Ma et al., 2013).

♦ **N-type** (*neuronal*, or $Ca_V2.2$): as for the L-type, these channels open upon large depolarization (HVA) but, differently from those subtypes, they are inactivated by depolarization. Therefore, they may open in bursts and inactivate with time (50 - 80 ms) and voltage (above -30 mV) upon sustained depolarizations. Differently from L-type, they are insensitive to DHPs and do not need to be phosphorylated, but they are selectively blocked by ω-conotoxin GVIA, peptide toxin of the marine snail *Conus geographicus*. N-type channels contribute most of the Ca^{2+} influx at the synaptic terminal that triggers neurotransmitter and hormone release. In addition, they are also key modulators of neurotransmitter release in sympathetic neurons. A synthetic

peptide blocker of N type Ca^{2+} channels (ziconotide) is under development for treating patients unresponsive to intrathecal opiates for relief of chronic pain

- **P/Q-type** (*Purkinje*, $Ca_V2.1$): These channels are classified as HVA and are the predominant Ca_Vs expressed by Purkinje cells (McDonough et al., 1997), where they contribute to most of the Ca^{2+} influx triggering neurotransmitter and hormone release. They are also expressed at the neuromuscular junction where they control neurotransmitter (acetylcholine) release leading to muscle contraction. They are insensitive to L-type and N-type blocker, but are blocked by polyamine fraction (FTX) from funnelweb spider (*Agelenopsis aperta*) (Araque et al., 1994).

- **R-type** (*resistant* current, $Ca_V2.3$): The role of CaV2.3 channels, belonging to the HVA Cavs, is less defined but may include neurotransmitter and hormone release, the generation of dendritic Ca^{2+} transients, synaptic plasticity, control of pain behaviour and myelinogenesis (Breustedt et al., 2003; Chen et al., 2000; Dietrich et al., 2003; Saegusa et al., 2000). They are blocked by the synthetic peptide toxin SNX-482, derived from *Tarantula venom*(Newcomb et al., 1998).

- **T-type** (*transient* current): these channels are activated by weak depolarizations, near the resting potential (i.e. -60 mV) and undergo rapid voltage-dependent inactivation as the depolarization producing their opening ultimately triggers their closure (Perez-Reyes, 2003). They are resistant to HVA blocker, as DHP, ω-conotoxin (ω-CTX) or ω-agatoxin (ω-AGA) and are expressed in a wide variety of cell types, where they are involved in shaping the AP and controlling patterns of repetitive firing. These channels are excellent generators of oscillations; indeed, they are believed to provide a pacemaker current in thalamic neurons that generate rhythmic cortical discharges associated with absence seizures (petit mal)(Powell et al., 2009). Accordingly, ethosuximide, which blocks T-type current, is an effective therapy for this kind of seizures (Brigo and Igwe, 2017).

	Type	Tissue expression	Functions	Blockers	Human channelopathies
$Ca_v1.1$	HVA, L-type	Skeletal muscle	Excitation-contraction coupling and Ca^{2+} homeostasis	DHP	Hypokalemic periodic paralysis, malignant hyperthermia susceptibility
$Ca_v1.2$	HVA, L-type	Heart, smooth muscle, Endocrine cells, SNC, SNP	Excitation-contraction coupling; hormone release; regulation of transcription; synaptic plasticity, AP propagation in sinoatrial and atrioventricular node	DHP	Timothy syndrome
$Ca_v1.3$	HVA, L-type	Sensory cells, Endocrine cells, CNS, PNS, heart, smooth muscle	Neurotransmitter release in sensory cells, control of cardiac rhythm and atrioventricular node conductance at rest, mood behaviour, hormone secretion	DHP (↓)	Deafness, sinoatrial and atrioventricular node dysfunction
$Ca_v1.4$	HVA, L-type	Retina, PNS, liphoid tissue	Neurotransmitter release in retinal cells	DHP (↓)	Congenital stationary night blindness
$Ca_v2.1$	HVA, P/Q-type	CNS, heart, pancreas	Neurotransmitter release in central neurons and neuromuscular junction; excitation-secretion coupling in pancreatic β-cells	ω-AGA-IVA	Familial hemiplegic migraine, spinalcerebellar ataxia, and episodic ataxia.
$Ca_v2.2$	HVA, N-type	CNS, PNS	Neurotransmitter release in central and sympathetic neurons, sympathetic regulation of the circulatory system, activity and vigilance state control, sensation and transmission of pain	ω-CTX-GVIA	Myoclonus-dystonia-like syndrome
$Ca_v2.3$	HVA, R-type	CNS, PNS, heart, testes, pituitary	Neurotransmitter release, repetitive firing, long-term potentiation, post-tetanic potentiation, neurosecretion	SNX-482	Developmental and epileptic encephalopathies
$Ca_v3.1$	LVA, T-type	CNS, ovary placenta, heart	Thalamic oscillations	Mibefradil	Cerebellar ataxia, childhood cerebellar atrophy, epilepsy, autism spectrum disorder
$Ca_v3.2$	LVA, T-type	Kidney, liver, adrenal cortex, CNS, heart	Smooth muscle contraction, smooth muscle proliferation, aldosterone secretion, cortisol secretion	Mibefradil	Idiopathic generalized epilepsy, autism spectrum disorder, primary aldosteronism
$Ca_v3.3$	LVA, T-type	CNS	Thalamic oscillations	Mibefradil	Schizophrenia

Table 2. **Tissue expression of voltage-gated Ca^{2+} channel family.** (modified from: Catterall et al., 2005; Lory et al., 2020).

1.3. Voltage-gated potassium channels

Potassium channels are found in all living organisms and play several roles in both excitable and no-excitable cells. These channels are distributed throughout the brain and in mature neurons play a critical role in membrane hyperpolarization, which is necessary after each AP for returning the membrane to a negative resting potential to terminate the AP signal. There is a multiplicity of roles played by K^+ channels which is allowed by their diversity. The primitive K^+ channel (KcsA), isolated from *Streptomyces lividans*, is a tetramer composed of four identical subunits consisting in two transmembrane (TM) domains connected by a pore region, in which the ion-selectivity filter resides (Doyle et al., 1998). Based on this structure, K^+ channels are divided in three classes, depending on the number of transmembrane domains (TM) contained in the main subunit: (i) 2TM, (ii) 4TM and (iii) 6TM (González et al., 2012; Fig. 2).

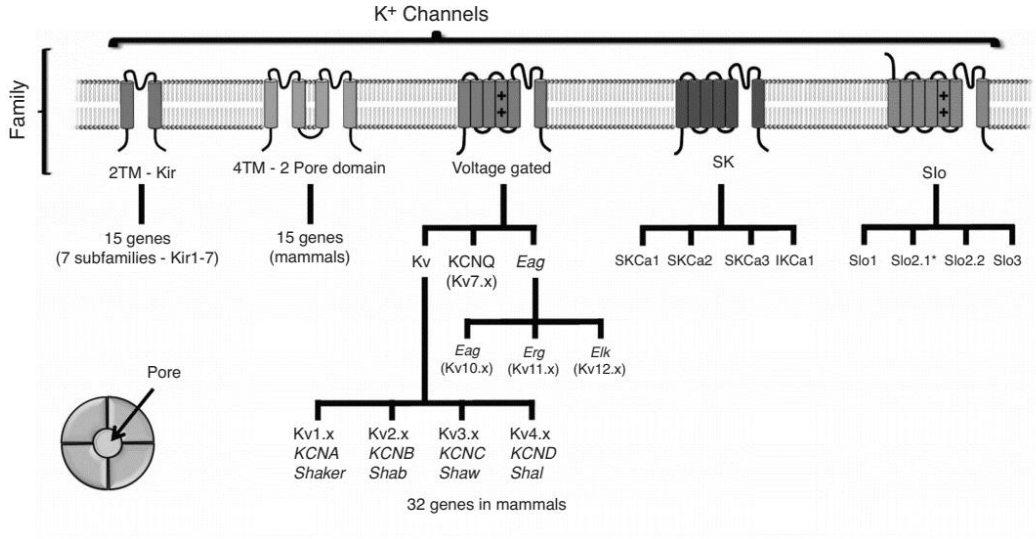

Figure 2. ***Potassium channel families arranged according to their subunit structure.*** Potassium channel families can be grouped in those having two transmembrane segments (2TM; Kir), 4TM (2-pore domain), 6TM (voltage gated and SK), and 7TM (Slo). Note that for the sake of simplicity the large-conductance Slo channel family includes the Slo2.x channels, which have only six transmembrane domains. The 6TM domain class can be divided into four families: Voltage-gated Kv, voltage-gated KCNQ-type (KCNQ); ether-a-go-go (Eag), and Ca^{2+}-activated channels (SK). Subdivisions of the voltage-gated Kv channels into four subfamilies and Eag into three subfamilies are also named according to the Drosophila melanogaster genes. In the SK family IKCa1 stands for intermediate conductance Ca^{2+}-activated K^+ channel. Modified from: González et al., 2012).

1.3.1. 2TM or inward rectifier K^+ channels

The inward rectifier family of K^+ channels (Kir) has the same structural pattern of the primitive KcsA channel, that is tetramers composed of subunit containing two TM (Hibino et al., 2010). As K^+ is more concentrated inside the cell, at membrane potentials above the reversal K^+ equilibrium (E_K, usually about -90 mV) potassium current flowing outwardly; the electrochemical gradient ions allows this ion to enter the cell only at potentials below the E_K. However, Kir channels present a greater inflow rather than outflow from the cell cytoplasm and, under physiological conditions, generate K^+ conductance at potentials negative to equilibrium potential of K^+ (E_K) (Noble, 1965). This inward rectification is due to Mg^{2+} and/or polyamines that intracellular block channel's pore (Lopatin et al., 1994; Matsuda et al., 1987). Moreover, gating in Kir channels is also modulated by nucleotides such as ATP, ADP, phosphorylation, G-proteins and PIP_2 (this lipid is essential for normal channel functioning) (Huang et al., 1998; John et al., 2003; Lin et al., 2002). Kir channels are efficiently blocked by low Ba^{2+} concentration (in the μM range, sensitivity depends on Kir subtype) and Cs^+; Kir3.x and Kir1.1 are also blocked by ***Tertiapin***, a toxin present in the honeybee venom (Kanjhan et al., 2005). In mammals, they are divided in 7 subfamilies (Kir1.x – Kir7.x), that could be classified into four functional groups (Hibino et al., 2010): (i) classical Kir (Kir2.x), (ii) G-protein-gated channels (Kir3.x), (iii) ATP-sensitive K^+ channels (Kir6.x) and (iv) K^+-transport channels (Kir1.1, 7.1, 4.x, 5.1).

(i) All classical Kir channels (Kir2.x) are expressed in the brain and their expression is restricted to neurons, soma, and dendrites where they are important in determining the resting potential and neuronal excitability(Day et al., 2005). Interestingly, Kir2.1 and Kir2.3 are located in the microvilli of Schwann cells where they can play the role of "keepers" of the external K^+ concentration by absorbing the excess of K^+ secreted by the neurons during excitation (Mi et al., 1996).

(ii) These channels are also known as GIRK (G-protein-coupled inward rectifier) and they are first reported by Kurachi and collaborators and are formed by a variety of combinations of the four subunits (Kir3.1-4) (Kurachi et al., 1986). To date Kir3.1 and Kir3.3 subunits function only to assemble forming heteroteramic channel (Kir3.1/Kir3.3 and Kir3.2/Kir3.3)(Jelacic et al., 2000). GIRK are activated by the βγ of $G_{i/o}$ protein (Wickman and Clapham, 1995) and PIP_2 is essential to allow $G_{\beta\gamma}$ binds Kir channels; its depletion, induced by PLC, mediates the inhibitory/desensitization effect of some neurotransmitter on GIRK channels (Huang et al., 1998). Following ligand stimulation, activated G protein subunits are released that directly interact with and open GIRK channels; subsequently GIRK become permeable to K^+, that outwardly flow throughout neuronal membrane, hyperpolarizing it and consequence decreasing excitability. In the brain they are localized in dendritic spines, in the postsynaptic density as well as extra synaptic sites and are involved in the generation of slow inhibitory postsynaptic potential (Hibino et al., 2010). Different types of GIRK channels are, however, found in synaptic and extra synaptic regions of neurons. GIRK channels are activated by a large family of GPCRs, including dopamine 2 (D_2) serotonin 1A (5-HT1A), μ-, κ-, and δ-opioid, cannabinoid 1 (CB1), and γ-aminobutyric acid type B ($GABA_B$) and adenosine receptors (Dascal and Kahanovitch, 2015; Kim and Johnston, 2015).

(iii) ATP-sensitive K^+ channels (K_{ATP}, or Kir6.x) show a weak inward rectification and have constitutive activities. They are octameric channels composed by four Kir6.x and four sulfonylurea receptor subunit (SUR1, 2A and 2B (Shyng and Nichols, 1997). In hypothalamic glucose-sensitive neurons extracellular glucose removal causes a cell hyperpolarization and an inhibition of AP firing (Ibrahim et al., 2003). Moreover, Kir6.2 channels are involved in the generation of the glucose-sensitive K^+ current in neurons, hence the increase in neuronal excitation observed when the concentration of external glucose raises is due to closure of K_{ATP} channels (Miki et al., 2001). They are also expressed in peripheral cell, i.e. in β cells and δ cells of the pancreatic islets

of Langerhans where they mediate insulin secretion upon hematic glucose increase.

(iv) K^+-transport channels (Kir1.1, 7.1, 4.x, 5.1) are most expressed in glial cells. In particular, Kir4.1 can form homo- or hetero-tetramers with Kir5.1 (Hibino et al., 2004). Kir5.1, on the other hand, is unable to form functional homo-tetramers and only play physiological roles in combination with Kir 4.1 or Kir4.2. Furthermore, Kir4.1 controls neuronal function by exerting a K^+-buffering capacity (Newman, 1984). Instead, in cortical astrocytes , Kir4.1 and Kir4.1/Kir5.1 channels are expressed in perisynaptic processes whereas Kir4.1/Kir5.1 are only expressed at the end feet (Lichter-Konecki et al., 2008).

1.3.2. 4TM or two-pore domain K^+ channels

Two-pore family (K2P), known also as background K^+ channels, are dimers composed by subunits thus containing, in total, four TM. The K2P channels are regulated by an extensive variety of stimuli: for example, pH, temperature, and membrane stretch (Talley et al., 2001). More evidences link these channels to anaesthesia and different pathologies in the nervous system, as neurodegeneration, neuropathic pain, depression, and epilepsy (Bayliss and Barrett, 2008; Honoré, 2007; Sabbadini and Yost, 2009). Depending on stimuli, K2P were divided into six subfamilies: (i) mechano-gated; (ii) alkaline-activated; (iii) Ca^{2+}-activated; (iv) weak inward rectifiers; (v) acid-inhibited; and (vi) halothane-inhibited channels (Honoré, 2007).

1.3.3. 6TM or voltage-gated K^+ channels

Voltage-gated K^+ channels (K_V) are composed of four transmembrane subunits, each of which is analogous to a single domain of the principal subunits of Na^+ or Ca^{2+} channels (Long et al., 2005). They include 40 different channels that are classified into 12 distinct groups based on their amino acid sequence homology (Kv1– Kv12). They are composed by α-subunits, that consists of six helices (S1–S6), can assemble into homo- and heterotetramers within each subfamily, leading to a wide diversity of different channel

complexes. The diversity of K^+ channels allows neurons and other excitable cells to precisely tune their electrical signalling properties by expression of different combinations of K^+ channel subunits. Mutations in Kv channels generally lead to some form of hyperexcitability in affected tissue and are related to a variety of disorders, ranging from ataxia to cardiac arrhythmias. For example, the long QT syndrome, a delay in ventricular repolarization that can cause heart arrhythmias, results from a malfunction of the KV11.1 (HERG) K+ channel, which is responsible for repolarizing the ventricle after contraction.

They are characterized by containing a voltage-sensor domain between S1 and S4 (Long et al., 2005). The vertebrate α-subunit of voltage-gated K^+ delayed rectifier family (K_v channels) is composed by twelve members (Kv1–Kv12) according to amino acid sequence similarity. Usually, K^+ currents mediated by 6TM channels can be classified into A-type (inactivating, given by K_V1.4, 3.3, 3.4, 4.1, 4.2, 4.3-containing channels) or delayed rectifier (non-inactivating) currents.

During a sustained depolarizing voltage pulses, A-type K^+ current activates and then inactivates rapidly (within 5-10 ms), producing a transient response. Fast inactivation may play a role in setting the AP interval since the K_v-dependent repolarization phase gets shorter as I_A inactivates and the excitable cell is ready to fire a new AP (Hoffman et al., 1997). Kv 4.2 also encodes A-type K+ currents in dendrites of CA1 pyramidal neurons where it antagonizes the back propagation of centrally generated APs, dampening the development of Long Term Potentiation (LTP) (Chen et al., 2006). Furthermore, Kv3.3 appears to inhibit either excitability or Ca^{2+} signal propagation in cerebellar Purkinje cells (Zagha et al., 2010) and mutations in Kv3.3 cause spinocerebellar ataxia in humans (SCA13) (Figueroa et al., 2010). Kv4.1 and Kv4.2 are responsible for the somato-dendritic A-type currents. For example, in different neuronal types, KV4 channels prolong the latency to the first spike in a train of APs; they

also slow down repetitive spike firing and shorten APs (Covarrubias et al., 2008).

Other Kvs are the classical delayed rectifier, a name used by Hodgkin and Huxley to describe main outward K^+-current in the squid giant axon activated later than the Na^+ currents (Hodgkin and Huxley, 1952b). According to this classical definition, these channels not only terminate the AP and restore K^+ permeability of the resting membrane, but they also shape AP waveform (Gutman et al., 2005). A detailed pharmacological study comparing several delayed rectifiers including Kv1.1, Kv1.2, Kv1.3, and Kv1.5, found that all have submillimolar sensitivity to 4-AP and flacainide; tens of micromolar sensitivity to capsaicin, nifedipine, ditiazem, and resiniferatoxin (Grissmer et al., 1994). They also have different sensitivity to external TEA. Therefore, both, Kv1.1 and Kv1.2 have low nanomolar sensitivity to dendrotoxin (DTX), while Kv1.2 and Kv1.3 have low nanomolar sensitivity to charybdotoxin (CTX). Kv2.x channels are the counterpart of Shab in Drosophila. This family is composed of Kv2.1, the mayor delayed rectifier present in CNS neurons. On the other hand, Kv3.x channels are the counterpart of the Drosophila Shaw channel. While Kv3.3 and Kv3.4 produce A-type currents, Kv3.1 and Kv3.2 are delayed rectifiers expressed prominently in the brain. They are blocked by micromolar 4AP and TEA and, in particular, Kv3.2 channels are blocked by verapamil and by the toxin from the sea anemone Stichodactyla helianthus (ShK). Kv3.2 knockout mice are susceptible to epileptic seizures (Gutman et al., 2005). Of note, Kv7 channels are also known as the KCNQ subfamily in humans. The Kv7.1, in association with KCNE3 and minK, are the major determinants of the cardiac IKs current, which is involved in the repolarization of ventricular AP (Nerbonne and Kass, 2005). Instead, the heteromeric channel Kv7.2/Kv7.3 determines subthreshold excitability and produces the M-current (muscarinic-current) found in neurons (Wang et al., 1998). This channel is sensitive to external pH and is widely distributed throughout the brain, sympathetic and dorsal root ganglia (DRG), and expressed at high levels in hippocampus and amygdala. Mutations in the KCNQ2/KCNQ3 genes give rise to an idiopathic

form of epilepsy (Gutman et al., 2005). The Eag channel family derives its name from a Drosophila behavioural mutant, ether-`a-go-go, characterized by an enhanced neuro-transmitter release at the neuromuscular junction. Known as the KCNH gene family in humans, it consists of three closely related subfamilies of genes defined by sequence homology, Kv10 (truly Eag), Kv11 (Erg), and Kv12, and they all produce slowly activating currents. Kv12 are expressed primarily in the nervous system and produce a slowly activating and deactivating current.

Another family of 6TM K^+ channels is the Ca^{2+}-dependent K^+ channel (KCa) family, consisting in three different subtypes: the large conductance Ca^{2+}-activated K^+ channel (BK or KCa1.1), the intermediate conductance Ca^{2+}-activated K^+ channel (IK, or KCa3.1) and the small conductance Ca^{2+}-activated K^+ channel (SK or KCa2.x). The BK channel subtype is blocked by the scorpion toxin CTX, the highly selective scorpion toxin ***iberiotoxin*** (IbTX) and are also highly sensitive to external TEA (100-200 μM). In the CNS, these channels are present in most regions of the mammalian brain. In neurons, BKs serve functions such as, for example, the repolarization of the AP (Hu et al., 2001) and produce the fast phase of the after hyperpolarization (fAHP) following an AP. Therefore, they are expressed also at presynaptic level where, by co-localizing with Ca_Vs, they regulate neurotransmitter release (Raffaelli et al., 2004). Then, both insufficient and excessive BK channel activity could lead to CNS disfunctions, as epilepsy, dyskinesia, cerebral ischemia and pain (Chen et al., 2009; Lee and Cui, 2009; Liao et al., 2010).

The IK channel is distributed in peripheral tissues, including secretory epithelia, blood cells and lymphocytes, but it appears almost absent from neuronal and muscle tissue (Sforna et al., 2018). Selective blockers of this channels are small organic molecules like TRAM-34 and ICA-17043, recently proposed as immunosuppressors for the treatment of autoimmune disorders such as rheumatoid arthritis, inflammatory bowel disease and multiple sclerosis as they inhibit lymphocyte T proliferation (Jensen et al., 2002). The

last but not the least family is the SK channels, activated by increases in the intracellular calcium concentration. They are ubiquitous in the CNS and mediate a variety of functions in health and disease, as excitability control by mediating medium AHP (mAHP) following a single AP (Lorenzon and Foehring, 1992). Additionally, SK channels, activated through muscarinic type 1 or group I metabotropic glutamate receptors and IP_3 signalling, mediate slow cholinergic and glutamatergic inhibition of layer 2–3 and 5 pyramidal neurons in several cortical areas (Gulledge et al., 2007). Finally, SKs are also involved in pacemaker activity and synaptic response (Bond et al., 2005). The bee venom ***apamin*** is the prototypical, highly specific blocker of SK channels.

Structural classes	Functional groups	Channels
2TM	Classical Kir	Kir2.x
	G-protein-gated	Kir3.x
	ATP-sensitive	Kir6.x
	K^+ transport	Kir1.1, 4.x, 5.1, 7.1
4TM	Mechano-gated	K_{2p}4.1 (TRAAK), 2.1 and 10.1 (TREK1 and 2)
	Alkaline activated	K_{2p}5.1 (TASK2), 16.1 and 17.1 (TALK1 and 2)
	Ca^{2+}-activated	K_{2p}18.1 (TRESK1)
	weak Kirs	K_{2p}7.1 (KCNK7), 1.1 and 6.1 (TWIK1 and 2)
	acid-inhibited	K_{2p}3.1, 9.1 and 15.1 (TASK1, 3 and 5)
	halothane-inhibited	K_{2p}13.1 and 12.1 (THIK1 and 2)
6TM	A-type	Kv1.4, 3.3, 3.4, 4.1, 4.2 and 4.3
	Classical delayed rectifier	Kv1.1, 1.2, 1.3 and 1.5
	Ca^{2+}-dependent K^+ channel	KCa1.1 (BK), 2.x (SK), 3.1 (IK)

Table 3. Classification of K^+ channels.

Chapter II - Cholinergic system and neurodevelopment

In the CNS, acetylcholine (ACh) is a major neurotransmitter implicated in higher brain functions, including cognitive processes. The term "cholinergic system" defines all those components of the nervous system whose actions are mediated by the neurotransmitter ACh. Besides, during brain development, ACh regulates many events by activating its receptors (AChRs). Thus, in the developing CNS, both ACh receptor classes, muscarinic (mAChR) and nicotinic (nAChR) receptors are involved in neuronal proliferation, differentiation and survival, as well as synapse formation, axonal pathfinding and neurotransmitter release (Abreu-Villaça et al., 2011). Cholinergic neurons are present in both PNS and CNS. Within the CNS there are either projection neurons, that connect different areas of the brain, or cholinergic interneurons. Cholinergic interneurons are present in various brain substrates, including the caudate-putamen nucleus, the nucleus accumbens, the olfactory tubercle and the Calleja Islands complex, where they exert important modulating actions (Ferreira-Vieira et al., 2016). Within the basal forebrain (BF), the nucleus basalis of Meynert (NBM) represents the main source of cholinergic projection neurons (Kilimann et al., 2014). Indeed, specific degeneration of NBM neurons is an early and prodromal event for the pathogenesis of Alzheimer's disease (Hampel et al., 2018), one of the most common form of dementia, and predicts cognitive decline in Parkinson's disease (A. Schulz et al., 2018). Moreover, alterations in BF development, as those that may be induced by premature birth, are associated with neonatal complications and cognitive deficit in adulthood (Grothe et al., 2017).

2. Acetylcholine

In 1913, H. Dale and A. Ewins isolated ACh from ergot (fungus *Claviceps*), by a "lucky accident" (Ewins, 1914) and only ten years later they find it as a natural constituent of the mammalian body (Dale and Dudley, 1929). To date, its mode of action at peripheral synapses, especially in neuromuscular

junction, has been extensively studied and it is considered the principal neurotransmitter in sympathetic and parasympathetic ganglia of the autonomic nervous system, in adrenal medulla and in skeletal muscle. ACh basically transmits fast excitation through nicotinic receptors that depolarize cell membrane to the threshold for electrical firing. However, in some areas (e.g. cardiac muscle) it transmits a slower excitatory or inhibitory signal through mAChRs linked to second messenger signalling.

In 1948, Feldberg W. and Vogt M. demonstrated that Ach was synthetized in CNS and acts as a neurotransmitter (Feldberg and Vogt, 1948). To date, its role is still under debate even if we know that is involved in many mechanisms, as attention, memory, it can also act as a neuromodulator or a neurotrophic factor.

ACh is an ester whose chemical structure is composed by choline and acetic acid (Fig. 3). Its synthesis takes place in the cytoplasm of cholinergic neurons from its precursor choline, an essential nutrient provided mostly from the diet and transported to the brain *via* blood flow in free form (yolk egg, liver, vegetables).

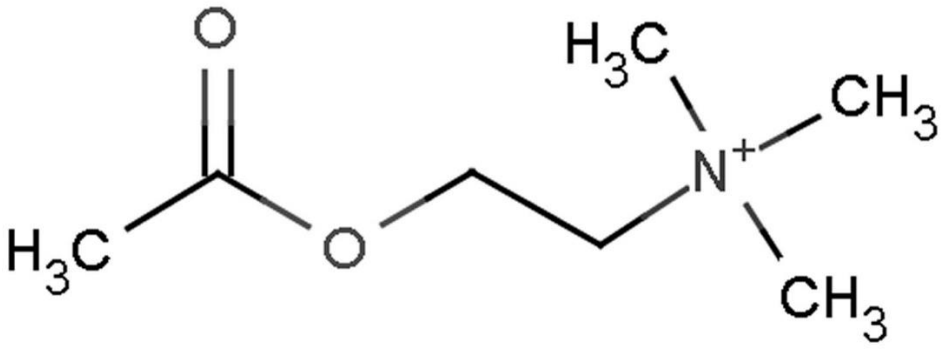

Figure 3. ***Structure of ACh.***

Choline participates to a number of physiological processes in every cell (e.g. it maintain membrane integrity). However cholinergic neurons have especially large requirements for this nutrient to supply the cargo for cholinergic vesicles. Neurons can hydrolyse phosphatidylcholine, a

membrane phospholipid, to choline; however, the *de novo* synthesis of choline provides to only with a very small fraction of the total choline necessary for the synthesis of ACh. Therefore, choline is taken up into the cytoplasm from the extracellular space by two transporter systems: first is the ubiquitous low-affinity (K_m=50 μM), sodium independent transport system; second is the high-affinity (K_m=1-5 μM), saturable and sodium, ATP and chloride-dependent transport system that is also specific of cholinergic neurons. Once choline is in the cytoplasm, it reacts with mitochondrial bound acetyl coenzyme A, a metabolic intermediate of the Krebs cycle, that it is transported by citrate to the cytoplasm. This reaction is catalysed by the cytoplasmatic enzyme choline acetyltransferase (ChAT), an enzyme specific to cholinergic nerve terminals and whose labelling by immunochemistry has much facilitated the mapping of cholinergic pathways. This enzyme is not saturable, but its activity is limited by the availability of choline.

Unfortunately, even if more than a hundred compounds have been reported as ChAT inhibitors, none of them is indeed able to achieve the desired *in vivo* efficacy (Kumar et al., 2017). On the other hand, synthesis of Ach is inhibited by drugs which compete for choline uptake, as ***hemicholinium*** or ***triethylcholine*** (Sterling et al., 1986).

Hence, the neurotransmitter is transported by the vesicular ACh transporter (VAChT) from the cytosol into synaptic vesicles by a proton electrochemical gradient to move ACh to the inside of the vesicle. ACh H^+ antiporter channel is inhibited by ***vesamicol***, a drug that reduces ACh storage and interferes with neurosecretion (Prior et al., 1992).

It seems that two pools of Ach-filled vesicles exist: one (depot pool) consists in vesicles located close the nerve terminals, read to be release. The other (reserve pool) replaces the depot pool and it is required to sustain ACh release during sustained or intense nerve stimulation. Indeed, the depolarization of the nerve terminals allow the entry of Ca^{2+} through Ca_Vs. The increase of intracellular Ca^{2+} promotes fusion of vesicular membranes with the plasma membrane,

allowing exocytosis of ACh in the synaptic cleft, where it can activate both mAchRs and nAchRs. Some toxins, as ***botulinum toxin***, produced by the anaerobic bacillus *Clostridium botulinum*, and ***β-bungarotoxin***, a protein in a cobra snake venom, efficiently inhibit Ach release. Of note, ACh present at the synaptic cleft is rapidly inactivated by the enzyme ACh esterase (AChE), localized on the membrane of the postsynaptic cell. This enzyme hydrolyze ACh into acetic acid and choline, that is continuously reuptaken into the presynaptic cholinergic neuron by an active transport system. The enzyme AChE is extremely efficient (10000 molecules of ACh each second) and numerous compounds that inhibit its activity have been developed to prolong and potentiate the action of ACh. For example, ***physostigmine***, which can cross the blood brain barrier, and ***neostigmine*** reversibly bound AChE; also insecticide, as organophosphorus compounds and methyl carbamates, irreversibly inhibit AChE (Casida and Durkin, 2013). Interestingly, it has been demonstrated that AChE modulates other multiple biological functions beyond cholinergic neurotransmission, as neurogenesis, cell adhesion, synaptogenesis, amyloid fibre assembly and activation of dopamine receptors (Paraoanu and Layer, 2008) (Fig. 4).

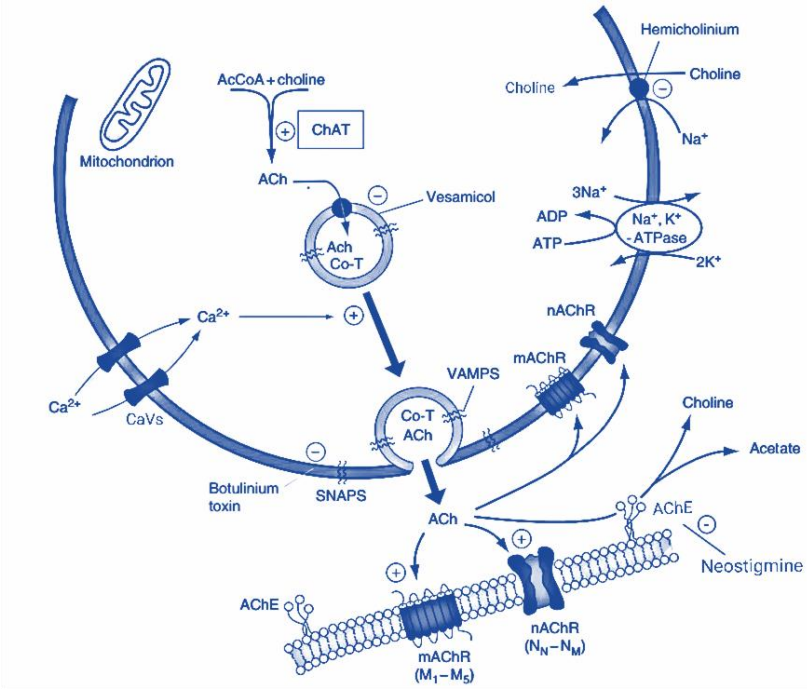

Figure 4. ***Acetylcholine signalling pathway.*** (Taken from: Malenka, 2009).

2.1. Acetylcholine receptors

Neurons may respond to neurotransmitters and/or neuromodulator release from itself (autoreceptors) or adjacent neurons (heteroreceptors); cholinergic nerve terminals contain both. The neurotransmitter ACh acts by activating its receptors and promoting either stimulation or inhibition of neuronal excitability, depending on receptor type and neuronal localization of the receptor. ACh receptors have been classified into two different categories: (i) nicotinic receptors (nAchRs), which are ionotropic receptors mediating fast synaptic transmission, and (ii) muscarinic receptors (mAchRs), which are metabotropic receptors modulating much slower events.

2.1.1. Nicotinic Ach Receptors

The nAChR was the first neurotransmitter receptor to be isolated and purified, in 1970, from electric organ of fish *Torpedo* and *Electrophorus electricus* (Miledi et al., 1971; Olsen et al., 1972). The nAChRs are ligand-gated ion channels permeable to cations (K^+, Na^+ and, in several instances, Ca^{2+}) and each receptor is a pentamer consisting of five subunits (α, β, γ, δ and ε) around a central ion channel pore (Cooper et al., 1991). Distinct subtypes of nAchRs are expressed in different structures and, depending on their location, they are classified in three families, with different combination of subunits. The α subunit is where Ach binds the receptor thus inducing a conformational change responsible for ion flow through the central pore of the receptor. Cation selectivity is due to the presence of areas enriched in negative charges within the pore, that act as a reminder for the positive charges of the cations. In neurons, combinatorial assembly of up to nine different α subunits and three β contributes to a wide variety of pentamers with distinct pharmacological, electrophysiological and kinetic properties. There are four traditional conformation states of the nAChR: resting (closed channel with an unoccupied agonist-binding site), active (open channel), desensitized (closed channel with high-affinity agonist binding), and an inactive state that is a more prolonged desensitized state (Changeux et al., 1984). With acute exposure to high concentrations of ACh or

non-selective nAChR agonists such as nicotine, the equilibrium between these conformation states shifts to an active state, allowing signal transduction followed by subsequent desensitization of the receptor. However, under sustained exposure to low concentrations of agonists, the desensitized conformational state of the receptor can be stabilized and become refractory to agonist activation (Jones et al., 2012).

In the CNS, most of the nicotinic receptors are expressed at the presynaptic neuronal membrane and their main role is to regulate neurotransmitter release, whereas nicotinic receptors expressed in the peripheral nervous system are mainly post-synaptic. Agonists at the nAChR can improve, while antagonists impair, performances in cognitive tasks (Ferreira-Vieira et al., 2016). ***Nicotine*** is the main agonist of the nicotinic receptor, while ***curare*** is the main antagonist. Of note, nAChRs are responsible for autosomal dominant nocturnal frontal lobe epilepsy, modulate pain transmission and seems to be involved also in autism, schizophrenia, Parkinson's disease, nicotine addiction, Alzheimer's disease, Tourette's syndrome and anxiety disorders (Becchetti et al., 2015; Lee et al., 2002; Posadas et al., 2013; Tregellas and Wylie, 2019; Umana et al., 2013) (Fig. 5).

2.1.2. Muscarinic Ach receptors

Muscarinic receptors (mAChRs) are G-protein-coupled receptors that modulate a wide variety of neuronal functions. On the basis of selective agonists and antagonists, they are further classified into five subtypes ($M_{1\text{-}5}$), with distinct anatomical locations in the periphery and CNS. In the CNS, mAChRs are involved in regulating a large number of cognitive, behavioural, motor, and autonomic functions although some of these are also influenced by nAChRs.

The M_1, M_3, and M_5 receptors are typically coupled to pertussis toxin-insensitive G_q, that stimulates phospholipase C (PLC). Their activation therefore induces hydrolysis of membrane phosphatidylinositol-4,5-diphosphate to form inositol triphosphate (IP_3) and diacylglycerol (DAG).

Intracellular IP_3 induces release of Ca^{2+} from the endoplasmic reticulum, which could activate several events, like smooth muscle contraction. On the other hand, DAG activates protein kinase C (PKC), resulting in phosphorylation of several proteins. Therefore, the activation of $G\alpha_q$-protein-coupled muscarinic receptors can also activate phospholipase A_2, leading to the release of arachidonic acid and then eicosanoid synthesis. Furthermore, $M_{1,3,5}$ receptors may also regulate K^+ channels, usually promoting their closure, thus facilitating cell excitability (Brown, 2018), but in some cases are also reported to inhibit Na^+ conductance through activation of PKC (Cantrell et al., 1996; Cantrell and Catterall, 2001).

The M_2 and M_4 receptors, instead, are coupled to pertussis toxin-sensitive G_i which lead to inhibition of adenylyl cyclase (AC) and consequent decrease in cyclic adenosine monophosphate (cAMP), activation of inwardly rectifying K^+ channels and inhibition of voltage-gated Ca^{2+} channels (Brown, 2018). Functional consequence are hyperpolarization and inhibition of excitable membranes. Moreover, in literature was described that M_2 can also enhance K_v currents (Cruzblanca, 2006; Harata et al., 1991). Therefore, stimulation of mAChRs can promote the opening or closing of Ca^{2+}, K^+, or Cl^- channels, which might facilitate either depolarization or hyperpolarization, depending on the cell type where these receptors are expressed (Ferreira-Vieira et al., 2016). The first selective agonist identified for mAChRs was the alkaloid ***muscarine***, from the mushroom *Amanita muscaria*, and, so far, it has not been possible to find an agonist with specific selectivity for a particular mAChRs isoform. While the best-known antagonists of the mAChRs are *belladonna* alkaloids, such as ***atropine*** and ***scopolamine***, which blocks all mAChRs (Ferreira-Vieira et al., 2016). Another kind of ligand, as ***gallamine***, competes with classical muscarinic ligands (Fig. 5).

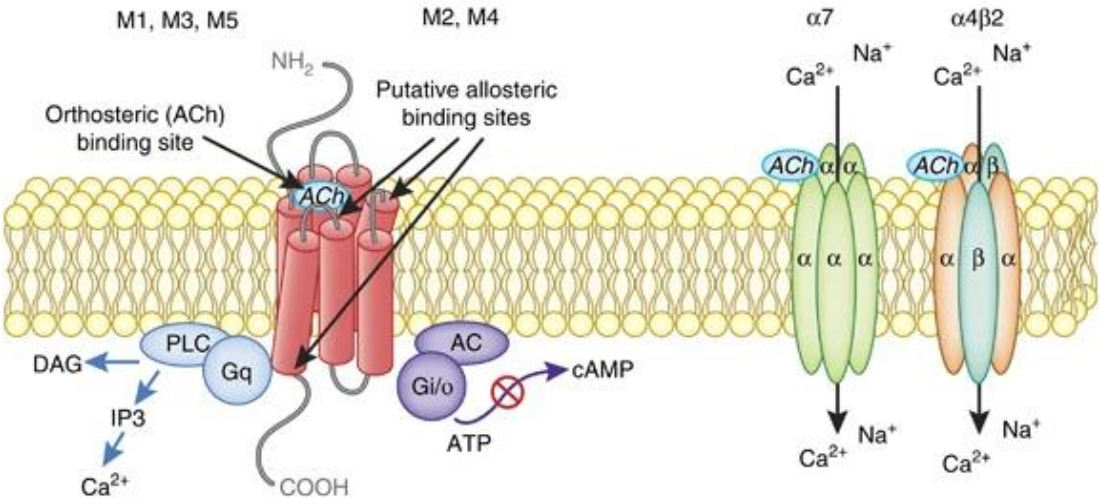

Figure 5. ***The structure and signalling pathways of mAChRs and nAChRs.*** Each mAChR subtype is a seven-transmembrane protein, which belongs to two major functional classes based on G-protein coupling. The M1, M3, and M5 mAChRs selectively couple to the G_q/G_{11}-type G-proteins resulting in the generation of inositol-1,4,5-trisphosphate (IP3) and 1,2-diacylglycerol (DAG) through activation of the phosphoinositide-specific phospholipase-Cβ leading to increased intracellular calcium levels. The M2 and M4 mAChRs preferentially activate G_i/G_o-type G-proteins, thereby inhibiting adenylate cyclase, reducing intracellular concentration of cAMP, and prolonging potassium channel opening. All mAChR subtypes show a high sequence homology across species, particularly in the orthosteric ACh-binding sites. Neuronal nAChRs are pentameric ligand-gated ion channels. The most abundant neuronal subunits are α4, β2, and α7, with the heteromeric α4β2 receptor subtype in highest abundance. The heteromeric α4β2 receptor subtype can exist in two different forms: (α4)2(β2)3 receptors show low Ca^{2+} permeability and high affinity to ACh and nicotine, whereas (α4)3(β2)2 receptors have high Ca^{2+} permeability. By contrast, the α7 nAChR also shows high permeability to Ca^{2+} relative to the heteromeric α4β2 nAChRs. The action of α4β2 nAChRs can enhance intracellular levels of Ca^{2+} by secondary activation of Ca_Vs, whereas α7 nAChRs preferentially increase Ca^{2+} release from ryanodine-sensitive intercellular stores through CICR. The capacity of these different nAChR subtypes to couple to Ca_V or CICR mechanisms results in distinct patterns of Ca^{2+} signalling that can provide a broader control of synaptic plasticity and neurotransmitter release, as well as gene transcription. (Modified from: Jones et al., 2012)

2.2. *Role of Ach in neurodevelopment*

Molecules such as ACh and glutamate act as both neurotransmitters and neuromodulators; as neuromodulators, they change neural information processing by regulating synaptic transmitter release, altering baseline membrane potential, and spiking activity, and modifying long-term synaptic plasticity. Compared to neurotransmitters, neuromodulators have slower, longer lasting, and more diffuse effects on neuronal physiology, often due to effects at metabotropic receptors rather than ionotropic receptors. Their effect

on synaptic transmission or cellular excitability depends on the type of pre- or postsynaptic receptor the modulator binds to. For example, the effect of ACh varies greatly depending on whether or not it binds to nicotinic compared to muscarinic ACh receptors (Giocomo and Hasselmo, 2007).

In a developmental context, activation of a given set of neurotransmitter receptors may promote neural cell replication, initiate the switch from replication to differentiation, enhance or retard axonogenesis or synaptogenesis, evoke or prevent apoptosis, or enable the appropriate migration and localization of specific cell populations within each brain region. At the same time, these multiple developmental roles of neurotransmitters render the developing brain vulnerable to neuroactive chemicals that elicit or block neurotransmitter responses, with sensitivity extending through all phases of brain assembly, from the early embryonic stage through adolescence (Slotkin, 2004).

In literature it has been reported that cholinergic neurons can synthesize ACh during their migration and that these neurons can release ACh from their growth cones prior to target contact or synapse formation and also along the neurite and at the soma (Allen and Brown, 1996). Nicotinic receptors subunits are the first membrane proteins to appear during CNS development; functional nAChRs were revealed by patch-clamp measurements in fetal mouse cerebral cortex as early as on E10 (Atluri et al., 2001). On the other hands, in the human fetal brain, nAChRs are detected in the first trimester, gradually increasing up to midgestation (Morelli et al., 2017). Moreover there is evidence that nAChR levels remain constant or decrease throughout postnatal life depending on the brain region and receptor composition (Falk et al., 2002). These changes in nAChR expression occur during critical prenatal and postnatal periods of neuronal development, involving mechanisms associated with neurogenesis, cell migration and differentiation, and synaptogenesis (Abreu-Villaça et al., 2011). Instead, mAChRs are present in both the forebrain and the hindbrain during early developmental stages; they

has been demonstrated in human fetal brain from early gestation (Gremo et al., 1987). On the other hand, in the rat, they appear in the spinal cord on E13 and on E15 they are evident in the rhombencephalon and mesencephalic structures and on E16, in forebrain regions (Schlumpf et al., 1991). The mAChRs have been shown to mediate effects of ACh on proliferation, differentiation, and survival. In embryonic P19 carcinoma cells, a widely accepted in vitro model for early neurogenesis, muscarine induces proliferation in progenitor cells by activation of M1, M3 and M5 receptors and mobilization of intracellular Ca^{2+} stores, whereas M2 receptor activity mediates neuronal differentiation (Resende et al., 2008; Young and Poo, 1983)

ACh can alter several processes in neuronal development, and the molecular basis for a number of these developmental effects of ACh signalling have been elucidated recently. For example, one fundamental role for ACh signalling through nAChRs is to regulate the timing of expression of the chloride transporter that is necessary for the ability of GABA to hyperpolarize, and therefore inhibit, central neurons (Liu et al., 2006). Disrupting nAChR signalling delays the switch from GABA-mediated excitation to inhibition; recent studies have also shown that nAChRs contribute to the maturation of GABAergic (Zago et al., 2006) and glutamatergic (Lozada et al., 2012) synapses, highlighting an important role for ACh signalling in synaptic development. In addition, signalling through nAChRs is also important for establishing critical periods for activity-dependent shaping of visual cortical function (Morishita et al., 2010) and maturation of thalamocortical (Hsieh et al., 2002) and corticothalamic (Horst et al., 2012) glutamatergic synapses.

In literature it has been demonstrated that nicotine exposure alters dopaminergic and noradrenergic systems in development (Muneoka et al., 2001; Ribary and Lichtensteiger, 1989). Developmental nicotine exposure can also result in alterations of the serotonergic system, with age-dependent reductions in serotonin turnover observed in the forebrain, brainstem and cerebellum of exposed animals (Muneoka et al., 2001; Slotkin et al., 2007).

Alterations in the serotonergic system may contribute to some aspects of attention deficit hyperactivity disorder (ADHD) symptomology (Oades, 2007), with disruptions in the cerebellum of particular interest, given the emerging role for this structure in cognition and sensory processing (Arnsten, 2006). Therefore, it is important to note that inappropriate modulation of the endogenous cholinergic system, with its extensive cortical innervation may also be a significant contributor to the neurochemical and behavioural deficits observed following developmental exposure (Heath and Picciotto, 2009).

3. The basal forebrain area

The BF region is a broad topographic term describing a heterogeneous set of cellular structures on the medial and ventral cerebral hemisphere (Hardenacke et al., 2013). It has a complex architecture: It comprises BF cholinergic neurons (BFCN) within the medial septal nucleus, the vertical and horizontal diagonal bands of Broca and the NBM (M. Mesulam, 2013). This complex region contains magnocellular neurons that provide the major cholinergic projections to the cerebral cortex, hippocampus and amygdala (Ferreira-Vieira et al., 2016) (Fig. 6). Indeed, this innervation of the neocortex by BFCN is an integral part of cortical activation as it supports cognitive functions, such as alertness, memory, attention, and learning. In simplified terms, the function of the BFCN is sometimes described as a kind of "background tuning" (Hardenacke et al., 2013). Furthermore, BF neurons modulate blood supply to the neocortex and thereby glucose metabolism. This process is considered as an elementary prerequisite for cognitive functions (Hardenacke et al., 2013). Importantly, the degeneration and loss of cholinergic neurons within the BF, especially in the NBM, represents a pathological correlate of the well-documented cholinergic derangement in Alzheimer's disease (AD) patients (Kilimann et al., 2014), and also predicts cognitive decline in Parkinson's disease (PD) (J. Schulz et al., 2018). A better understanding of functional features of human NBM neurons may help to clarify disease mechanisms and to develop disease-modifying drugs in order to improve cognitive outcome in these pathologies.

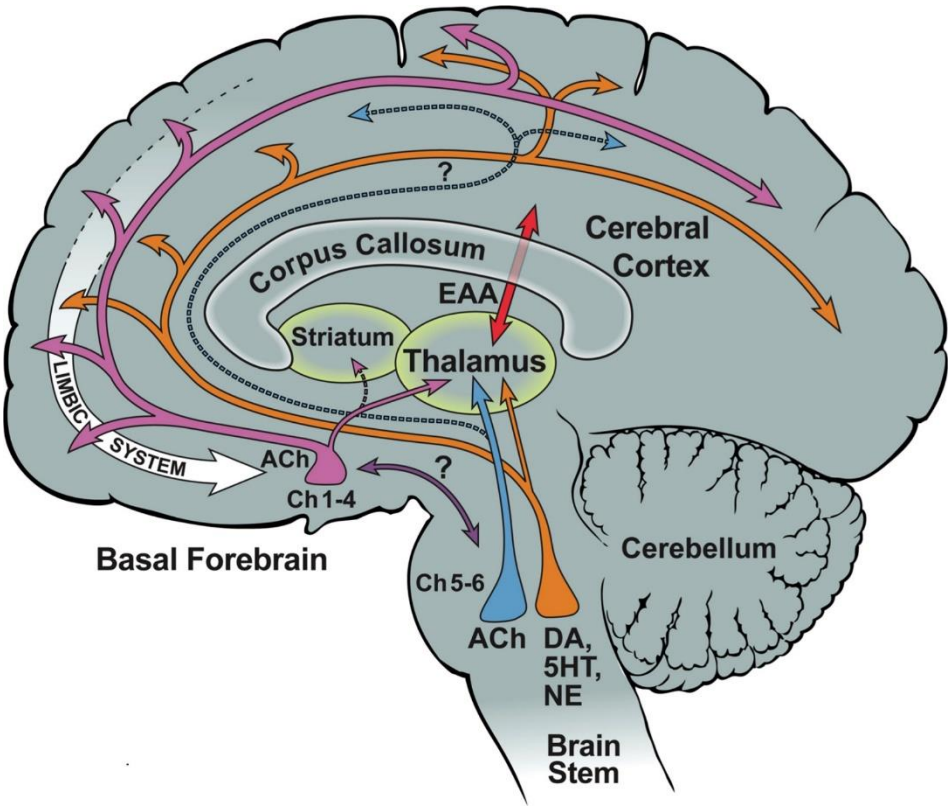

Figure 6. ***Cholinergic circuitry of the human nucleus basalis.*** ACh, acetylcholine; DA, dopamine; EAA, excitatory amino acids; NE, norepinephrine; 5HT, serotonin. Question marks indicate that the connection has not been confirmed in the human brain (M. M. Mesulam, 2013).

3.1. Basic notions of human forebrain embryogenesis

The evolvement of cerebral cortex is considered one of the most critical developmental processes underlying cognitive differences between humans and lower mammals. Indeed, defective development of the cerebral cortex is a major cause of intellectual disability disorders. In order to understand the molecular basis of these disorders and to develop future therapies for their treatment, a thorough understanding of cerebral cortex development is required. The entire nervous system originates from the neural plate that, during the third week of gestation in humans, forms neural folds which converge to create the neural tube and canal. Cells at the edge of each neural fold escape from the line of union and form the neural crest alongside the tube, divided in a dorsal part (alar plate) and a ventral part (basal plate). Within the fourth week, the rostral part of the neural tube undergoes a flexion at the level of the future midbrain, shaping the mesencephalon. Slight constrictions mark

its junction with the prosencephalon (future forebrain) and rhombencephalon (future hindbrain) (Mtui, 2016). The primary prosencephalon divides into two major components, the epichordal caudal diencephalon and the rostral secondary prosencephalon. The secondary prosencephalon is the entire prechordal part of the neural tube and includes the rostral diencephalon or hypothalamus, the optic vesicles, the preoptic region, and the telencephalon (ten Donkelaar, 2015). The alar plate of the prosencephalon expands on each side to form telencephalon (cerebral hemispheres), while the basal plate remains in place as diencephalon. In the telencephalon, mitotic activity takes place in the ventricular zone, just outside the lateral ventricle. Daughter cells migrate to the outer surface of the expanding hemisphere and form the cerebral cortex (Mtui, 2016). The two major telencephalic subdivisions are the pallium (the roof) and the subpallium (the base). The pallium gives rise to the cerebral cortex, whereas the basal ganglia and most cortical interneurons derive from the subpallium. the embryonic forebrain appears to be organized into transverse (prosomeres) and longitudinal subdivisions (alar and basal plates). The relationship between these postulated segments and telencephalic subdivisions, however, remains controversial. The dorsal and ventral domains of the developing telencephalon are distinguished by different patterns of gene expression, reflecting the initial acquisition of regional identity by progenitor populations (Zaki et al., 2003). The caudal part of the ventricular eminences or caudal ganglionic eminence (CGE) primarily gives rise to the subpallial parts of the amygdala. Therefore, the medial ganglionic eminence (MGE) is involved in the formation of the globus pallidus and the NBM. The nucleus basalis complex develops the earliest ACh sterase activity in the human telencephalon (Kostović, 1986) and sends widely distributed fibres to the anlage of the neocortex and limbic cortex via the external capsule by the end of the second trimester of gestation (Vasung et al., 2010). The timing of neuronal development in different brain regions have been extensively studied in rodents (ten Donkelaar et al., 2014). Structures such as the globus pallidus, the nucleus of the horizontal limb of the diagonal band of Broca, the

caudate–putamen complex ,and the olfactory tubercle arise early, whereas medium-sized and small cells in the BF develop over a much longer period of time, until P4 (ten Donkelaar, 2015). In the forebrain, differentiation is temporally regulated, with neuronal stem cells (NSCs) gradually losing their pluripotency, first generating neurons, and thereby astrocytes and finally oligodendrocytes. Hence, neural circuits are established before the formation of glial cells, which support the circuitry. Several factors influence NSCs proliferation or differentiation and regulate the length of cell cycle, of cell division, and extrinsic and intrinsic determinants. Cellular differentiation requires that neural progenitors first acquire a regional identity, which is often conferred by homeodomain transcription factors, followed by subtype specification and differentiation, which are induced by other transcription factors and signalling molecules (Dennis et al., 2016).

3.2. Nucleus Basalis of Meynert: anatomy and histology

The BF region is located above and parallel to the optic nerve, with the medial boundary being the wall of the lateral ventricle. This brain area was first described by Reil in 1809 and then was named substantia innominata (SI) of Reil by Theodore Meynert (Putnam, 1873), today known the SI of Reichert. However, instead of labelling a region, some investigators describe the SI as a discrete group of magnocellular neurons within the BF and Meynert first described a group of magnocellular hyperchromic neurons located in the SI of the human BF in 1873, naming it the nucleus of the ansa lenticularis; Kölliker later renamed it the NBM (Kölliker and von Ebner, 1903). The intricacy of this area has led to multiple names for this cluster of cells, resulting in substantial inconsistencies across studies. Ultimately, in 1942, the term NBM was established and is now widely used. The nucleus basalis is well delineated in certain mammalian species such as dolphins (*Delphinus delphis*), but sparsely distributed and less organized in others such as in the rat (*Rattus norvegicus*), where it is referred to as nucleus basalis magnocellularis (Gorry, 1963).

The NBM is an "open" nucleus with no distinct boundaries and it forms several clusters within the BF. Therefore, attempts have been made to subdivide this 'nucleus' (Liu et al., 2015). Detailed human anatomical studies show that the NBM is a flat, nearly horizontal structure extending anteriorly from the olfactory tubercle to the hippocampus, spanning 13–14mm in the sagittal plane. It reaches its greatest cross-sectional diameter under the anterior commissure in SI, with a medio-lateral width of 16–18 mm (Mesulam and Geula, 1988). The anterior part of the NBM reaches the horizontal limb of the nucleus of the diagonal band of Broca ventrally, the ventral globus pallidus medially, and the lateral extension of the anterior commissure laterally. The posterior portion of NBM reaches the ansa lenticularis dorsally, the putamen laterally, the posterior tip of the amygdala ventrally, and the optic tract medially (Bosch, 1978).

Histologically, NBM is characterized by the presence of magnocellular and hyperchromatin neurons containing conspicuous nucleus; it contains about 200,000 neurons per hemisphere, with the highest neuronal density under the anterior commissure (Koulousakis et al., 2019). Since nearly 90% of nucleus basalis neurons are cholinergic, by using histochemical and immunohistochemical labelling for AChE and choline acetyl-transferase (ChAT), Mesulam and colleagues (Mesulam et al., 1983) were able to identify the various cholinergic loci in the subhuman primates' BF and introduced the nomenclature Ch1–Ch4 to describe four cholinergic cell groups rostrocaudally. The Ch1 and Ch2 sectors are contained within the medial septal nucleus and the vertical limb nucleus of the diagonal band, respectively. The Ch3 sector is contained mostly within the lateral portion of the horizontal limb nucleus of the diagonal band. Finally, the Ch4 sector is comprised of cholinergic neurons in the nucleus basalis and parts of the diagonal band nuclei. The prefix Ch underlines the cholinergic nature of these cell groups and the Ch4 group is the largest out of the BF cholinergic groups and are mixed with a heterogeneous population of non-cholinergic neurons (Koulousakis et al., 2019).

Cholinergic neurons of the NBM express estrogen receptors, glutamate receptors and calbindin, as well as ACh receptors (Manns et al., 2001). The 10% of non-cholinergic interneurons of the NBM include galaninergic neurons, which inhibit cholinergic neurons, and nicotinamide adenine dinucleotide phosphate-diaphorase (NADPH-d) containing neurons, implicated in nitric oxide (NO) synthesis (Benzing and Mufson, 1995; Mufson et al., 2000). Furthermore γ-aminobutyric acid (GABA)-ergic neurons are distributed throughout the BF (Gritti et al., 1994).

However, the NBM is the major source of cholinergic input to the cerebral cortex and projects to most cortical areas (Cummings and Benson, 1987). Several works, including neuroimaging studies, show how the degeneration of these cholinergic pathways, especially the NBM, are involved in various forms of dementia. Hence, the study of the anatomy and function of this cholinergic nucleus is relevant to better understand the role it plays in these pathologies.

3.3. Connectivity: afferent and efferent projections of the NBM

Retrograde axonal tracing experiments cannot be performed in human subjects; therefore, we assume that the afferent and efferent connections of the human NBM are very similar to those demonstrated in primates. Direct axonal tracing experiments in non-human primates show that despite widespread efferent projections from the NBM to the entire neocortex, reciprocal afferent connections from cortex to NBM are not symmetrical and are restricted to limbic and paralimbic areas (Gratwicke et al., 2013). NBM has rich afferent and efferent connections. Its input arises primarily from the limbic system and related structures and its output projects to most of the neocortex the principal inputs that arrives to NBM from orbitofrontal, insular, temporopolar, parahippocampal, entorhinal and cingulate regions. Subcortical afferent input arises from the hypothalamus, septal nuclei, nucleus accumbens, amygdala and peripeduncular nucleus of the midbrain (Cummings and Benson, 1987).

Studies from Russchen and colleagues (Russchen et al., 1985) on macaques have warned that the NBM also receives neuronal projections from the reticular formation of the brain stem and from the nucleus of the solitary tract, with other surrounding cholinergic nuclei of the BF. According to retrograde tracer experiments in primate studies, efferent connectivity between individual NBM subsectors and cortical areas shows topographical specificity (Mesulam et al., 1983):

- **Ch4am** (anterior-medial), provides the major cholinergic projection to frontal, parietal and cingulate cortices situated along the medial wall of the hemisphere. There are also minor projections directed to the hypothalamus, hippocampal formation, ventral somatosensory cortex, amygdala, ventrolateral orbital, middle insular, parahippocampal regions and the inferior parietal lobule.
- **Ch4al** (anterior-lateral), the principal source of cholinergic projections to frontoparietal opercular regions and the amygdala. Additional projections are directed to the olfactory bulb, medial frontal pole, dorsomedial motor cortex, ventrolateral orbital cortex, insular, inferotemporal area and parahippocampal region.
- **Ch4id** (intermedio-dorsal) and **Ch4iv** (intermedio-ventral) present similar projections patterns: the main projections reach the ventrolateral orbital, insular, periarcuate, peristriate and parahippocampal areas as well as to the inferior parietal lobule. Minor projections occur to the medial frontal pole, dorsomedial motor cortex, frontoparietal opercular areas, the amygdala, anterior auditory cortex, and the temporal pole.
- **Ch4p**: it has a major projection to the superior temporal gyrus and the temporal pole. And minor projections confined to adjacent inferotemporal and posterior insular regions.

Due to the complex topographical arrangement of the efferent connectivity of Ch4, there is a substantial overlap of projections between the individual

subsectors according to primate tracing studies (Gratwicke et al., 2013). The anatomical analysis shows that NBM is mainly involved in a unidirectional flow of neuronal impulses ranging from limbic and paralimbic structures to the neocortex. All this is confirmed and supported by the fact that limbic and paralimbic areas (particularly hippocampal, amygdala and piriform regions) receive substantially higher levels of cholinergic input than adjacent neocortical association areas. Overall, the heterogeneous neural input to NBM from predominantly limbic structures combined with its dominant cholinergic output to the entire neocortex places it in a unique position in the brain where it can influence all aspects of complex behaviour according to the prevailing emotional or motivational state (Cummings and Benson, 1987; Gratwicke et al., 2013)

3.4. Functions of NBM

Despite detailed information about NBM's anatomy, connections or neurochemistry are available to date, its functions have not yet been fully clarified. Most experimental studies confirm that lesions or stimulations of NBM can lead to different consequences that mainly involve learning, memory, and modulation of the behavioural state.

3.4.1. NBM and memory

A role of NBM in memory tasks has been suggested by the observation that lesions of the medial forebrain nuclei, or isolated lesions of the NBM combined with anticholinergic treatment, result in a memory defect (Cummings and Benson, 1987). Low doses of cholinergic antagonists typically impair the animal's ability to perform various memory tasks, whereas cholinergic agonists facilitate these performances (Richardson and DeLong, 1991). Moreover, lesions to NBM cholinergic system or the use of anticholinergic agents in rodents and primates reduce cortical cholinergic functions and therefore compromise learning and memory on a variety of tasks by acting directly on cortical plasticity. It has been observed that the appearance of these

plastic changes is associated to cortical EEG desynchronization (transition from slow synchronized delta waves to fast gamma and theta waves) which is, in turn, associated to plasticity and learning. Subsequent studies demonstrated that physiological changes induced in the cortex of rats by NBM stimulation indeed have all the features of physiological associative memory: associativity, specificity, rapid acquisition, consolidation, conservation, and long-term extinction. Thus, compelling evidence exists that NBM plays an integral role in new memory formation (Gratwicke et al., 2013)

3.4.2. NBM and attention

A parallel line of investigation into the functions of the NBM hypothesizes a role in attention. In a scientific study on rats carried out by McGaughy and colleagues (McGaughy et al., 2002), selective NBM lesions correlated to differences in ACh levels and attention. Immunotoxin IgG-saporin (SAP) was used to perform a selective NBM lesion. Rats were tested in a five-choice serial reaction time task (5CSRTT) designed to assess visual attention. Rats with extensive damage in the nucleus magnocellular revealed a higher impairment of this activity. These rats had significantly lower levels of cortical ACh. These data provided the first direct evidence for a relationship between selective damage in the BF, decreased cortical ACh efflux and impaired attention. Memory and attention are not mutually exclusive activities. Indeed, if we consider all the phases of a learning process (selection of the sensory stimulus, manipulation in working memory, construction of associations for recall), they are closely connected one each other and dependent upon attention. Indeed, both human neuroimaging and computational modelling studies suggest that cholinergic activity in the sensory cortex serves to enhance signal detection (and thus attention) and, by doing so, to facilitate the formation of novel input associations (memory formation) (Gratwicke et al., 2013).

3.4.3. NBM and the modulation of the behavioural state

It has long been known that cholinergic projections of the NBM to the cortex are intimately involved in the regulation of cortical activation and arousal. Systemic injections of cholinergic agonists reliably desynchronize cortical EEG activity, whereas cholinergic antagonists synchronize EEG activity (Richardson and DeLong, 1991). The desynchronization of the neocortical EEG also corresponds to the presence of fast gamma waves, typical of the waking and alarm state. Otherwise, the failure to desynchronize the EEG due to a lesion of the NBM, produces slow synchronized delta waves (present in the state of sleep) with corresponding behavioural unresponsiveness / coma. Several studies have shown how cholinergic fibres of the rat's BF have a maximum discharge activity during the waking states to which the activity of the cortical gamma waves are related (emphasizing cortical excitation) and also the theta cortical oscillations (favouring synaptic plasticity). Summing up and analysing all these results it can be assumed that the function of the NBM is to regulate the behavioural state, allowing enhanced cognitive functions, attention and perception that lead to the enhancement of the ability to process and learn new information. Consequently, the degeneration of this nucleus compromises this state of activation, thus altering attention, perception of stimuli and the formation of new memories, as is the case in dementia (Gratwicke et al., 2013).

3.5. The importance to know better NBM

A better understanding of functional features of the human NBM is therefore required to clarify developmental aspects of cholinergic neurons and disease mechanisms that could support innovative therapeutic approaches to counteract the cognitive impairment produced by NBM cholinergic system dysfunction and/or degeneration.

In literature, it has been well established that neuronal loss within the cholinergic NBM correlates with cognitive decline in dementing disorders

such as Alzheimer's disease (AD) (Liu et al., 2015). Therefore, cell loss in NBM was first identified in Parkinson Disease (PD) by Lewy in 1913. Indeed, when directly comparing PD and AD cases, the loss is comparable (Rogers et al., 1985) or more extensive in PD than in AD (Candy et al., 1983) and the loss was more apparent among PD with dementia (PDD) cases. Furthermore, the role of NBM was investigated in many other neuropsychiatric disorders, as schizophrenia (Williams et al., 2013), Pick's disease, Creutzfeldt–Jakob disease (Rogers et al., 1985), dementia pugilistica (Uhl et al., 1982) and Down's syndrome (Casanova et al., 1985; Liu et al., 2015). The potential for neuromodulatory treatment targeting the NBM is now being realised, in particular deep brain stimulation in dementia (Gratwicke et al., 2013) and stereotactic gene delivery of trophic factors (Rafii et al., 2014). Moreover, in the era of regenerative medicine, increasing knowledge of functional features of human cholinergic neuroblasts could help to arrange efficient cell-based therapies to treat neurodegenerative disorders (Gallina et al., 2008; Guarnieri et al., 2018; Parmar, 2018). In spite of this, most of present knowledge on cholinergic system development and functioning has been obtained from studies in animal models and waits for confirmation and implementation using human experimental model tissue.

Studies focusing on the pharmacological and/or functional characteristics of human neurons isolated from the embryonic or fetal brain are limited in number (Hellström-Lindahl et al., 1998; Lepski et al., 2011; Sah, 1995). Indeed, most data concerning this issue have been collected from rodent tissues (Hedrick and Waters, 2010; Nakajima et al., 1985). Alternatively, immature neurons of human origin have been obtained from induced pluripotent stem cells (iPSCs) (R. Liu et al., 2013; Song et al., 2013) or embryonic stem cells (ESCs) (Bissonnette et al., 2011; Yang et al., 2019), but results need to be confirmed in developing "native" neurons.

Recently, my research group gathered important information on the characteristics of human fetal NBM (hfNBM) neuroblasts isolated from 12-

week-old human fetuses and we demonstrated that this cell culture possesses the hallmarks of cholinergic neurons (Morelli et al., 2017). Indeed, these neuroblasts express the enzymes required for ACh synthesis (choline acetyltransferase) and degradation (AChE) as well as the specific vesicular ACh transporter. Moreover, hfNBM cells can release ACh in the culture medium and express all subtypes of mAChRs (with predominance of M_2 and M_3 subtypes) and a variety of nAChRs. Furthermore, hfNBM neuroblasts exhibit tetrodotoxin- (TTX)-sensitive Na^+ current and a repertoire of voltage-dependent K^+ currents, as well as cholinergic receptor-mediated responses. Interestingly, intravenous injection of hfNBM cells in NBM-lesioned rats resulted in selective colonization of the lesioned NBM by differentiating cholinergic neurons injected cells and recovery of the cognitive impairment produced determined by the lesion (Morelli et al., 2017).

For this reason, the first aim of this thesis was to take advantage from the availability of hfNBM cultures to investigate the electrophysiological properties of immature, non-differentiating, cholinergic neurons from the human developing CNS and their functional responses to cholinergic agonists.

Chapter III – Purinergic system in PNS and CNS

Adenosine is a purine nucleoside indispensable for DNA synthesis; therefore, adenosine plays an essential role as neuromodulator also in biochemical processes and signal transduction, being correlates with molecules such as ATP, ADP and AMP. Therefore, adenosine is an endogenous neuromodulator that recently emerged as a most pervasive mechanism for intercellular communication in the nervous system. The first report on adenosine actions by Drury and Szent-Györgyi (Drury and Szent-Györgyi, 1929) mainly considered the profound cardiac actions. Thirty-four years later, Berne identified a physiological role for adenosine as a mediator of coronary vasodilation in response to myocardial hypoxia (Berne, 1963). In 1970s, Sattin and Rall showed that adenosine, in the CNS, increases cAMP in mammalian brain slices, an effect inhibited by methylxanthines (i.e. caffeine and theophylline) (Sattin and Rall, 1970). Later, a depressant role of adenosine on the firing of cortical and cerebellar neurons and on excitatory synaptic potential amplitude in cortical and hippocampal slices was demonstrated (Dunwiddie and Hoffer, 1980; Kostopoulos et al., 1975; Okasa and Ozawa, 1980; Phillis et al., 1979). Moreover, it was shown that adenosine inhibits on the release of several neurotransmitters in different brain areas, as Ach, dopamine, noradrenaline excitatory amino acids and serotonin (Corradetti et al., 1984; Harms et al., 1979, 1978; Michaelis et al., 1979).

At central level, it carries out numerous actions: acts as an endogenous anticonvulsant, influences control of motility, pain, learning and memory (Pedata et al., 2007). Moreover, it has a further crucial role in the modulation of emotional states, conditioning social interactions, and aggressive behaviours. In physiologic conditions, extracellular adenosine exerts an inhibition on synaptic transmission, and this makes it a highly protective neuromodulator. Adenosine is a paramount chemical mediator which can activate specific biologic responses and its action mainly occurs through purinergic receptors activation. To date, it is well recognised that purinergic

signalling plays a fundamental role in several biological systems, from invertebrates to mammals, and purinergic-mediated effects including both short-term (neurotransmission, endothelial-mediated vasodilatation, platelet aggregation) and long-term (cell proliferation, differentiation, migration and death) phenomenon have been demonstrated.

4. Adenosine

The nucleoside adenosine is formed by an adenine and ribose molecule joined through an N9-glicosidic bond (Fig. 7) and is continually formed both at intracellular and extracellular level (Fredholm et al., 2001).

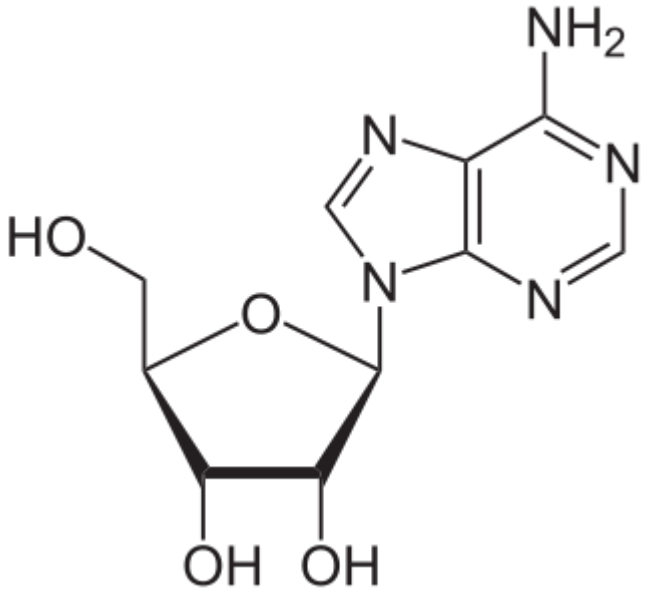

Figure 7. *Structure of Adenosine.*

Adenosine is produced from dephosphorylation of adenosine monophosphate (AMP) by the enzyme 5'- nucleosidase (5'-NT), that is present at both intracellular and extracellular level (Zimmermann et al., 1998). adenosine can also be formed through the breakdown of nucleotides which are released into extracellular space, through coupled ectonucleotidases: CD39 that converts ATP/ADP to AMP and CD73 that hydrolyses AMP to adenosine. A further enzyme able to generate adenosine by sequential hydrolysis of ATP, is the alkaline phosphatase (Zimmermann, 2000). Another possible source of extracellular adenosine is represented by released cAMP. In the extracellular

space, cAMP can be converted to 5'-AMP by ecto-phosphodiesterase, and then to adenosine by 5'-ectonucleotidase. The 5'-NT is inhibited by ATP and it has an elevated affinity towards AMP; for this reason, when the cell is exposed to an intense metabolic activity with increased ATP consumption and consequent elevated production of AMP, the enzyme has very high enzymatic activity (Pedata et al., 2007). Therefore, during low energetic support conditions as in epileptic attacks, hypoxia or ischemia, production of adenosine is much raised (Latini and Pedata, 2001). Alternatively, cAMP can be converted into 5'-AMP within the cell and then released in the extracellular space, where it represents a further source of adenosine. This suggests that many neurotransmitters that act on metabotropic receptors whose signalling is linked to adenylate cyclase, by favouring the accumulation of cAMP, may regulate the adenosine levels and thus the inhibitory effects in the CNS (Latini and Pedata, 2001).

After electrical stimulation in vitro, adenosine seems to originate directly from cells, while in ischemic experimental models in vitro, adenosine might have also an extracellular origin due to the degradation of the adenosine nucleotides released following changes in membrane permeability (Pedata et al., 1993). Under normal physiological conditions, extracellular adenosine levels are between 20 and 300 nM, rising to a low micromolar range under extreme physiological situations (intensive exercises or low atmospheric oxygen levels) and high micromolar levels (30 μM) in pathological conditions such as ischemia (Newby, 1984).

Adenosine concentrations are regulated by a bidirectional flow mediated by transporters. These transporters are divided into two categories: (i) those capable of a bidirectional transport across the plasma membrane of both purines and pyrimidines, according their concentration gradient (equilibrative transporters, ENT1 and ENT2) and (ii) transporters that mediate the nucleotide influx thank to the coupling with sodium transporters (concentrative, CNT1 and CNT2) (Baldwin et al., 1999; Williams and Jarvis, 1991). The equilibrative transporters work bidirectionally in order to maintain

the intracellular and extracellular concentrations of adenosine in a range of 30-300 nM (Jacobson et al., 1997). Inhibitors of adenosine equilibrative transporters, such as dypiridamole, might increase or decrease the efflux of adenosine differently according to the physiopathological conditions. It has been observed that TTX completely blocks adenosine release in brain slices electrically stimulated and that a reduction of extracellular Ca^{2+} concentration can cause a remarkable reduction of adenosine release (Pedata et al., 1990). It was demonstrated that adenosine efflux occurring in vivo from the striatum under normoxic physiological conditions does not arises from extracellular degradation of nucleotides and is not inhibited by dypiridamole (Melani et al., 2012). Under these conditions the efflux of adenosine is Ca^{2+}-sensitive and is inhibited by TTX (Dobolyi et al., 2000; Pazzagli et al., 1993). On the all observations in vitro and in vivo led to speculate that adenosine efflux under normoxic physiological conditions is consequent to electrical activity propagated along the typical modality of nervous cells that involves activity of voltage-gated Na^+ channels. In fact, the TTX sensitivity and the Ca^{2+} dependency of adenosine release indicate that adenosine release occurs by an excitation-secretion modality which is typical of neurotransmitters. Observation that the presence of adenosine is associated with intracellular vesicles support the notion that adenosine is stored in vesicles and released by exocytosis in an excitation- secretion modality typical of neurotransmitters (Corti et al., 2013).

Finally, adenosine metabolism is regulated by two enzymes: adenosine deaminase (ADA) and adenosine kinase (AK). ADA degrades adenosine to inosine and it is present both at intracellular and at extracellular sites where is anchored to the plasma membrane (Franco et al., 1986). AK is an enzyme that converts adenosine to AMP, it is characterized by high specificity. Since the endogenous levels of adenosine are in the nanomolar range, it is likely that under physiological conditions the main degradation pathway is the phosphorylation operated by AK, while the action of ADA is important only

for the significant increases in adenosine concentration, such as those that occur during ischemia (Latini and Pedata, 2001).

4.1. Purinergic receptors

The existence of adenosine receptors was proved unequivocally when the first adenosine receptors were cloned in 1990 (Maenhaut et al., 1990). Based on the responses of various tissues to purines, Burnstock proposed that there are distinct receptors that bind adenosine or ATP, designated P1 and P2 receptors, respectively (Burnstock et al., 1978). Originally, the "P" in P1 and P2 was meant to designate purinergic receptors. However, it has been discovered that some of the P2 receptors bind pyrimidines, UTP or UDP, preferentially over the purine, ATP. Hence, the "P" in P2 is now used to designate purine or pyrimidine. Despite these exceptions, P1 and P2 receptors collectively are still generally referred to as purinergic receptors. In addition to adenosine, various synthetic adenosine analogues activate P1, but not P2, receptors and synthetic ATP or UTP analogues activate P2, but not adenosine, receptors. P1 receptors were initially distinguished into two classes (A_1 and A_2 receptors) based on their excitatory or inhibitory actions on adenylyl cyclase (Van Calker and Hamprecht, 1979). Later work defined four different subtypes of P1 receptors: A_1, A_{2A}, A_2B and A_3 receptors (A_1R, $A_{2A}R$, $A_{2B}R$, A_3R) (Fredholm et al., 2001). On the other hand, P2 receptors appeared to be more heterogeneous and in 1994 Abbracchio and Burnstock have classified P2 receptors in two major families: (i) P2X ligand-gated ion channel receptors and (ii) P2Y G-protein-coupled receptors (Abbracchio and Burnstock, 1994). Receptors for both ATP and adenosine are widely distributed in the nervous system as well as in other tissues and physiological effects of adenosine on almost all tissues have been described.

The development of synthetic compounds that activate P1 or P2 receptors has been important for elucidating how these receptors function because some of these compounds are more potent and selective than the parent purines and

most are more stable than the short-lived endogenous compounds adenosine and ATP.

4.1.1. P1 adenosinergic receptors

As stated above, molecular cloning and pharmacological studies have identified four subtypes of adenosine P1 receptors: A_1R, $A_{2A}R$, $A_{2B}R$ and A_3R (Fredholm et al., 2001). All of them have already been cloned at least from rat, mouse and human. All receptors are metabotropic heteromeric G-protein coupled receptor (GPCR). Typically, their structure is formed by a polypeptide chain characterized by 7 transmembrane hydrophobic domains with α helix structure (7TM, helices 1-7) of approximately 25 residues followed by one short membrane-associated helix (helix 8). TM domains are closely associated by three extra-cellular loops (ECL1-3) and three intracellular loops (ICL1-3) (Cristalli et al., 2008). Biochemical experiments and computational approaches have revealed the importance of the TM3 and TM7 in binding the endogenous ligand and agonist molecules (Rivkees et al., 1995). All adenosine receptors present an extra-cellular amino terminus (N-terminus) and a cytosolic carboxy terminus (C-terminus), (Cristalli et al., 2008). The extracellular N-terminus contains one or more glycosylation sites, while the intracellular C-terminus provides sites for phosphorylation and palmitoylation, thereby playing a role in receptor desensitization and internalization mechanisms (Borea et al., 2018). Structural data report a close similarity between adenosine receptors of the same subtype among mammalian species, except for A_3Rs. This subtype is the latest cloned and pharmacologically characterized and presents a considerable structural variability among different species. For instance, almost 30% difference in the amino acid sequence is found between humans and rat (Linden et al., 1993).

A_1R, $A_{2A}R$ and A_3R present a particularly high affinity for the endogenous ligand, being activated by nanomolar concentrations of adenosine (Fredholm et al., 2001). On the other hand, the affinity values of $A_{2B}R$ for adenosine in binding and functional experiments are higher than 1 μM (Fredholm et al.,

2001). Physiological extracellular adenosine concentrations are sufficient to activate A_1R, $A_{2A}R$ and A_3R subtypes, but not $A_{2B}R$, which require higher concentrations (micromolar range) of adenosine to be activated (Frenguelli et al., 2007; Latini and Pedata, 2001). Therefore, higher adenosine concentrations are only reached under pathological conditions, such as during hypoxia or ischemia in vivo (Pedata et al., 2001) and in vitro (Latini et al., 1999).

Furthermore, A_1R and A_3R subtypes are associated with G_i activation, adenylyl cyclase inhibition and decrease of intracellular cAMP levels, while $A_{2A}R$ and $A_{2B}R$ are linked to G_s proteins that activate the same enzyme increasing cAMP concentration in the cytosol. However, adenosine receptors have also been reported to couple to other G-proteins than G_s, modulating different second messenger systems. For instance, in addition to their effects on adenylate cyclase adenosine A_1R, $A_{2B}R$ and A_3R are also coupoled with G_q and G_o proteins (Antonioli et al., 2013; Burnstock et al., 2011). Furthermore, A_1R and A_3R can also activate phospholipase D (PLD) (Fredholm et al., 2001).

Since adenosine receptors have been studied for a long time, there are several useful pharmacological tools available at present. Numerous adenosine analogues have been developed that selectively bind one of the four different subtypes of P1 receptors. For examples, NECA was long considered to be a selective $A_{2A}R$ agonist but it has been largely demonstrated that it is an unselective agonist at all P1 receptors, only slightly preferring $A_{2A}R$ subtypes (Fredholm et al., 2001) (Fig. 8).

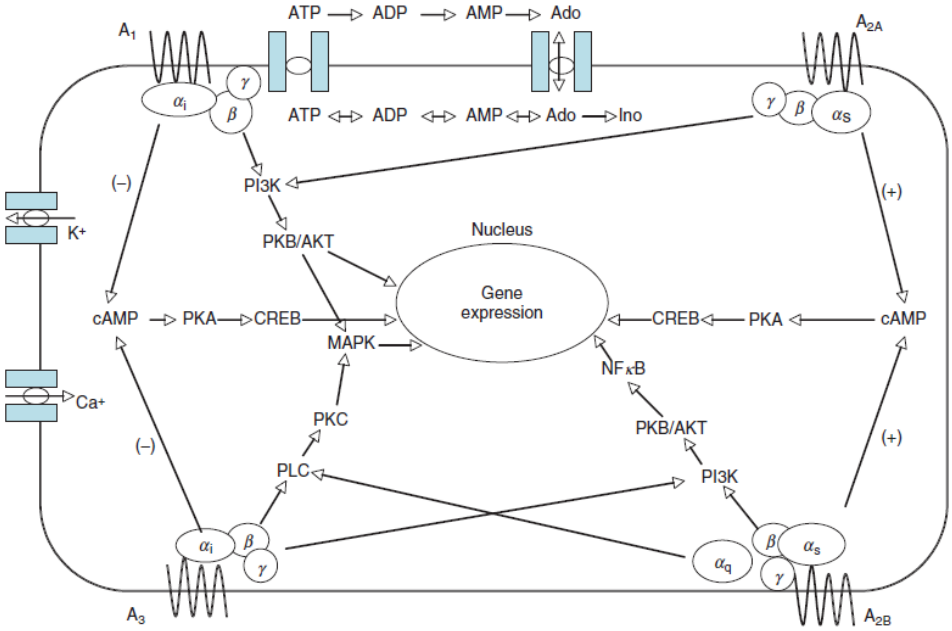

Figure 8. ***Signalling pathway associated with adenosine receptor.*** ATP, adenosine triphosphate; ADP, adenosine diphosphate; AMP, adenosine monophosphate; Adp, adenosine; Ino, inosine; CREB, cyclic AMP response element-binding protein; MAPK, mitogen-activated protein kinase; NFkB, nuclear factor-kappa B; PI3K, phosphatidylinositol 3-kinase; PKA, protein kinase A; PKB, protein kinase B; PKC, protein kinase C; PLC, phospholipase C. (Taken from: Malenka, 2009).

4.1.1.1. A_1Rs

The A_1R is highly conserved with an 87%-92% homology between different species. It is coupled with the $G_{i/0}$ protein, leading to inhibition of adenylate cyclase, activation of several types of K^+ channels (probably via β,γ-subunits), inactivation of N- and P/Q-type Ca^{2+} channels, stimulation of phospholipase C, and stimulation of phospholipase D (Burnstock et al., 2011; Fredholm et al., 2001). The highest levels of A_1R expression are found in the CNS, suggesting a particularly important role of adenosine in brain functions. In particular, in rat the highest expression of A_1R has been found in the cortex, hippocampus, cerebellum and dorsal horn of the spinal cord; intermediate levels in basal ganglia structures including the striatum (Dixon et al., 1996). Neuronal A_1Rs are localized both pre- and postsynaptically (Deckert and Jorgensen, 1988); in the hippocampus subcellular analysis of nerve terminals revealed that A_1R immunoreactivity is strategically located in the active zone of presynaptic terminals, as expected on the basis of the ability of A_1R agonists to depress

neurotransmitter release. It has also been demonstrated that A_1R immunoreactivity is evident at postsynaptic sites together with NMDA receptors and with N- and P/Q-type Ca^{2+} channels, emphasizing the importance of A_1Rs in the control of dendritic integration (Rebola et al., 2003). Moreover, A_1Rs can be found also extrasynaptically on dendrites and on the axonal fibres of the hippocampus (Rivkees et al., 1995; Swanson et al., 1995). Activation of A_1Rs along the axon may be a powerful extra synaptic mechanism by which adenosine alters axonal electric transmission to inhibit neurotransmitter release (Swanson et al., 1995). Under physiological conditions A_1Rs mediate sedative-hypnotic, anti-epileptic and anti-nociceptive effects by exerting a tonic inhibition of synaptic transmission both in vitro and in vivo (Dunwiddie, 1985). At presynaptic level, the activation of A_1R reduces Ca^{2+} influx through the preferential inhibition of N-type and, probably, Q-type channels, with a consequent decrease in neurotransmitters release (McCool and Farroni, 2001). In fact, adenosine, by stimulation of A_1R, has been found to inhibit the release of all classic neurotransmitters: glutamate, acetylcholine, dopamine, noradrenaline and serotonin (Ribeiro, 1995). In particular, a powerful suppression of glutamate release from presynaptic terminals has been described in the hippocampus (Corradetti et al., 1984). At postsynaptic level, A_1Rs mediate a direct hyperpolarization of neurones via activation of G-protein-coupled inwardly rectifying potassium (GIRK) channels (Kir 3.2 and 3.4 channels) and by a direct increase of Cl^- conductance thus, stabilizing the membrane potential (Greene and Haas, 1991; Takigawa and Alzheimer, 2002). Out from CNS, high levels of A_1R expression are found in adrenal glands, eye, and atria. Intermediate levels are found in skeletal muscles, liver, kidney, adipose tissue, gastrointestinal smooth muscles, and bronchi. Lung and pancreas present low level of A_1R expression (Fredholm et al., 2001).

The A_1R full agonist 2-chloro-N-(6)-cyclopentyladenosine (CCPA), and to a lesser extent CPA, and the antagonist 8-Cyclopentyl-1,3-dipropylxanthine (DPCPX) are highly selective compounds active at nanomolar concentrations,

in human, rat and mouse tissues. Allosteric enhancers for this receptor subtype, such as PD81723 and analogues, are also available and increase the agonist binding and its effects (Bruns and Fergus, 1990; Van Der Klein et al., 1999).

4.1.1.2. $A_{2A}Rs$

The $A_{2A}R$ is highly conserved with a homology of 90% between different species. This receptor is associated to a G_s protein, which stimulates adenylate cyclase leading to increase of intracellular cAMP concentrations and mobilize the intracellular Ca^{2+} (Mirabet et al., 1997; Moreau and Huber, 1999). These receptors are expressed throughout all the CNS, however they are principally located in the basal ganglia, as caudate-putamen, nucleus accumbens and olfactory tubercle (Dixon et al., 1996; Jarvis et al., 1989; Rosin et al., 1996). In particular, this receptor subtype is expressed on striatopallidal GABAergic-enkephalin neurones, where it colocalises with dopamine D2 receptors, but not on GABAergic-dynorphin striatal neurones (Fredholm and Svenningsson, 2003). High levels of adenosine $A_{2A}R$ mRNA have also been found in striatum, while lower levels have been found in hippocampus and cortex (Dixon et al., 1996; Svenningsson et al., 1997). Besides postsynaptically, $A_{2A}Rs$ are also located presynaptically on different GABAergic, cholinergic, glutamatergic neuron types (Hettinger et al., 2001; Rosin et al., 2003). In the CNS they are also expressed on astrocytes (Biber et al., 1999; Lee et al., 2003), microglia (Pedata et al., 2014) , oligodendrocytes (Stevens et al., 2002), blood cells and vasculature (Phillis, 2004). In recent years, particular interest has been dedicated to study receptor dimerization, either in homomeric and heteromeric structures, since this phenomenon seems to frequently occur in numerous cell types and can modify the pharmacological profile of receptors and their functional role. Various lines of evidence indicate that such an interaction occurs postsynaptically in the striatum between $A_{2A}R$ adenosine and D_2 dopamine receptors, where this heterodimerization inhibits D_2 receptor functions (Ferre et al., 1991). Therefore, A_1R and $A_{2A}R$ heteromers are

located presynaptically in glutamatergic terminals of the striatum, exerting opposite effects on the modulation of glutamate release through a "concentration-dependent switch" mechanism by which low adenosine concentrations inhibit, while high concentrations stimulate, glutamate release (Ciruela et al., 2006). In the nervous system, $A_{2A}R$ activation mediates excitatory actions, contrary to the A_1R that exerts synaptic inhibition (Latini et al., 1996; Pedata et al., 1984; Sebastião and Ribeiro, 1996; Spignoli et al., 1984). Electrophysiological investigations about the role of $A_{2A}Rs$ under physiological conditions have shown that they increase synaptic neurotransmission. In fact, the $A_{2A}R$ G_s-mediated signalling increases cAMP level, which activates PKA (Gubitz et al., 1996). Furthermore, PKA phosphorylates the P-type Ca_v, that directly modulates the mechanisms of vesicle release. Vesicle exocytosis can also be regulated by βγ subunits of the G_s protein, which can promote the phosphorylation, mediated by PKC, of N-type Ca_v (Gonçalves et al., 1997; Gubitz et al., 1996). In fact, in the hippocampus in vitro, $A_{2A}R$ stimulation results in a Ca^{2+}-dependent release of Ach (Cunha et al., 1995; Spignoli et al., 1984). Moreover, the selective stimulation of adenosine $A_{2A}Rs$ augments the amount of glutamate released in hippocampus and striatum of young rats (Corsi et al., 2000, 1999; Popoli et al., 1995), supporting the theory about that $A_{2A}Rs$ increase excitatory amino acid release. In addition, $A_{2A}R$ also enhance long-term potentiation (LTP), a form of synaptic plasticity associated with memory, central for learning process (Almeida et al., 2003). In fact, a decreased LTP in the nucleus accumbens was found in knock-out (KO) mice for the $A_{2A}R$ (D'Alcantara et al., 2001). It is worth noticing that the role of $A_{2A}Rs$ in the striatum is recently gaining interest considering their heterodimerization with D2 dopamine receptors. The association between $A_{2A}R$ and D2 receptors results in an antagonistic interaction which provided a rationale for evaluating $A_{2A}R$-selective antagonists in Parkinson's disease. It was suggested that $A_{2A}R$ antagonists not only provide symptomatic relief but also decelerate dopaminergic neuron degeneration in patients (Xu et al., 2005). Finally, $A_{2A}Rs$

are also highly present in spleen, thymus, immune cells both on cells of innate (macrophages, mast cells, monocytes, dendritic cells, and granulocytes) and on cells of adaptive (lymphocytes) immunity (Antonioli et al., 2014; Haskó et al., 2008). Lower levels are also found in the heart, lung, and blood vessels (Fredholm et al., 2001). As mentioned above, NECA is an unselective adenosine receptor agonist; however, based on evidence that 2-substitution of NECA molecule increased selectivity, CGS21680 was developed as an $A_{2A}R$ selective agonist (Hutchison et al., 1989). This compound is less potent and selective in humans than in rats (Kull et al., 1999), but it has been replaced by another recently developed $A_{2A}R$ agonist, ATL-146, which is 50 fold more potent than CGS21680 at the human receptor (Rieger et al., 2001). Among the numerous $A_{2A}R$ antagonists, the most selective so far are SCH58261 and SCH442416 and the structurally related ZM241385 (Poucher et al., 1995).

4.1.1.3. $A_{2B}Rs$

The $A_{2B}R$ show a low affinity for adenosine (EC_{50} = 5-20 µM; (Beukers et al., 2000; Fredholm et al., 2001; Sachdeva and Gupta, 2013) and are associated, as the $A_{2A}R$, to G_s protein; for these reason they were initially considered a receptor subtype with a little physiological importance (Sun and Huang, 2016). Recently we are beginning to understand the importance of this receptor and how much they are involved in many diseases. Moreover, in physiological conditions, for their low affinity to adenosine, they are not activated. However, they are activated in pathological conditions, when adenosine reaches concentrations of micromolar order; for these reasons it could represent an interesting therapeutic target. In addition to being coupled to G_s protein, the $A_{2B}R$ can be coupled to G_q protein (Gao et al., 1999; Linden et al., 1999; Panjehpour et al., 2005), involving MAPK and arachidonic acid. In general, $A_{2B}R$ are widely expressed in numerous tissues and organs, including the vascular system, smooth muscle, gastrointestinal tract, brain tissue and bladder (Wang and Huxley, 2006; Yaar et al., 2005). However, the presence of these receptors is influenced by environmental stimuli, such as inflammation,

cellular stress, trauma and hypoxia, which may increase their expression (Fredholm et al., 2001; Hart et al., 2009; Haskó et al., 2009; Kolachala et al., 2005; Kong et al., 2006; Xaus et al., 1999). In addition, A_{2B}Rs are expressed both in the CNS and PNS (Dixon et al., 1996). They are expressed ubiquitously in the brain and their mRNA has been detected in all rat cerebral areas studied (Dixon et al., 1996; von Lubitz, 1999), with a prevalent presence on hippocampal neurons (Kessey and Mogul, 1997; Mogul et al., 1993) and on glial cells (Fiebich et al., 1996; Peakman and Hill, 1994). These receptors appear to induce the release of excitatory amino acids and acetylcholine, while they reduce the release of γ-amino butyric acid (GABA) in rat cortex (Phillis et al., 1993). In addition, at hippocampal level, they modulate the LTP process (Kessey and Mogul, 1997).

The signalling pathways generated by A_{2B}Rs stimulation are strongly influenced by the signalling of other receptors that affect the PLC/PKC pathway. In brain slices, cAMP accumulation due to the activation of the A_{2B}R, is markedly increased by drugs that stimulate PKC (Fredholm et al., 1987; Hollingsworth et al., 1985). At peripheral level, A_{2B}R subtype is particularly abundant in the gastrointestinal tract, mainly in caecum, colon, urinary bladder, lung, blood vessels and adipose tissue (Fredholm et al., 2001). Increasing evidences indicate a role for this receptor in the modulation of inflammation and immune responses in selected pathologies like cancer, diabetes, as well renal, lung and vascular diseases (Borea et al., 2018). In addition, A_{2B}R plays proinflammatory roles in human asthma and chronic obstructive pulmonary disease (COPD) and murine colitis (Kolachala et al., 2008; Wendell et al., 2020). In phase I clinical trials, CVT-6883, a potent and selective A_{2B}R antagonist, was demonstrated to be safe, well tolerated, and sustainable at a once-daily chronic dosage (Kalla and Zablocki, 2009). It may provide a new therapeutic option for several disease areas, including asthma, COPD, and pulmonary fibrosis (Wendell et al., 2020).

Potent $A_{2B}R$ agonists with affinity values in the low nanomolar range have been lacking till recently, when a new class of non-adenosine compounds, as pyridine derivatives, has been synthesised by Beukers and colleagues (Beukers et al., 2004). Among them, LUF5835 is a full agonist with an EC_{50} of 10 nM at human $A_{2B}R$ expressed in CHO cells. Unfortunately, its selectivity towards A_1R and $A_{2A}R$ is not adequate to discriminate between them in native tissues. The situation is somewhat more favourable for antagonists, as some potent and relatively selective compounds have been found among anilide derivatives of xanthines with K_i values in the low nanomolar range, such as MRS1754 (Ji et al., 2001), that is over 200-fold selective for $A_{2B}R$ versus all other P1 receptors (Kim et al., 2000).

4.1.1.4. A_3Rs

The A_3Rs have a high affinity for adenosine (EC_{50} = 300 nM) and are coupled to Gi proteins, whose activation inhibits the Adenylate Cyclase, stimulates the phospholipase C and B and induces the uptake of Ca^{2+} and its release from intracellular reserves (Sachdeva and Gupta, 2013). Their activation can lead to both protective and harmful effects (Cheong et al., 2013); in nonneuronal cells it was observed that a non-excessive activation prevents apoptosis mechanisms, while a persistent and intense activation induces toxic effects (Yao et al., 1997). The A_3R evokes the same effects mentioned for A_1R (Englert et al., 2002), inducing Ca^{2+} mobilization (Englert et al., 2002; Shneyvays et al., 2005, 2004) and interacts with MAPK (Schulte and Fredholm, 2003). The expression of A_3R adenosine receptor in the brain is generally lower than that of the other subtypes (Ji et al., 1994) and is highly species-dependent (Fredholm et al., 2001, 2000). These receptors show a significant difference between the various species under the pharmacological profile, the distribution and their function. By the sensitive technique of real time PCR, A_3Rs are found in both neuronal and non-neuronal elements, i.e. astrocytes, microglia, and vasculature of the cerebral tissue (Zhao et al., 1997) with widespread distribution. In the rat, a significant expression of A_3Rs is found

in cerebellum and hippocampus (Dixon et al., 1996) where they are mainly expressed at the presynaptic level (Lopes et al., 2003). In literature discrepancies about the role of adenosine A_3Rs in the CNS are present. An excitatory role of A_3R has been supported by evidence indicating that, in the rat hippocampus, its activation attenuates long-term depolarization (LTD) and allows induction of LTP elicited by a subliminal weak-burst protocol (Costenla et al., 2001). Additional evidence for an excitatory role of adenosine A_3Rs came from studies carried out in hippocampal slices (Pugliese et al., 2007). In the same brain area, A_3R activation through a selective agonist has been shown to antagonize the adenosine A_1R-mediated inhibition of excitatory neurotransmission (Dunwiddie and Fredholm, 1997). However, further electrophysiological studies refused this hypothesis, since several authors demonstrated that no significant interaction between A_1R and A_3R occurs in the rat cortex and hippocampus (Brand et al., 2001; Lopes et al., 2003). Conversely, an inhibitory action has been attributed to A_3Rs by Brand and colleagues, who demonstrated that, in rat cortical neurons, the selective activation of A_3R is involved in inhibition of excitatory neurotransmission, suggesting a synergic action with the inhibitory effect mediated by A_1R activation (Brand et al., 2001). Despite results obtained by A_3R stimulation, evidence that selective block of A_3Rs does not affect neurotransmission in the CA1 region of the hippocampus under normoxic conditions, indicates that endogenous adenosine at physiological concentration does not exert tonic activation of A_3Rs (Dunwiddie and Fredholm, 1997; Pugliese et al., 2003). In oligodendrocytes A_3R represents the main cause of toxicity due to the action of adenosine; in fact, the selective 2-Cl-IB-MECA A_3R agonist, chlorinated derivative of N6-(3-iodo-benzyl)-adenosine-5′-N-methyluronamide (IB-MECA), induces apoptosis in oligodendrocytes, while the selective antagonist MRS 1220 is protective when the extracellular concentration of adenosine rises to 10 μM, as it occurs following ischemia (González-Fernández et al., 2014). The toxic effect is due to the generation of reactive oxygen radicals (ROS) and the depolarization of the mitochondrial membrane (Brady et al., 2004; Cao et

al., 2011), which leads to the release of pro-apoptotic proteins, activating the intrinsic pathway of apoptosis (González-Fernández et al., 2014; Masino and Boison, 2013).

In the periphery, A_3R subtype is mainly found in rat testis (Meyerhof et al., 1991) and mast cells, in accordance with the fact that for a long time the unique role assigned to this receptor have been mast cell degranulation and histamine release. Intermediate levels are found in the lung, spleen, thyroid and liver (Linden et al., 1993; Salvatore et al., 1993). Interestingly, A_3R is overexpressed in several cancer cells and tissues and is therefore likely to have an important antitumoral role (Borea et al., 2015). An emblematic feature of the adenosine A_3R, the most recently discovered one, is its insensitivity to the antagonistic actions of methylxanthines, such as caffeine and theophylline, the traditional blockers of adenosine receptors (Fredholm, 1995). Hence, most A_3R antagonists are dihydropyridines, pyridines and flavonoids (Baraldi and Borea, 2000). Another class of highly selective compounds are isoquinoline and quinazoline derivatives, such as VUF5574 that presents a K_i value of 4 nM vs human A_3R but not vs the rat isoform (Van Muijlwijk-Koezen et al., 2000). In this regard, it is worth noticing that significant species differences in the affinity of adenosine A_3R antagonists have been noted, as expected from the high structural inter-species variability already mentioned. The affinity values of several A_3R blockers are typically more than 100-fold greater on human than rat receptors, as described for MRS1220. The unique rat-selective compound is the A_3R agonist MRS1523. In contrast, the affinity of the most widely used A_3R agonist, Cl-IB-MECA, does not vary beyond an order of magnitude between the species examined, at least among mammals. The high affinity (low nanomolar range) and selectivity (more than 100-fold vs A_1R and $A_{2A}R$) of this compound towards A_3R turns it into the most used pharmacological tool for investigating A_3R-mediated effects (Jeong et al., 2003).

5. Foreword - Role of adenosine A_{2B} receptors in oligodendrocyte differentiation

Oligodendrocyte progenitor cells (OPCs) are a population of cycling cells in the developing and adult CNS that, under opportune stimuli, differentiate into mature myelinating oligodendrocytes (OLs). During brain injury or demyelinating pathologies, OPCs are recruited to the site of lesion to remyelinate damaged axons. Growing evidence shows that failure of myelin formation in demyelinating diseases such as multiple sclerosis (MS) arises from the disruption of OPC differentiation (Levine et al., 2001). For this reason, therapeutic strategies aimed at fostering this process could be of interest in this pathology. Adenosine is emerging as an important player in OPC differentiation and it is demonstrated that adenosine A_{2A}Rs inhibit cell maturation by reducing voltage-dependent K^+ currents (Coppi et al., 2013a). On the other hand, we know little about the role of A_{2B}R subtype in OL.

Furthermore, the bioactive lipid mediator sphingosine-1-phosphate (S1P) and its receptors (S1P1–5) are also crucial modulators of OPC development and Sun and colleagues demonstrated an interaction between this pathway and the A_{2B}R in peripheral cells (Sun et al., 2015). For these reasons, the second aim of this thesis is to study the role of A_{2B}R in OL and to investigate a possible crosstalk between A_{2B}R and S1P pathway.

5.1. Oligodendrocyte differentiation

Before being able to produce myelin, oligodendroglia cells progress through a series of highly regulated steps of differentiation from OPCs to mature OLs (Barateiro and Fernandes, 2014; De Castro and Bribián, 2005). During embryonic development, OPCs are generated in restricted areas, such as the subventricular zone (SVZ), and present a significant migratory ability that allow them to spread and populate the brain and spinal cord (Emery, 2010). Their differentiation and maturation are postnatal processes characterized by the loss of proliferative activity and the acquisition of an elaborate morphology with highly branched processes (De Castro and Bribián, 2005).

Oligodendrogliogenesis involves a sequence of distinct phases that can be identified by the expression of stage-specific surface antigens and by morphological changes (Gard and Pfeiffer, 1990; Jung et al., 1996; Levi et al., 1986; Warrington et al., 1992). On these bases, a classification into three stages of differentiation has been proposed: proliferating OPCs, post-mitotic pre-OLs and mature myelinating OLs (Barateiro and Fernandes, 2014; Coppi et al., 2015, 2013a; Szuchet et al., 2011). The initial stage of maturation presents a bipolar (or tripolar) morphology, typical of proliferating OPCs (Fumagalli et al., 2011). Several are the markers of precocious maturation stages, such as platelet-derived growth factor receptor a (PDGFa), nerve glial antigen 2 (NG2) or the OL transcription factor 2 (Olig2) (Ligon et al., 2006; Nishiyama et al., 2002; Pringle et al., 1992; Yu et al., 1994).

When OPCs start to differentiate in pre-OLs, secondary ramifications emerge from the soma and the expression of new molecular markers, typical of intermediate steps of maturation, is detected, such as O4 (Szuchet et al., 2011) and the recently deorphanized P2Y-like GPR17 receptor (Coppi et al., 2013b; Emery, 2010; Fumagalli et al., 2011; Lecca et al., 2008). During this phase, cells acquire the typical phenotype of postmitotic, but not yet myelinating, immature OLs characterized by a complex multipolar morphology (Back et al., 2001).

Finally, when OLs reach the fully mature, myelinating phase, they acquire a highly ramified profile and immunoreactivity for myelin specific structural proteins such as 2',3'-Cyclic-nucleotide-3'-phosphodiesterase (CNPase), myelin associated glycoprotein (MAG) and myelin basic protein (MBP) (Scolding et al., 1989; Zhang, 2001). Mature OLs synthesize large amounts of myelin, giving rise to multilamellar myelin sheaths that wrap and insulate neuronal axons which allow electrical isolation and saltatory conduction of electric impulses.

It is known that, during their maturation, oligodendroglial cells display different functional voltage-gated ion channels (Barres et al., 1990; Sontheimer

and Kettenmann, 1988; Williamson et al., 1997) including either inward or outward rectifying K^+ channels, Na^+ currents and different subtypes of Ca^{2+} channels (Verkhratsky et al., 1990) and the density of channels differs within age and region (Spitzer et al., 2019). Such a heterogeneity may therefore reflect different cellular states, where densities of ion channels define a particular cell function.

When OPCs first appear, i.e. at embryonic day 13 (E13) in the mouse, they have no detectable voltage-gated ion channels nor glutamate receptors and may be therefore considered in a naive state (Spitzer et al., 2019). The first ion channels detected are K_V and glutamate AMPA and/or Kainate receptors (AMPARs/KARs), at E18. OPCs with these properties are considered migrating cells because of the strong expression of migratory genes at this time point. The fraction of OPCs with detectable Na_V increases sharply around birth. It is conceivable that OPCs with high Na_V and K_V, and low AMPA/KAR, densities reflect a high proliferation state because (i) OPCs in S/G2/M phase have a higher density of Na_V than OPCs in G0/G1 phase (Spitzer et al., 2019), (ii) the higher the fraction of this type of OPC, the higher the proportion of OPCs in G2/M phase (Spitzer et al., 2019), (iii) proliferating 5-ethynyl-2-deoxyuridine (EdU)-positive OPCs show this pattern of ion channel expression (Clarke et al., 2012), (iv) this state of OPCs is the most prominent during the OPC recruitment phase (the period of highest proliferation) in myelin regeneration (Gautier et al., 2015). OPCs expressing Na_V, K_V, AMPA/KARs, and NMDARs are typically found throughout oligodendrogliogenesis during development, when myelin gene expression starts (Marques et al., 2018; Spitzer et al., 2019), and during the beginning of the differentiation phase of myelin regeneration (Gautier et al., 2015) and so it might reflect a ''primed'' OPC state for differentiation. Either K_V or AMPA/KAR channels were expressed in nearly all recorded postnatal OPCs, whereas, intriguingly, not all OPCs express Na_V or NMDARs, as their density reaches a maximum after the first postnatal week, when myelination starts, and then declines when myelination decays. The last state of OPC maturation

is distinguished by low Na_V density, lack of NMDARs and high AMPA/KAR density and is observed at a time when OPC cell-cycle time lengthens, differentiation genes are downregulated and senescent molecular signature genes appear. In this phase, OPCs differentiation potential declines and thus it can be considered a ''quiescent'' OPC state.

Among K^+ currents, OPCs show outward currents conductances mainly composed by component is represented by delayed rectifying K^+ currents (IK) (Sontheimer and Kettenmann, 1988) characterized by scarce time- and voltage-dependent inactivation and by a threshold for activation around -40 mV. They also express a transient outward K^+ current (IA), which is typically found in undifferentiated OPCs and presents a rapid time-dependent inactivation (approximately 50 ms) and a voltage-dependent inactivation at potentials from -40 and above (Gallo et al., 1996). A subpopulation (about 60%) of immature OPCs also express inward, tetrodotoxin-sensitive, Na^+ currents (I_{Na}) typically found in neurons, with a rapid time-dependent inactivation (less than 1 ms) and a current peak amplitude at about -10 mV (Kettenmann et al., 1991). I_{Na} is never observed in mature oligodendroglial stages, as previously reported by my research group (Coppi et al., 2013b) and others (Sontheimer et al., 1989). Of note, a subpopulation fraction of electrically excitable, spiking, $NG2^+$ OPCs, able to generate full action potentials when stimulated by depolarizing current injection, have been described in brain slices, but the functional role of this "electrically excitable" OPC subpopulation is still unknown (Káradóttir et al., 2008). Of note, single action potentials have also been detected in a minority of cultured OPCs (Barres et al., 1990).

During maturation, membrane outward K^+ conductance (both IK and IA) in OPC undergo a strong downregulation up to almost completely disappearance in mature OLs (Barres et al., 1990; Coppi et al., 2013a; Sontheimer and Kettenmann, 1988). In parallel with outward K^+ current downregulation, there is a gradual increase in the expression of inwardly rectifying K^+ currents (Kir), activated at potentials lower than -100 mV. Indeed,

Kir currents are the main conductance observed in mature OLs (Knutson et al., 1997). Among the mentioned currents, IK are crucially linked to cell cycle regulation and hence to myelin formation (Chittajallu et al., 2005) because of the following: (i) a downregulation of IK occurs as OL lineage cells mature (Barres et al., 1990; Sontheimer and Kettenmann, 1988) and (2) pharmacological block of IK induced by tetra-ethyl-ammonium (TEA) in cultured OPCs is sufficient to inhibit their proliferation and differentiation (Chittajallu et al., 2005; Coppi et al., 2013b; Gallo et al., 1996; Knutson et al., 1997). Hence, treatments aimed at modulating these currents may affect OL proliferation and myelination.

Steps and markers of oligondendroglial differentiation described above are observed not only in the brain but also in the spinal cord, where a significant fraction of OPCs also persists throughout adult life.

What is clear is that these changes in voltage-gated channels will have a profound effect on how OPCs sense neuronal activity and on the effect neuronal inputs will have on OPCs (Coppi et al., 2013a; Spitzer et al., 2019).

Therefore, neurotransmitters, cytokines and growth factors have been shown to regulate glutamate receptor expression in OPCs (Gallo et al., 1994; Lundgaard et al., 2013; Malerba et al., 2015; Spitzer et al., 2019; Stellwagen and Malenka, 2006; Zonouzi et al., 2011). Accordingly, a combination of G-protein coupled receptors, growth factors, and cytokines may modify K^+ current expression. This heterogeneity in physiological properties may cause differences in the myelination potential of OPCs and implicate distinct functions or cell states (Fig. 9).

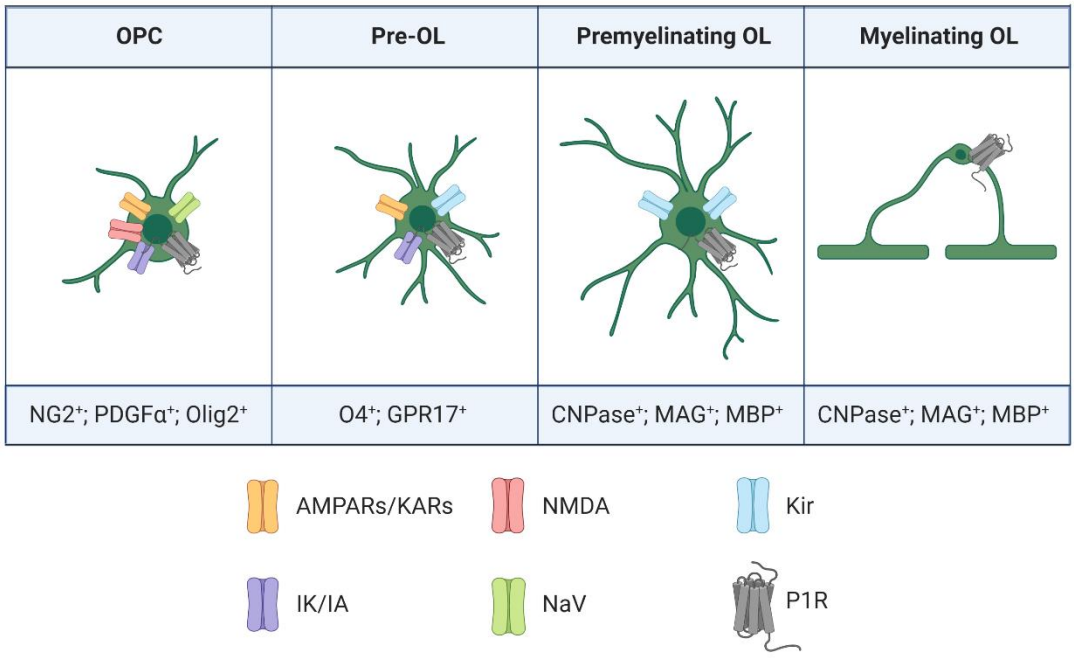

Figure 9. ***Schematic representation of morphological and antigen/channel expression changes during oligodendrogliogenesis.*** A typical oligodendrocyte precursor cell (OPC) is positive to the antigens: nerve glial antigen 2 ($NG2^+$), platelet-derived growth factor alpha (PDGFa+) and to the transcription factor Olig2 (Olig2+) and express glutamate AMPA and/or kainate receptors (AMPARs/KARs) and voltage-dependent Na+ (Nav) and K+ (IK/IA) channels. A typical pre-Oligodendrocyte (Pre-OL) is positive to the markers: oligodendrocyte 4 (O4+), the purinergic-like receptor GPR17 (GPR17+) and express AMPARs/KARs, inward-rectifier potassium channels (Kir) and IK/IA channels. Premyelinating OLs and myelinating OLs are positive to the antigens: 2′,3′-Cyclic-nucleotide-3′-phosphodiesterase (CNPase+), myelin associated glycoprotein (MAG+) and myelin basic protein (MBP+) and express Kir channels. During oligodendrogliogenesis P1Rs are expressed at all maturation stages.

5.1.1. Role of adenosine in oligodendrocyte differentiation

All P1 receptors are expressed at all maturational stages of oligodendroglial cells (Fields, 2004; Stevens et al., 2002) and exert a key role in cell development. Furthermore, the expression by OLs of the equilibrative nucleoside transporters ENT1 and ENT2, as well as adenosine degrading enzymes, such as adenosine deaminase and adenosine kinase, has been demonstrated (González-Fernández et al., 2014), supporting the notion that purinergic signalling exerts a prominent role in these cells (Burnstock et al., 2011). Indeed, it was demonstrated that adenosine can affect numerous OPC functions such as migration, proliferation and maturation (Coppi et al., 2015, 2013a, 2013b;

Fields, 2004; Fields and Burnstock, 2006; Stevens et al., 2002), with distinct effects mediated by different receptor subtypes, as described below.

5.1.1.1. A_1Rs in oligodendrogliogenesis

Exogenous adenosine added to OPCs cultured in the presence of the mitogen PDGF, leads to a concentration-dependent reduction of cell proliferation and promotes differentiation towards pre-myelinating oligodendrocytes, an effect that is mainly mediated by A_1Rs (Stevens et al., 2002). Furthermore, tonic electrical stimulation of co-cultures of OPCs with dorsal root ganglion neurons also promotes myelination by increasing the number of MBP^+ cells (Stevens et al., 2002), an effect blocked by a cocktail of A_1R, A_{2A}R and A_3R antagonists, suggesting that endogenous adenosine released in response to impulse activity promotes oligodendrocyte development and myelination (Stevens et al., 2002). In addition, A_1R agonists have been reported to stimulate OPC migration (Othman et al., 2003). On these basis, it was proposed that A_1Rs on OPCs prompt myelination thus offering new approaches for the treatment of demyelinating diseases of the CNS, such as MS. In accordance, $A_1R^{-/-}$ mice developed more severe EAE with worsened demyelination, axonal injury, and enhanced neuroinflammation and activation of microglia/macrophages (Tsutsui et al., 2004). Furthermore, A_1Rs promotes myelin repair by recruiting endogenous progenitor cells in an experimental model of optic nerve demyelination (Asghari et al., 2013) and, when activated on astrocytes, exert immunosuppressive properties (G. Liu et al., 2018).

Such protective effects, however, are at variance from what has been described in in vivo neonatal rats, where the treatment with A_1R agonists reduces white and gray matter volume, induces ventriculomegaly (Turner et al., 2002) and decreases the expression of MBP, similarly to what observed in neonatal rats reared in hypoxia (Ment et al., 1998). Ventriculomegaly was also observed in mice lacking the enzyme adenosine deaminase which degrades adenosine (Turner et al., 2003). Moreover, hypoxia-induced periventricular white matter injury (PWMI, a form of brain injury present in preterm infants) was

prevented in $A_1R^{-/-}$ mice (Turner et al., 2003). These data support the notion that adenosine, acting on A_1Rs, mediates hypoxia-induced brain injury and ventriculomegaly during early postnatal development. Such an effect could be attributed to the fact that adenosine, which is released in huge amounts during hypoxic-ischemic conditions (Latini and Pedata, 2001), activates A_1Rs leading to premature differentiation and reduced proliferation of oligodendroglia precursors. Indeed, studies on OPCs and pre-OLs in hypoxic conditions, when increased glutamate outflow impairs neuronal functions (Rossi et al., 2000) and synaptic transmission (Colotta et al., 2012), revealed a reduced proliferation and an accelerated maturation, as demonstrated by the increased expression of the cell cycle regulatory proteins p27 (Kip1) and phospho-cdc2 (Akundi and Rivkees, 2009). This series of events would lead to a reduced number of OLs available for myelination, thus contributing to PWMI (Rivkees and Wendler, 2011). So, strategies aimed at stimulating OPC proliferation in neonatal hypoxia/ischemia may be of value to prevent PWMI.

Accordingly, Cao and co-workers (Cao et al., 2019) found that OLs pre-treated with 100 μM caffeine or the A_1 antagonist DPCPX (100 nM) during hypoxia showed a significant reduction in A_1R and Olig2 expression, at early stages, and a decreased CNPase expression, at later stages of hypoxia. In addition, they demonstrated that either hypoxia or adenosine treatment induced significant elevation in resting $[Ca^{2+}]_i$, which was restored to normal levels when cells were treated with caffeine or DPCPX. During hypoxia, adenosine increase leads to A_1R activation which resulted in excessive Ca^{2+} release from intracellular stores (Annunziato et al., 2013; Gao et al., 2014), a condition that is considered to initiate cell injury (Cao et al., 2019) (Fig. 10).

5.1.1.2. A_{2A}Rs in oligodendrogliogenesis

The first functional characterization of the adenosine A_{2A}R subtype in OPCs has been reported by our group of research (Coppi et al., 2013a). We demonstrated that the selective A_{2A}R agonist CGS21680 inhibits IK currents in cultured OPCs and delays in vitro OPC differentiation since it increases the

percentage of $NG2^+$ immature OPCs and reduces $O4^+$ pre-OLs and MAG+ mature OLs along 12 days of cell culture, without affecting neither cell viability nor proliferation (Coppi et al., 2013a). These effects were completely prevented in the presence of the selective $A_{2A}R$ antagonist SCH58261 (Coppi et al., 2013a). Tetraethylammonium (TEA), at 3 mM concentration which blocks sustained IK but not transient IA currents in cultured OPCs, mimics and occludes the effect of the $A_{2A}R$ agonist on membrane currents, confirming that this purinergic receptor subtype electively affects IK in cultured OPC (Coppi et al., 2013a). In keeping with data demonstrating that IK inhibition impairs proliferation and maturation of cultured OPCs (Attali et al., 1997; Coppi et al., 2013b; Gallo et al., 1996) and blocks myelin deposition in the embryonic spinal cord (Shrager and Novakovic, 1995), it appears that $A_{2A}R$ stimulation inhibits OPC differentiation by reducing IK currents. In line with this assumption is the observation that selective activation GPR17, a Gi-coupled P2Y-like receptor, enhances TEA-sensitive IK and improves OPC differentiation (Coppi et al., 2013b).

Recently, Fontenas and colleagues (Fontenas et al., 2019) demonstrated that the $A_{2A}R$ antagonist SCH-58261 induced ectopic OPC migration from motor exit point in transition zones in zebrafish larvae, an effect that is not shared by antagonists at the other adenosine receptor subtype .

A pathological condition associated with defects in cell metabolism and OPC maturation is the Niemann-Pick type C 1 (NPC) disease, an autosomal recessive and progressive neurovisceral disorder characterized by intracellular cholesterol accumulation and myelin defects (Kodachi et al., 2017; Walterfang et al., 2010). De Nuccio and colleagues observed that in primary cultures of OPCs exposed to a cholesterol transport inhibitor (U18666a), used to induce the NPC1-like phenotype in vitro, $A_{2A}R$ expression was significantly decreased whereas treatment with the $A_{2A}R$ agonist CGS21680 triggered a protective effect by reducing cholesterol accumulation and mitochondrial membrane potential (mMP) alterations in U18666a-treated OPCs (De Nuccio

et al., 2019). Consistent with data from Coppi et al., the same study demonstrates that CGS21680 induced a decrease in the percentage of $O4^+$, $O1^+$ and MBP^+ in control OPCs (Coppi et al., 2013b; De Nuccio et al., 2019). In contrast, after 48 h of U18666a treatment, CGS21680 overcame the maturation arrest induced by the compound, even when $A_{2A}R$ stimulation occurred 24 h after U18666a exposure. Finally, the same study also demonstrated that protein-kinase A (PKA) activation is responsible for the $A_{2A}R$-dependent effect on cholesterol accumulation since the PKA inhibitor KT5720, but not the extracellular signal-regulated kinases 1/2 (ERK1/2) inhibitor PD98059, prevented the cholesterol redistribution induced by CGS21680 in NPC-OPC. The dual effect of CGS21680 on OPC differentiation, arresting OLs maturation in control cultures and promoting differentiation in U18666a-treated cultures, is in keeping with differential effects by CGS21680 previously reported in a model of Huntington's disease (HD), where the compound induces opposite effects in the striatum of Huntington versus wild-type mice (Martire et al., 2007).

However, other intracellular pathways, in addition to IK block, could contribute to the $A_{2A}R$-mediated inhibition of OPC differentiation. OPCs also express the tyrosine kinase fibroblast growth factor (FGF) receptor whose activation promotes cell proliferation and inhibits the expression of myelin components (Besnard et al., 1989). As an example, in PC12 cells (a cell line that was confirmed to express the $A_{2A}R$ and FGFRs), the simultaneous activation of both $A_{2A}R$ and FGF receptors by robust activation of the mitogen activated protein kinase (MAPK/ERK) pathway, brings to increased differentiation and neurite extension (Flajolet et al., 2008). It is possible that a crosstalk between $A_{2A}Rs$ and FGF receptors regulates cell maturation also in OPCs.

Of note, upregulation of $A_{2A}R$ expression has been observed in cerebral white matter of patients with secondary progressive MS and a higher density of brain $A_{2A}R$ appeared to correlate with higher disability scale scores in MS patients (Rissanen et al., 2013). On these bases, it has been hypothesized that

$A_{2A}R$ upregulation on brain cells is associated with disease progression. In agreement, in a mouse model of MS, the experimental autoimmune encephalomyelitis (EAE), $A_{2A}R$ antagonists protected from disease development (Mills et al., 2012), suggesting that activation of $A_{2A}Rs$ glial and neuronal cells is responsible for EAE development in mice. Moreover, in a rat model of focal brain ischemia (by middle cerebral artery occlusion: MCAo), systemic administration of $A_{2A}R$ antagonists after ischemia prevented the activation of JNK mitogen activated kinase (Melani et al., 2009) and subsequent activation cascade of caspase3 and the pro-apoptotic regulator DP5 (Yin et al., 2005), involved in OL death (Howe et al., 2004; Jurewicz et al., 2006). Accordingly, selective $A_{2A}R$ antagonists also prevented myelin disorganization in the basal nuclei and striatum of MCAo rats (Melani et al., 2009). So, it emerges from above data that $A_{2A}R$ activation is deleterious in demyelinating disorders. Moreover, in a rat model of focal brain ischemia (by middle cerebral artery occlusion: MCAo), the myelin damage inflicted to the striatum by the ischemic insult is significantly prevented by the $A_{2A}R$ antagonist SCH58261 that reduced the activation of JNK mitogen activated kinase in oligodendrocytes and subsequent activation of caspase3-mediated oligodendrocyte cell death (Melani et al., 2009).

In keeping with these data, it can be concluded that the activation of $A_{2A}Rs$ by adenosine released during a demyelinating insult contributes to brain damage by hampering OPC maturation and myelin deposition. Such a role might appear in contrast with the observation that A_{2A} R agonists proved protective in EAE models by decreasing immune cell infiltration and lymphocyte Th1 cell activation (Y. Liu et al., 2018) . Furthermore, genetic ablation of both central and peripheral $A_{2A}Rs$ exacerbates brain damage and neuroinflammation in EAE (Ingwersen et al., 2016; Yao et al., 2012). Indeed, $A_{2A}Rs$ expressed on peripheral leucocytes are known to exert important anti-inflammatory effects, i.e. by reducing adhesion cell factor production and neutrophil activation (Sitkovsky et al., 2004). Thus, genetic ablation of adenosine $A_{2A}Rs$ on blood cells exacerbates leucocyte infiltration, neuroinflammation and brain damage

in a model of chronic inflammation such as EAE (see: Pedata et al., 2014). It appears that, beside disadvantageous central effects on OPC differentiation, $A_{2A}R$ stimulation may also alleviate neuroinflammation by peripheral mechanisms, thus complicating the role of this endogenous nucleoside in neurodegenerative diseases. Successive studies contributed to elucidate the multifaceted role played by $A_{2A}Rs$ in EAE. Ingwersen et al. demonstrated that $A_{2A}Rs$ were upregulated predominantly on T cells and macrophages/microglia within the inflamed tissue and preventive EAE treatment with $A_{2A}R$-specific agonist inhibited myelin-specific T cell proliferation ex vivo and ameliorated disease, while application of the same agonist after disease onset exacerbated non-remitting EAE progression and tissue damage (Ingwersen et al., 2016). Similarly, Chen and co-workers (Chen et al., 2019) demonstrated that the administration of the selective $A_{2A}R$ antagonist SCH58261 at 11-28 days post-immunization with MOG prevented neurological deficits and reduced local infiltration and demyelination. By contrast, the same treatment was ineffective when administered at the beginning of the onset of EAE (i.e., 1-10 after immunization). So, it appears that, while providing anti-inflammatory effects on T cells and thus protection at early stages, $A_{2A}R$ seems to play a detrimental role during later stages of the disease and may thus contribute to sustained tissue damage within the inflamed CNS. Hence, the identification of the effective therapeutic window to optimize the beneficial effects of $A_{2A}R$ antagonists is of crucial importance to support SCH58261 as a candidate for the treatment of MS in human (for a review see: (Rajasundaram, 2018)). (Fig. 10)

5.1.1.3. $A_{2B}Rs$ in oligodendrogliogenesis

The functional role of the $A_{2B}R$ in OLs has not yet been clarified. Among adenosine receptors, the $A_{2B}R$ is the least studied and still remains the most enigmatic adenosine receptor subtype because of the relatively low potency of adenosine at this receptor (EC_{50} value of 24 μM) (Burnstock et al., 2011) and the very few specific agonists that have been described so far. Therefore, Wei

and co-workers, who demonstrate that pharmacological blockade of $A_{2B}R$ with selective antagonists or receptor knock out the in a rodent model of EAE, protects from myelin disruption and neurological impairment due to this pathological condition (Wei et al., 2013). However, unless the lack of preclinical studies where $A_{2B}R$ agonists are administered in EAE mice up to date, it cannot be ignored that the $A_{2B}R$ subtype shares with the $A_{2A}R$ the anti-inflammatory impact in many different pathologies (Dettori et al., 2020; Eckle et al., 2008; Pedata et al., 2016; Yang et al., 2006) so, possible side effects could arise in MS patients treated with $A_{2B}R$ blockers (Fig. 10).

5.1.1.4. A_3Rs in oligodendrocyte survival

No data are present in the literature about the effect/s of A_3Rs on oligodendrocyte differentiation. However, Results obtained by Gonzalez-Fernandez and colleagues (González-Fernández et al., 2014) demonstrate that the A_3R agonist 2-CI-IB-MECA induces apoptosis of cultured $O4^+$ OLs isolated from rat optic nerve through the activation of Bax and Puma proapoptotic proteins. Furthermore, incubation of ex vivo preparations of optic nerve with adenosine or 2-CI-IB-MECA induces OL damage and myelin loss, effects prevented by the A_3R antagonist MRS220 (González-Fernández et al., 2014). Moreover MRS220 also prevented OL damage and myelin loss in the optic nerve exposed to in vitro ischemic like conditions, i.e. oxygen–glucose deprivation (González-Fernández et al., 2014). Thus, data suggest that adenosine, via activation of A_3Rs, triggers OL death and contributes to white matter ischemic damage (Fig. 10).

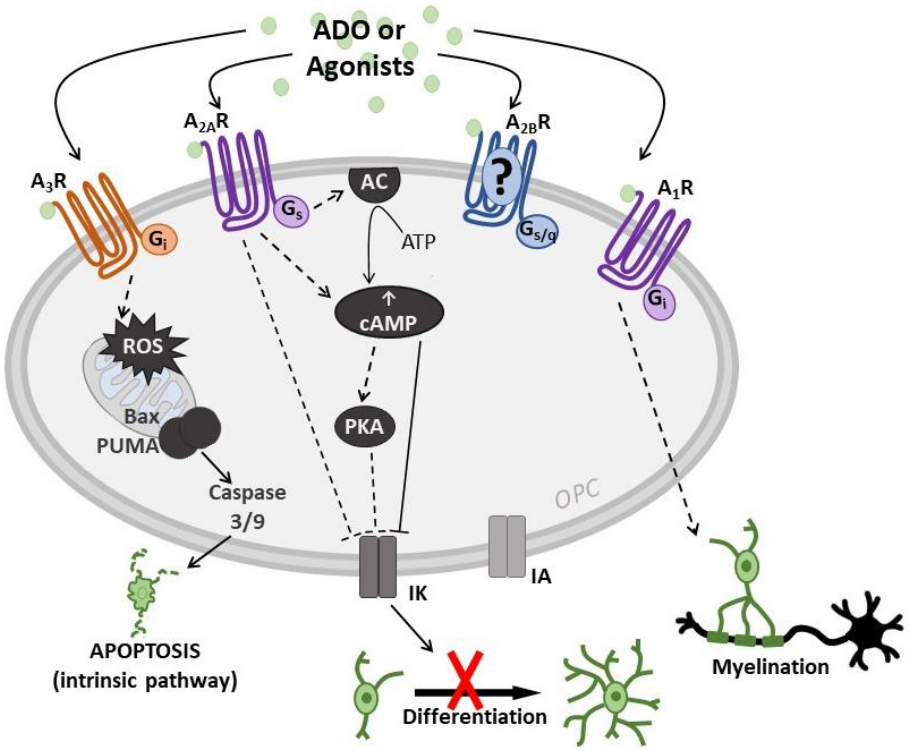

Figure 10. ***Effects of A_1, A_{2A} and A_3 receptor (A_1R, $A_{2A}R$ and A_3R) activation on OPCs and intracellular pathways involved.*** The activation of A_1Rs by adenosine (ADO) or other receptor agonists facilitates myelin deposition by Gi coupling. The stimulation of G_s-coupled receptors A_{2A}R leads to adenylyl cyclase (AC) activation causing an increase in intracellular cAMP, which, in turn, closes IK channels and inhibits OPC differentiation possibly by a mechanism involving protein kinase A (PKA) activation. The activation of A_3Rs induces OPC apoptosis by activating the intrinsic pathway through reactive oxygen species (ROS) production and following activation of Bax and PUMA.

5.2. *Multiple sclerosis*

Multiple sclerosis (MS) is a chronic disease of the CNS that mainly presents in young adults, creating a substantial health-care burden at individual, family and community levels (Ontaneda et al., 2017). MS is primarily considered to be an immune-mediated disease and is characterized by focal areas of inflammatory demyelination that spread in the brain and in the spinal cord with time, driven by an infiltration of lymphocytes. In according, the first years of relapsing–remitting MS, the form of MS that many individuals with the disease initially develop, are characterized by recurrent episodes of neurological dysfunction from which the individual usually recovers (Compston and Coles, 2002), and the frequency of such episodes can be even

markedly reduced by treatments that modulate or suppress the immune system (Comi et al., 2017). The classic pathological hallmark of MS was long considered to be the presence of focal white matter demyelinating lesions. However, pathological changes are also detectable in normal-appearing white matter, as well as in the CNS grey matter, with the presence of focal grey matter lesions and grey matter atrophy (Calabrese et al., 2015; Filippi et al., 2012). Axonal damage and diffuse microglial activation dominate MS-related pathological changes and are accompanied by progressive, mostly untreatable, accumulation of neurological disability affecting many functional domains from mobility to cognition. Current available MS therapies target immune modulation with some efficacy, however, concomitantly with adverse side effects (English and Aloi, 2015). Damaged OLs no longer generate myelin and remyelination requires generation of new mature OL from the differentiation of OPCs (Dawson et al., 2003). Therefore, these cellular resources are especially active after demyelinating episodes in early phases of MS, indeed OPCs actively proliferate and migrate in the lesioned area (Levine et al., 2001). Efficient remyelination is accomplished when new OLs reinvest nude neuronal axons and restoring the normal properties of impulse conduction. However, when the disease progresses, this fundamental process fails (Levine et al., 2001). Multiple causes seem to contribute to such transient decline, including the failure of OPCs to differentiate and enwrap the vulnerable neuronal axons; for example, the observation that OPCs are present in MS lesions but fail to differentiate into mature OLs (Chang et al., 2000; Levine et al., 2001) suggests that the remyelination process is blocked at a premyelinating stage in demyelinating lesions. Unfortunately, the precise mechanisms underlying cognitive impairment in MS are still largely unknown, and efficacious treatments for this aspect of the disease are lacking. Pathological changes in CNS white matter and specific neuronal grey matter structures could play a crucial role in the pathogenesis of MS-related cognitive impairment (DeLuca et al., 2015). Alterations in the physiological crosstalk between the immune and nervous systems might also have a role, as such

crosstalk modulates synaptic transmission and the induction of synaptic plasticity in the CNS (Di Filippo et al., 2008).

5.2.1. S1P as a target for MS

S1P is a soluble signalling molecule involved in a wide range of immunological, cardiovascular, and neurological processes through interaction with five members of a G-protein-coupled receptor family (S1PR1-5) (Rosen et al., 2009). S1P levels are primarily regulated by sphingosine kinase 1 and 2 (SphK1 and SphK2), and S1P-degrading enzymes, such as S1P phosphatases (SPPs), that convert S1P to sphingosine, and S1P lyase, which terminally cleaves this sphingolipid (Brinkmann et al., 2002). Furthermore, SphK1 and SphK2 sequence differences arise from alternative splicing, which affects their differential subcellular localization and biochemical properties (Alemany et al., 2007); therefore, the S1P pools synthesized by individual kinases could play different roles in each cell. In particular, S1P synthesized by SphK1, localised in the cytoplasm and endoplasmic reticulum, can be transported out of the cell and exert mitogenic and anti-apoptotic effects in an autocrine manner (O'Sullivan and Dev, 2017). S1P receptors were originally described as endothelial differentiation genes (edg) and build a subclass of G protein-coupled lipid receptors, which are most homologous to the lysophosphatidic acid (LPA) receptors (Binder et al., 2015). So far, 5 subtypes of S1P receptors have been identified, denoted S1P1–5, that bind S1P with high affinity (Kihara et al., 2014) with binding constants ranging from 1 to 10 nM, except for S1P4, which has a ten-fold lower affinity (Mandala et al., 2002).

S1PR-mediated signalling is essential for development of the neural tube and vascular system during embryogenesis (Mizugishi et al., 2005). In the mature CNS, S1P regulates the activation of neuronal progenitor cells and their migration to possible lesions (Blanc et al., 2015). S1P-dependent signalling influences the synthesis of neurotrophic factors and pro-inflammatory cytokines, as well as cellular communication (Wollny et al., 2017).

Four of the five S1P receptors (S1PRS), (S1P1R, S1P2R, S1P3R, and S1P5R) are expressed in both neurons and glial cells within the CNS, where S1P1R is the most abundant (Dev et al., 2008; Fig. 11). The level of expression of S1P1R and S1P3R changes over a lifespan, under pathological conditions, and depends on the environmental milieu (Watson et al., 2010). Mice with a S1P1R receptor deletion are characterized by abnormal formation of the neural tube and blood vessel failure that leads to embryonic death; however, mortality at the embryonic stage is not observed upon deletion of the other four S1PRs (Mizugishi et al., 2005).

A disrupted balance between S1P and ceramide has been documented in AD patients and reported in other neurodegenerative diseases. Activity of SphK1s and level of S1P decline in brain regions that are affected relatively early in AD (Couttas et al., 2014; He et al., 2010) increase in ceramide concentration in the cerebrospinal fluid and serum is suggested to be an appropriate biomarker of AD (He et al., 2010; Satoi et al., 2005). It was also reported that S1P concentration exhibits a strong inverse correlation with tissue Aβ levels and hyperphosphorylation of tau protein in post-mortem brain from AD patients (He et al., 2010). In addition, endogenously released Aβ peptides induced significant inhibition of both expression and activity of SphKs in PC12 cells transfected with the human gene for Aβ precursor protein (Gassowska et al., 2014); moreover, another study demonstrated decreased SphK1 expression under Aβ peptide toxicity in PC12 cells (Cieślik et al., 2015). Importantly, small interfering RNA knockdown of SphK1 increases Aβ accumulation and decreases learning and memory function in an AD mouse model, revealing SphK1 modulation as a potential target for AD treatment (Zhang et al., 2013).

5.2.2. Fingolimod

Fingolimod (FTY720; Gilenya®, Novartis), a sphingosine analogue, was approved as the first oral MS therapy by the United States Food and Drug Administration (FDA), the European Union, and several other countries (Chun and Brinkmann, 2011; Fig. 11). In 1995, Fujita synthesized FTY720 (2-

amino-2[2-(4-octylphenyl)ethyl]-1,3-propanediol) using the natural compound myriocin (Adachi et al., 1995). Myriocin was previously isolated by the same group from the culture broth of *Isaria sinclairii*, the imperfect or asexual stage of the genus *Cordyceps sinclarii* (cordycipitaceae), a subfamily of parasitic fungi (Zhou et al., 2009). Remarkably, extract and powder from the near relative *Cordyceps sinensis* has been widely used in Traditional Chinese Medicine for its energy boosting effect and to grant eternal youth (Zhou et al., 2009). FTY720 turned out to be an even more potent immunosuppressant when tested in vitro in a mouse allogenic mixed lymphocyte reaction assay, and in vivo in different animal models (Fujita et al., 1996; Suzuki et al., 1996; Yanagawa et al., 1998). Indeed, FTY720 was described as an immunosuppressant 10–100 times more potent than cyclosporine A and its main immunomodulatory mechanism of action is based on its effect on lymphocyte homing (Fujita et al., 1996; Yanagawa et al., 1998).

5.2.2.1. Fingolimod modulates S1P pathway

Furthermore, FTY720 is a pro-drug which requires SphK to become active; it was demonstrated that both enzymes can phosphorylate FTY720 in vitro (Billich et al., 2003). However, SphK2 is 30-fold more efficient due to a lower Km value of FTY720 for SphK2 compared to SphK1 (Billich et al., 2003). Indeed, SphK2 is the only enzyme which activates FTY720 in vivo, since only SphK2 knockout mice are resistant to FTY720-induced lymphopenia (Zemann et al., 2006) and lack FTY720-mediated protection from disease symptoms in experimental autoimmune encephalomyelitis (EAE), a widely used animal model for multiple sclerosis (Imeri et al., 2016). FTY720, but not FTY720-P, acts also as a direct inhibitor of SphK1, but very high concentrations (50 mM) are needed to achieve 50% inhibition (Tonelli et al., 2010; Vessey et al., 2007). As a pharmacological target with oncogenic potential, SphK1 is of interest for cancer therapy (Shida et al., 2008). Considering the toxicity profile of FTY720 at 0.5 mg per day in patients, however, it is unrealistic to believe that such high doses can be tolerated. Nevertheless, numerous preclinical studies have

shown pro-apoptotic and antitumor effects of FTY720 with tumour cell lines in vitro and in tumour models in mice, which could be partly attributed to inhibition of SphK1 (Pchejetski et al., 2010). Therefore, it was found that FTY-720-P inhibit S1P lyase, the enzyme responsible for irreversible S1P degradation, activity in vitro and in vivo (Bandhuvula et al., 2005; Park et al., 2014). Since FTY720-P mimics S1P in structure, not surprisingly, that also binds to its receptors (Brinkmann et al., 2002; Mandala et al., 2002). In detail, FTY720-P binds with similar affinity as S1P to S1P1, S1P3, and S1P5, but shows much better binding to S1P4 than S1P (6 nM vs 90 nM), even if it is not a ligand for S1P2 (Mandala et al., 2002). Due to the diversity of S1P receptor subtypes with their distinct function and ubiquitous expression in the body, multiple effects can be expected from using FTY720, which may either have therapeutic benefit or cause adverse events (Kihara et al., 2014; O'Sullivan and Dev, 2017). As outlined above, because of FTY720-P binds and activates S1P receptor subtypes, except for S1P2, "active" FTY720 is pharmacologically considered an unselective S1P receptor agonist (Brinkmann, 2007; Brinkmann et al., 2002; Mandala et al., 2002). Moreover, it causes sustained desensitization of the S1P1-mediated signalling pathway by inducing receptor internalization and degradation, which on the cellular level results in functional antagonism (Brinkmann et al., 2004). This effect of FTY720 on S1P1 is unique and not seen with the endogenous ligand S1P, which also internalizes S1P1 upon binding but then dissociates in endosomes and the receptor recycles back to the plasma membrane (Myat et al., 2007). Similarly, S1P3, S1P4 and S1P5 are also internalized upon FTY720-P binding and then redistribute back to the cell surface (Brinkmann et al., 2004). Particularly, downregulation of S1P1 on T cells is supposed to account for the immunosuppressive effect of FTY720, whereas downregulation of S1P1 in other cell types, notably in endothelial cells, is likely responsible for the adverse events observed under long-term FTY720 treatment (Brinkmann, 2007). The agonistic effect of FTY720 on S1P3, S1P4 and S1P5 may account for additional biological effects with unknown consequences as outlined below. Since S1P1 is ubiquitously expressed in

almost every cell type, its downregulation by prolonged FTY720 treatment is expected to have multiple consequences on cellular responses and tissue homeostasis (Brinkmann et al., 2004). Therefore, S1P1 activation improves the endothelial barrier function, whereas S1P1 antagonism, notably also by prolonged FTY720 treatment, disrupts it, thereby increasing permeability and vascular leakage (Wilkerson and Argraves, 2014).

FTY720-P has an EC_{50} value of 7 to 10 nM for S1P3, which is comparable to the endogenous ligand S1P; however, its efficacy reached only 50% of S1P, suggesting a partial agonistic effect (Riddy et al., 2012). By definition, a partial agonist in the presence of a full agonist produces an antagonistic output. This could mean that in vivo, FTY720 can also antagonize S1P3 signalling rather than stimulate it, depending on the local S1P concentration.

On the other hand, the role of S1P4 in physiological processes is still poorly understood and therefore the effects of FTY720 mediated by S1P4 are unclear. S1P and FTY720-P associate with S1P4 with binding constants of 95 nM and 6 nM, respectively, which means that FTY720 is a much better ligand for this receptor than the endogenous ligand (Mandala et al., 2002). Therefore, S1P4 expression is restricted in the body and mainly found in lymphocytes and tissues of the immune and hematopoietic system (Gräler et al., 1998).

Finally, the S1P5 receptor was originally cloned as rat nerve growth factor-regulated G protein-coupled receptor Nrg-1 and later found to be identical to S1P5 (Glickman et al., 1999). It is predominantly expressed in the brain and spleen (Im et al., 2000; Malek et al., 2001) and in these tissues, it is further concentrated in OLs and natural killer cells (O'Sullivan and Dev, 2017). FTY720-P and S1P bind to S1P5 with equally high affinity. Moreover, S1P5 is also expressed on brain microcapillary endothelial cells where it contributes to the blood-brain barrier function and maintains the immunoquiescent state of brain endothelial cells (van Doorn et al., 2012).

In the last few years, several second-generation compounds with structural similarity to the FTY720 prodrug backbone, such as KRP203, CS-0777, and

RPC-1063, were synthesized and used in clinical trials; these S1PR modulators show higher selectivity for S1P1R than S1P3R (O'Sullivan and Dev, 2017). Therefore, recently, FDA has approved Siponimod (Mayzent®; Novartis, approved in march 2019) and Ozanimod (Zeposia®; Celgene Corporation, approved on march 2020) as oral treatments for relapsing forms of MS (Fda and Cder, 2020, 2019). Both are a highly selective S1PR1 and S1PR5 (Pan et al., 2013; Sørensen, 2016) and, as FTY720, they limit the capacity of lymphocytes to egress from peripheral lymphoid organs (Pan et al., 2013; Scott et al., 2016). In addition, FTY720 has reached clinical trials for other nervous system diseases, like amyotrophic lateral sclerosis (ALS), acute stroke, Rett syndrome, glioblastoma, and schizophrenia. Its potential utility has also been demonstrated in numerous in vitro and in vivo models of neurological disorders, like spinal cord injury, Huntington's disease, epilepsy, and toxicity of Aβ (O'Sullivan and Dev, 2017).

On the other hand, patients with MS undergoing long-term treatment with FTY720 showed reduced brain volume loss, reduced number of relapses, and a significantly slower progression of disability suggesting that FTY720 has also a neuroprotective properties (De Stefano et al., 2017). Patients treated with FTY720, might be more susceptible to serious infections, such as disseminated or CNS herpetic infection, because of reduced number of circulating lymphocytes (Cohen et al., 2010). The above side effects determine some limitations with FTY720 therapy to patients with cardiovascular and immune risk factor, especially in patients with diagnosed immunodeficiency syndrome (Yoshii et al., 2017).

The therapeutic effect of FTY720 in MS and its animal model experimental autoimmune encephalomyelitis (EAE) is attributed to the downregulation of S1P1 on lymphocytes resulting in their retention within lymph nodes (Balatoni et al., 2007; Brinkmann, 2007; Brinkmann et al., 2002; Mandala et al., 2002; Matloubian et al., 2004). In addition, there is also evidence supporting the concept of anti-inflammatory, glioprotective and neuroprotective actions of

S1PR modulators in the CNS (Choi et al., 2011; Kim et al., 2011; Soliven et al., 2011).

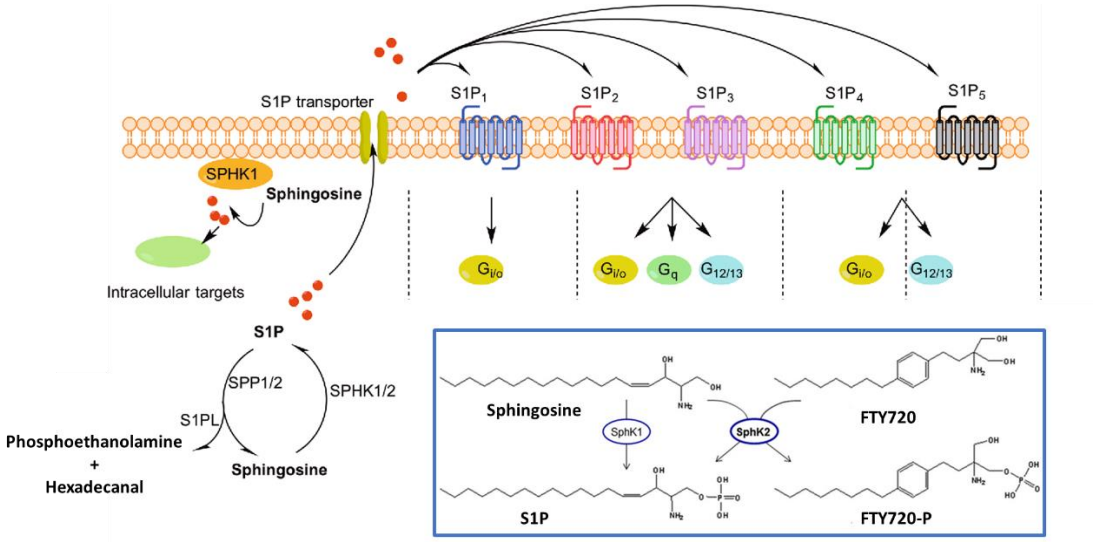

Figure 11. ***S1P and S1P signalling pathways FTY720.*** S1P is generated intracellularly from the phosphorylation of sphingosine by sphingosine kinases (SphK1 and SphK2). S1P propagates its signals by interacting with its intracellular targets or is transported extracellularly to activate its cell surface receptors (S1PR1-5). Intracellular S1P is recycled into sphingosine by S1P-specific ER phosphatases (SPP1 and SPP2) or irreversibly degraded by S1P lyase (S1PL). The S1PRs are coupled to different G proteins ($G_{i/o}$, G_q, and $G_{12/13}$) to regulate downstream biological responses. Fingolimod (FTY720) shows high analogy to sphingosine and is phosphorylated by sphingosine kinases, mainly SphK2, which is the predominant SphK isoform in the brain. Fingolimod is a prodrug of fingolimod phosphate that can signal via S1P receptors and activate intracellular targets of S1P (Modified from: Brunkhorst et al., 2014; Tsai and Han, 2016).

5.2.2.2. Fingolimod in oligodendrogliogenesis

S1P1-5 are found in oligodendroglial cells, where they regulate several processes, ranging from cell proliferation and maturation to branches elongation (Jaillard et al., 2005; Jung et al., 2007; Miron et al., 2008). Mature OLs express S1P5 and at lesser extent S1P1 S1P2 and S1P3, whereas OPCs express at a higher level S1P1 than S1P2, S1P3 and S1P5 (Jung et al., 2007; Novgorodov et al., 2007; Yu et al., 2004).

In vitro studies have demonstrated that FTY720-P regulates the survival, differentiation and process dynamics of cultured rodent and human OL lineage cells (Coelho et al., 2007; Jung et al., 2007; Miron et al., 2008). Furthermore, it has been demonstrated that treatment of mice with FTY720 protects against acute cuprizone-induced OL injury, demyelination and

axonal loss without promoting remyelination in this model (Kataoka et al., 2005; Rothhammer et al., 2017). The protective effect of FTY720 in the cuprizone model may be mediated not only by direct actions on S1PR on OLs, but also by indirect or antinflammatory actions on astrocytes and microglia (Kim et al., 2011).

Moreover, FTY720-P, through S1P5, triggers two distinct functional responses depending on the OL developmental stage; it leads to process retraction in pre-OLs, whereas it increases the survival of mature cells (Jaillard et al., 2005). In addition, migration of OPCs, which normally migrate over considerable distances during brain development, is inhibited by S1P5 activation (Novgorodov et al., 2007). FTY720 was also shown to protect human OLs from apoptosis induced by serum and glucose deprivation, suggesting a neuroprotective effect by activating S1P5 (Miron et al., 2008). In agreement, it was demonstrated that also Siponimod can modulate glial cell function and attenuate demyelination (O'Sullivan et al., 2016).

6. Role of adenosine A_3Rs in pain

Pain control is a vast, unmet medical need with a high societal cost impact (Goldberg and McGee, 2011). Current treatments (opioids, non-steroidal anti-inflammatory drugs, antidepressants or anticonvulsants) are frequently inadequate or associated with adverse side effect (Goldberg and McGee, 2011; Maloy et al., 2014; Pizzo and Clark, 2012). Therefore, new therapeutics for managing patient pain are being developed.

Several early electrophysiological studies reported that adenosine and its analogues inhibit Ca^{2+}-dependent plateau potentials and Ca_V activation in isolated rat DRG neurons (B. Y. A. C. Dolphin et al., 1986; Gross et al., 1989; MacDonald et al., 1986). However, adenosine receptors subtypes were initially poorly characterized, with only A_1R and a "generic" A2 subtype being described based on their ability to modulate intracellular cAMP accumulation. Nevertheless, MacDonald and colleagues (MacDonald et al., 1986) argued that neither A_1R nor A_{2A}R seems to be entirely responsible for Ca^{2+} current inhibition in rat DRG neurons, leading to the possibility that a hypothetically different adenosine receptor could be involved. Building on this observation, a part of this study was aimed to fill a major gap by investigating whether the A_3R modulates membrane currents and excitability in isolated rat DRG neurons.

6.1. Pain

Recently, the International Association of the Study of Pain (IASP) has revised the definition of pain as "*An unpleasant sensory and emotional experience associated with, or resembling that associated with, actual or potential tissue damage*" (Raja et al., 2020). Pain has physiologic, behavioural, and aversive emotional components, and is an adaptive response to actual or potential damage to the body. Without its alerting, pain would not reliably trigger escape from danger and avoid a future damage. When it becomes chronic, however, pain loses its adaptive role as a defender of the body's integrity and becomes a pressing

medical problem. As mentioned above, pain has also an emotional and motivational component, and as there are different types of pain, some inconsistencies arise from the literature in its classification. According to the IASP, pain can be classified based on the region of the body involved (e.g., head, visceral), pattern of occurrence's duration (acute and chronic), or the system whose dysfunction could be causing pain (e.g., gastrointestinal, nervous). Thus, pain has been classified into three major classes: nociceptive pain, neuropathic pain and inflammatory pain (Woolf et al., 1998).

The ascending pain pathway begins with primary afferent nociceptors that have cell bodies in dorsal root ganglia (DRG) and that make synapses in the dorsal horn of the spinal cord. The peripheral terminals of primary afferent nociceptors are morphologically undifferentiated free nerve endings, that express several receptors and/or ionic channels. When activated, noxious stimulus-detecting channels produce depolarizing currents within the peripheral terminals of primary nociceptors that can initiate trains of action potentials transmitted to the dorsal horn of the spinal cord. Nociceptive neurons of dorsal root ganglia represent "first order" neurons that synapse on "second order" neurons within the dorsal horn. These second order neurons may be local interneurons or projection neurons that carry nociceptive information to the brainstem and thalamus (Nestler et al., 2002; Fig. 12).

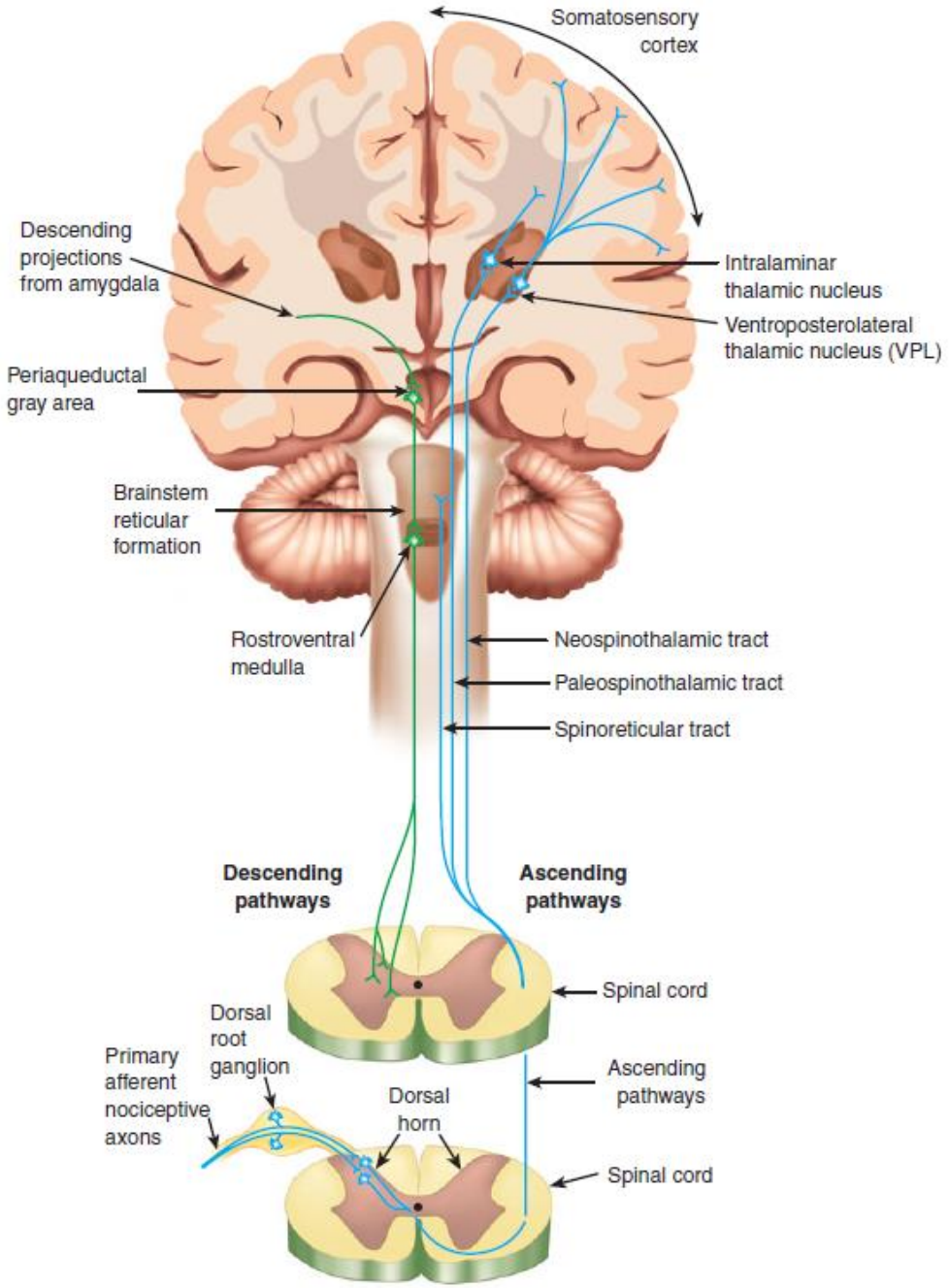

Figure 12. ***Nociceptive pathways.*** Taken by (Nestler et al., 2002).

6.1.1. The Dorsal Root Ganglia in chronic pain

The DRG contains cell bodies of the primary sensory neurons responsible for modulation and transduction of sensory information to the spinal cord. The primary sensory neuron is a pseudounipolar neuron with one branch extending to the peripheral receptive field and the other entering the spinal cord (Aldskogius et al., 1986).

In humans, there are 31 pairs of "mixed" spinal nerves carrying sensorimotor information between the spinal cord and the periphery. These spinal nerves are formed by dorsal afferent sensory axons (dorsal rootlets) and ventral efferent motor axons (ventral rootlets). As the dorsal sensory root fibres travel laterally, their processes connect via a T-junction with their cell bodies, which form the DRG. The T-junction of the DRG neurons can act as an impediment to electrical impulses traveling from the peripheral nociceptor to the dorsal root entry zone of the spinal cord, can participate in the propagation of the electrical pulse, or can act as a low-pass filter to electrical information from the periphery (Gemes et al., 2013; Fig. 13).

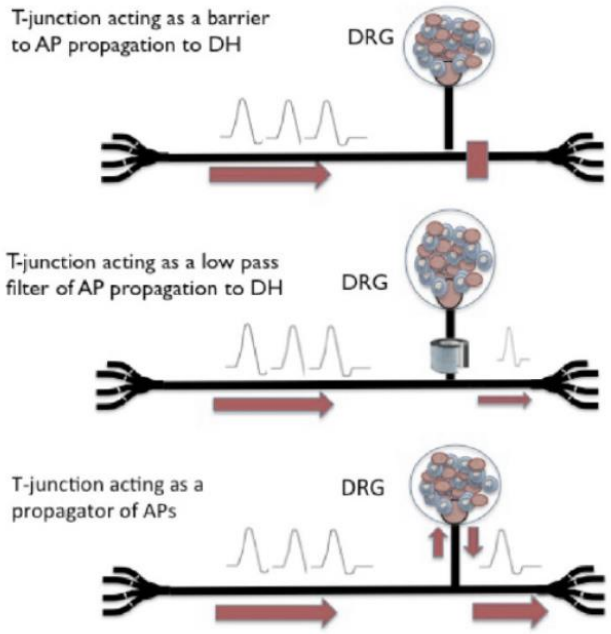

Figure 13. ***Role of T-junction of DRG.*** The T-junction acts either as (i) a barrier to the propagation of actionpotentials (APs) to the dorsal horn (DH) of the spinal cord, (ii) a low-pass filter tothe propagation of APs to the DH, or (iii) an active participant in the propagationof APs to the DH of the spinal cord. Taken by (Krames, 2015).

The cell bodies of the DRG neurons are separated from each other by an envelope of satellite glial cells (SGCs) that respond to peripheral and central processes including nociception, peripheral afferent fiber injury, and inflammation. Glial cells have important roles in pathological states such as pain and inflammation (Aldskogius and Kozlova, 1998; Cherkas et al., 2004; Watkins and Maier, 2002), are involved in the regulation of transmission at the

synapse (Haydon, 2001), elicit Ca^{2+} waves that transmit signals over long distances (Newman, 2003), and express numerous receptors to neurotransmitters and other bioactive molecules (Kamiya et al., 2006).

As most studies of the DRG are performed in rats, it should be stated that human and rat differ with respect to the number of spinal segments and thus primary sensory nerves (Gelderd and Chopin, 1977). In 1985, Harper and Lawson classified rat DRG neurons into small- (20-27 μm), medium- (33-38 μm), and large- (45-51 μm) sized, depending on cell bodies diameter (Harper and Lawson, 1985). These neurons give rise to C (less than 1.4 m/s), Aδ (2.2-8 m/s), and Aα/β (more than 14 m/s) fibres, respectively (Harper and Lawson, 1985). Because of its important roles in the modulation of sensory processing, including nociceptive pain, and the development of neuropathic pain, along with its anatomic accessibility to clinical intervention (Hasegawa et al., 1996, 1993), the DRG is an excellent clinical target for pain control.

6.1.2. Ionic channels and Pain

Much is known regarding the role of Na^+, K^+, and Ca^{2+} current changes and their up- and down-regulation in the development of neuropathic pain.

In 1983, Wall and Devor showed that electrical impulses in peripheral afferent fiber injury may originate not only from the damaged fiber, but also from within the DRG itself, and that systemic application of lidocaine suppressed ectopic impulse discharges generated both at sites of experimental nerve injury and within axotomized DRG cells (Wall and Devor, 1983; Wu et al., 2002). These studies suggest that electrical impulses originating in the DRG are mostly due to activation of normal or abnormal Na^+ channels, which play a very important role in the development of hyperexcitability and neuropathic pain. Observations by Sukhotinsky and colleagues support the hypothesis that ectopic firing in DRG neurons induces central sensitization and clinical allodynia (Sukhotinsky et al., 2004).

DRG neurons co-express several types of Na^+ channels, in particular TTX-resistant $Na_V1.8$, and it is hypothesized that various subtypes of these channels are associated with neuropathic pain (Dong et al., 2007; Ekberg et al., 2006; Gold et al., 2003; Joshi et al., 2006). Na^+ channels within the DRG after peripheral afferent fiber injury can change expression and gating properties and can give rise to spontaneous action potential activity or pathological burst firing, which is the electrophysiological signature of neuropathic pain (Devor et al., 1993; Waxman et al., 1999).

Besides the up-regulation of TTX-resistant Na^+ channels, nerve injury leads to striking reduction in voltage-gated K^+ channel subunits expression in DRG neurons, suggesting that also K^+ channels play an important role in the development of hyperexcitability of injured nerves (Ishikawa et al., 1999; Kajander et al., 1992; Kawano et al., 2009; Rasband et al., 2001). Therefore, modulating the expression and/or function of these channels can help normalizing membrane functions and provide potential mechanisms by which electrical fields can chronically modulate these cells.

It is reasonable that an increase in voltage-activated Ca^{2+} currents may contribute to inflammation-induced increase in afferent nerve input associated with neuropathic pain: (i) an increase in T-type Ca^{2+} currents in peripheral afferent terminals is associated with a decrease in nociceptive threshold (Bilici et al., 2001); (ii) inflammatory injuries are associated with an increase in the α-subunit protein thought to underlie P/Q-type Ca^{2+} currents (Westenbroek and Byers, 1999); (iii) persistent inflammation results in an increase in Ca^{2+}-dependent transmitter release from primary afferents (Neubert et al., 2000) and the selective N-type Ca^{2+} blocker ω-conotoxin GVIA (ω -CTX) inhibits dorsal root stimulus-evoked excitatory postsynaptic currents in lamina I dorsal horn neurons by 60% (Heinke et al., 2004); (iv) inflammation and nerve injury appear to have opposite effects on the expression of several ion channels (Amir et al., 2006), and nerve injury results in a decrease in both HVA and LVA Ca^{2+} currents in primary afferents (McCallum et al., 2006, 2003); (v)

persistent inflammation alters the density and distribution of Ca_V channels in subpopulations of rat cutaneous DRG neurons (Lu et al., 2010) and aberrant expression and/or activity of N-type Ca^{2+} channels is associated with neuropathic pain (Hannon and Atchison, 2013).

After chronic constriction injury of the peripheral axon, LVA Ca^{2+} currents are significantly reduced, so the cell becomes less stable and more likely to initiate or transmit bursts of action potentials thus contributing to increased excitability. Loss of inward Ca^{2+} currents in DRG neurons after peripheral nerve injury induces the by closure of KCa (BK and SK) channels thus contributing to increased sensory neuron excitability (Lirk et al., 2008), and restoring the inward Ca^{2+} current leads to decreased neuronal excitability (Hogan et al., 2008).

Furthermore, Ca_V channels are crucial mediators of neuropathic pain, as confirmed by the fact that α2δ ligands, ie, gabapentinoids, are a first line treatment for this type of pain (Field et al., 2007; Vink and Alewood, 2012). In addition, ziconotide, a derivative of v-CTX, was FDA approved in 2000 (Prialt) for intrathecal treatment of severe and refractory chronic pain (Brookes et al., 2016; Jain, 2000; McDowell and Pope, 2016).

6.1.3. Role of Adenosine in Pain

Adenosine receptor system is a widely studied target, which evidently was successful for neuropathic pain control in several experimental paradigms, and researchers are putting efforts in building its clinical roadmap. Adenosine receptors act by different mechanisms and their targeting for neuropathic pain involves several important pathways such as MAPK, ERK, BDNF signalling, neurotransmitters as well as the ion channel modulations, as mentioned above.

6.1.3.1. *A_1Rs in pain*

A_1Rs are present on the small, medium and large-sized sensory neurons as well as on the periaqueductal grey and brainstem, which are involved in pain perception (Sawynok, 2013). The role of A_1R in neuropathic pain has been well studied and it was found that mice deficient of A_1R showed increased neuropathic pain-like behaviour (Wu et al., 2005). Therefore, A_1R downregulation was found in neuropathy induced by Resiniferatoxin (RTX), a derivate of capsaicin that mainly affect the non-selective cation TRPV1 channel (Kan et al., 2018). In addition, it was found that A_1R co-localised with TRPV1 and Kan and colleagues speculates that development of neuropathic pain by TRPV1 was due to a reduction in adenosine levels and adenosine A_1R density (Kan et al., 2018). On the other hand, it was demonstrated that peripheral nerve injury increases A_1R expression in glial cells (Luongo et al., 2012). Besides, 5′-chloro-5′-deoxy-(±)-ENBA, a potent A_1R agonist, attenuated mechanical allodynia, thermal hyperalgesia and microglia activation, induced by Spared Nerve Injury of sciatic nerve, an effect prevented by DPCPX (Luongo et al., 2012).

Furthermore, A_1R was involved in caffeine inhibition of oxcarbazepine response, an anticonvulsant used in the management of neuropathic pain (Sawynok et al., 2010), in Paeoniflorin-induced effect, a monoterpene glycoside which alleviates neuropathic pain, and TRR469 anti-hyperalgesia, a novel allosteric modulator that inhibit neuropathic pain (Andoh et al., 2017; Vincenzi et al., 2014). Finally, A_1Rs are involved in electroacupuncture mediated antinociception, which acts through the suppression of astrocyte action and up-regulation of TNF-α (Zhang et al., 2018).

Unfortunately, the therapeutic utility of A_1R agonists is limited by their adverse cardiovascular effects.

6.1.3.2. *A_{2A}Rs and A_{2B}Rs in pain*

As mentioned above, A_{2A}R and A_{2B}R are present on different kinds of cells, such as glial and inflammatory cells; activation of A_{2A}R promotes pro-inflammatory cytokines and inhibits anti-inflammatory cytokines (Haskó et al., 2008). Centrally, A_{2B}R is located in the microglia and astrocytes whereas, in the periphery, it is found on immune and inflammatory cells (Merighi et al., 2017; Sawynok et al., 2010). It was reported that the expression of microglia and astrocytes was enhanced in wild-type mice exposed to sciatic nerve injury and this response was attenuated in A_{2A}R knockout animals (Bura et al., 2008), indicating the involvement of this receptor in the neuropathic pain.

In contrast, it was seen that in chronic constriction injury-induced neuropathic pain in rats, a single intrathecal injection of ATL313, an A_{2A}R agonist, reversed the allodynic effect *via* PKA and PKC signalling (Loram et al., 2013). Indeed, A_{2A}R agonist decreased mechanical allodynia and reduced the expression of CD11b mRNA, a microglial activation marker, and TNFα, but it did not affect IL-10 expression after spinal neuropathic avulsion pain surgery (Kwilasz et al., 2018). Furthermore, A_{2A}R agonists increased IL-10 levels in the cerebrospinal fluid of rats with neuropathic pain (Malcangio et al., 2013). Consistently with these data, peri-sciatic administration of an A_{2A}R agonist reduces neuropathic pain and prevented sciatic inflammatory neuropathy (SIN) (Kwilasz et al., 2019). Finally, administration of A_{2A}R antagonist SCH58261 (50 nM) prevents BDNF secretion as well as microglia proliferation, thus regulating the microglial activity during neuropathic pain (Gomes et al., 2013). At variance, there are very few pieces of evidence on the involvement of A_{2B}R in neuropathic pain; therefore, limited studies were conducted based on this receptor. However, it has been shown that mice with adenosine deaminase deficiency develop an adenosine-induced pain behaviour, that was prevented only by A_{2B}R antagonist PSB1115 (Hu et al., 2016). In confirm, coadministration of low doses (10mg/kg) with a low dose of morphine enhanced the efficacy of morphine (Abo-Salem et al., 2004).

6.1.3.3. A_3Rs in pain

It has been demonstrated that A_3R activation reduces the excitability of the neurons and decreases the activity of astrocytes, thus decreasing inflammation in the nervous tissues (Wahlman et al., 2018). A_3Rs are expressed in DRG neurons, with species-specific differences being described (Ray et al., 2018; Usoskin et al., 2015). This receptor is also present at spinal and supraspinal sites, thus it emerges as a good target for anti-nociceptive activity as well as prophylactic action of neuropathic pain (Little et al., 2015), but the mechanisms behind this anti-hyperalgesic effect are not clearly understood. It was also discovered that amitriptyline, a tricyclic antidepressant, has an antinociceptive activity through the A_3R pathway (Cho et al., 2018). In addition, A_3R also reduced CCI-induced pain behaviour at the spinal cord level through the GABAergic pathway (Ford et al., 2015).

The well-known A_3R agonists IB-MECA and Cl-IB-MECA acted in opiate receptor-independent way and were found to be five times more potent than opioids, also more efficacious than morphine (Chen et al., 2012). Furthermore, IB-MECA inhibited neuropathic pain by blocking the activation of NADPH (nicotinamide adenine dinucleotide phosphate oxidase) as well as of MAPK (mitogen-activated protein kinase) (Janes et al., 2014; Terayama et al., 2018) and NFκB (nuclear factor kappa-light-chain-enhancer of activated B cells) along with increased production of IL10 and decrease in levels of TNFα and IL1β. (Janes et al., 2014). Indeed, IBMECA or Cl-IB-MECA are in phase II/III clinical trials for other indications such as rheumatoid arthritis, hepatitis, psoriasis, dry eye, and glaucoma and are showing safety data which may guarantee a rapid translational potential.

The recently synthetized and highly selective A_3R agonist MRS5698, and the more water-soluble congener MRS5980, proved effective in preventing allodynia and hyperalgesia associated with traumatic nerve injury, chemotherapy, and bone cancer in rodents (Ford et al., 2015; Janes et al., 2014; Little et al., 2015). These second-generation, highly selective A_3R agonists are

at least several orders of magnitude more selective than the early generation exemplified by IB-MECA and Cl-IB-MECA (Janes et al., 2014; Little et al., 2015; D. K. Tosh et al., 2014). Finally, A_3R agonist prevents astrocyte and microglial activation and elevates the level of anti-inflammatory cytokines and decreases the level of proinflammatory cytokines (Janes et al., 2015).

The adenosine A_3R has stood out as one of the most potential targets for the management of chronic neuropathic pain.

Aims of the study.

Aim I – *Study about electrical oscillatory activity and muscarinic effects on K^+ and Na^+ currents in human foetal cholinergic neurons from the nucleus basalis of Meynert.*

The Nucleus Basalis of Meynert (NBM) is the major source of cholinergic input to the cerebral cortex and projects to most cortical areas and is implicated in several roles, as memory, attention and behaviour. It has been demonstrated that the degeneration of NBM is involved in various forms of dementia, as Alzheimer and Parkinson diseases, but also in schizophrenia.

The first aim of this thesis was to take advantage from the availability of human foetal nucleus basalis of Meynert (hfNBM) cultures to investigate the electrophysiological properties of immature, non-differentiating, cholinergic neurons from the human developing CNS and their functional responses to cholinergic agonists. For this purpose, we used electrophysiological patch-clamp recordings and selective cholinergic agonist and/or antagonist, to investigate functional metabotropic receptors in hfNBM cultures.

Aim II – *Study about the effect of adenosine A_{2B} receptors on K^+ currents and cell differentiation in cultured oligodendrocyte precursor cells and modulation sphingosine-1-phosphate signalling pathway.*

Oligodendrocytes are the only myelinating cells in the brain and differentiate from their progenitors (OPCs) throughout adult life. However, this process fails in demyelinating pathologies. Adenosine is emerging as an important player in OPC differentiation and all its receptors (named A_1, A_{2A}, A_{2B} and A3) are expressed in oligodendroglial cells, at all maturation stages. Our group recently demonstrated that A_{2A}Rs inhibit cell maturation by reducing voltage-dependent K^+ currents. To date, no data are available about the A_{2B}R. On the other hand, the bioactive lipid mediator sphingosine-1-phosphate (S1P) and its receptors (S1P1–5) are also crucial modulators of OPC development. In addition, an interaction between this pathway and the A_{2B}R activation is reported in peripheral cells. The second aim was to study the role of A_{2B}Rs in

modulating K^+ currents and cell differentiation in rat OPC cultures. We also investigated the possible interplay between A_{2B}Rs and S1P signalling. All experiments were performed by electrophysiological recordings and biochemical assays, as real-time quantitative polymerase chain reaction experiments (RT-PCR), Western blot, small interference RNA transfection and immunofluorescence analysis.

Aim III – *Study about the role of adenosine A3 receptor activation in inhibition of pronociceptive N-type Ca^{2+} currents and of cell excitability in dorsal root ganglion neurons.*

Recently, studies have focused on the antihyperalgesic activity of the adenosine A3 receptor (A_3R) in several chronic pain models, but the cellular and molecular basis of this effect is still unknown. Therefore, our last aim was to investigate the expression and role of A_3R on the excitability of small- to medium-sized, capsaicin-sensitive, dorsal root ganglion (DRG) neurons isolated from 3- to 4-week-old rats, by using patch-clamp and RT-PCR experiments and immunofluorescence analysis.

Materials and Methods.

1. Cell culture preparation

1.1. Human foetal NBM neuroblast cultures

The use of human foetal tissue for research purposes was approved by the National Ethics Committee and the local ethic committee for investigation in Humans of the University of Florence (Permit Number: 678304).

Human foetuses biopsies were obtained from therapeutic medical abortions after women approved and signed the informed consent document, as already reported (Gallina et al., 2008). Cell used in the present study were isolated from two female 12-weeks old human foetuses and have been already characterized as cholinergic neuroblasts by qRT-PCR, immunofluorescence and cytofluorimetric analysis, as reported in previous work (Morelli et al., 2017). Cell suspensions were mechanically dispersed and cultured in Coon's modified Ham's F12 medium (Euroclone, Milan, Italy) supplemented with 10% FBS (Hyclone, Logan, UT), as described (Morelli et al., 2017). Cells were split from plates when confluent: approximately twice a week for the first 10-12 passages, then once a week/every 10 days for later passages. Thus, the whole period of observation in the present research was, from p9 to p25, about 3-3.5 months.

In the present work, we refer to hfNBM cells as cholinergic neuroblasts on the basis of previous work (Morelli et al., 2017) in which we the expression of specific neuronal vs glial markers was elucidated in detail, as well as markers of immature stem-like cells. It should be considered that the same cell cultures, prepared from the same tissue isolations, were used in the present research.

1.2. OPC cultures

Purified cortical OPC cultures were prepared as described elsewhere (Coppi et al., 2013b; Malerba et al., 2015). Wistar rat pups (postnatal day 1–2) were killed and cortices removed, mechanically and enzymatically dissociated, suspended in DMEM medium containing 20% foetal bovine serum (FBS), 4 mM L-glutamine, 1 mM Na-pyruvate, 100 U/ml penicillin, 100 U/ml

streptomycin (all products are from EuroClone, Milan, Italy), and plated in poly-D-lysin coated T75 flasks (1 flask per animal). After 2–3 days in culture, OPCs growing on top of a confluent monolayer of astrocytes were detached by 5 h of horizontal shaking. Contaminating microglial cells were eliminated by a 1 h pre-shake and by further plating detached cells on plastic culture dishes for 1 h. OPCs, which do not attach to plastic, were collected by gently washing the dishes and plated onto poly-DL-ornithine-coated (final concentration: 50 µg/ml, Merck) 13 mm-diameter glass coverslips laid in 24 multiwell chambers (l0^4 cells/well) for electrophysiological and immunocytochemical experiments, or on poly-DL-ornithine-coated 25 mm-diameter glass coverslips laid in 6 multiwell chambers (l05 cells/well) for Western blot or real-time polymerase chain reaction (RT-PCR) experiments. OPC cultures were maintained in Neurobasal medium (Thermo Fisher Scientific) containing 2% B27, 4 mM L-glutamine, 1 mM Na-pyruvate, 100 U/ml penicillin, 100 U/ml streptomycin, 10 ng/ml platelet derived growth factor-BB (PDGF-BB) and 10 ng/ml basic fibroblast growth factor (bFGF; both mitogens were from PeproTech EC Ltd, London, UK) to promote cell proliferation. In some cases, OPC were allowed to differentiate into mature OLs by mitogen withdrawal. The day at which cells were deprived of mitogens is indicated as t_0. According to our previous results (Coppi et al., 2013a, 2013b), cells cultured in mitogen-free medium undergo gradual maturation as demonstrated by the increase in myelinrelated proteins such as MAG and MBP. After 7 days in these conditions (t_7), the expression of myelin-related proteins reaches a peak so most of our analysis were performed at this time point. In order to study the effect of $A_{2B}R$ and/or SphK/S1P signalling pathway on oligodendroglial maturation, selective ligands for these targets were added every two days from t_0 to t_7.

1.3. DRG neuronal cultures

Animal experiments were performed according to Directive 2010/63/EU of the European Parliament and of the European Union Council (September 22,

2010) and to the Italian Law on Animal Welfare (DL 26/2014). The protocol was approved by the University of Florence Institutional Animal Care and Use Committee and by the Italian Ministry of Health. All efforts were made to minimize animal suffering and to use a minimal number of animals needed to produce reliable scientific data. Sprague-Dawley rats (3-4 weeks old, Envigo, Udine, Italy) of both sexes were housed in a temperature- and humidity-controlled vivarium (12-hour dark/ light cycle, free access to food and water) and sacrificed by cervical dislocation. Primary DRG neurons were isolated and cultured as described (Fusi et al., 2014; Nassini et al., 2015). Briefly, ganglia were bilaterally excised and enzymatically digested using 2 mg/mL of collagenase type 1A and 1 mg/mL of trypsin (both compounds from Sigma-Aldrich, Milan, Italy) in Hank's balanced salt solution (25-35 minutes at 37°C). Cells were then pelleted and resuspended in Dulbecco's modified Eagle's medium supplemented with 10% heat inactivated horse serum, 10%heat-inactivated foetal bovine serum, 100 U/mL penicillin, 0.1 mg/mL streptomycin, and 2-mM L-glutamine for mechanical digestion. After centrifugation (1200g, 5 minutes), neurons were suspended in the above-mentioned medium, enriched with 100 ng/mL of mouse nerve growth factor and 2.5 mM of cytosine-b-D-arabino-furanoside free base, and then plated on 13- mm or 25-mm glass coverslips coated by poly-L-lysine (8.3 mM) and laminin (5mM). Dorsal root ganglion neurons were cultured for 1 to 2 days before being used for experiments. In a set of experiments, DRG cultures were maintained in the absence of nerve growth factor. However, no difference was found in any of the effects tested in the present research, and data were pooled.

2. *Electrophysiology – Whole-cell patch clamp*

For these studies patch clamp experiments in whole-cell configuration have been performed. For this purpose, cells were transferred to a recording chamber (1 ml volume) mounted on the platform of an inverted microscope (Olympus CKX41, Milan, Italy) and superfused at a flow rate of 1.5 ml/min with a standard extracellular solution, depending on the cell investigated

(Table 4), by a three-way perfusion valve controller (Harvard Apparatus).

	hfNBMs	OPCs	DRGs
Standard extracellular solution (mM)			
HEPES	10	5	10
D-glucose	5	10	10
NaCl	140	140	147
KCl	3	5.4	4
$MgCl_2$	2	1.2	1
$CaCl_2$	1	1.8	2
pH	7.4 with NaOH	7.3 with NaOH	7.4 with NaOH
Standard pipette solutions (mM)			
K-Aspartate	130	-	-
K-gluconate	-	130	130
KCl	-	-	10
NaCl	-	6	4.8
$MgCl_2$	2	2	2
$CaCl_2$	5	-	1
Na_2-*ATP*	5	2	2
Na_2-*GTP*	0.1	0.3	0.3
EGTA	11	0.6	3
HEPES	10	10	10
pH	7.2 with KOH	7.4 with KOH	7.4 with KOH
LJP	14.5 mV	14.5 mV	15 mV

Table 4. Electrophysiological solutions. 4-(2-hydroxyethyl)piperazine-1-ethanesulfonic acid, N-(2-hydroxyethyl)piperazine-N′-(2-ethanesulfonic acid) (**HEPES**); ethylene glycol-bis(2-aminoethylether)-N,N,N′,N′-tetraacetic acid (**EGTA**); Liquid Junction Potential (**LJP**).

Borosilicate glass electrodes Harvard Apparatus, Holliston, Massachusetts USA) were pulled with a Sutter Instruments puller (model P-87) to a final tip resistance suitable for each cell investigated (2÷4MΩ, 4÷7MΩ and 1.5÷3MΩ for hfNBMs, OPCs and DRGs, respectively). Then, data were acquired with an Axopatch 200B amplifier (Axon Instruments, CA, USA), low pass filtered at 10 kHz, stored, and analysed with pClamp 9.2 software (Axon Instruments, CA, USA). All the experiments were carried out at room temperature (RT: 20–22°C).

Cells were voltage-clamped at -60 mV as previously described (Coppi et al., 2012), except for OPC (-70 mV), and input resistance (Rin) and membrane capacitance (Cm) were routinely measured by fast hyperpolarizing voltage

pulses (from -60 to -70 mV, 40 ms duration). Only cells showing a stable Cm and Rs before, during, and after drug application were included in the analysis. In some experiments, cell resting membrane potential (Vm) was determined immediately after seal breaking-through by switching the amplifier to the current-clamp mode.

Current amplitude (measured as pA) was normalized to respective cell capacitance (Cm, measured in pF) and expressed as current density (pA/pF) in averaged results. All drugs were dissolved in extracellular solution and were applied by superfusion with a three-way perfusion valve controller (Harvard Apparatus, Holliston, MA USA) after a stable baseline was obtained. A complete exchange of bath solution in the recording chamber was achieved within 28 s.

2.1. Electrophysiology - Protocols used in hfNBMs

K^+ currents were evoked by a voltage ramp protocol (1 s depolarization from -120 to +150 mV) once every 15 s before, during, and after drug treatments. Ramp-evoked outward currents were measured at +150 mV and quantified by averaging current values recorded between +139 and +149 mV. On the other hand, ramp-evoked inward currents were measured at -120 mV quantified by averaging current values recorded between -109 and -119 mV.

In the present work, we refer to "muscarinic effect" of ACh on ramp currents when a sustained increase of +150 mV currents was observed in the absence of any change in -120 mV currents. We refer to "nicotinic effect" of ACh on ramp currents when a concomitant increase in +150 mV and -120 mV current were measured, both responses fading before drug removal. In some cases, both the nicotinic and muscarinic effects were observed in the same cell during Ach application.

Control ramps were obtained by averaging the last 4 traces (1 min) of baseline and were compared to those measured during the last min of drug application (muscarinic effect) or at the peak (nicotinic effect). Net ACh- or CCh-activated

currents were obtained by subtraction of the control ramp from the ramp recorded in the presence of the compound as described above. Concentration-response curve of CCh was obtained by averaging at least 4 individual experiments for each CCh concentration.

Na^+ currents were isolated by substituting extracellular K^+ with equimolar Cs^+ and by using the following Cs^+-based pipette solution (mM):

CsCl 120; NaCl 4.8; $CaCl_2$ 1; $MgCl_2$ 2; Na_2-ATP 5; Na_2-GTP 0.1; EGTA 11; HEPES 10 (pH 7.4 with CsOH), in order to block K^+ conductance.

Na^+ currents evoked in Cs^+-replacement conditions by a 0 mV step depolarization (40 ms) from a holding potential (Vh) of -90 mV once every 5 s. Current-to-voltage relationship of Na^+ currents was obtained by a series of depolarizing voltage steps from -60 to +60 mV (10 mV step depolarization, 40 ms step duration, 2 s inter-step interval; Vh=-90 mV). Control values of Na^+ current amplitude were measured by averaging the last 12 traces (1 min) of baseline and were compared to those measured during the last min of drug application. Activation/inactivation curves of Na^+ currents were obtained by a series of depolarizing voltage steps from -100 to +60 mV (10 mV step depolarization, 60 ms step duration, 2 s inter-step interval; Vh=-110 mV; post-step potential = 0 mV). Open-channel current-to-voltage relationship of Na^+ current was used to calculate Na^+ conductance (G) and normalized to the maximal Na^+ conductance recorded during the depolarizing voltage step protocol (G/G_{max}).

Curves obtained by this method were then fitted by a Boltzmann equation:

$$\frac{G}{G_{max}} = 1 - \frac{1}{1 + e^{\frac{V - V_{1/2}}{k}}}$$

Therefore, concentration-response curves were obtained by fit of data to four-parameter logistic equation:

$$Y = \min + \frac{(\max - \min)}{1 + 10^{(LogEC50 - X)nH}}$$

where EC50 is the half-maximally effective concentration, X is the logarithm of concentration, nH is the Hill coefficient and min and max are the bottom and the top of the curve, respectively.

Finally, current-clamp recordings were performed as described (Coppi et al., 2012). Electrical activity was elicited in hfNBM neuroblasts by depolarizing current steps injection (100 pA increment, from -100 pA to +700 pA; 600 ms, 2 s inter-episode interval). Sampling rate for current-clamp recordings was 50 μs.

In some experiments we substituted intracellular EGTA with equimolar BAPTA (1,2-bis(2-aminophenoxy)ethane-N,N,N′,N′-tetra-acetic acid).

Where indicated, the antibiotic neomycin (500 μM) was added to the pipette solution to prevent PLC activation (Felder et al., 1990; Mlinar et al., 1995). In those experiments, at least 10 min we waited after seal breakthrough before starting the experiment to allow complete intracellular diffusion of the drug. Where indicated, pertussis toxin (PTx; 1 μg/ml) was added to the culture medium and maintained overnight (o/n).

2.2. *Electrophysiology - Protocols used in OPCs*

In all electrophysiological experiments, the following adenosine receptor antagonists were added to the extracellular solution in order to prevent nonspecific adenosine receptor activation upon the superfusion with various $A_{2B}R$ agonists: DPCPX, SCH58261 and MRS1523, all at 100 nM concentration, in order to block A_1R, $A_{2A}R$ and A_3R respectively.

It is known that the vast majority of voltage-dependent currents expressed by OL cells are K^+ currents. Therefore, Na^+ currents are recorded in about 60% of cells only at the stage of bipolar, undifferentiated OPCs whereas appreciable Ca^{2+} currents can only be evoked in very high extracellular Ba^{2+} conditions (i.e 90 mM $[Ba^{2+}]_o$) (Coppi et al., 2013b).

A voltage ramp protocol (800 ms depolarization from −120 to +80 mV) was recorded every 15 s to evoke a wide range of overall voltage-dependent membrane currents before, during and after drug treatments. Variations in membrane potential (Vm) induced by drug treatments were measured by calculating the reversal potential (the "zero current" potential) of ramp-evoked currents before, during and after drug application. Outward K^+ currents were evoked by two different depolarizing voltage-step protocols, in order to separate delayed rectifier outward K^+ currents (IK) from transient outward (IA) conductances. A first protocol consisted in 10 mV depolarizing voltage steps from −40 to +80 mV (200 ms each, 1 s inter-step interval) preceded by a 100 ms pre-step potential (Vpre) at −80 mV. This protocol activates a mixture of outward IK and IA currents in cultured OPCs. Since transient IA currents present a voltage-dependent inactivation at potential positive to −80 mV, a second protocol was applied in the same cell with a pre step at −40 mV, to selectively inactivate IA thus leaving the IK component unchanged (IK protocol). Net IA current was then obtained in each cell by digital subtraction of the two current traces. Current-to-voltage relationships (I-V plots) of IK or IA currents were obtained by measuring current amplitude at the steady state (200–250 ms after step onset) of the IK protocol or at the peak of subtracted trace (1–20 ms after step onset), respectively.

2.3. Electrophysiology - Protocols used in DRG neurons

Ca^{2+} currents were isolated by replaced of K^+ with equimolar Cs^+ and by using the following Cs^+-based pipette solution (mM):

CsCl 120; Mg_2-ATP 3; EGTA 10; and HEPES 10 (pH 7.4 with CsOH).

In addition, TTX (1 mM), A887826 (200 nM) were added to block TTX-sensitive and TTX-insensitive Na^+ channels, respectively. As reported in Results, ramp experiments revealed that Cl-IB-MECA–inhibited Ca^{2+} currents in DRG neurons were completely prevented in the presence of extracellular Cd^{2+}. The effect of Cd^{2+} was not different when applied at 100 mM, 500 mM, or 1 mM concentrations (Fig. 43). So, when studying the effect of this compound on Ca^{2+}

currents evoked in isolation, Ni^{2+} (100 mM) was added to the extracellular solution to exclude T-type Ca^{2+} channels, which do not seem to be involved in A3AR-mediated effect. For this reason, the hypothetical, additional, involvement of T-type Ca^{2+} channels in A3AR-mediated Ca^{2+} channel modulation was not investigated in the present research and will be addressed in a separate work.

A voltage-ramp protocol (800-ms depolarization from +65 to -135 mV; holding potential, or Vh, of -75 mV) was used to evoke a wide range of overall voltage dependent currents before, during, and after drug treatments. TRPA1- or TRPV1-mediated currents were detected as inward currents activated in -60 mV (corresponding to -75 mV after liquid junction potential correction) clamped cells on superfusion of the respective agonists allyl isothiocyanate (AITC) and capsaicin, respectively, as already shown elsewhere (Fusi et al., 2014; Nassini et al., 2015).

Voltage-dependent Ca^{2+} channels' currents were evoked in Cs^{+}-replacement conditions by a 0 mV step depolarization (200 ms, V_h of -65 mV) once every 30 seconds, a time that allowed complete recovery from eventual Ca^{2+} channel inactivation and minimized Ca^{2+} current run down. The current-to-voltage relationship of Ca^{2+} currents was obtained by eliciting 10 depolarizing voltage steps (200-ms duration, 10-mV increments, 5-second interval) from -50 to +50 mV starting from a V_h of -65 mV.

On the other hand, Na^{+} currents were isolated by using Cs^{+}-based pipette solution and by adding Cd^{2+} (100 mM) and Ni^{2+} (100 mM) to a Cs^{+}-substituted extracellular solution. Na^{+} currents were evoked in Cs^{+}-replacement conditions by a 0 mV step depolarization (40 ms, V_h of -90 mV) once every 5 seconds.

Cell capacitance was used to estimate neuronal diameter by assuming an approximated spherical cell shape according to the calculated Cm for all biological membranes of 1 $\mu F/cm^2$ and to the equation of the sphere surface: $A = 4\pi r^2$ (Jain, 2000).

Current-clamp recordings were performed as described (Coppi et al., 2012) in the standard extracellular solution, by lowering $CaCl_2$ (2 mM). A ramp current protocol consisting in 1 second injection of 30 pA positive current from the resting membrane potential (only cells showing a Vm of at least -50 mV were chosen) was used to evoke action potential (AP) firing in a typical DRG neuron once every 30 seconds. After at least 3 minute recording of a stable baseline, Cl-IB-MECA (100 nM) was applied for 8 to 10 minutes. Action potential firing was quantified by counting the number of APs evoked by a ramp current (1 second). When the Cl-IB-MECA was applied in the presence of MRS1523 (100 nM; A_3R antagonist) or PD173212 (1 mM; N-type Cav blocker), the blocker was added at least 10 minutes before the agonist. Current-clamp recordings were filtered at 10 kHz and digitized at 1 kHz. All current-clamp values reported in Table 5 are the average of at least 3 episodes and have been corrected for liquid junction potential. All AP parameters refer to the first AP generated by the ramp, and in particular:

- The rate of AP depolarization and hyperpolarization was measured as the first derivative of membrane potential over time (mV/ms);
- AP threshold was defined as the point at which the derivative first exceeded 30 mV/ms;
- AP amplitude was calculated as the difference between the peak reached by the overshoot and the threshold;
- AP time to peak was measured as the time between the threshold and the voltage peak reached by the AP;
- Action potential half-width was measured as the time to reach half the AP amplitude (ms);
- Resting Vm was calculated as the averaged membrane voltage measured 200 ms before ramp current injection;
- The current needed to produce the first spike was defined as "current threshold" and measured as the minimal amount of current (pA) injected during the ramp protocol leading to the first AP initiation;

- The AP duration measured the difference between the time of reaching the threshold potential during the rising phase and the time when the repolarizing potential crossed the threshold value again;
- The fast afterhyperpolarization was measured as the difference between the voltage threshold and the minimum potential reached after the AP peak.

	Ctrl	Cl-IB-MECA	Ctrl	PD173212	Ctrl in PD173212	PD173212 + Cl-IB-MECA
	n=6		n=7		n=8	
V_{rest} (mV)	-61.2 ± 2.3	-60.1 ± 2.1	-63.6 ± 2.9	-59.7 ± 3.6*	-53.3 ± 4.0	-54.1 ± 2.6
AP-ttp (ms)	685.1 ± 100.7	684.6 ± 105.2	530.7 ± 61.9	504.2 ± 70.5	465.0 ± 73.54	480.1 ± 84.65
AP-hw (ms)	1.7 ± 0.2	2.6 ± 0.6	2.2 ± 0.6	4.4 ± 2.3	3.8 ± 2.0	2.6 ± 0.6
AP-a (mV)	65.0 ± 6.3	57.7 ± 7.9	60.6 ± 7.6	58.0 ± 12.4	57.6 ± 6.2	52. ± 6 5.5
Ith (pA)	16.0 ± 5.3	20.7 ± 7.4	4.0 ± 1.6	4.3 ± 2.0	3.3 ± 1.1	3.8 ± 1.1
APth (mV)	-15.7 ± 1.8	-14.5 ± 1.4	-12.7 ± 1.9	-14.1 ± 1.5*	-14.1 ± 2.6	-13.8 ± 2.4
APd (ms)	3.7 ± 0.4	3.2 ± 0.7	3.9 ± 0.7	4.5 ± 0.6†	4.3 ± 0.5	4.2 ± 0.8
fAHP (mV)	41.9 ± 2.9	39.5 ± 4.1	46.0 ± 2.1	34.8 ± 4.4*	37.4 ± 3.1	34.3 ± 4.0

Table 5. Action potential parameters. The following experimental groups were analysed: Control: Ctrl vs Cl-IB-MECA (100 nM; n=6); Ctrl vs PD173212 (1 mM; n=7); and PD173212 vs PD1732121Cl-IB-MECA (n=8). All action potential (AP) parameters are referred to the first action potential (AP) generated by the ramp. Resting Vm (V_{rest}) was calculated as the averaged membrane voltage measured 200 ms before ramp current injection. Action potential time to peak (AP-ttp) was measured as the time between the threshold and the voltage peak reached by the AP. Action potential half-width (AP-hw) was measured as the time to reach half the AP amplitude. Action potential amplitude (AP-a) was calculated as the difference between the peak reached by the overshoot and the threshold. The current needed to produce the first spike was defined as "current threshold" (Ith) and was measured as the minimal amount of current (pA) injected during the ramp protocol leading to the first AP initiation. Action potential threshold was defined as the point at which the derivative first exceeded 30 mV/ms. Action potential duration (APd) measured the difference between the time of reaching the threshold potential during the rising phase and the time when the repolarizing potential crossed the threshold value again. The fast afterhyperpolarization (fAHP) was measured as the difference between the voltage threshold and the minimum potential reached after the AP peak. The paired Student t test, n = 7. * $P < 0.05$; † $P < 0.01$ vs respective ctrl.

3. Quantitative RT-PCR analysis

Gene expression analysis was performed by RT-PCR, using $2^{(-\Delta\Delta CT)}$ comparative method of quantification (Schmittgen and Livak, 2008).

For OPC cultures, total RNA (500 ng), extracted with GenElute™ Mammalian Total RNA Miniprep (Sigma-Aldrich s.r.l. Milan, Italy) was reverse transcribed using iScript™ Advanced cDNA Synthesis Kit for RT-qPCR (Bio-Rad Laboratories S.r.l., Segrate (MI), Italy) according to the manufacturer's instructions. The design of MAG, MBP, S1P2, S1P3 and $A_{2B}R$ primers were performed employing Primer Express® Software v3.0.1 (Thermo Fisher Scientific INC. Monza (MB), Italy) that provides customized application-specific documents for absolute and relative quantitation. Rat oligonucleotide primers employed in gene expression studies are listed in Table 6.

The quantification of target gene mRNA levels was performed employing PowerUp™ SYBR™ Green Master Mix (Bio-Rad Laboratories S.r.l). Each measurement was carried out in triplicate, using the automated ABI Prism 7500 Sequence Detector System (Thermo Fisher Scientific INC) as described previously (Donati et al., 2007), by simultaneous amplification of the target gene together with the housekeeping gene (β-actin and glyceraldehyde-3-phosphate dehydrogenase: GAPDH) in order to normalize expression data. Results were analyzed by ABI Prism Sequence Detection Systems software, version 1.7 (Applied Biosystems, Foster City, CA). The $2^{(-\Delta\Delta CT)}$ method was applied as a comparative method for quantification and data were normalized to β-actin and GAPDH expression.

Oligo name	Sequence 5′ to 3′ (include modification codes if applicable)
MAG-FW	TTCCGAATCTCTGGAGCACCTGATAAG
MAG-RV	TCCTCACTTGACTCGGATTTCTGCGT
ACTB-FW	GAACACGGCATTGTCACCAACTGGGA
ACTB-RV	GCCTGGATGGCTACGTACATGGCT
MBP-FW	GCCCTCTGCCTTCTCATGCCC
MBP-RV	CCTCGGCCCCCCAGCTAAATCT
NG2 CSPG4-FW	ACCCTCAGCACTTTCTCCTGGAGAG

NG2 CSPG4-RV	CAAGCCTGTGTTTGTGGTGATGACAG
ADORA2B-FW	GTGGGAGCCTCGAGTGCTTTACAG
ADORA2B-RV	GCCAAGAGGCTAAAGATGGAGCTCTG
GAPDH-FW	AACCCATCACCATCTTCCAGGAGCG
GAPDH-RV	TCTCGTGGTTCACACCCATCACAAAC
SPHK1-FW	ACCTGCTTCCTCACTGGCACAGAAG
SPHK1-RV	CAGATGCATAACACCAGCCTCGCAG
SPHK2-FW	GAGTGAGTGGGAAGGCATTGTCACTG
SPHK2-RV	GAGCAACAGGTCAACACCAACAGTTTGC
S1PLYASE-FW	GTCAAGAACATGCCATTCCTGAAGTTGGA
S1PLYASE -RV	GAATTCTCCGTAAGCCTGCACCAGC
S1P2-FW	GGTGGAGAACCTTCTGGTGCTAATCG
S1P2-RV	GTGATGAAGGCTGAACCCTCTCGG
S1P3-FW	TGATCAAGATGAGGCCGTACGACGC
S1P3-RV	GGCTGTGAAGATGCTGATGAGAAAGG
S1P5-FW	GCTTCCATGCACCCATGTTCCTGC
S1P5-RV	CGCTCTATAGCAATGGCCAGGAGG
CNPASE-FW	TCTCCGAGGAGTACAAGCGTCTGG
CNPASE-RV	CTCCTTGAGCTGGGCACAGTCTAGT

Table 6. Sequences of rat oligonucleotide primers employed in gene expression studies of real-time polymerase chain reaction (RT-PCR). The following mRNA were used: rattus norvegicus myelin-associated glycoprotein (MAG); rattus norvegicus actin beta (Actb); rattus norvegicus myelin basic protein transcript variant 1 (MBP); rattus norvegicus chondroitin sulfate proteoglycan 4 (NG2 Cspg4); adenosine A_{2B} receptor (ADORA2B); glyceraldehyde-3-phosphate dehydrogenase (Gapdh); sphingosine kinase 1 (Sphk1); sphingosine kinase 2 (Sphk2); sphingosine 1-phosphate lyase (S1Plyase); sphingosine 1-phosphate receptor 2, 3, 5 (S1P2, S1P3, S1P5); 2′,3′-cyclic-nucleotide 3′-phosphodiesterase (CNPase). Forward (FW); reverse (RV).

For DRG cultures, total RNA was isolated using Nucleospin RNA (Macherey–Nagel Duren, Duren, Germany) with DNAse treatment according to the manufacturer's instructions. The expression of A_3Rs was evaluated by quantitative real-time polymerase chain reaction (RT-PCR) using gene-specific fluorescently labelled TaqMan MGB probe (minor groove binder). For the RT-PCR of A3ARs, a predeveloped assay was used: Adora3 Rn_00563680_m1. The amount of target mRNA was normalized to the endogenous reference, GADPH Rn 01749022_g1, and to a homogenate of the rat brain taken as a positive control, according to the $2^{(-\Delta\Delta CT)}$ method. Data are the result of 3 independent experiments performed in triplicate.

4. Western blot analysis

Primary rat cortical OPC culture were collected after 10 µM BAY60-6583 challenge for 10 min and lysed in a buffer containing 50mM Tris, pH 7.5, 120mM NaCl, 1mM EDTA, 6mM EGTA, 15mM $Na_4P_2O_7$, 20mM NaF, 1% Nonidet protease inhibitor and phosphatase inhibitor cocktail for 30 min at 4°C. Then lysates were centrifuged at 10.000xg, 15 min 4°C, supernatant collected for protein quantification and 15 µg of protein from total cell lysates were used to perform a SDS-polyacrylamide gel electrophoresis and Western blot analysis. The rate of phosphorylation of SphK1 and SphK2 were measured using the Sphingosine kinase activation antibody sampler kit (ECM Biosiences ECM Biosciences, Versailles, KY USA). Membranes were incubated overnight with the primary antibodies at 4°C and then with specific secondary antibodies for 1 h at room temperature. Binding of the antibodies with the specific proteins has been detected by Enhanced chemiluminescence (ECL), employing Amersham Imager 600. Densitometric analysis was performed by ImageJ software.

5. Small interference RNA transfection and gene downregulation

OPC were transiently transfected with Lipofectamine RNAi-MAX according to the manufacturer's instructions, as already reported (Bruno et al., 2018). Briefly, Lipofectamine RNAiMAX (Thermo Fisher Scientific) was incubated with siRNA in Neurobasal medium without serum and antibiotics at room temperature for 20 min, and afterwards the lipid/RNA complexes were added with gentle agitation to cells to a final concentration of 75 nM in B27-containing Neurobasal in the presence of PDGF-BB and bFGF. After 24 h, cell medium was changed with serum-free medium and then used for the experiments within 72 h from the beginning of the transfection. The specific gene knockdown was evaluated by RT-PCR.

6. Immunocytochemical analysis

OPC and DRG cultures grown on 13-mm diameter coverslips were fixed with 4% paraformaldehyde in 0.1 M phosphate-buffered saline (PBS, Pan-Biotech, Milan, Italy) for 10 min at RT.

Then OPC were washed twice with PBS and incubated with PBS containing 0.25% Triton X-100 (Sigma-Aldrich, Milan Italy) (PBST). After three washes in PBS, OPCs were incubated with 10% goat serum (Sigma-Aldrich, Milan Italy) in PBST (PBST-GS) for 30 min to block unspecific binding of the antibodies. OPCs were incubated for 2.5 hours at RT in rabbit anti-A_{2B}R-selective primary antibody (Alomone, Jerusalem, Israel) diluted 1:200 in PBST-GS. Cells were then washed 3 times with PBS and incubated 1 h at RT with goat AlexaFluor647 anti-mouse secondary antibody (AbCam, UK, Cambridge) diluted 1:500 in PBST-GS. Coverslip were mounted with Fluoroshield (Sigma-Aldrich, Milan Italy) containing 49,6-diamidino-2-phenylindole (DAPI) to visualize cells nuclei. Immunocytochemical images were captured by a SP8 laser scanning confocal microscope (Leica Microsystems, Mannheim, Germany), using a 63X oil-immersion objective (NA 1.40) and the collected images were analyzed with an open source software (ImageJ, version 1.49v National Institutes of Health, Bethesda, MD, USA).

For DRG cultures, rabbit polyclonal A3AR-selective primary antibody (Alomone Labs, Jerusalem, Israel) was diluted 1:200 in bovine serum dilution buffer (450-mM NaCl, 20-mM sodium phosphate buffer, pH 7.4, 15% fetal bovine serum, and 0.3% Triton X-100) and incubated for 2.5 hours at RT. Cells were then washed 3 times with phosphate-buffered saline and incubated for 1 hour at RT with a donkey anti-rabbit secondary antibody (diluted 1:500 in bovine serum dilution buffer) conjugated to AlexaFluor 488 (Life Technologies, Invitrogen, Milan, Italy). Coverslips were mounted with Vectashield mounting medium (Vector Laboratories, Burlingame, CA) containing 49,6-diamidino-2-phenylindole (DAPI) to visualize cells nuclei, digitized, and acquired by using an Olympus BX40 microscope equipped with

CellSens Dimension Software (Olympus, Hamburg, Germany). Control experiments were performed by incubating fixed cells with the secondary antibody alone to exclude nonspecific binding.

In both cases, control experiments were performed by incubating fixed cells only with the secondary antibodies and DAPI in order to exclude nonspecific binding.

7. Intracellular Ca^{2+} measurement

Intracellular cytosolic Ca^{2+} dynamic ($[Ca^{2+}]_i$) was evaluated in fura-2–loaded DRG neurons as described (Di Cesare Mannelli et al., 2016). Briefly, 10^4 cells were plated on round glass coverslips (25-mm diameter) and seeded for 1 to 2 days in a complete medium. Cells were loaded with 4 mM fura-2AM (Molecular Probes-Invitrogen Life technologies, San Giuliano Milanese, Italy) for 45 minutes at 37°C and then washed with the K^+-containing standard extracellular solution described above. Coverslips were mounted in a perfusion chamber and placed on the stage of an inverted reflected light fluorescence microscope (Zeiss Axio Vert. A1 FL-LED) equipped with fluorescence excitation (385 nm) based on LED. Before electrical field stimulation, cells were incubated for at least 5 minutes with different solutions containing the following molecules: control (standard extracellular solution), 1 μM TTX + 200 nM A887826, 30 nM Cl-IB-MECA, and 1 μM verapamil + 0.5 μM PD173212. Fura-2 fluorescence was recorded with a Tucsen Dhyana 400D CMOS camera (Tucsen Photonics, Co, Ltd, Fuzhou, China) with a frame rate of 40 Hz and a resolution of 1024 x 1020 pixels^2. Ca^{2+} dynamic was measured by single-cell imaging analysis at 35°C (Di Cesare Mannelli et al., 2016).

Images were recorded using Dhyana software SamplePro and dynamically analyzed with the opensource community software for bio-imaging Icy (Institute Pasteur, Paris, France). Ca^{2+} transients were induced by electrical field stimulation at 0.1 Hz frequency, 100 mV voltage, and 50 ms width duration. Preliminary experiments were performed to optimize stimulation

parameters in control condition (standard extracellular solution). Frequency, voltage, and duration were chosen to obtain a high number of responder cells, defined as "spiking" cells, without signs of membrane electroporation and stable fura-2 fluorescence. A signal-to-noise ratio of at least 5 arbitrary units was considered as Ca^{2+} transient. Spiking DRG neurons were identified as cells showing at least 5 Ca^{2+} transients in 1 minute. In spiking cells, the following parameters were evaluated as the mean of at least 3 different Ca^{2+} transients: the ratio between the fluorescence maximal variation induced by electrical field stimulation and basal fluorescence ($\Delta F/F$, measured as arbitrary units) and the decay time of Ca^{2+} transient (tau, τ). Tau was calculated according to the following equation: $Y = y_0 + A \times e^{(-x/\tau)}$.

According to the fitting function, the tau (τ) parameter represented the time necessary for $[Ca^{2+}]_i$ to reach 36.8% of the maximal value. Tau was therefore reported as the decay time value (s). At least 3 Ca^{2+} transients for each different treatment were analysed and averaged. The cell diameter of analyzed DRG neurons was measured in pixels using ImageJ software and transformed in micrometer by a specific calibration scale. Experiments were repeated in 4 different neuronal preparations. All DRG neurons (identified by transmitted light microscopy) found in an optical field (using 40X magnification objective) were analyzed. From 16 to 22 cells were evaluated blindly every experimental day for each experimental treatment.

8. Drugs

Acetylcholine (**ACh**), carbachol (**CCh**), atropine (**atr**), pertussis toxin (**PTX**), **neostigmine**, **neomycin**, 4-aminopyridine (**4-AP**), **EGTA**, **apamin**, tetraethylammonium (**TEA**), 1,1-dimethyl-4-diphenylacetoxypiperidinium iodide (**4-DAMP**), 2-[[6-Amino-3,5-dicyano-4-[4-(cyclopropylmethoxy) phenyl]-2-yridinyl]thio]-acetamide (**BAY 60-6583**), 8-cyclopentyl-1,3-dipropylxanthine (**DPCPX**), 3-propyl-6-ethyl-5-[(ethylthio)carbonyl]-2 phenyl -4-propyl-3-pyridine carboxylate (**MRS1523**), 7-(2-phenylethyl)-5-amino-2-(2-furyl)-pyrazolo-[4,3-e]-1,2,4-triazolo[1,5-c]pyrimidine (**SCH58261**), 8-(4-(4-(4-

Chlorophenyl)piperazide-1-sulfonyl)phenyl)-1-propylxanthine (**PSB603**), 8-[4-[((4-Cyanophenyl)carbamoylmethyl)oxy]phenyl]-1,3-di(n-propyl)xanthine (**MRS1754**), 5-[4-phenyl-5-(trifluoromethyl)-2-thienyl]-3-[3-(trifluoromethyl) phenyl]-1,2,4-oxadiazole (**SEW2871**), (R)-3-amino-(3-hexylphenylamino)-4-oxobutylphosphonic acid (**W146**), **forskolin**, 2-Chloro-N6-(3-iodobenzyl)-adenosine-59-N-methyluronamide (**Cl-IB-MECA**), 5-(4-butoxy-3-chloro phenyl)-N-[[2-(4-morpholinyl)-3-pyridinyl] methyl]-3-pyridinecarboxamide (**A 887826**), N-(2-methoxyphenyl)-N9-[2-(3-pyridinyl)-4-quinazolinyl]-urea (**VUF5574**), N6-cyclopentyladenosine (**CPA**) and **adenosine** were purchased from Sigma/Merck Life Science S.r.l. (Milan, Italy).

Verapamil was purchased from Calbiochem (Merck, Darmstadt, Germany).

N-[[4-(1,1-Dimethylethyl)phenyl]methyl-N-methyl-L-leucyl-N-(1,1-dimethyl ethyl)-O-phenylmethyl)-L-tyrosinamide (**PD173212**) were purchased from Alomone Labs (Jerusalem, Israel).

Tetrodotoxin (**TTX**), N-(4-cyanophenyl)-2-[4-(2,3,6,7-tetrahydro-2,6-dioxo-1,3-dipropyl-1H-purin-8-yl)phenoxy]-acetamide (**MRS1754**) and N-(4-acetylphenyl)-2-[4-(2,3,6,7-tetrahydro-2,6-dioxo-1,3-dipropyl-1H-purin-8-yl) phenoxy]acetamide (**MRS1706**) were purchased from Tocris (Bristol, United Kingdom).

2-amino-2-[2-(4-octylphenyl)ethyl]-1,3-propanediol (fingolimod)-phosphate (**FTY720-P**) was purchased from Cayman Chemical (Michigan, USA)

Methoctramine was a kind gift from Dr. Rosanna Matucci (University of Florence) and Prof. Carlo Melchiorre (University of Bologna).

Amidine analogs that inhibits sphingosine kinase, **VPC96047** and **VPC96091**, were kindly provided by Prof. K. Lynch (University of Virginia, USA)

The new, highly selective, $A_{2B}R$ agonist 2-{[(1H-imidazol-2-yl)methyl]thio}-6-amino-4-[4-(cyclopropylmethoxy)phenyl]pyridine-3,5-dicarbonitrile (**P453**) was previously described (Betti et al., 2018; Fig. 14).

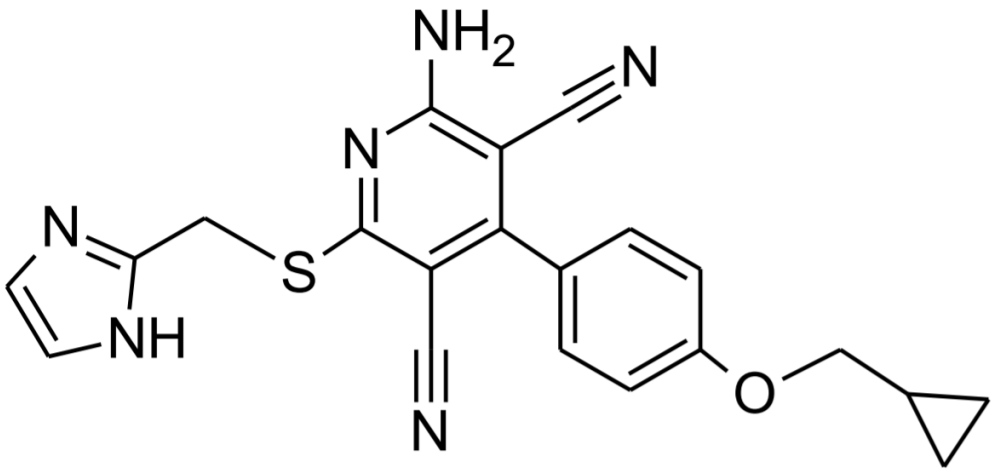

Figure 14. ***Chemical structure of the non-adenosine like $A_{2B}R$ agonist.*** (2-{[(1H-imidazol-2-yl)methyl]thio}-6-amino-4- [4-(cyclopropylmethoxy)phenyl]pyridine-3,5-dicarbonitrile) (**P453**).

The new, highly selective, A_3R agonist (1S,2R,3S,4R,5S)-4-(2-((5-chlorothiophen-2-yl)ethynyl)-6-(methylamino)-9H-purin-9-yl)-2,3-dihydroxy-N-methylbicyclo[3.1.0]hexane-1-carboxamide (**MRS5980**) was synthesized as reported previously (Fang et al., 2015; D. K. Tosh et al., 2014).

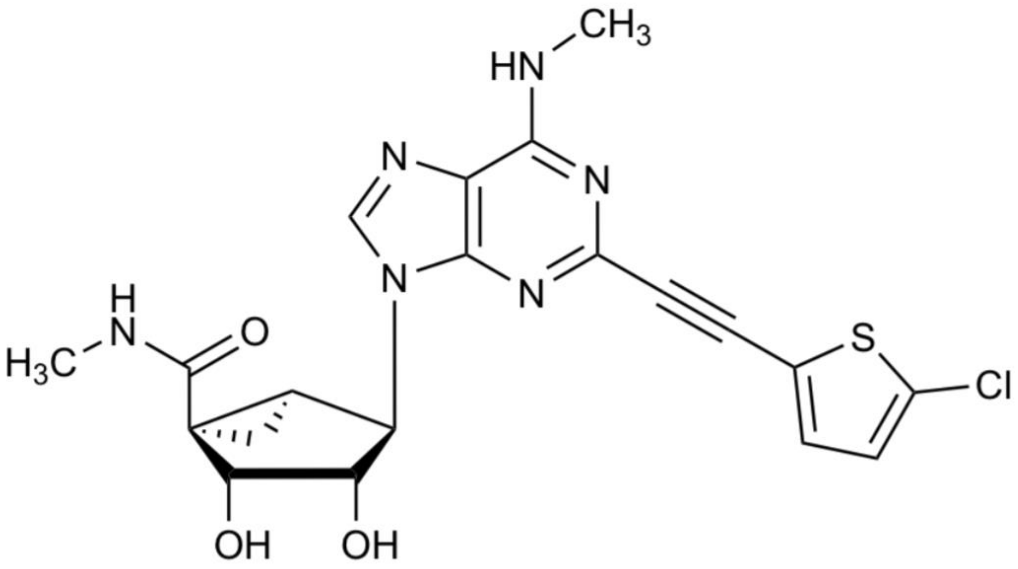

Figure 15. ***Chemical structure of the A3 receptor agonist.*** (1S,2R,3S,4R,5S)-4-(2-((5-chlorothiophen-2-yl)ethynyl)-6-(methylamino)-9H-purin-9-yl)-2,3-dihydroxy-N-methylbicyclo[3.1.0]hexane-1-carboxamide (**MRS5980**).

Ach, CCh, atropine, PTx, neostigmine, neomycin, 4-AP, EGTA, apamin, TEA, methoctramine, TTX were dissolved in distilled water.

4-DAMP, Cl-IB-MECA, A887826, MRS1523, VUF5574, DPCPX, CPA, PD173212, MRS5980, BAY 60-6583, SCH58261, PSB603, MRS1754, SEW2871, W146 and forskolin were dissolved in dimethyl sulphoxide (DMSO).

Control experiments were performed to confirm that the maximal concentration of DMSO used in our experiments was 0.1% and it did not alter electrophysiological properties nor drugs effects in hfNBM neuroblasts, OPCs nor DRGs.

All drugs were stored at -20°C as 10^3 to 10^4 times more concentrated stock solutions and dissolved daily in the extracellular solution to the final concentration and applied by bath superfusion.

	Drugs	Pharmacological activities	Provided by	IUPAC names
A_1R	**CPA**	Agonist	SIGMA	N6-cyclopentyladenosine
	DPCPX	Antagonist	SIGMA	8-cyclopentyl-1,3-dipropylxanthine
$A_{2a}R$	**SCH 58261**	Antagonist	SIGMA	7-(2-phenylethyl)-5-amino-2-(2-furyl)-pyrazolo-[4,3-e]-1,2,4-triazolo[1,5-c]pyrimidine
$A_{2A}R$	**BAY 60-6583**	Agonist	SIGMA	2-[[6-Amino-3,5-dicyano-4-[4-(cyclopropylmethoxy) phenyl]-2-yridinyl]thio]-acetamide
	P453	Agonist	Prof. Colotta, University of Florence	2-[[(1H-imidazol-2-yl)methyl]thio]-6-amino-4- [4-(cyclopropylmethoxy)phenyl]pyridine-3,5-dicarbonitrile
	MRS 1706	Antagonist	TOCRIS	N-(4-acetylphenyl)-2-[4-(2,3,6,7-tetrahydro-2,6-dioxo-1,3-dipropyl-1H-purin-8-yl) phenoxy]acetamide
	PSB-603	Antagonist	SIGMA	8-(4-(4-(4-Chlorophenyl)piperazide-1-sulfonyl)phenyl)-1-propylxanthine
	MRS 1754	Antagonist	SIGMA/TOCRIS	8-[4-[((4-Cyanophenyl)carbamoylmethyl)oxy]phenyl]-1,3-di(n-propyl)xanthine
A_3R	**Cl-IB-MECA**	Agonist	SIGMA	2-Chloro-N6-(3-iodobenzyl)-adenosine-59-N-methyluronamide
	MRS 5980	Agonist	Prof. Jacobson, NIH	1S,2R,3S,4R,5S)-4-(2-((5-chlorothiophen-2-yl)ethynyl)-6-(methylamino)-9H-purin-9-yl)-2,3-dihydroxy-N-methylbicyclo[3.1.0]hexane-1-carboxamide
	MRS 1523	Antagonist	SIGMA	3-propyl-6-ethyl-5-[(ethylthio)carbonyl]-2 phenyl -4-propyl-3-pyridine carboxylate

Table 7. Adenosine receptors ligands used in this thesis.

9. Data and Statistical analysis

Data are expressed as mean ± SEM (standard error of the mean). Two tailed Student's paired or unpaired t-tests or One-way ANOVA followed by Bonferroni post-test analysis were performed, as appropriated, in order to determine statistical significance ($P<0.05$).

In experiments of intracellular Ca^{2+} measurement, 3 different parameters were measured: (1) the ratio between DRG neurons defined as "spiking" (Ca^{2+} transient) and "not spiking" in each experimental condition; (2) $\Delta F/F$; and (3) tau of Ca^{2+} transient evoked in "spiking" cells. The effect of each treatment in changing the ratio between "spiking" and "not spiking" was evaluated using the X^2 test (PRIMER); other data (reported as mean ± SEM) were statistically analyzed using One-way ANOVA followed by Bonferroni analysis.

Data were analyzed using "Origin 10" (OriginLab, Northampton, Massachusetts, USA) or "GraphPad Prism" (GraphPad Software, San Diego, CA, USA) software.

Results and Discussions.

Aim I - *Electrical oscillatory activity and muscarinic effects on K^+ and Na^+ currents in human foetal cholinergic neurons from the nucleus basalis of Meynert*

Part of the following results were recently published in:

Coppi, E., Cherchi, F., Sarchielli, E., Fusco, I., Guarnieri, G., Gallina, P., Corradetti, R., Pedata, F., Vannelli, G.B., Pugliese, A.M., et al. (2020). ***Acetylcholine modulates K^+ and Na^+ currents in human basal forebrain cholinergic neuroblasts through an autocrine/paracrine mechanism.***
J. Neurochem. jnc.15209.

1.1. Electrophysiological characterization of a primary culture of hfNBM neuroblasts

Electrophysiological properties were recorded in hfNBM neuroblasts propagated up to p25, i.e. up to ~15 weeks in culture. As summarized in Fig. 16, cells exhibited stable passive and active membrane properties throughout this period of observation. Input resistance (Rin) and resting membrane potential (Vm) were not statistically different from p9 to p25 (Fig. 16A, B) and were, on average, 645.7 ± 48.7 MΩ (n=176) and -45.1 ± 1.6 mV (n=102), respectively. Cell capacitance (Cm: Fig. 16C), as directly proportional to cell size, significantly increased during the culture period starting from p20 and was, on average, 24.0 ± 2.4 pF from p9 to p18 (n=71) and 54.8 ± 3.5 pF from p20 to p25 (n=105). Active electrophysiological properties of hfNBM neuroblasts were also stable during cell culture: fast, TTX-sensitive Na^+ currents were present in about 64.3 % of cells (90 out of 140) from p9 to p25 and their amplitude was similar along passages (Fig. 16D-F). Overall voltage-dependent outward K^+ currents evoked by a voltage ramp protocol (Fig. 16G) were stable throughout cell culture (Fig. 16H) with an average amplitude of 2.9 ± 0.2 nA at +150 mV (n=85). A phase contrast image of typical hfNBM used for recording is shown in Figure 16I.

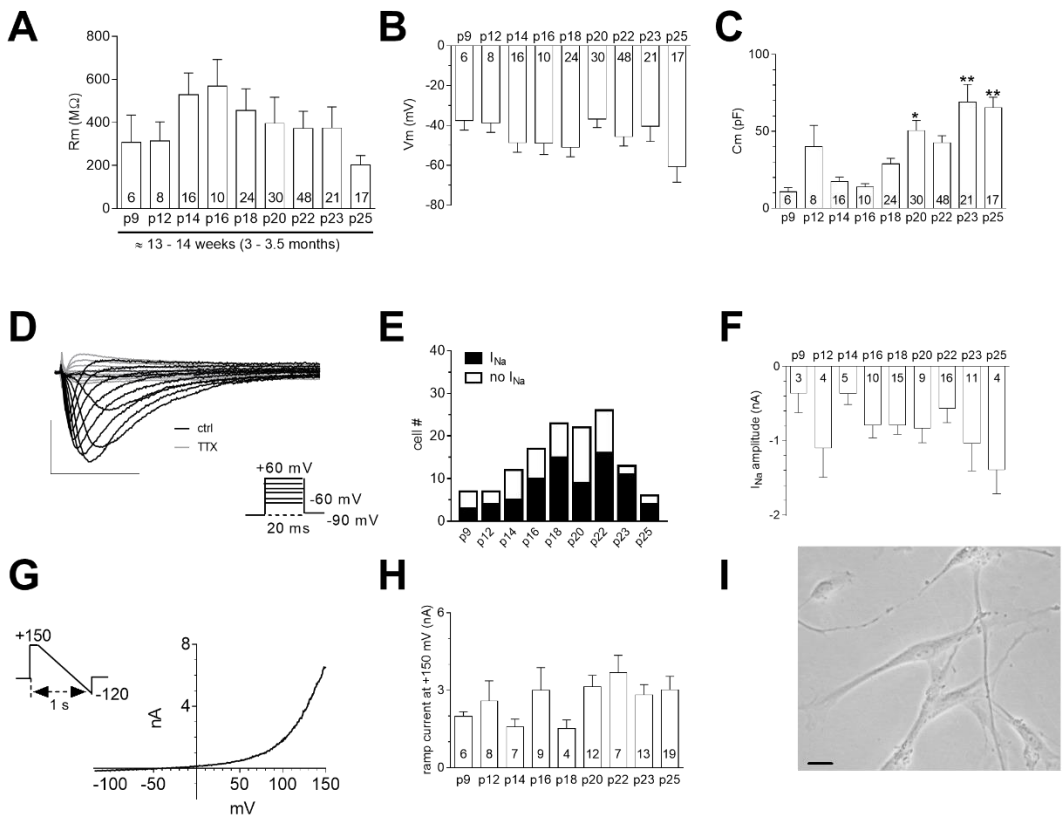

Figure 16. ***Electrophysiological properties of a primary culture of hfNBM neuroblasts.*** **A-C.** Pooled data of membrane resistance (Rm: **A**), resting membrane potential (Vm: **B**) and cell capacitance (Cm: **C**) measured in hfNBMs at different passages (p). *p<0.05 vs p9, p14, p16; **p<0.01 vs p9, p14, p16, p18, One-way ANOVA, Bonferroni's post-test. **D.** Original Na^+ current (INa) traces elicited in a hfNBM in the absence (control: ctrl) or presence of tetrodotoxin (TTX). Scale bars: 0.5 nA; 5 ms. **E.** Fraction of cells expressing (INa) or not expressing (no INa) Na^+ currents at distinct passages. **F.** Averaged INa amplitude was not different during cell culture. One-way ANOVA, Bonferroni's post-test. **G.** Original current trace elicited by a voltage ramp protocol. **H.** Averaged ramp-evoked outward currents measured at +150 mV in hfNBMs were not different at various passages. One-way ANOVA, Bonferroni's post-test. **I.** Phase contrast microphotograph showing cell morphology at p18. Number of cells is indicated inside the columns. Data are mean ± SEM.

1.2. *Effects of acetylcholine in hfNBM neuroblasts*

In previous work (Morelli et al., 2017) it was demonstrated the functional expression of nAChRs, whose activation elicits an inward current at -60 mV, and mAChRs, whose activation increases ramp-evoked K^+ currents. In the present work, we investigated the effect of ACh on hfNBM neuroblasts at different passages in culture to reveal whether significant changes in the response to the activation of these receptors by the physiological agonist occurred between p9 and p25. To this purpose, we recorded the response of

hfNBM neuroblasts to voltage ramps from -120 mV to + 150 mV (Fig. 17A, upper left inset). This permitted to simultaneously monitor possible modulation of inward (at -120 mV) and outward (at +150 mV) currents by ACh. Figure 17 illustrates the effects of ACh on ramp-activated outward currents in hfNBM neuroblasts from p9 to p25. Three different responses were observed. In the majority of cells (38 out of 73: 52.1%; Fig. 17A) application of ACh (20 µM, 5 min) produced an increase in ramp-activated outward currents that reached a steady-state level after 3 min and slowly reversed after drug washout. In a second group of cells (16 out of 73: 21.9%; Fig. 17B) we recorded a transient increase in ramp activated outward and inward currents. The effect peaked within the first minute of ACh application and rapidly faded before drug washout. In the third group of cells (19 out of 73: 26.0%; Fig. 17C) a combination of both responses was present. In the presence of the muscarinic antagonist atropine (100 nM, n=9), that *per se* did not elicit any effect on ramp-activated currents, the increase in +150 mV ramp-evoked currents elicited by Ach was fully antagonized in 5 cells. In the remaining 4 cells a transient increase in both inward and outward currents was recorded, indicating that the effect was mediated by nAChRs. On these bases, we define the former as a "muscarinic-like effect" of ACh, and the latter as a "nicotinic-like effect" of ACh on ramp currents. Figure 17E summarizes the panel of responses in the presence and in the absence of atropine. The relative distribution of the three responses to ACh application (i.e.: muscarinic-like, nicotinic-like, and both combined) did not show significant differences throughout cell passages (Fig. 17F).

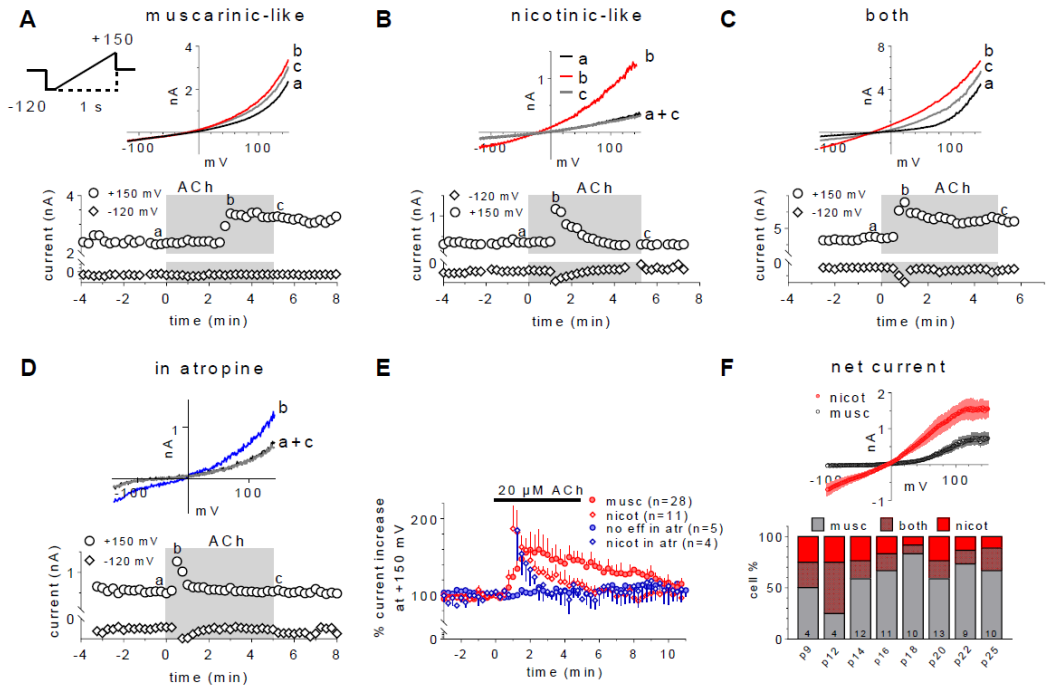

Figure 17. ***Effects of acetylcholine on ramp-activated currents in hfNBM neuroblasts.*** **A-C.** Representative time courses of whole-cell recordings illustrating three different responses to acetylcholine (ACh, 20 µM) application in subsets of hfNBM neuroblasts. Voltage ramps (from - 120 mV to + 150 mV; 1 s duration, every 15 s: see upper left inset in **A**) were imposed to hfNBM neuroblasts to simultaneously measure inward (at -120 mV) and outward (at +150 mV) currents during drug application (see also methods). **A.** Sustained, muscarinic-like, response (n=57) **B.** Rapidly desensitizing, nicotinic-like, response (n=16). **C:** Mixed, nicotinic-like and muscarinic-like, response (n=19). Note the simultaneous changes in inward and outward currents in **B** and **C**. Upper insets: original current traces recorded at time points indicated by letters in the corresponding time course. **D.** Representative time-course showing that the rapidly desensitizing response to ACh was not sensitive to atropine (atr: 100 nM), indicating nicotinic receptor activation. Note the simultaneous change in inward and outward currents. **E.** Effect of atropine on responses to ACh application. Averaged (mean ± SEM) time courses of ramp-activated outward currents measured at +150 mV and expressed as percent of baseline values in hfNBM neuroblasts at passages 9-25. In the presence of atropine (atr; 100 nM; n=9) neuroblasts showed either no response (n=5; blue circles) or fast desensitizing, nicotinic-like effect (nicot: n=4, open blue diamonds) to ACh application (20 µM). Muscarinic-like (musc: n=28, red circles) and nicotinic-like (n=11; open red diamonds) responses from parallel recordings in the absence of atropine are shown for comparison. **F.** Graph: Averaged ACh-activated net currents, obtained by subtraction of the control ramp from that recorded in ACh, during muscarinic (n=38, black trace) or nicotinic (n=35, red trace) responses. Histogram: fraction of cells showing muscarinic response (musc), nicotinic response (nicot) or both responses (both). No significant difference was found between groups, One-way ANOVA, Bonferroni's post-test. Numbers in the columns are the number of cells tested.

As hfNBM neuroblasts express high levels of the ACh degrading enzyme AChE (Morelli et al., 2017), the effect of ACh could be underestimated. Therefore, we applied ACh in the presence of the AChE inhibitor neostigmine (100 nM). As illustrated in Figure 18A, upon neostigmine application a slowly developing increase in ramp-activated outward currents (b, blue trace)

reminding the muscarinic-like response evoked by ACh itself was observed in all cells tested (n=6). ACh (20 µM), applied in the presence of neostigmine, elicited a further increase in ramp-activated outward currents (c, red trace). As summarized in Figure 18B, both these effects were prevented by atropine (100 nM: Fig. 18B, right panel), indicating their dependence on muscarinic receptor activation. As expected, the effect of ACh in neostigmine was significantly greater than that of ACh alone (Fig. 18C). Importantly, the effect of neostigmine itself was statistically significant indicating that, when AChEs are inhibited, endogenous ACh produced by hfNBM neuroblasts accumulates in the culture medium and activates AChRs. Notably, in 2 out of these 6 cells, the muscarinic-like effect of neostigmine was preceded by a transient increase in both inward and outward ramp-activated currents (Fig. 18D, E), characteristic of nicotinic receptor-mediated response in hfNBM cells (see: Morelli et al. 2017). Collectively, these data indicate that cultured hfNBM neuroblasts spontaneously release ACh which, in the presence of neostigmine, can activate nAChRs and/or mAChRs. This result is consistent with our previous observation that ACh is found in nM amounts in the culture medium of these cells (Morelli et al., 2017).

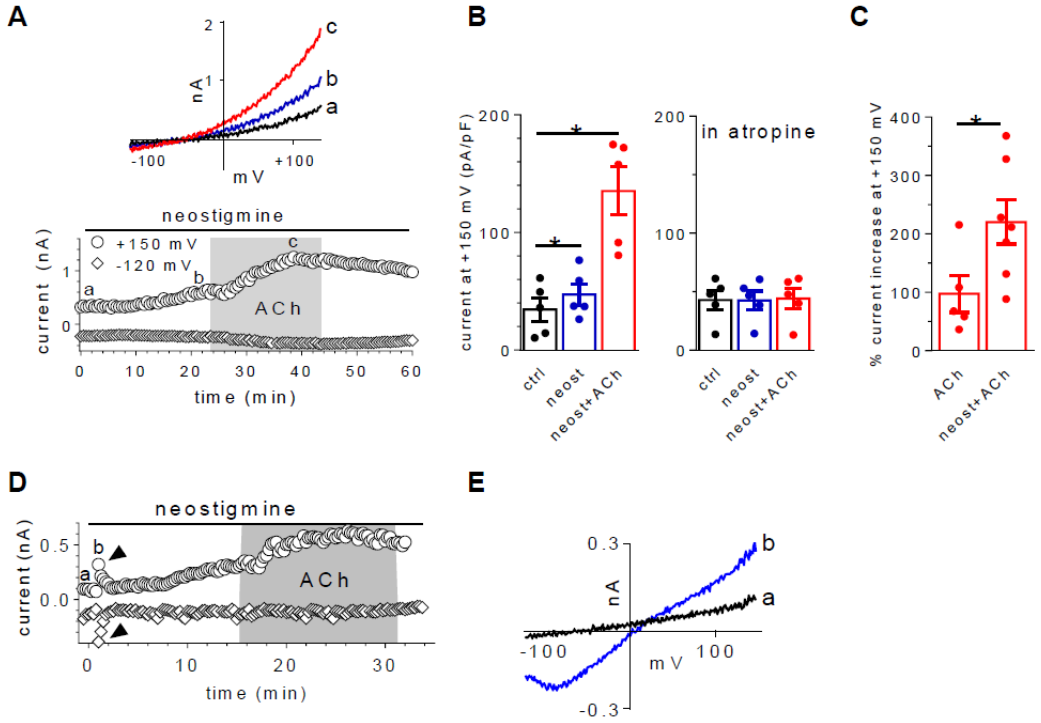

Figure 18. ***Block of acetylcholine-esterases reveals endogenous acetylcholine release and enhances the effect of acetylcholine application in hfNBM neuroblasts.*** **A.** Time course of ramp-activated currents recorded before, during, or after the application of the acetylcholine-esterase (AChE) inhibitor neostigmine (100 nM) alone or in combination with ACh (20 µM). Upper inset: original current traces recorded in the same cell at time points indicated by corresponding letters in the time course. **B.** Pooled data (mean ± SEM) of ramp currents measured at +150 in control (ctrl), neostigmine (neost) or neostigmine with ACh (neost + ACh) (n=5, left panel) or the same experimental conditions but in the presence of atropine (atr, n=5, right panel). *P < 0.05, paired Student's t-test. **C.** Pooled data of ACh-mediated effect (% increase of ramp-activated currents at +150 mV from the value measured during the last minute before ACh application) in the absence or presence of neostigmine. *P < 0.05, unpaired Student's t-test. **D.** Time course of ramp activated currents recorded before and during the application of the AChE inhibitor neostigmine (100 nM) applied alone or in combination with ACh (20 µM). Arrowheads indicate the transient nicotinic effect elicited by neostigmine. **E.** Original current traces recorded in the same cell at time points indicated by corresponding letters in the time course.

1.3. *Muscarinic M2 receptors modulate K⁺ conductance in hfNBM neuroblasts*

Next, we characterized the muscarinic receptors and the intracellular pathways implicated in the response of hfNBM neuroblasts to ACh by using the muscarinic agonist carbachol (CCh). CCh concentration-dependently increased ramp-activated outward currents (Fig. 19A, B) with an EC50 value of 1.7 µM (C.I.: 1.1 – 2.7 µM; Fig. 19C). The effect of CCh (50 µM) was prevented by atropine (100 nM; Fig 17D) confirming that the response to the agonist was

mediated by muscarinic receptors. Fig. 19D also summarizes the sensitivity of CCh-evoked responses to a variety of K^+ channel ligands. Thus, the K^+ currents modulated by CCh resulted insensitive to the small conductance Ca^{2+}-activated K^+ (SK) channel blocker apamin (100 nM) and to the inward rectifying K^+ (Kir) channel blocker Ba^{2+} (2 mM), but were blocked by the delayed rectifier K^+ channel blocker TEA (10 mM). We conclude that mAChR activation in hfNBM neuroblasts enhances TEA-sensitive K^+ currents.

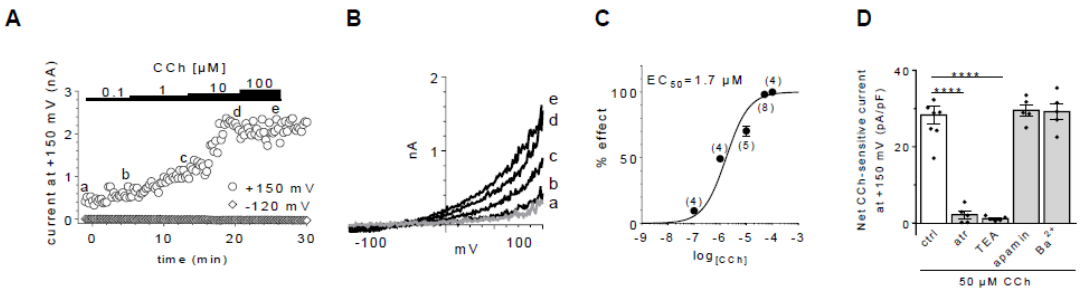

Figure 19. ***Effect of carbachol on ramp-activated K⁺ currents in hfNBM neuroblasts.*** **A.** Time course of carbachol (CCh) concentration-dependent effect on ramp-activated outward currents in a representative neuroblast. **B.** Original current traces recorded at points indicated by corresponding letters in the time course; same cell shown in **A. C.** Average concentration-response curve. Given are the mean ± SEM of at least 4 determinations. When not visible error bars are smaller than symbols. Curve represents the best fit to four-parameter logistic equation (see methods). The calculated EC_{50} of CCh effect on ramp currents is 1.7 µM (confidence limits: 1.1 - 2.7 µM). **D.** Pooled data (mean ± SEM) of net CCh (10 µM)-activated currents at +150 mV in control conditions (ctrl: n=8), in the presence of atropine (atr: 100 nM; n=5), in tetraethylammonium (TEA: 10 mM; n=5), in apamin (100 nM; n=5) or in Ba^{2+} (2 mM; n=5). One-way ANOVA, Bonferroni post-test.

In the attempt to elucidate the intracellular pathway/s involved in the action of CCh, we first recorded the effect of the agonist using patch pipettes containing 500 µM neomycin, known to prevent PLC activation (Felder et al., 1990). Intracellular neomycin did not significantly affect the response to CCh (10 µM; Fig. 20A) indicating that PLC was not involved in this specific effect of the agonist. Similarly, when the elevation of intracellular Ca^{2+} was prevented by the presence of BAPTA (10 mM) in the recording pipette, CCh still produced an increase in ramp-activated outward currents (Fig. 20B) indicating that intracellular Ca^{2+} mobilization was not required for the response to CCh. Finally, to test the dependence of CCh effect on G protein activation, we incubated hfNBM neuroblasts in pertussis toxin (PTx; 1 µg/ml,

overnight). In all neuroblasts recorded (n = 6). PTx treatment prevented CCh to affect ramp-activated outward currents (Fig. 20C) showing that the response in hfNBM neuroblasts was mediated by G_i/G_o–coupled, likely M2 and/or M4, receptors.

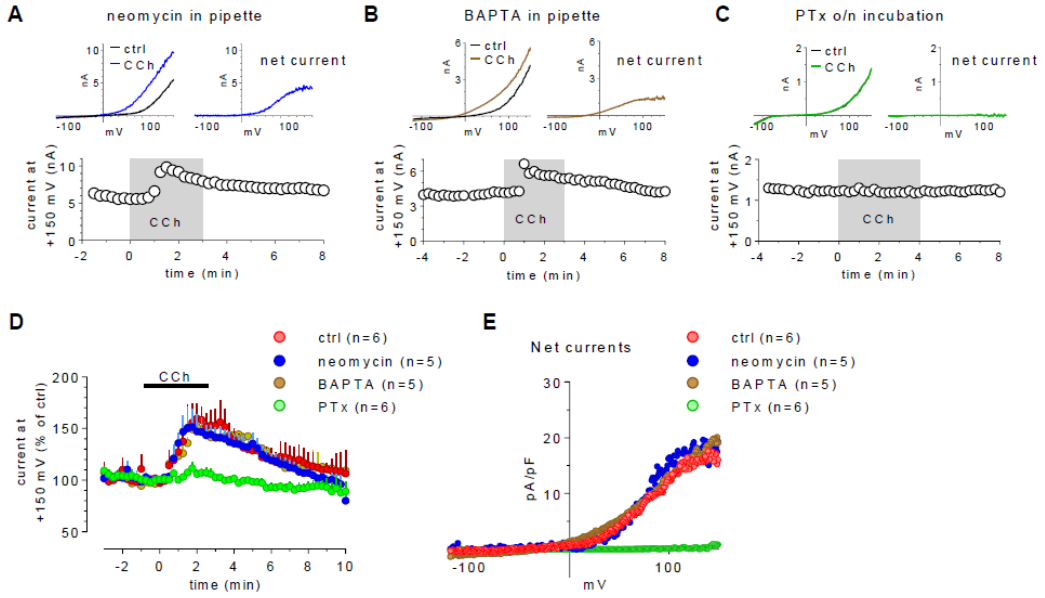

Figure 20. ***Carbachol-evoked increase of ramp-activated K⁺ currents in hfNBM neuroblasts is mediated by Gi protein activation.*** **A-C.** Time courses of carbachol (CCh: 10 µM)-mediated effect on ramp-activated K^+ currents in different experimental conditions: neomycin (500 µM)-containing pipettes (n=5) (**A**), BAPTA (10 mM)-containing pipettes (n=5) (**B**) or pertussis toxin (PTx: 1 µg/ml)-incubated cells (n=6) (overnight: o/n) (**C**). Upper insets: original current traces recorded in representative cells before (control: ctrl) or after CCh application (left panels) and respective net CCh-activated currents (right panels), obtained in each cell by subtraction of the control ramp from the ramp recorded in CCh. **D.** Averaged time courses of CCh-mediated effect in different experimental conditions. For the sake of clarity, error bars (SEM) are shown in a single direction. **E.** Averaged net CCh-activated currents measured in the same experiments shown in **D.** For the sake of clarity, error bars are not shown.

As the G_i/G_o-coupled M2 and the $G_{q/11}$-coupled M3 are the most abundant muscarinic receptors expressed by hfNBM neuroblasts (Morelli et al., 2017), we tested the sensitivity of CCh effect to the selective M2 antagonist methoctramine (1 µM: Fig. 21A) and to the selective M3 blocker 1,1-dimethyl-4-diphenylacetoxypiperidinium iodide (4-DAMP; Fig. 21B). Both compounds did not modify ramp-activated K^+ currents *per se*. Consistently with PTx block, CCh-mediated effect on K^+ currents was significantly antagonized by metochtramine but not by 4-DAMP, (Fig. 21C, D) demonstrating the involvement of M2, but not M3, mAChRs.

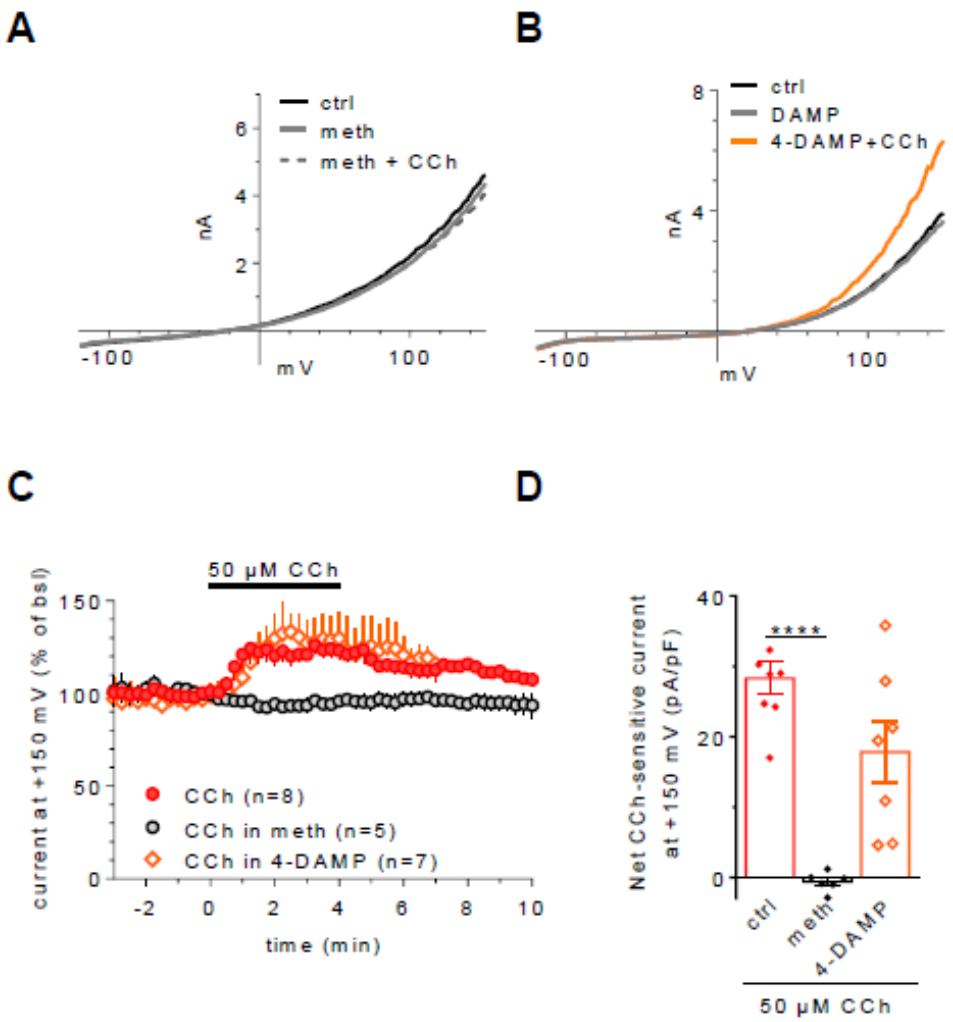

Figure 21. ***The M2 muscarinic receptor subtype is responsible for the increase in K⁺ current induced by carbachol in hfNBM neuroblasts.*** **A-B.** Original current traces recorded in typical cells where carbachol (CCh: 50 µM) was applied in the presence of the M2 antagonist methoctramine (meth: 1 µM: **A**) or the M3 antagonist 4-DAMP (1 µM: **B**). **C.** Averaged (mean ± SEM) time courses of net ramp-activated currents in hfNBM cells in different experimental conditions. Data are expressed as % of control (ctrl). For the sake of clarity, error bars (SEM) are shown in a single direction. **D.** Pooled data of net CCh activated currents at +150 mV, obtained by subtraction of the control ramp from the ramp recorded in CCh, in control conditions (ctrl: n=8), in 1 µM methoctramine (n=5) or in 1 µM 4-DAMP (n=7). **** P <0.0001, One-way ANOVA, Bonferroni post-test.

1.4. Muscarinic M3 receptors decrease Na⁺ currents in hfNBM neuroblasts

The effect of cholinergic agonists on Na^+ currents in hfNBM neuroblasts was tested in conditions of K^+ channel block by Cs^+ replacement (see methods). As

shown in Figure 22, Na^+ currents elicited by single voltage steps (from -90 mV to 0 mV; 40 ms) were efficiently isolated in these experimental conditions and were concentration-dependently inhibited by CCh (1-50 µM) and ACh (1-50 µM). Both effects were fully antagonized by atropine (100 nM; Fig. 22A, B), showing that inhibition of Na^+ currents was produced by activation of muscarinic receptors. Similar results were obtained when Na^+ currents were evoked by a sequence of depolarizing voltage steps (from -90 mV to +60 mV; 40 ms) to investigate muscarinic modulation in a wider range of membrane potentials (Fig. 22C-F).

To further define the characteristics of Na^+ current modulation by muscarinic receptors we have studied the effects of ACh (50 µM) and CCh (50 µM) on activation and inactivation properties of Na^+ currents. As illustrated in Fig. 22G-J, ACh, (Fig. 22G, H) but not CCh (Fig. 22I, J), caused a depolarizing shift in the activation curve and a hyperpolarizing shift in the inactivation curve.

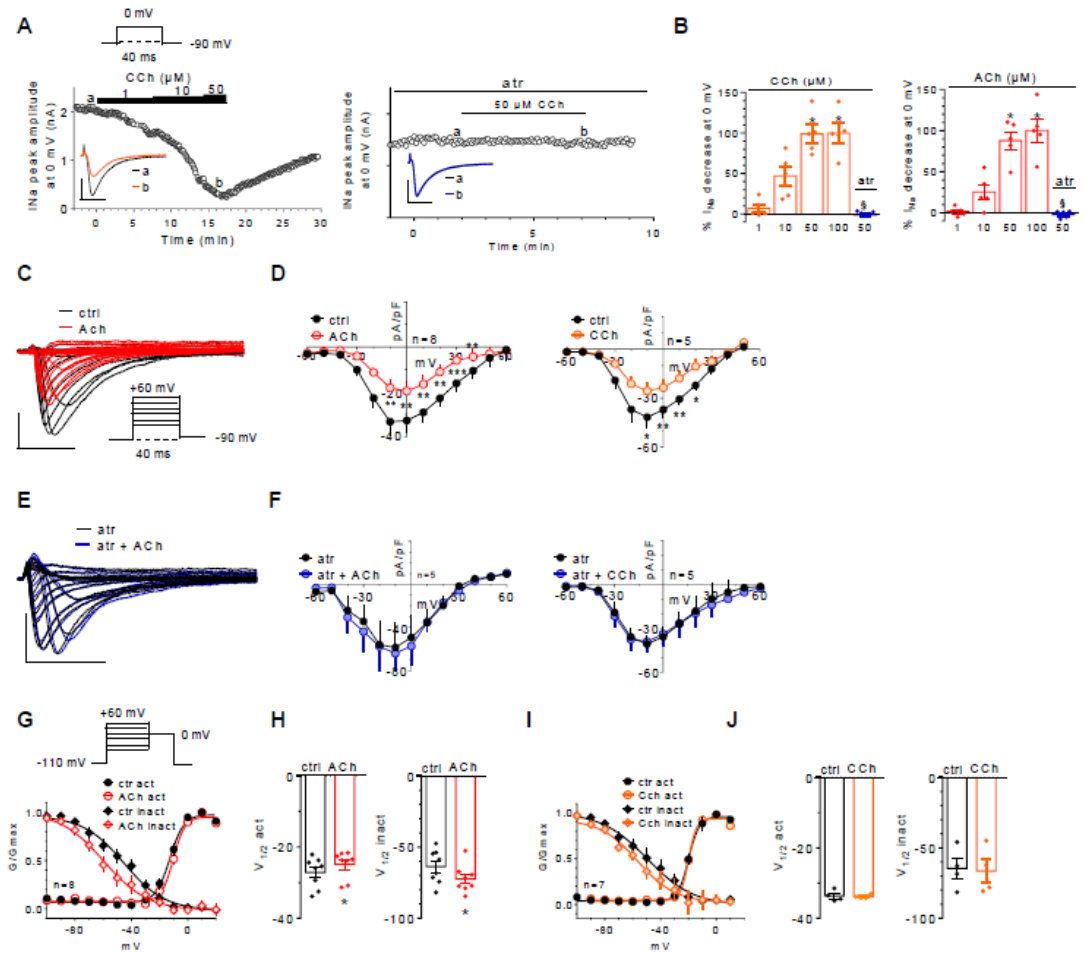

Figure 22. ***Muscarinic receptor activation by acetylcholine or carbachol decreases Na⁺ currents in hfNBM neuroblasts.*** **A.** Time courses of carbachol- (CCh)-mediated effect on Na^+ current (INa) elicited by voltage pulses (upper diagram) in the absence (left panel) or in the presence (right panel) of atropine (100 nM). Insets: original INa traces recorded at time points indicated by letters in the corresponding time-course. Scale bars: 1 nA, 5 ms. **B.** Pooled data (mean ± SEM) of CCh- (left panel; n=5) or acetylcholine- (ACh: right panel; n=8) mediated INa decrease at different concentrations or in the presence of atropine (atr; 100 nM). Data were expressed as % INa decrease. * P <0.05 vs 1 µM CCh (left panel) or 1 µM ACh (right panel). § P <0.05 vs 50 µM CCh (left panel) or 50 µM ACh (right panel); One-way ANOVA, Bonferroni post-test. **C-F.** Original current traces (**C,E**) and averaged I-V plots (**D,F**) recorded before and during ACh (50 µM) or CCh (50 µM) applied alone (**D**) or in the presence of 100 nM atropine (**F**). Paired Student's t-test. Scale bars: 0.5 nA, 5 ms. **G,I.** Activation and inactivation curves elicited by a depolarizing voltage step protocol (from -100 to +60 mV, 40 ms; final step = 0 mV: upper inset) in ACh (G, n=8) or CCh (I, n=7) compared to control conditions (ctrl). Lines represent fittings with Boltzmann equation. **H,J.** Pooled data of half-activation ($V_{1/2}$ act) or half-inactivation ($V_{1/2}$ inact) voltages in ctrl and in the presence of ACh (**H**, n=8) or CCh (**J**, n=7). Note that ACh significantly modifies $V_{1/2}$ act and $V_{1/2}$ inact. Activation curve: $V_{1/2}$ = -27.2 ± 1.5 mV in ctrl and -24.0 ± 1.4 mV in ACh; *P < 0.05; paired Student's t-test; slope factor = 5.0 ± 0.6 in ctrl and 4.2 ± 0.6 mV in ACh, P > 0.05; paired Student's t-test; ACh inactivation curve: $V_{1/2}$ = -63.8 ± 4.2 mV in ctrl and -72.4 ± 3.4 mV in ACh; P < 0.05, slope factor = 14.5 ± 1.7 in ctrl and 15.6 ± 2.2 mV in ACh; P > 0.05; paired Student's t-test, n=8. Data are mean ± s.e.m.

In order to depict the intracellular signaling pathway/s involved in the modulation of Na^+ current amplitude by muscarinic receptor activation, we tested the effects of CCh (50 µM) in hfNBM neuroblasts incubated in PTx overnight or using patch pipettes containing neomycin in control conditions. As illustrated in Fig. 23A, G_i/G_o protein block was ineffective in preventing Na^+ current reduction by CCh, whereas the effect was fully blocked by neomycine showing that PLC pathway was involved in the effect. Furthermore, the action of CCh was abolished by the selective M3 receptor antagonist 4-DAMP (1 µM; Fig. 23B), demonstrating that the effect of CCh was mediated by the M3 mAChRs.

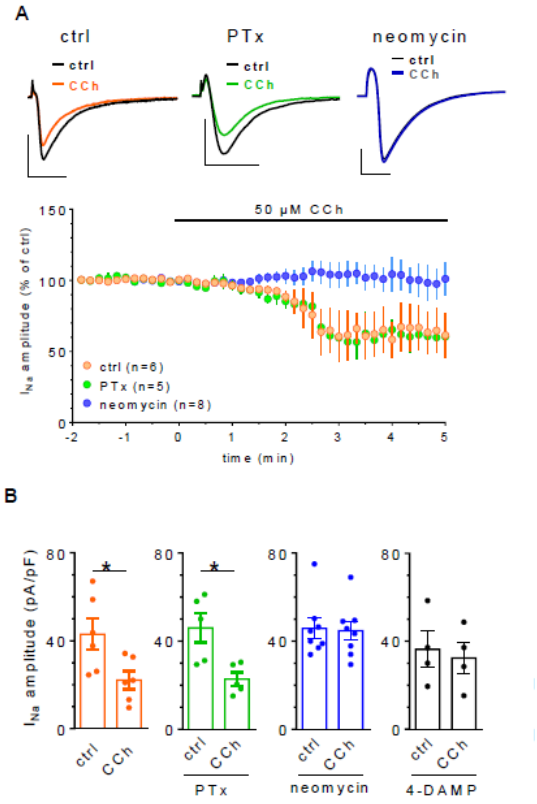

Figure 23. ***Muscarinic M3receptors inhibit Na+ currents in hfNBM neuroblasts by activating phospholipase C.*** **A.** Averaged time courses of Na^+ current (INa) amplitude recorded before, during or after the application of carbachol (CCh: 50 µM) in control conditions (ctrl; n=6), in cell incubated with pertussis toxin (PTx: 1 µg/ml overnight; n=5) or in cells patched with neomycin (500 µM)-containing pipettes (n=8). Upper insets: original current traces recorded before or at the end of CCh application in representative cells. Scale bars: 1 nA, 5 ms. **B.** Pooled data (mean ± SEM) of INa amplitude recorded before (ctrl) or at 5 min of CCh (10 µM) application in different experimental conditions. 4-DAMP shows the effect of CCh in the presence of the selective M3 blocker 1,1-dimethyl-4-diphenylacetoxypiperidinium iodide. *P < 0.05, paired Student's t-test.

1.5. An oscillatory activity in membrane voltage was observed in hfNBMs upon depolarizing current injection

Finally, we studied the electrical activity of hfNBMs in the current-clamp mode. For these experiments, a physiological-like, low-EGTA (0.1 mM) containing, pipette solution was used, at variance from that used in voltage-clamp experiments previously described (10 mM EGTA). To our surprise, as shown in Figure 24, we observed an oscillatory activity in membrane voltage upon positive current injection in hfNBMs, which, to our knowledge, has never been described before in neuronal cells. In particular, we observed three different responses, as follow. In a group of cells (18 out of 30), an oscillatory, periodic-like activity was recorded upon depolarizing current injections (Fig. 24A). These oscillations were defined by us “voltage waves" and were observed between 100 and 900 pA of injected current, depending on cells. Voltage waves presented an averaged frequency of 89.4 ± 14.7 Hz and an amplitude of 148.2 ± 6.1 mV (values measured at +500 pA step, n=18). No evidence of frequency accommodation was detected up to 1 s of current injection (Fig. 24E). A second, minor group of cells (3 out of 30) presented a single, immature action potential (AP) evoked at current values between 700 and 900 pA (Fig. 24B). A third group of cells (6 out of 30) presented both phenomena, with the single AP being evoked at higher current values, where voltage waves disappeared (Fig. 24C). In the 3 (out of 30) remaining cells, no electrical activity was recorded. Of note, only 1 cell (at p12) was found to fire multiple APs (and up to 11 APs at 600 pA current injection: Fig. 24F). In that case, however, multiple APs clearly accommodated during the 500 ms of current injection. Considering all oscillating cells (18 of 30 with waves only and 6 with waves plus single AP), it appears that the majority of hfNBMs (24 out of 30 cells: 80%) presented voltage waves (Fig. 24D). No difference was found in wave frequency nor amplitude at different passage in culture, as shown in Figure 24G.

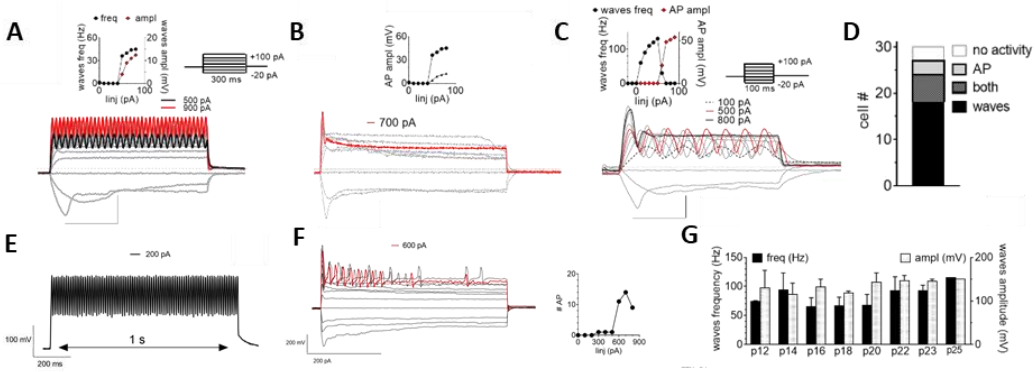

Figure 24. ***Electrical activity in hfNBMs.*** **A-C.** Original voltage traces recorded in the current-clamp mode in a representative hfNBMs where a rhythmic oscillatory activity (**A**), a single action potential (AP: **B**) or both events (**C**) were observed. Upper panels: oscillation parameters (waves frequency: waves freq; waves amplitude: waves ampl) or AP amplitude are plotted vs the current injected. **D.** Fraction of cells examined showing voltage waves, a single AP, both phenomena or no electrical activity. **E.** Original voltage traces recorded in the current-clamp mode in a representative hfNBM neuroblast where the current injection (200 pA) was prolonged to 1 s. No signs of wave frequency accommodation were observed. **F.** Left panel: Original voltage traces recorded in the current-clamp mode in a representative hfNBM neuroblast where multiple action-potential-like waveforms of activity were evoked by a depolarizing current step protocol (from 0 to +800 pA current injection, 500 ms). Right panel: the number of AP (right y axis) were pooled as a function of the current injected in the same cell. **G.** Averaged values of waves frequency or amplitude were not different during the period of observation. One-way ANOVA, Bonferroni post-test.

Of note, only 10 out of the 30 oscillating cells also express INa currents when investigated in the voltage-clamp mode. Differently, when considering the totality of cells presenting the single AP (9 out of 30 cells: 30 %; 3 cells with AP only plus 6 cells with AP plus waves), the majority of them (7 out of 9 cells) also expressed INa. Of note, TTX was unable to prevent single AP either in 4 cells tested, even if efficiently prevented INa in the same cell (Fig. 25A). All cells recorded in the current-clamp mode presented a negative peak at hyperpolarizing current values. The peak waveform was sharp at -200 pA whereas it assumed a rounded shape at -100 pA values, resembling the Ih-dependent "sag". Consistently with this observation, the -200 pA-elicited negative peak was insensitive to the Ih blocker ZD7288 (50 μM: Fig. 25B, left panel), whereas the -100 pA-elicited "sag" was significantly reduced by the Ih blocker ZD7288 (50 μM: Fig. 25B, right panel). Similar results were obtained with 100 μM ZD7288 (n=3, data not shown). Of note, TTX (1-10 μM) was unable to block voltage oscillations (Fig. 25D: left and central panels and upper inset and Fig. 25E). Similarly, a subsequent application of the voltage-

dependent Ca^{2+} channel (Ca_V) blocker Cd^{2+} was unable to block voltage oscillations (1 mM: Fig. 25D: right panel). Figure 25E shows pooled data demonstrating that neither TTX, Cd^{2+}, nor the combination of both compounds was able to affect voltage waves in hfNBMs. We then tested the effect of intracellular Ca^{2+} chelation by using a high (10 mM) EGTA-containing pipettes. In these experimental conditions, the fraction of voltage wave-presenting cells was greatly reduced (11 out of 46 cells investigated: 24%; Fig. 25F upper panel). The population of single AP-expressing cells in these conditions was unchanged (12 out of 46 cells: 26%). No electrical activity was found in 23 out of 46 cells recorded in high EGTA. Since BAPTA is more effective as a Ca^{2+} chelator than EGTA, we repeated above experiments by using high BAPTA (10 mM)-containing pipettes. As shown in figure 25F and 25G (left panel), none of the 8 cells tested in 10 mM BAPTA oscillated whereas 2 of them presented a single AP (not shown). It is worth to note that, once initiated, voltage waves were not different in low (0.1) or high (10 mM) EGTA conditions in terms of frequency (Fig. 25G right panel, filled columns, left y axis) or amplitude (dotted columns, right y axis). It appears that intracellular Ca^{2+} chelation reduces the fraction of oscillating hfNBMs.

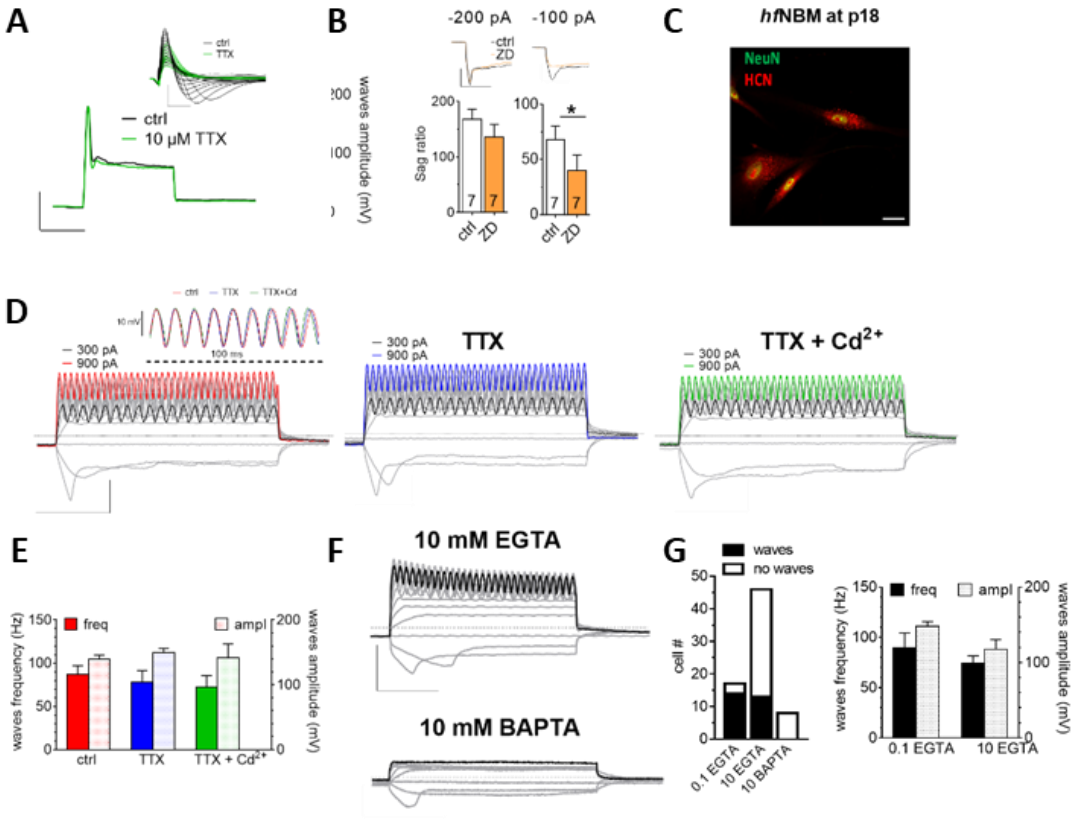

Figure 25. ***Only intracellular Ca^{2+} chelation reduces the fraction of oscillating hfNBMs.*** **A.** Original voltage traces recorded in a representative cell where a TTX-insensitive AP was elicited at +800. Scale bars: 100 mV; 20 ms. Upper inset: TTX abolished INa in the same cell. Scale bars: 1 nA; 10 ms. **B.** Pooled data of sag ratio recorded at -200 pA (left panel) or -100 pA (right panel) in control (ctrl) or in 50 µM ZD7288; *p < 0.05, paired Student's t-test. Upper insets: respective original current traces. **C.** Representative image of hfNBMs at p18 expressing HCN3 channels (red) and the nuclear neuronal marker NeuN (green). **D.** Original voltage traces recorded in a representative hfNBM in the absence (left panel) or presence of tetrodotoxin (TTX) alone (central panel) or in co-application with Cd^{2+} (right panel). **E.** Averages voltage waves parameters, measured at 900 pA of current injection, were not different in distinct experimental conditions. One-way ANOVA, Bonferroni's post-test. **F.** Original voltage traces recorded in a representative hfNBM in a high-EGTA (10 mM)-containing pipette (upper panel) or in a BAPTA (10mM)-containing pipette (lower panel). **G.** *Left panel*: the fractions of cells presenting or not voltage waves in different experimental conditions were quantified. *Right panel*: averaged waves frequency or amplitude were not different in 0.1 or 10 mM EGTA. Unpaired Student's t-test. Number of cells is indicated inside the columns. Data are mean ± SEM.

In order to describe the ionic current/s subtending voltage oscillations, we used a less invasive protocol consisting in a single step at +500 pA (500 ms duration) repeated once every 30 s to obtain reproducible oscillations during a relatively long time (up to 30 min: Fig. 26).

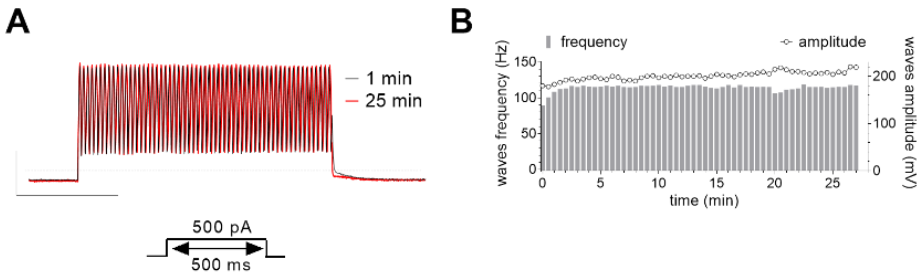

Figure 26. ***Long-term recording of stable voltage waves in a typical hfNBM neuroblast.*** **A.** The frequency (left y axis) and amplitude (right y axis) of voltage waves was pooled as a function of time in a representative cell where a stable recording was performed up to 30 min by using a single step protocol of 500 pA current injection (500 ms duration: inset of B). **B.** Original voltage traces recorded in the same cell at the beginning (1 min: black trace) or after 25 min (red trace) of current-clamp recording.

Sensitivity of voltage oscillations to different channel blockers and/or receptor agonists and antagonists was than tested. As shown in Figure 27, oscillations were unaffected by cholinergic agonists (Ach 50 µM; Fig. 27A and B, right panel) or antagonists (atropine 100 nM: Fig. 27A and B, right panel), as well as by the Ih blocker ZD7288 (Fig. 27C and D, upper right panel). On the contrary, oscillations were completely blocked by a high concentration (10 mM) of the unselective K^+ channel blocker TEA (Fig. 27A and B, right panel). Among the subtype/s of K^+ channels possibly involved in voltage waves, on the basis of their sensitivity to BAPTA and EGTA, likely candidates are Ca^{2+}-activated K^+ channels. Accordingly, the selective blocker of big-conductance Ca^{2+}-activated K^+ (BK) channels iberiotoxin completely prevented voltage waves initiation (200 nM: Fig. 27C and D, upper left panel). The involvement of BK channels in this phenomenon was confirmed by its sensitivity to a low concentration (0.2 mM) of TEA (Fig. 27C and D, lower left panel), which is known to selectively block this channel subtype without interfering with delayed rectifier IK conductances. Both IbTx and TEA effects were rapidly reversed upon washout (Fig. 27A, C). Of note, also the Kir channel blocker Ba^{2+}, applied at 2 mM concentration, efficiently blocked voltage waves but its effect was not reversed by up to 10-15 min washout in 4 cells tested (Fig. 27C and D, lower right panel) probably because, differently from TEA, it caused massive depolarization of resting membrane potential leading cells to death. None of the drugs tested

significantly affected cell resting membrane potential excluded Ba^{2+}, which significantly depolarized hfNBMs (Fig. 27I). Finally, in conditions of intracellular Ca^{2+} stores depletion by thapsigargin (1 μM), voltage waves transiently disappeared as long as the compound dialyzed cell cytoplasm, i.e. 7 - 8 min after seal breakthrough (Fig. 27E and F, left panel) (Thastrup et al., 1990). After this period, waves recurred with a significantly slower frequency (Fig. 27E-G) and with a different shape (Fig. 27F right panel), but unchanged amplitude (Fig. 27G). Under these experimental conditions, 1 mM Cd^{2+} was sufficient to abolish oscillations (Fig. 27E and F, right panel, and 27G). Only 1 out of 5 cells tested with intracellular thapsigargin did not show any oscillatory activity. Consistently with current-clamp results, immunocytochemical analysis revealed the expression of BK channels in hfNBM culture (Fig. 27H).

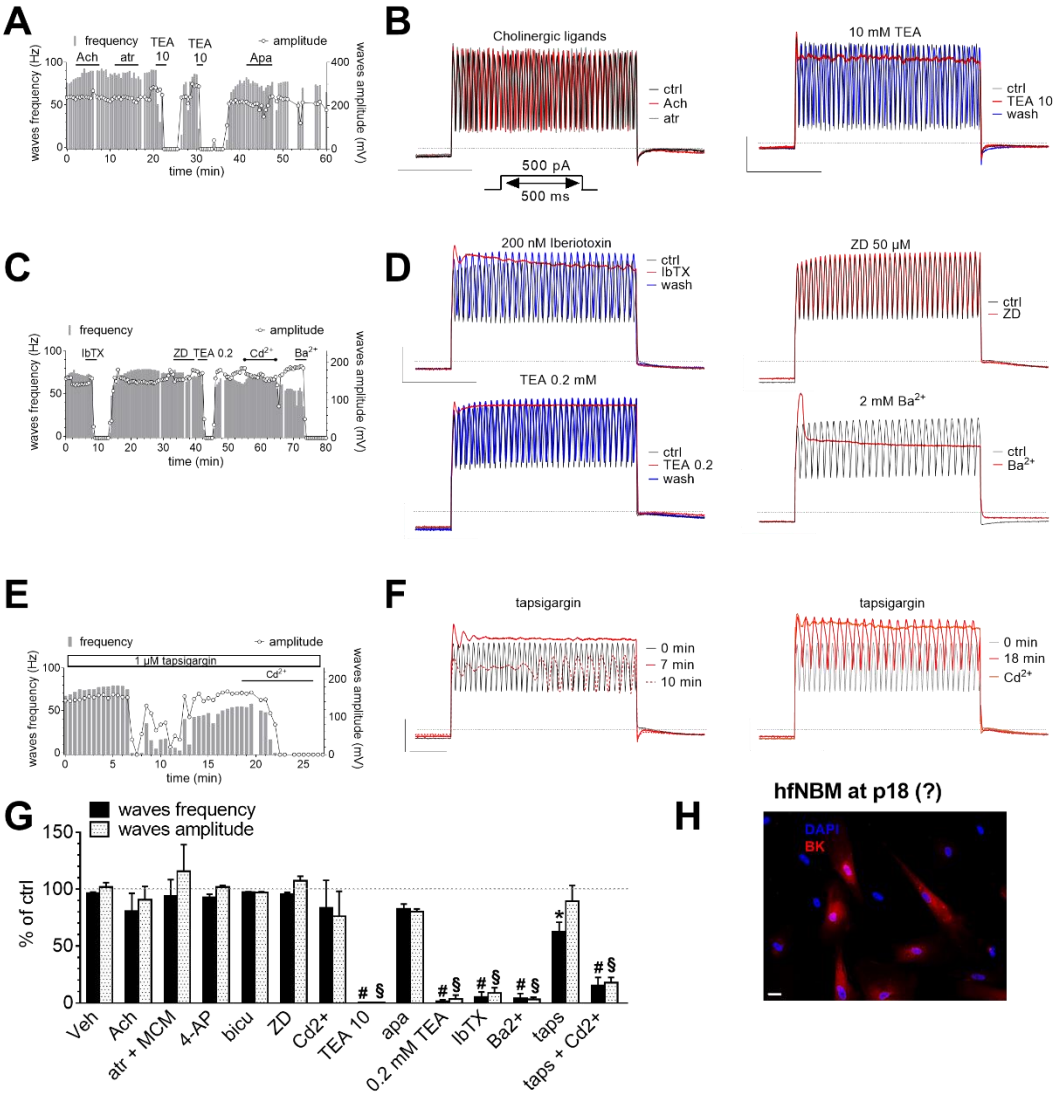

Figure 27. ***Voltage waves recorded in hfNBMs are prevented by BK or Kir channel inhibition and are impaired by thapsigargin.*** **A, C, E.** The frequency or amplitude of voltage waves were pooled as a function of time in representative hfNBMs. **B, D, F.** Original voltage traces recorded in respective cells. Acetylcholine (Ach); atropine (atr); tetraethylammonium (TEA); Iberiotoxin (IbTx); ZD7688 (ZD); thapsigargin (taps) effect was measured at different times after seal breakthrough (0, 7, 10 and 18 min) (**F**). **G.** Pooled data of waves frequency or amplitude expressed as % of ctrl. *p<0.05; #p<0.0001 vs Veh for frequency; §p<0.0001 vs Veh for amplitude, One-Way ANOVA, Bonferroni's post-test. Vehicle (Veh; n=4) was 0.1% phosphate buffer saline (PBS). MCM (mecamilamine) 10 µM; 4-AP (4-amino-pyridine): 1 mM; bicu (bicuculline): 1 µM; apa (apamin). **H.** Representative image of hfNBMs at p20 expressing BK channels (red) and the nuclear neuronal marker NeuN (green).

1.6. Discussion

In the years of my doctorate, I contributed to provide detailed electrophysiological characterization of hfNBM neuroblasts kept in culture up to 3.5 months (p25). Our results indicate that these cells spontaneously release ACh and that activation of G_i/G_o-coupled M2 mAChRs positively modulates voltage-dependent K^+ currents whereas stimulation of $G_{q/11}$ protein-coupled M3 receptors produces inhibition of Na^+ currents via PLC-dependent mechanism(s). A detailed description of hfNBM cultures as cholinergic neuroblasts is provided in our previous work (Morelli et al., 2017). Here we characterized major passive and active membrane properties in hfNBM neuroblasts at increasing passages to describe whether or not the culture underwent functional maturation. Our results show that immature electrophysiological properties (i.e. a relatively depolarized resting membrane potential and the lack of TTX-sensitive action potentials) were maintained for at least 3 months in culture, regardless the number of passages and in vitro proliferation of these cells. Only cell capacitance showed significant increase during hfNBM cell culture starting from p20, indicating an increase in cell size, in line with previous data (Lepski et al., 2011). Furthermore, the expression of INa only in a portion of cells is in line with that reported by Lepski and co-workers in similar human fetal-derived neuronal progenitor cells (Lepski et al., 2011). However, it is at variance from what reported by Sah in human fetal neurons isolated from the whole brain (Sah, 1995) where all cells investigated expressed Na^+ currents. We hypothesize that differences in the isolation (i.e. NBM vs whole brain) or cell maintenance (absence of mitogens vs N2/fibroblast growth factor-supplemented medium) could justify this discrepancy. Consistent with the expression of both nAChRs and mAChRs in our hfNBM cell culture (Morelli et al., 2017), ACh modulated voltage-dependent currents in hfNBM neuroblasts by activating either or both mAChRs and nAChRs and these effects remained constant throughout culture passages. An important finding was that endogenous ACh released by hfNBM

neuroblasts is able to activate both mAChRs and nAChRs. Indeed, exposure of cells to the AChE inhibitor neostigmine produced a small but significant atropine-sensitive muscarinic-like effect. In addition, a rapidly-desensitizing nicotinic-like response was occasionally observed upon neostigmine application. It should be considered that these data were obtained in continuously perfused (1.5 ml/min) cells, so the relatively small effect of neostigmine on ramp currents could be underestimated by partial wash out of the endogenously released ACh. These results indicate that cultured hfNBM neuroblasts spontaneously release ACh which is actively hydrolyzed by AChEs. Consistently, nanomolar levels of ACh were detected in the culture medium of these cells (Morelli et al., 2017). Of note, as this value was measured in the absence of AChE inhibitors, it might be underestimated. The lack of effect of atropine per se on ramp currents confirms rapid ACh degradation by AChE activity in hfNBM cultures. In fully developed cholinergic neurons of the NBM, stimulation of AChRs modulates excitability and firing activity likely influencing the cholinergic system output in cortical areas (Khateb et al., 1997; Zhang et al., 2000). However, the existence of an active ACh release and expression of a panel of AChRs in this immature phase of neuronal development suggests that autocrine/paracrine ACh release could participate in migration and/or differentiation, maturation and neuronal specification of hfNBM neuroblasts within NBM in vivo (Abreu-Villaça et al., 2011). However, since there are extrinsic sources of ACh in the in vivo BF (e.g., from brainstem), the specific role of autocrine ACh release in NBM development remains to be better clarified. In our work, we characterized mAChR subtypes responsible for the action of ACh on hfNBM neuroblasts by using the selective muscarinic agonist CCh. Although activation of nAChR by high concentrations of CCh has been reported (Liu et al., 2007; Nguyen et al., 2013), this action was not apparent in hfNBM cultures because all CCh-mediated effects were blocked by atropine. Consistent with relatively abundant expression of M2 and M3 mAChR subtypes in hfNBM cell cultures (Morelli et al., 2017), we found two distinct atropine-sensitive muscarinic responses in these cells. Namely,

stimulation of the M2 receptor subtype activates a G_i/G_o protein responsible for the enhancement of a TEA-sensitive, Ba^{2+}- and apamine-insensitive, K^+ current whereas the stimulation of $G_{q/11}$-coupled M3 subtype receptors decreased Na^+ currents via a PLC-dependent mechanism. The latter effect is in agreement with the observation that CCh inhibits INa in hippocampal neurons by $G_{q/11}$-coupled muscarinic receptors in a protein kinase C-dependent manner (Cantrell et al., 1996). Interestingly, the endogenous agonist ACh, but not CCh, also induced a negative shift in the inactivation curve, and a positive shift in the activation curve, of Na^+ currents. In mature NBM cholinergic neurons in vivo, this type of channel modulation would lead to narrowing of the voltage window for Na^+ channel opening, decrease in neuron excitability and reduction of cholinergic tone in the brain (Dong and Xu, 2002; Keynes et al., 1992). The discrepancy between CCh and ACh effects on the voltage-dependence of Na^+ conductance could be due to differential activation of intracellular pathways by different agonists acting on the same receptor/s subtype/s (Ilyaskina et al., 2018). In spite of the scarce/null excitability of hfNBM immature neuroblasts described in the present research, it appears that cholinergic modulation is complex in the developing NBM and, even if it would have no effects at this stage in terms of firing or neurotransmitter release, it indicates that the machinery is already present and, if retained, would have an impact on CNS circuitry in the adult. In particular, we suggest that ACh released in the NBM will lead to inhibition of neuronal excitability by activating mAChRs, which enhance K^+ currents (thought G_i/G_o-coupled M2 receptors) and inhibit Na^+ currents (thought $G_{q/11}$-coupled M3 receptors). However, ACh acting at nAChRs elicits a depolarizing inward current (Morelli et al., 2017) that would excite NBM neurons (Fig.28). These results are in agreement with previous work demonstrating that nicotinic receptors increase, while muscarinic receptors decrease, the excitability of BF cholinergic neurons (Khateb et al., 1997). So, the weight assigned to each component of cholinergic modulation in the NBM circuitry in vivo will depend on the interaction between Na^+ channels,

muscarinic or nicotinic receptors, and K^+ channels targeted by cholinergic input. ACh has been demonstrated to have trophic and/or migratory impact on proliferating neuroblasts in forebrain areas (Bruel-Jungerman et al., 2011; Resende and Adhikari, 2009; Zheng et al., 1994) as other neuromodulators do in different immature cells (Coppi et al., 2015). Indeed, ACh has been shown to promote a favorable environment for progenitor proliferation, neurite extension and synaptogenesis (for review: (Bruel-Jungerman et al., 2011)). However, the effects of ACh on developing BF cholinegic neurons in humans remain unknown. On the basis of present data, we may hypothesize that autocrine ACh released within the developing NBM drives neuronal excitability and, possibly, cell fate of fetal cholinergic neuroblasts.

Most of cells were not excitable, with only a minority (about 25%, this percentage being stable upon time) of them presenting a single spike. This phenomenon, already described in our previous work (Morelli et al., 2017), was TTX-insensitive and was also observed in cells devoid of Na^+ currents. On these bases, we hypothesize that it is Ca^{2+}-dependent. On the whole, the lack of mature APs, as a landmark of attained neuronal differentiation (Prè et al., 2014), confirms that hfNBM neuroblasts retain immature features during the entire culture period. This notion is not in contrast with previous literature. The lack of full APs in human fetal neurons is consistent with data obtained by others in similar preparations, i.e. telencephalic vesicles isolated from 12 week fetuses and maintained in mitogens at least for at least 6 weeks (Lepski et al., 2011), or cortical neurons isolated during the second trimester of gestation (Mo et al., 2007). At variance, full APs have been reported in prenatal (Levine et al., 1995) or perinatal (Nakajima et al., 1985) rodent BF neurons, as well as in ESC- (Bissonnette et al., 2011) or iPSC-derived (M. L. Liu et al., 2013) human cholinergic neurons. As no data are present to date about the electrical activity in human NBM neurons at this time of gestation nor at corresponding developmental stages in rodents (the earlier time point analyzed during rodent gestation is E17, which is very close to birth: (Levine et al., 1995)), we reasoned that the lack of full APs is not surprising in hfNBM cultures. Indeed,

these cells exemplify an immature, still proliferating, step of neuroblast differentiation, as confirmed by the lack of changes in active nor passive membrane electrophysiological properties throughout the culture period.

The most relevant finding of the present work is probably the rhythmic, oscillatory activity in cell voltage recorded in the vast majority of cells upon depolarization. This active phenomenon, named by us "voltage waves", was unexpected and inedited. It was observed in 80% of hfNBMs recorded in low (0.1 mM) EGTA. The high frequency (about 80-100 Hz) of these oscillations resembles the firing frequency recorded in the NBM of behaving monkeys (Martinez-Rubio et al., 2018) or in different regions of the in vivo human brain, for example in as the globus pallidus of parkinsonian patients (Alam et al., 2016; Lee et al., 2020). Importantly, alterations in these firing activities has been reported in patients with dystonia or PD (Alam et al., 2016; Lee et al., 2020). However, in our case, oscillations differ from standard APs in their waveform. Of note, their frequency fits also with the "gamma-band rhythm" (30-100 Hz) recorded in many cortical areas, for example in the visual cortex of macaque monkeys during visual exploration (Brunet et al., 2015). Gamma oscillations are known to be related to different cognitive capacities, from selection by attention to formation of Hebbian assemblies (Fries, 2015, 2009; Singer, 1999). We can only speculate that voltage waves recorded by us in hfNBMs could represent the ancestors of adult gamma rhythm.

The description of voltage waves in hfNBMs is only at its infancy and to decipher the intracellular mechanisms underlying this phenomenon is complex at best. Most classical blockers of neuronal conductances, i.e. TTX for INa, Cd^{2+} for ICa, were totally ineffective in modulating voltage waves, including ZD7288. This compound is a selective blocker of Ih current, known to participate to electrical oscillatory activity in different kind of rhythmically firing pacemaker cells, i.e. in sinoatrial node cells (Wahl-Schott et al., 2014). Importantly, intracellular Ca^{2+} buffering by high intracellular EGTA or BAPTA respectively impaired or abolished voltage waves. However, EGTA

did not modify the frequency nor amplitude of the voltage waves, once elicited. So, we conclude that intracellular Ca^{2+} rise plays a role in triggering voltage waves but not in maintaining them.

Of note, K^+ emerged as the leading ion in this phenomenon since the unselective K^+ channel blocker TEA (10 mM) abolished oscillations. This notion, together with the sensitivity to EGTA or BAPTA, gave us a clue about the involvement of BK and SK channels, known to participate in the conversion of intracellular Ca^{2+} oscillation into propagative electrical signals in different cell systems (Saeki et al., 2019). Accordingly, the selective BK channel blocker IbTx prevented voltage waves in all cells tested, a result confirmed by TEA at 0.2 mM, a concentration considered selective to BK channel block. The fact that the Ca_V blocker Cd^{2+} did not affect oscillations in physiological-like conditions, i.e. intact intracellular Ca^{2+} homeostasis, let us hypothesize that Ca_Vs channels were not involved in the event. However, when tested in conditions of intracellular Ca^{2+} store depletion by thapsigargin, oscillations presented a significantly lower frequency and were completely prevented by Cd^{2+} demonstrating that, when intracellular Ca^{2+} rise cannot be achieved by store release, external Ca^{2+} entering from Ca_Vs compensates, even if not so efficiently as demonstrated by their lower frequency.

Importantly, previous data demonstrated that intracellular Ca^{2+} oscillations can trigger propagative electrical signals (Saeki et al., 2019) and these events have been indeed related to BK channel opening. However, the high frequency of hfNBM oscillations is at variance from those reports that describe strikingly slower frequencies (in the range of 0.3-1 HZ). A similar observation can be made for the facilitating effect of nicotine in spontaneous Ca^{2+} waves observed in cortical neurons (Wang et al., 2014).

Beyond BK channels, other players are involved in the event, i.e. Kir channels, as their selective blocker Ba^{2+} prevents waves initiation but this effect, differently from IbTx and TEA, is irreversible upon washout as most cells depolarized to death. These data demonstrate that: i) Kir channels are essential

for maintaining Vm polarization and ii) a polarized Vm is required to evoke voltage waves (Fig.28).

In trying to understand this unexplored phenomenon, we have to consider that hfNBMs are immature, still proliferating, neuroblasts isolated from the developing foetal human brain, a rare source of cells. Indeed, the vast majority of previous studies devoted to describe the behaviour of immature neurons have been performed by using iPSCs (M. L. Liu et al., 2013; Song et al., 2013) or ESCs (Bissonnette et al., 2011) committed to neuronal phenotype or in rodent-derived neuronal precursors (Nakajima et al., 1985). These cell sources are profoundly different from hfNBMs which are non-manipulated, genuine neuroblasts: immature, but already committed toward the cholinergic phenotype. These cells in culture retain, under defined experimental conditions and over a relatively long-time frame (3-3.5 months), peculiar immature neuronal features, among which we should include the oscillatory activity in membrane potential.

In finding a functional explanation to voltage waves, it is worth to note that intracellular Ca^{2+} waves are frequently associated to cell migration and, in particular, recurrent Ca^{2+} oscillations involving BK channels have been described to mediate in vitro glioblastoma cell migration (Catacuzzeno and Franciolini, 2018). So, as an alternative explanation beyond adult NBM firing precursors, a possible functional role for voltage waves is their involvement in hfNBM migration. Consistently, we demonstrated that intravenously injected in NBM-lesioned rats, hfNBMs migrated to the injured area (Morelli et al., 2017). Furthermore, we have evidence that serum-starved hfNBMs are attracted by 10% FBS in the lower chamber of a Boyden chamber-based migration assay (manuscript in preparation). Hence, we speculate that voltage waves in hfNBMs may serve to promote cell migration.

Furthermore, malfunctioning of BK channels is responsible for several diseases involved in different pathologies. It was found that intracellular amyloid-β (Aβ) inhibits these currents in cortical neurons (Yamamoto et al.,

2011) and that BK deficient mice show impaired spatial memory (Typlt et al., 2013). Importantly, early memory dysfunction observed in a transgenic mouse model of AD is prevented by chronic activation of BK channels (Wang et al., 2015).

Finally, in line with previous works (Lepski et al., 2011; Morelli et al., 2017; Song et al., 2013), we also observed an immature AP which was elicited in 30% of hfNBMs. Of note, only 1 cell was found to fire more than one AP upon depolarizing current injection, resembling classical AP firing. The single AP was insensitive to high intracellular EGTA or BAPTA and to TTX, even if the compound efficiently blocked INa which are responsible for APs in adult neurons. At present, the ionic channel/s underlying this phenomenon remain unknown.

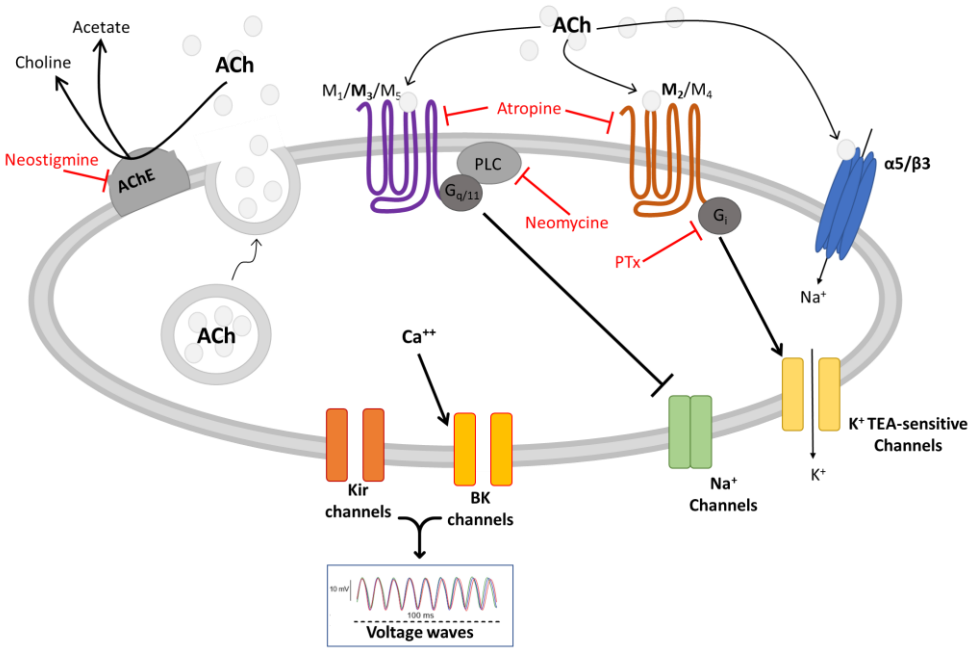

Figure 28. *Schematic representation of the results discussed in this section.*

Aim II - *Adenosine A_{2B} receptors inhibit K^+ currents and cell differentiation in cultured oligodendrocyte precursor cells and modulate sphingosine-1-phosphate signalling pathway.*

The following results were recently published in:

Coppi, E., Cherchi, F., Fusco, I., Dettori, I., Gaviano, L., Magni, G., Catarzi, D., Colotta, V., Varano, F., Rossi, F., et al. (2020). ***Adenosine A_{2B} receptors inhibit K^+ currents and cell differentiation in cultured oligodendrocyte precursor cells and modulate sphingosine-1-phosphate signaling pathway***.
Biochem. Pharmacol. 177.

2.1. Selective A_{2B}R stimulation inhibits voltage-dependent K^+ currents in cultured OPCs.

Electrophysiological recordings were performed on 221 cells showing, on average, a Vm of -60.8 ± 1.6 mV, a Cm of 7.2 ± 0.3 pF of and a Rm of 840.1 ± 49.7 MΩ. All experiments were performed in the continuous presence of the A_1R, A_{2A}R and A_3R antagonists DPCPX, SCH58261 and MRS1523, respectively (100 nM each). As shown in Figure 29A, we applied a voltage ramp protocol (from -120 to +80 mV, 800 ms duration: upper inset of Fig. 29A) in cultured OPCs in the absence or presence of the selective A_{2B}R agonist BAY60-6583 (10 μM) and we found that the compound reversibly inhibited ramp-evoked outward currents (Fig. 29A and lower inset). BAY 60-6583-inhibited current, obtained by subtraction of the ramp recorded in the presence of BAY 60-6583 from the control ramp, is a voltage-dependent outward conductance (Fig. 29B). In agreement, immunofluorescence experiments confirmed A_{2B}R expression on $NG2^+$ cells (Fig. 29C). The maximal effect of BAY60-6583 was reached within 5 min application (lower inset of Fig. 29A) and was statistically significant in 51 cells investigated (Fig. 29D: 41.9 ± 2.8% current inhibition). Of note, ramp-evoked outward currents were absent, as well as the effect of BAY60-6583, when extra- and intra-cellular K^+ ions were replaced by equimolar Cs^+ (Fig. 29D), demonstrating that the current involved in A_{2B}R-

effect is a voltage-dependent K^+ current. The effect of BAY60-6583 on K^+ currents was concentration-dependent (Fig. 29E) with an EC50 = 0.6 µM (Fig. 29E, left panel: confidence limits: 0.04 – 9.4 µM), and prevented by the selective $A_{2B}R$ antagonist MRS1706 (10 µM: Fig. 29E, F). In accordance with K^+ current inhibition, BAY60-6583 caused a concentration-dependent depolarization in cultured OPCs and this effect was also concentration-dependent and prevented by the $A_{2B}R$ antagonist MRS1706 (Fig. 29G and Table 7).

We further investigated which subtype/s of K^+ currents are targeted by $A_{2B}Rs$. OPCs are known to express sustained, delayed rectifier, IK currents and a transient, rapidly inactivating, IA conductance (Knutson et al., 1997; Sontheimer and Kettenmann, 1988). We applied a voltage-step protocol (from -40 to +80 mV, 200 ms duration, lower inset in Fig. 29H) to activate both IA and IK in the absence or presence of 10 µM BAY60-6583. As shown in figure 29H-I, both K^+ currents were inhibited in the presence of the $A_{2B}R$ agonist, as demonstrated by a significant decrease in either transient IA (Fig. 29I, left panel) or steady state IK (Fig. 29I, right panel) starting from a voltage of 0 mV. Above data were obtained in OPCs at t_0, which correspond to the period at which most cells are immature $NG2^+$ OPCs (Coppi et al., 2013a, 2013b). We also tested BAY60-6583 effects on mature oligodendrocytes (OLs) allowed to differentiate by mitogen withdrawal for 7 days (t_7). At these time point, as it previously shown (Coppi et al., 2013b, 2013a), oligodendroglial cultures are mostly composed by highly ramified, MBP^+ and MAG^+ mature OLs (Attali et al., 1997; Gallo et al., 1996; Knutson et al., 1997; Sontheimer and Kettenmann, 1988).

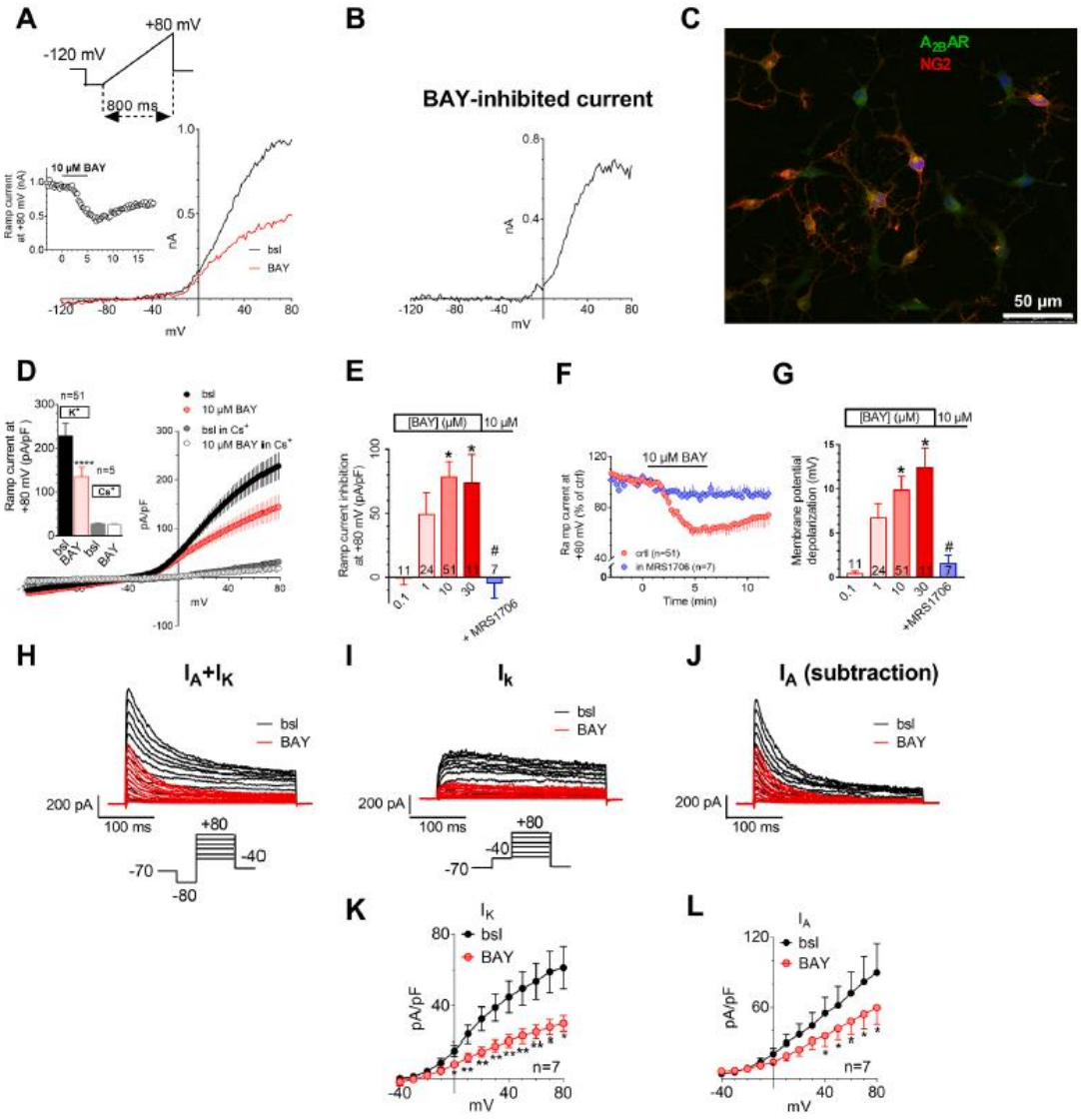

Figure 29. ***The $A_{2B}R$ agonist BAY60-6583 inhibits IK and IA outward K^+ currents in cultured OPCs.*** **A.** Original whole-cell patch clamp current traces evoked by a voltage ramp protocol (from −120 to +80 mV, 800 ms: upper inset) in a typical OPC before (baseline: bsl, black trace) or after the application of BAY60-6583 (BAY: 10 µM; 5 min, red trace). Inset: time course of ramp-evoked currents at +80 mV in the same cell. **B.** Net BAY60-6582-inhibited current, obtained by subtraction of the trace recorded in BAY60-6582 from the control ramp, in the same cell. C. Confocal image of immunofluorescence staining for $A_{2B}R$ (green) and NG2 (red) in OPC cultures (at t_0). Cell nuclei are marked with DAPI (blue). Scale bar: 50 µm. **D.** Averaged ramp-evoked currents, and pooled data at +80 mV (mean ± SEM), recorded in the absence (bsl) or presence of 10 µM BAY60-6583 under control conditions (K^+; n=51) or in Cs^+-replacement experiments (n=5). ****P < 0.0001 vs respective bsl, paired Student's t-test. **E.** Pooled data of K^+ current inhibition obtained in different experimental conditions in cultured OPCs. *P < 0.05 vs 0.1 µM BAY60-6583; #P < 0.05 vs 10 µM BAY60-6583, One-way ANOVA, Bonferroni post-test. Number of observation is written in the columns. **F.** Averaged time courses of ramp-evoked currents at +80 mV in cultured OPCs before and after the application of BAY60-6583 (10 µM) under control conditions (ctrl: red circles; n=51) or in the presence of the selective $A_{2B}R$ antagonist MRS1706 (10 µM: blue diamonds: n=7). **G.** Pooled data of membrane potential depolarization induced by BAY60-6583 in cultured OPCs under different experimental conditions. *P < 0.05 vs 0.1 µM BAY60-6583; #P < 0.05 vs 10 µM BAY60-6583, One-way ANOVA, Bonferroni post-test. Number of observations is written in the columns. **H, I.** Original current traces evoked by two different voltage-step protocols (from −40 to +80

mV, V_{pre}=-40 mV; 200 ms: lower panel in H; or from −40 to +80 mV, V_{pre}=-80 mV; 200 ms: lower panel in I) in a representative OPC before (bsl: black traces) or after the application of BAY60-6583 (10 µM, 5 min; red traces). **J.** Net IA current in the same OPC obtained by subtraction of traces reported in **H** and **I**. Scale bars: 200 pA; 100 ms. **K, L:** Averaged current-to-voltage relationship (I-V plot) of steady-state, sustained, IK currents (**K**) or peak, transient, IA currents (**L**) recorded in the absence (bsl: black circles) or in the presence (red circles) of 10 µM BAY60-6583 in 7 cells investigated. *P < 0.05; **P < 0.01 paired Student's t-test. All experiments were performed in the presence of the A_1R, A_{2A}R and A_3R antagonists DPCPX, SCH58261 and MRS1523, respectively (all 100 nM).

	Vm (mV)	**n**
CTRL	−58.3 ± 2.4	n = 51
10 µM BAY	−48.4 ± 2.5 ****	
CTRL	−57.5 ± 3.4	n = 6
VEH	−56.1 ± 4.1	
CTRL	−55.1 ± 3.0	n = 23
50 nM P453	−43.0 ± 3.9 **	
MRS1706	−61.4 ± 5.2	n = 7
MRS1706 + 10 µM BAY	−56.3 ± 4.2	

Table 8. Selective A_{2B}R stimulation depolarizes cell membrane potential (Vm) in cultured OPCs. Membrane potential (Vm) was measured during the last min preceding drug application (baseline, bsl) or after 5 min application of A_{2B}R agonists: BAY 60–6583 (BAY: 10 µM) or P453 (50 nM), or vehicle (Veh: 0.1% DMSO). The A_{2B}R antagonist MRS1706 (10 µM) was applied at least 10 min before BAY60-6583. ** P < 0.01; ****P < 0.0001 vs respective bsl, paired Student's t-test.

As shown in figure 30A-C, BAY 60-6583 (1–30 µM) inhibited outward K^+ currents in OLs at t7 and presented a concentration-dependent effect similar to what observed in immature OPCs (Fig. 30D-F).

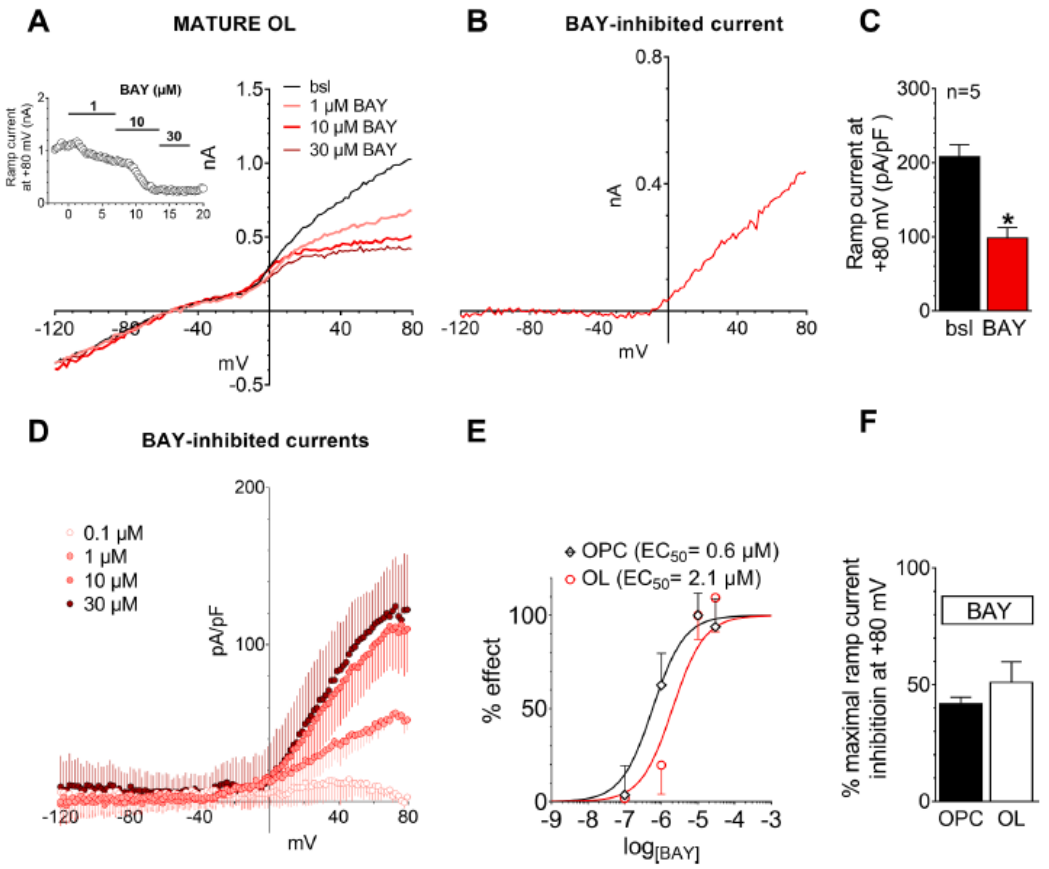

Figure 30. ***The $A_{2B}R$ agonist BAY60-6583 inhibits ramp-evoked outward currents in mature OLs.*** **A.** Original whole-cell patch clamp current traces activated by a voltage ramp protocol (from −120 to +80 mV, 800 ms) in a typical OL at t_7 before (baseline, bsl) or after BAY60-6583 (BAY) applied at different concentrations (1–10-30 μM). Inset: time course of ramp-evoked currents at +80 mV in same cell. **B.** Net BAY60-6583-inhibited current, obtained by subtraction of the trace recorded in 10 μM BAY60-6583 from the control ramp, in the same cell. **C.** Pooled data (mean ± SEM) of ramp current amplitude at +80 mV, recorded in the absence (black column) or presence (red column) of 10 μM BAY60-6583 in 5 cells investigated. * $P < 0.05$, paired Student's t-test. **D.** Averaged BAY60-6583-inhibited currents, recorded in the presence of different agonist concentrations, in mature OLs at t_7. At least n = 4 in each experimental group. **E.** Concentration-response curve of BAY60-6583-mediated inhibition of ramp currents at +80 mV in cultured OPCs (EC50 =0.6 μM, confidence limits: 0.04 – 9.4 μM: black diamonds) or in mature OLs (EC50 = 2.1 μM, confidence limits: 0.2 – 23.6 μM: red circles). **F.** Pooled data of maximal ramp current inhibition achieved by BAY60-6583 (10 μM) in OPCs (black column) or OLs (open column) at +80 mV. $P > 0.05$, unpaired Student's t-test. All experiments were performed in the presence of the A_1R, $A_{2A}R$ and A_3R antagonists DPCPX, SCH58261 and MRS1523, respectively (all 100 nM).

We also tested the functional effect of a newly synthesized, highly selective, $A_{2B}R$ agonist: P453 (Betti et al., 2018). As shown in figure 31A, and similarly to BAY 60-6583, P453 at a concentration of 50 nM significantly inhibited ramp-evoked currents in 23 cells tested and significantly depolarized OPCs, as reported in Table 7. The effect was concentration dependent (Fig. 31B), blocked by the $A_{2B}R$ antagonist MRS1706 (10 μM: Fig. 31B, D) and prevented by Cs^+-

replacement of K^+ ions (Fig. 31C), thus confirming that $A_{2B}R$ activation inhibits K^+ currents in cultured OPCs. Of note, averaged P453-inhibited current was superimposable to BAY-inhibited current (Fig. 31D: black circles and grey diamonds). When tested on the voltage step protocol, P453 inhibited both IA and IK currents (Fig. 31E, F), similarly to BAY60-6583.

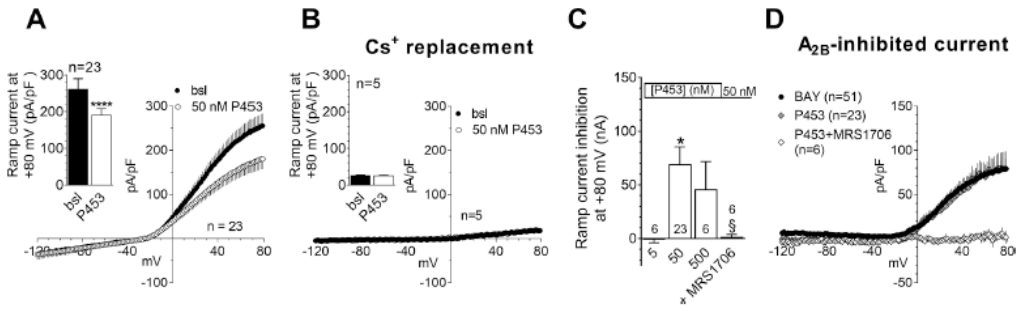

Figure 31. ***The effect of the prototypical $A_{2B}R$ agonist BAY60-6583 on IK and IA currents is mimicked by P453, a recently synthetized $A_{2B}R$ agonist.*** **A.** Averaged ramp evoked currents, and pooled data at +80 mV (mean ± SEM), recorded before (baseline: bsl) or after P453 application (50 nM, 5 min) in 23 OPCs tested. ****P < 0.0001, paired Student's t-test. **B.** Averaged ramp-evoked currents, and pooled data at +80 mV, recorded in the absence (bsl) or presence of the $A_{2B}R$ agonist P453 (50 nM) in Cs^+-replacement experiments (n=5). No significant difference was found in ramp currents measured at +80 mV in the absence or presence of P453, paired Student's t-test. **C.** Pooled data of ramp current inhibition at +80 mV induced by different concentrations of P453 or by 50 nM P453 applied in the presence of the $A_{2B}R$ antagonist MRS1706 (10 µM). *p < 0.05 vs 5 nM P453; §p < 0.05 vs 50 nM P453, One-way ANOVA, Bonferroni post-test. Number of observations is written in the columns. **D.** Net A_{2B}-inhibited currents, obtained by subtraction of the trace recorded in the presence of $A_{2B}R$ agonists from the control ramp, in different experimental groups. Note that no A_{2B}-inhibited current is recorded when P453 (50 nM) is co-applied with the $A_{2B}R$ antagonist MRS1706 (10 µM).

We also tested the unselective adenosine agonist NECA. The compound was applied, as in all other experimental groups, in the continuous presence of the A_1R, $A_{2A}R$ and A_3R antagonists DPCPX, SCH58261 and MRS1523 (all 100 nM), respectively, to isolate $A_{2B}R$-mediated effects. As shown in figure 32A, NECA (50 µM) mimicked BAY60-6583-mediated inhibition of ramp-evoked K^+ currents. The effect was significant in 8 cells tested (Fig. 32B), prevented by the selective $A_{2B}R$ antagonist PSB603 (10 µM: Fig. 32C, D) and concentration-dependent (Fig. 32D), with an EC50=1.9 µM (confidence limits: 0.4 – 9.0 µM: Fig. 32E).

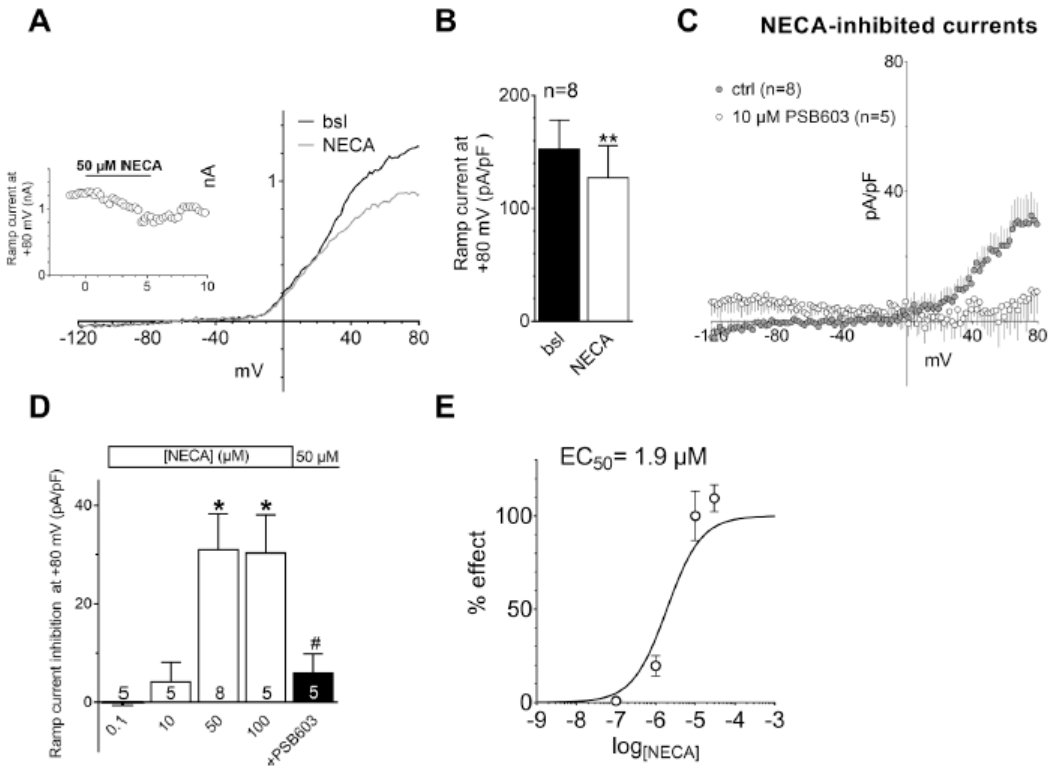

Figure 32. ***The effect of BAY60-6583 on ramp-evoked K⁺ currents is mimicked by the unselective adenosine receptor agonist NECA.*** **A**. Original whole-cell patch clamp current traces activated by a voltage ramp protocol (from −120 to +80 mV, 800 ms) in a typical OPC before (baseline: bsl, black trace) or after the application of NECA (50 µM; 5 min, grey trace). Inset: time course of ramp-evoked currents at +80 mV in same cell. **B.** Pooled data (mean ± SEM) of ramp-evoked currents at +80 mV in the absence (bsl) or presence of 50 µM NECA in 8 cells tested. **P < 0.01, paired Student's t-test. **C.** Averaged NECA-inhibited currents, obtained by subtraction of the trace recorded in NECA from the control ramp in each cell, measured in the absence (control: ctrl; n = 8) or in the presence of the $A_{2B}R$ antagonist PSB603 (PSB, 10 µM; n = 5). **D.** Pooled data of ramp current inhibition measured at +80 mV in the presence of NECA at different concentrations or at 50 µM in the presence of the $A_{2B}R$ antagonist PSB603. *P < 0.05 vs 0.1 µM NECA; #P < 0.05 vs 50 µM NECA, One-way ANOVA, Bonferroni post-hoc test. Number of observations is written in the columns. **E.** Concentration-response curve of NECA-mediated inhibition of ramp currents at +80 mV. EC50 = 1.9 µM, confidence limits = 0.4 – 9.0 µM. All experiments were performed in the presence of the A_1R, $A_{2A}R$ and A_3R antagonists DPCPX, SCH58261 and MRS1523, respectively (all 100 nM).

In order to confirm the involvement of IA and IK currents in the $A_{2B}R$-mediated effect, we applied BAY60-6583 in the presence of a combination of the IA blocker 4-AP (500 µM) plus the IK blocker TEA (3 mM: Fig. 33A) (Gutman et al., 2005). It has previously shown that, in cultured OPCs, 3 mM TEA inhibits delayed rectifier IK currents whereas 500 µM 4-AP selectively blocks transient IA conductances (Coppi et al., 2013b, 2013a). As shown in figure 33A, a co-application of both compounds fully prevented ramp current inhibition mediated by this $A_{2B}R$ agonist whereas TEA alone did not

significantly block BAY60-6583-mediated effect (Fig. 33B). Concerning the intracellular mechanism by which the G_s-coupled $A_{2B}R$ inhibits IK, we tested the hypothesis of intracellular cAMP being involved, in accordance with G_s coupling of $A_{2B}Rs$ and with previous data showing that increased levels of this intracellular metabolite decreased steady state outward K^+ conductances in ovine OPCs (Soliven et al., 1988). The adenylyl cyclase activator forskolin (FSK; 20 µM) mimicked and occluded the effect of BAY 60-6583 on ramp-evoked K+ currents in cultured OPCs (Fig. 33C-D) thus confirming that $A_{2B}R$ inhibit IK currents by increasing cAMP levels.

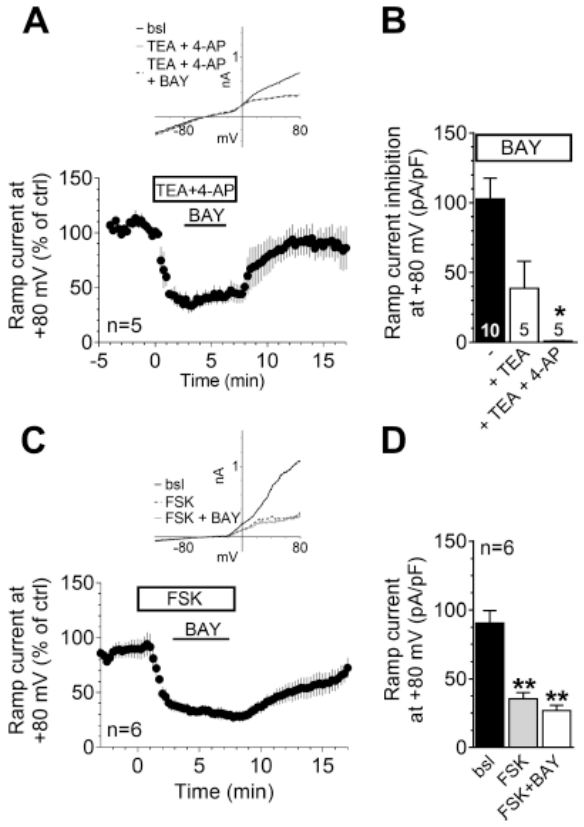

Figure 33. ***The effect of BAY60-6583 on ramp-evoked K⁺ currents is occluded by a combination of the K⁺ channel blockers TEA and 4-AP and by the adenylyl cyclase activator forskolin.*** **A.** Averaged time course (mean ± SEM) of ramp-evoked currents measured at +80 mV in cultured OPCs before or after the application of a combination of the IK blocker tetraethylammonium (TEA; 3 mM) plus the IA blocker 4- amynopyridine (4-AP; 500 µM) or during the subsequent application of BAY60-6583 (BAY; 10 µM). Upper panel: original ramp current traces recorded in a typical OPC at representative time points: in control conditions (bsl; black trace); after 3 min of TEA with 4-AP (TEA + 4-AP; grey trace) or after 5 min of 10 µM BAY60-6583 applied in the presence of TEA with 4-AP (TEA + 4- AP + BAY; dotted black trace). **B.** Pooled data of BAY60-6583-inhibited currents measured at + 80 mV in the absence (n = 10) or presence of 3 mM TEA (+TEA) alone or in combination with 500 µM 4-AP (+TEA + 4-AP). *P < 0.05; One-way ANOVA, Bonferroni post-hoc test. Number of observations is

written in the columns. **C, D.** Averaged time course (**C**) and pooled data (**D**) of ramp-evoked currents measured at +80 mV in cultured OPCs before or after the application of the adenylyl cyclase activator forskolin (FSK; 20 µM) and during the subsequent application of BAY60-6583 (BAY; 10 µM). Upper panel in C: original ramp current traces recorded in a typical OPC at representative time points: in control conditions (bsl; black trace); after 3 min of FSK (dotted grey trace) or after 5 min of 10 µM BAY60-6583 applied in the presence of FSK (FSK + BAY; grey trace). **P < 0.01 from bsl, paired Student's t-test, n = 6. All experiments were performed in the presence of the A_1R, $A_{2A}R$ and A_3R antagonists DPCPX, SCH58261 and MRS1523, respectively (all 100 nM).

2.2. *$A_{2B}R$ activation stimulates SphK1 phosphorylation in cultured OPCs*

In the attempt to identify a putative cross-talk between $A_{2B}R$ and SphK/S1P signalling pathways, as already proposed by others in peripheral cells (Sun et al., 2015), we studied whether BAY60-6583, applied at the same concentration found to inhibit K^+ currents (10 µM), could affect the activation of one or both isoforms of SphK, SphK1 and SphK2, known to be expressed in oligodendroglial cells (Saini et al., 2005). It has been previously demonstrated that SphK activation requires phosphorylation and then translocation to the plasma membrane, where the substrate is located (Hait et al., 2007; Pitson et al., 2003). We quantified the phosphorylation of both these enzymes after 10 min application of BAY60-6583 (10 µM) in OPC cultures and we found that the $A_{2B}R$ agonist significantly increased SphK1, but not SphK2, phosphorylation in cultured OPCs (Fig. 34A, B).

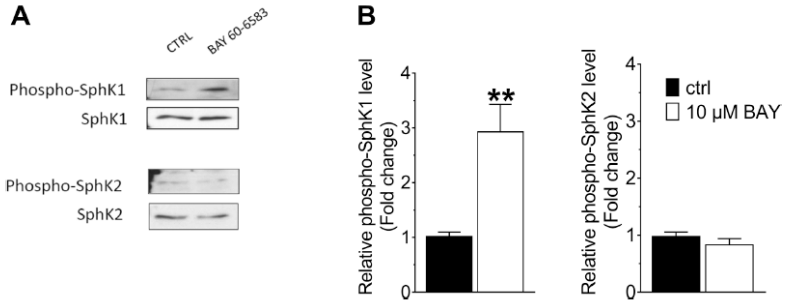

Figure 34. ***$A_{2B}R$ activation increases SphK1 phosphorylation in cultured OPCs.*** **A.** Western Blot analysis of phospho-SphK1 (upper panel) and phospho-SphK2 (lower panel) performed in total cell lysates of OPC cultures after 10 min application of BAY60-6583 (BAY; 10 µM). **B.** Pooled data (mean ± SEM) of phospho-SphK1 (left panel) and phospho-SphK2 (right panel) levels measured in control conditions (ctrl) or in 10 µM BAY60-6583. In the histogram, band intensity corresponding to phospho-SphK1 or phospho-SphK2 was normalized to SphK1 or SphK2 total content of three independent experiments performed in triplicate (-fold change over control). **P < 0.01, unpaired Student's t-test.

2.3. FTY720-P interferes with A_{2B}Rs in decreasing outward K^+ currents in cultured OPCs

Based on the latest results, we next tested the hypothesis of a possible involvement of SphK1/S1P pathway in A_{2B}R-mediated K^+ current inhibition in OPCs. As shown in Figure 35A, cell preincubation with the pan SphK1/2 inhibitor VPC96047 (500 nM, at least 30 min pre-incubation) did not prevent BAY60-6583 (10 µM)-mediated ramp current inhibition. Of note, VPC96047-preincubated cells presented a significant increase in ramp currents at +80 mV under baseline conditions (bsl), i.e. before the application of BAY60-6583, vs respective, non-VPC-pre-incubated, matched controls (Fig. 35B), indicating that sustained SphK inhibition affects K^+ current amplitude in cultured OPCs. The S1P analogue FTY720-P, at a concentration of 1 µM, mimicked the effect of BAY60-6583 in inhibiting ramp currents (Fig. 35C). Of note, 1 µM FTY720-P reduced the effect of a subsequent application of the A_{2B}R agonist (Fig. 35G), indicating these two effects are not additive. Differently, a low (10 nM) concentration of FTY720-P did not modify ramp current amplitude *per se* (Fig. 35D) and significantly increased the effect of a subsequent application of BAY60-6583, as shown in figure 35G. Finally, the product of SphK activity, S1P, did not modify ramp-evoked currents in cultured OPCs (Fig. 35E, F), nor the inhibitory effect of BAY60-6583 on them (Fig. 35G), at concentrations ranging from 10 nM to 1 µM.

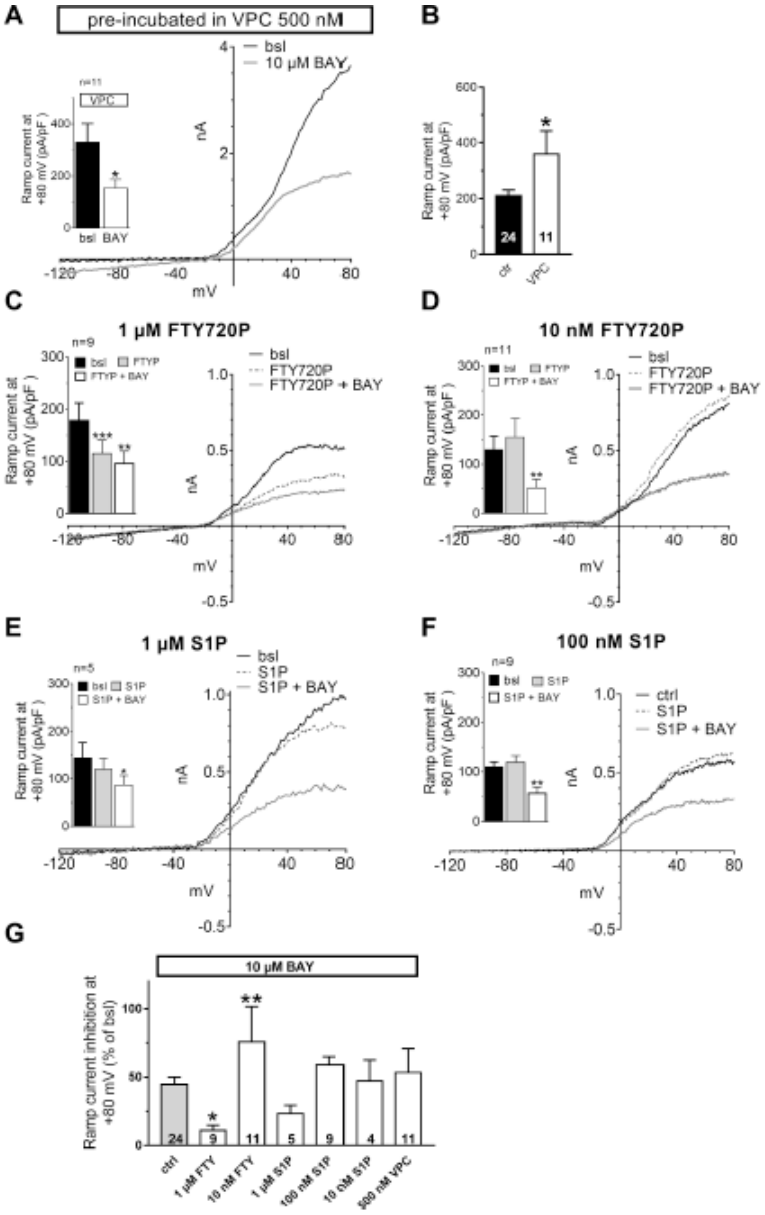

Figure 35. ***The effect of BAY60-6583 on ramp-evoked currents is differently modulated by FTY720-P depending on the concentration applied.*** **A.** Original ramp current traces recorded before (baseline: bsl; black trace) or after the application of BAY60-6583 (BAY: 10 µM, 5 min; grey trace) in a typical OPC pre-incubated (at least 45 min) with the pan-SphK inhibitor VPC96047 (VPC: 500 nM). Inset: pooled data (mean ± SEM) of ramp-evoked currents at +80 mV recorded before or after 10 µM BAY60-6583 in 11 cells tested. *P < 0.05; paired Student's t-test. **B.** Pooled data of ramp-evoked currents at +80 mV recorded in control OPCs (ctrl), OPCs not incubated with VPC96047 and before the application of BAY60-6583 (n = 24), or in OPCs pre-incubated with VPC96047 (500 nM; n = 11). *P < 0.05; unpaired Student's t-test. **C-F.** Original ramp current traces, and respective pooled data at +80 mV (insets), recorded during baseline (bsl), after the application of FTY720-P (FTY: 1 µM in C; 10 nM in D) or S1P (1 µM in E; 100 nM in F) or after a subsequent application of BAY60-6583 (10 µM). *P < 0.05; **P < 0.01; ***P < 0.001vs bsl, paired Student's t-test. **G.** Pooled data of ramp current inhibition at +80 mV, expressed as % of bsl, induced by 10 µM BAY60-6583 in different experimental conditions. *P < 0.05; **P < 0.01 vs ctrl, One-way ANOVA, Bonferroni post-test. Number of observations is written in the columns. All experiments were performed in the presence of the A_1R, $A_{2A}R$ and A_3R antagonists DPCPX, SCH58261 and MRS1523, respectively (all 100 nM).

2.4. A_{2B}Rs and S1P pathway interact to modulate oligodendrocyte maturation in vitro

To study oligodendroglial cell maturation in vitro, OPCs were lead to differentiate into mature OLs by mitogen withdrawal and gene-related targets of cell maturation were studied (see Table 6). As shown in figure 36A and 36B, a significant and time-dependent increase in MAG and MBP expression were found, with a maximal peak after 7 days (t_7). Moreover, we studied the expression of A_{2B}Rs during oligodendroglial differentiation and we found out that this receptor is overexpressed during cell maturation (Fig. 36C). Interestingly, A_{2B}R expression was not affected by low (10 nM) nor high (1 µM) concentration of FTY720-P whereas it was dramatically decreased when the 7 days differentiation period was carried out in the presence of the pan SphK1/2 inhibitor VPC96047 (500 nM). Similarly to the A_{2B}R, also S1P5 displays a time-dependent expression during OL differentiation, in line with previous data in the literature about the expression of S1P receptors in mature OLs (Jung et al., 2007; Novgorodov et al., 2007; Yu et al., 2004). S1P5 mRNA levels presented a time-dependent increase during cell maturation but were not significantly changed in the presence of high doses of FTY720-P nor VPC96047 whereas 10 nM FTY720-P induced a significant upregulation of the receptor (Fig. 36D).

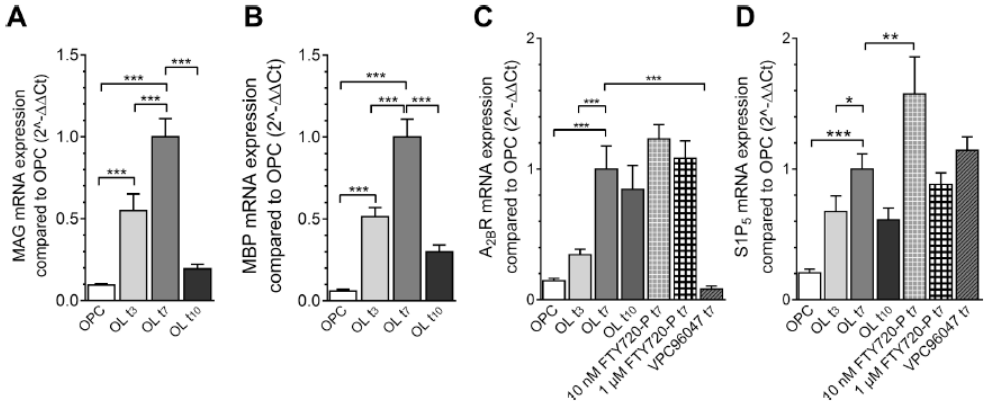

Figure 36. ***Time course of the expression of oligodendrocyte markers, A_{2B}R and S1P5 receptor during oligodendroglial cell differentiation in vitro.*** **A, B.** Gene expression analysis of oligodendrocyte differentiation markers MAG (**A**) and MBP (**B**) performed by Real Time-PCR (RT-PCR) from OPC cultures at t_0 (OPC) to oligodendrocyte cultures (OL) after 3, 7 and 10 days of differentiation (t_3, t_7, t_{10}). **C, D.** Gene expression analysis of A_{2B}R (**C**) and S1P5 (**D**) performed by RT-PCR from OPC to OL cultures at t_3, t_7, t_{10}. Mature OL at t_7 were challenge with or without 10 nM and 1 µM FTY720-P or 500 nM VPC96047. RT-PCR was performed by

using SYBR green probe and specific rat primers, as reported in Table 6. The $2^{(-\Delta\Delta CT)}$ method was applied as a comparative method of quantification and data were normalized to β-actin expression. Data are means ± SEM of three independent experiments performed in triplicate. *P < 0.05; ** P < 0.01; *** P < 0.001, One-way ANOVA, Bonferroni post-test.

We finally investigated the involvement of $A_{2B}R$ agonists in oligodendroglial cell maturation at t_7, alone or in combination with various S1P analogues or SphK inhibitors (Fig. 37). The $A_{2B}R$ agonist BAY60-6583 (10 μM) dramatically reduced MAG or MBP expression at t_7 (Fig. 37A, B:), indicating that $A_{2B}R$ stimulation counteracts OPC maturation towards OLs. The opposite effect was observed when cells were grown in the presence of the pan SphK1/2 inhibitor VPC96047 or the selective SphK1 inhibitor VPC96091 (both at 500 nM: Fig. 37A, B), thus indicating that SphK inhibition promotes OPC maturation. Furthermore, in line with electrophysiological data, the $A_{2B}R$ agonist BAY 60-6583 still inhibited cell maturation when applied in the presence of either of the two SphK inhibitors tested, VPC96047 and VPC96091. The S1P analogue FTY720-P, at a concentration of 1 μM, mimicked the effect of BAY 60-6583 in inhibiting oligodendroglial cell differentiation (Fig. 37A, B) and a combination of both compounds did not produce any additional effect (Fig. 37A, B). These results are also consistent with what observed on IK currents (see Fig. 35C). On the contrary, 10 nM FTY720-P positively affected oligodendrocytes differentiation by increasing MAG expression, a result consistent with previous data (Jung et al., 2007) and with the present research (see Fig. 35D, G). OL differentiation was also significantly decreased by the recently described $A_{2B}R$ agonist P453 and, similarly to BAY60-6583, the effect of P453 was not reverted by VPC96047 (Fig.37A, B). Data in literature show that mice with a targeted deletion of S1P1 did not show an obvious clinical phenotype, but there were subtle abnormalities in myelin (Kim et al., 2011). Interestingly, recent results demonstrated that S1P1 deficiency caused delayed differentiation of OPCs into OLs at 3 weeks (Dukala and Soliven, 2016). For this reason, we employed the specific S1P1 agonist and antagonist, SEW2871 and W146 respectively, to analyze the contribution of S1P1 in BAY60-6583-mediated inhibition of OPC differentiation. As reported in figure 37C and 37D,

neither SEW2871 (1 μM) nor W146 (10 μM) exerted any significant effect on OPC differentiation. Moreover, MAG and MBP expression after BAY60-6583 stimulation were not significantly affected by the S1P1 blocker W146, ruling out a role for S1P1 in BAY60-6583-mediated inhibition of oligodendroglial differentiation. Notably, S1P2 expression was significantly downregulated in OL at t7 compared to OPC as shown in figure 37E. Finally, S1P3 expression was upregulated during OL differentiation and this effect was significantly enhanced in the presence of BAY60-6583 (Fig. 37F).

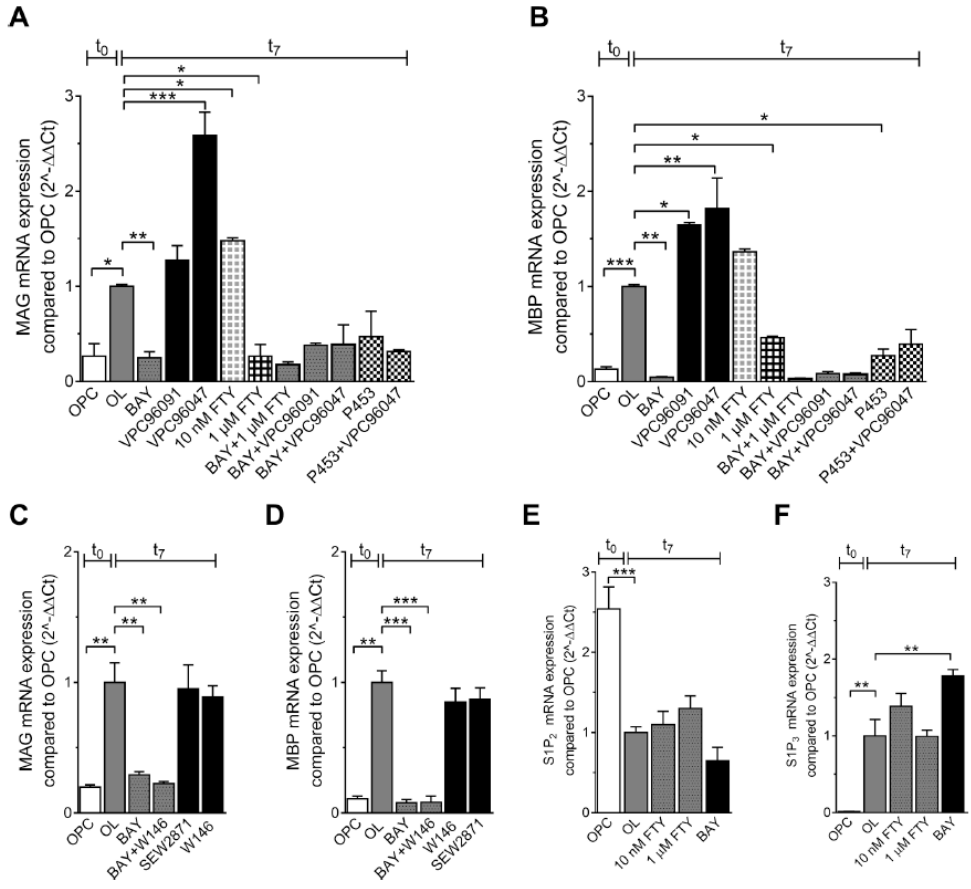

Figure 37. ***A_{2B}R- and SphK/S1P axis-mediated effects on oligodendrocyte differentiation in vitro.*** **A-D.** Gene expression analysis of oligodendrocyte differentiation markers MAG (**A** and **C**) and MBP (**B** and **D**) by Real Time-PCR (RT-PCR) in OPC at t_0 and in OL at t_7 in different experimental conditions. **E, F.** Gene expression analysis of S1P2 (**E**) and S1P3 (**F**) by RT-PCR in OPC at t_0 and in OL at t_7 in different experimental conditions. BAY60-6583 (BAY, 10 μM), VPC96091 (500 nM); VPC96047 (500 nM); FTY720-P (FTY: 10 nM or 1 μM), P453 (500 nM), SEW2871 (1 μM), W146 (10 μM). RT-PCR was performed by using SYBR green probe and specific rat primers, as reported in Table 6. The $2^{(-\Delta\Delta CT)}$ method was applied as a comparative method of quantification and data were normalized to β-actin expression. Data are means ± SEM of three independent experiments performed in triplicate. * $P < 0.05$; ** $P < 0.01$; *** $P < 0.001$, One-way ANOVA, Bonferroni post-test.

2.5. $A_{2B}R$ silencing by siRNA enhances oligodendrocyte maturation in vitro and affects S1P pathway

In order to confirm above data obtained with $A_{2B}R$ ligands, we took advantage of the interference RNA strategy to test the impact of transient $A_{2B}R$ silencing in OPC cultures. Figure 38A shows that transfection of OPCs with scramble silencing RNA (SCR-siRNA) did not affect BAY60-6583- mediated inhibition of ramp currents. On the contrary, when cells were transfected with a pool of specific $A_{2B}R$ silencing RNA duplexes ($A_{2B}R$-siRNA), the effect of the $A_{2B}R$ agonist was significantly reduced (Fig. 38B), i.e. BAY60-6583-inhibited current was halved (Fig. 38C, D). However, total outward currents evoked by the voltage ramp protocol at +80 mV were not different in the two groups (94.9 ± 16.0 pA/pF in the SCR-siRNA group, n=12, vs 88.0 ± 8.8 pA/pF in the $A_{2B}R$-siRNA group, n=14; p = 0.1576, unpaired Student's t-test; data not shown). As shown in figure 38E, downregulation of $A_{2B}R$ expression in $A_{2B}R$-siRNA-transfected OPCs was about 50 % (open bars) at 3 days post-transfection. Importantly, $A_{2B}R$-siRNA transfection significantly reduced NG2 and increased CNPase expression, an earlier marker of differentiation, demonstrating that $A_{2B}R$ silencing enhanced OPC maturation (Fig. 38E). Furthermore, a significant reduction in S1P3, S1P5 and SphK1, but not SphK2, expression was observed. Finally, the expression of S1P degrading enzyme S1P lyase was strikingly enhanced in $A_{2B}R$ siRNA-transfected cells (Fig. 38E, black bars).

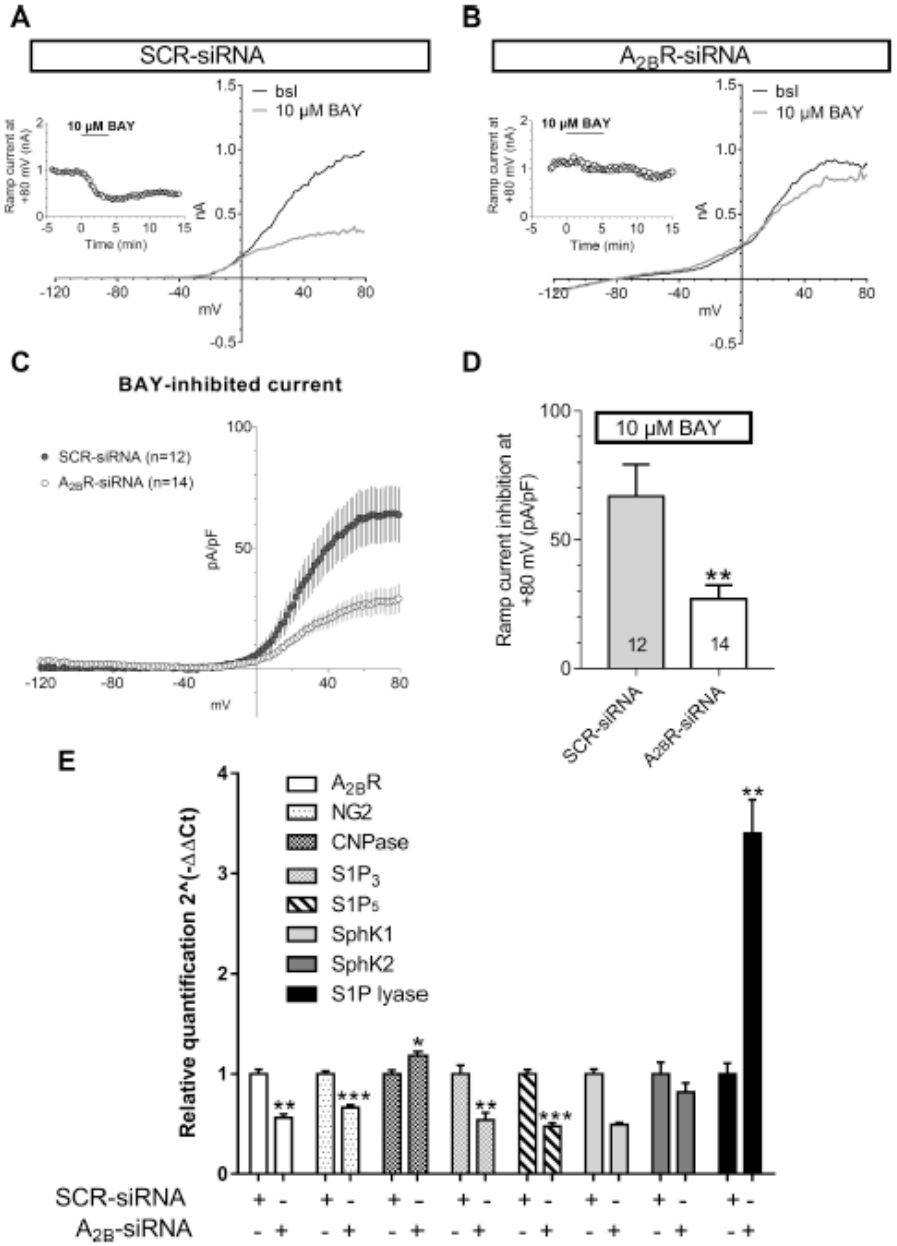

Figure 38. ***A_{2B}R silencing in cultured OPCs by small interference RNA (siRNA) prevents the effect of BAY60-6583 on K^+ currents, facilitates cell maturation and interferes with S1P signaling.*** **A, B.** Original ramp current traces recorded before (baseline: bsl; black traces) or after the application of BAY60-6583 (BAY: 10 µM; grey traces) in typical OPCs transfected with scramble (SCR)-siRNA (**A**) or A_{2B}-siRNA (**B**). Insets: time courses of ramp-evoked currents at +80 mV in respective cells. **C.** Averaged BAY60-6582-inhibited currents, obtained by subtraction of the trace recorded in BAY60-6582 (10 µM) from the control ramp, measured in OPCs transfected with SCR-siRNA or A_{2B}-siRNA. **D.** Pooled data of BAY-inhibited current at +80 mV recorded in OPCs transfected with SCR-siRNA (n = 12) or A_{2B}-siRNA (n = 14). ** P < 0.01, unpaired Student's t-test. **E.** Relative quantitative mRNA analysis was performed by Real-Time PCR in OPCs transfected with SCR-siRNA or with A_{2B}-siRNA; the content of housekeeping gene glyceraldehyde 3-phosphate dehydrogenase (GAPDH) was analyzed in parallel. Results are expressed as fold changes according to the $2^{(-\Delta\Delta CT)}$ method, utilizing as calibrator the expression of each gene in scrambled siRNA-transfected cells. Data are means ± SEM of three independent experiments performed in triplicate. * P < 0.05, ** P < 0.01, *** P < 0.001; unpaired Student's t-test. All experiments were performed in the presence of the A_1R, A_{2A}R and A_3R antagonists DPCPX, SCH58261 and MRS1523, respectively (all 100 nM).

2.6. Discussion

The present work has provided the first description of A_{2B}R-mediated effects in oligodendroglial cell cultures. We demonstrate here that selective A_{2B}R activation inhibits IK and IA currents and delays maturation of cultured OPCs. Furthermore, A_{2B}Rs activate SphK1 and differently modulate S1P3, S1P5 and S1P lyase expression levels. Adenosine participates to a number of OPC functions, from cell migration to myelin production (Coppi et al., 2015; Fields and Burnstock, 2006). My group recently contributed to address this issue (Coppi et al., 2013a) by demonstrating that A_{2A}R stimulation counteracts oligodendroglial cell differentiation in vitro by inhibiting TEA-sensitive IK currents that are necessary to OPC maturation (Gallo et al., 1996). In the present work, we demonstrated that similar effects are achieved by selective A_{2B}R stimulation: the A_{2B}R agonist BAY60-6583 decreased IK currents and inhibited OPC differentiation into mature OLs when added in the culture medium of these cells. These data are consistent to the notion that the inhibition of TEA-sensitive IK current in cultured OPCs prevents cell differentiation (Attali et al., 1997; Chittajallu et al., 2005; Coppi et al., 2013a; Gallo et al., 1996; Knutson et al., 1997). However, differently from A_{2A}Rs, A_{2B}Rs not only inhibit IK conductances but also IA transient currents. This discrepancy could be due to the fact that A_{2B}Rs, differently from A_{2A}Rs, may also activate G_q proteins (Antonioli et al., 2019). Finally, in accordance with K^+ channel inhibition, the A_{2B}R agonist BAY60-6583 also significantly depolarized cell membrane potential. Cell depolarization could be one of the mechanisms by which A_{2B}Rs modulate cell cycle and maturation, as suggested by other authors (Chen et al., 2014; Rao et al., 2015). A_{2B}R-mediated IK inhibition was obtained in the present work by using three different A_{2B}R agonists: the prototypical, commercially available, selective A_{2B}R agonist BAY60-6583, a recently synthetized A_{2B}R agonist P453, described by Betti and co-workers (Betti et al., 2018) and, lastly, the unselective adenosine receptor agonist NECA. All compounds were applied in the continuous presence of saturating concentrations of A_1R, A_{2A}R and A_3R antagonists to avoid

nonspecific effects on other adenosine receptor subtypes. We can conclude that ramp current inhibition observed in the presence of the above mentioned compounds is $A_{2B}R$-mediated. We also investigated the intracellular pathway by which $A_{2B}Rs$ inhibit K^+ currents. Our previous data showed that the G_s-coupled $A_{2A}R$ decreases ramp-evoked K^+ currents in purified OPCs (Coppi et al., 2013a), whereas the G_i-coupled GPR17 receptor increases (Coppi et al., 2013b) the same conductances. So, we tested the hypothesis of intracellular cAMP being involved. Indeed, the adenylyl cyclase activator forskolin inhibited ramp currents and occluded the effect of a further application of BAY60-6583, demonstrating that $A_{2B}R$-mediated effect is mediated by intracellular cAMP rise (Fig. 39).

Silencing experiments demonstrate that $A_{2B}R$ downregulation is, *per se*, a signal for enhancing OPC differentiation. Given the notoriously low affinity of this receptor for the endogenous ligand adenosine, we discourage the hypothesis that $A_{2B}R$ could be activated by adenosine released from OPC cultures under control conditions. Furthermore, constitutive activation of $A_{2B}R$ is also improbable because we did not observe any modification in ramp currents when the $A_{2B}R$ antagonist MRS1706 was applied alone in OPCs. So, we hypothesize that $A_{2B}R$ could dimerize with some other receptors (an option that has been previously reported for this adenosine receptor subtype: (Fusco et al., 2019, 2018)) or, indeed, could promote the maintenance of high levels of S1P by some still unknown mechanisms. Consistently with this hypothesis, we demonstrate here that SphK inhibition by VPC96047 counteracts the overexpression of $A_{2B}Rs$ observed in OPC cultures during the 7 days of maturation. Furthermore, either SphK inhibition or $A_{2B}R$ silencing produce enhanced OPC differentiation, thus corroborating our hypothesis of crosstalk and, in particular, of reciprocal control between these two pathways (Fig. 39). Of note, data by Gonçalves and co-workers reported that $A_{2B}R$-KO mice are devoid of any obvious behavioural phenotype when tested by open field, elevated plus-maze or Y-maze paradigms (Gonçalves et al., 2015). Here we found some important effects of $A_{2B}Rs$ on in vitro OPC maturation, which is

inhibited by $A_{2B}R$ agonists and enhanced by receptor silencing. Thus, theoretically, $A_{2B}R$-KO mice would present increased, or more efficient, myelination, a fact that is not necessarily linked to appreciable differences in behavioural tests.

S1P activates a family of G-protein coupled receptors, S1P1-5 that modulate a variety of cell functions (Strub et al., 2010). S1P is reported to act as a mitogen in glial cells and neural progenitors, i.e. it increases cell proliferation and promotes the production of neurotrophic factors, (Bassi et al., 2006; Harada et al., 2004; Yamagata et al., 2003). As an example, PDGF-stimulated OPC proliferations is attenuated in S1P1 silenced cells (Jung et al., 2007) or by SphK inhibitors. Thus, it appears that high levels of this metabolite support the undifferentiated OPC phenotype whereas a decrease in S1P production, or an increase in S1P degradation, would promote OPC maturation. This notion is confirmed by the present work as SphK inhibition by VPC96047 or VPC96091 markedly increased MAG and MBP expression in OL cultures at t_7 and also significantly increased IK currents when incubated for 45 min in OPC cultures, an effect that has already been linked to increased OPC maturation (Coppi et al., 2013b). Furthermore, we provide here the first demonstration of an interplay between SphK and $A_{2B}R$ activation in OPCs as demonstrated by the fact that: (i) an acute application of the $A_{2B}R$ agonist BAY60-6583 promotes SphK1 (but not SphK2) phosphorylation; (ii) the SphK inhibitor VPC96047 prevents the increase in $A_{2B}R$ expression observed during OPC maturation; (iii) $A_{2B}R$ silencing decreases SphK1 (but not SphK2), S1P3 and S1P5 levels and highly increases S1P lyase expression.

Of note, either Western blot, RT-PCR or silencing experiments demonstrated that $A_{2B}R$ activation specifically affects SphK1 isoform. However, to our surprise, neither of the two SphK inhibitors tested, VPC96047 (which blocks both SphK1 and 2) and VPC96091 (which selectively inhibits SphK1) were able to prevent BAY60-6583-mediated effect either on ramp currents nor on OPC differentiation, demonstrating that $A_{2B}R$mediated response overrides the pro-

differentiating effect of SphK inhibition. However, the fact that $A_{2B}R$ silencing strikingly increased S1P lyase expression suggests an interplay between $A_{2B}R$ and S1P signalling more at the level of S1P degradation, rather than its synthesis.

Indeed, in conditions of altered S1P degradation, we hypothesize that inhibition of S1P synthesis by VPC96047or VPC96091 would have little impact on S1P levels. This concept is in accordance with previous data showing that increased S1P levels found in mixed glial cell cultures after treatment with remyelination promoting antibody rHIgM22, were not associated to an increased expression and/or phosphorylation of SphK1 or 2 but rather to a decrease in S1P lyase (Grassi et al., 2019). Of note, increased S1P levels are associated to mitogenic effects, as mentioned above.

An additional proof that $A_{2B}Rs$ are critical modulators of OPC maturation resides in the fact that this receptor subtype is clearly upregulated during cell differentiation, an effect that is completely prevented when cells are differentiated in the presence of the pan SphK inhibitor VPC96047. S1P5 receptor, whose expression is limited to the oligodendroglial lineage (Jaillard et al., 2005), is also upregulated during oligodendrogliogenesis, a result that was previously reported by others (Yu et al., 2004) but, differently from $A_{2B}R$, its upregulation is not modified when OPCs are differentiated in the presence of VPC96047. Fingolimod (FTY-720) is the first oral MS disease therapeutic agent and the first human medicine to be approved that targets S1P receptors. Emerging evidence indicates that its immunomodulatory role could be supported by an additional protective effect exerted at central level, possibly on OPCs, by facilitating myelin production. Results from in vitro studies have shown that the effect of FTY720-P on cultured oligodendrocyte lineage cells is complex at best as is affected by developmental stage of OPCs, concentration and duration of treatment (Miron et al., 2008; Novgorodov et al., 2007).

Here we found that FTY720-P differently affected BAY60-6583-mediated K^+ current inhibition depending upon the concentration applied. When

administered at 1 μM, it mimicked and partially occluded the effect of a subsequent BAY60-6583 application on voltage-dependent K^+ currents. This confirms, again, that S1P and $A_{2B}R$ pathways converge. On the other hand, the effect of BAY60-6583 on ramp currents was significantly enhanced in the presence of 10 nM FTY720-P. Similarly, 10 nM FTY720-P increased, whereas 1 μM decreased, MAG expression after 7 days of OPC maturation. Contrasting effects of this compound depending on the concentration used have been previously reported by others. For example, Jung and collaborators demonstrated that high (1 μM) and low (10 nM) doses of FTY720-P mediate opposite effects in rat OPC cultures (Jung et al., 2007). Similarly, Miron et al. reported that the effects of fingolimod on process dynamics in mature oligodendrocytes depended on both concentration and treatment duration (Miron et al., 2008). Differently from FTY720-P, when S1P is used as a ligand, the effect on ramp currents was not observed. This apparent discrepancy may be ascribed to the fact that receptor ligation by FTY720-P is restricted to all S1P receptors except S1P2. Moreover, the functional outcome induced by S1P receptor modulators could differ from one ligand to another since it could differently affect receptor fate. Indeed, it has been shown that FTY720P can induce S1P1 receptor degradation, whereas S1P affects receptor recycling. Finally the lack of effect exerted by exogenous S1P is in agreement with previous data in different cellular models, such as skeletal muscle cells, were agonist-induced S1P intracellular production opposite actions compared to exogenous S1P (Cencetti et al., 2013, 2010; Donati et al., 2005). This effect can be explained by a localized release of bioactive lipid in membrane microdomain where the availability of certain receptor subtypes is limited. The spatial regulation of S1P biosynthesis within the cell, together with its localized partitioning into plasma membrane domains, determines the subset of engaged S1P receptors and thus the biological outcome (Donati et al., 2013).

The differentiation of OPCs in our experimental model is reduced after the treatment with high (μM) concentrations of FTY720-P, in agreement with

previous results obtained in rat cultured OPC (Coelho et al., 2007; Jung et al., 2007; Miron et al., 2008).

Among the different S1P receptors expressed in OPCs, namely S1P1, S1P2, S1P3 and S1P5, binding of S1P to S1P1, S1P2, and S1P3 receptors has been shown to promote cell proliferation whereas binding to S1P5 is associated with anti-proliferative effect (Gonda et al., 1999; Malek et al., 2001). However, in the present work, neither the S1P1 agonist SEW2871 nor its antagonist W146 were able to affect OPC differentiation nor the effect of BAY60-6583 on it, thus ruling out a role of this receptor subtype in this phenomenon.

Differently, Dukala and Soliven reported that deletion of S1P1 in oligodendroglial lineage cells leads to a delayed differentiation of OPCs into OLs in the mouse brain solely during early myelination stages (i.e. at P14 and P21) but not at 3 months (Dukala and Soliven, 2016; Kim et al., 2011). So, we hypothesize that differences in the in vivo time window analyzed by those authors vs the in vitro stage of differentiation investigated in the present work could justify the discrepancy.

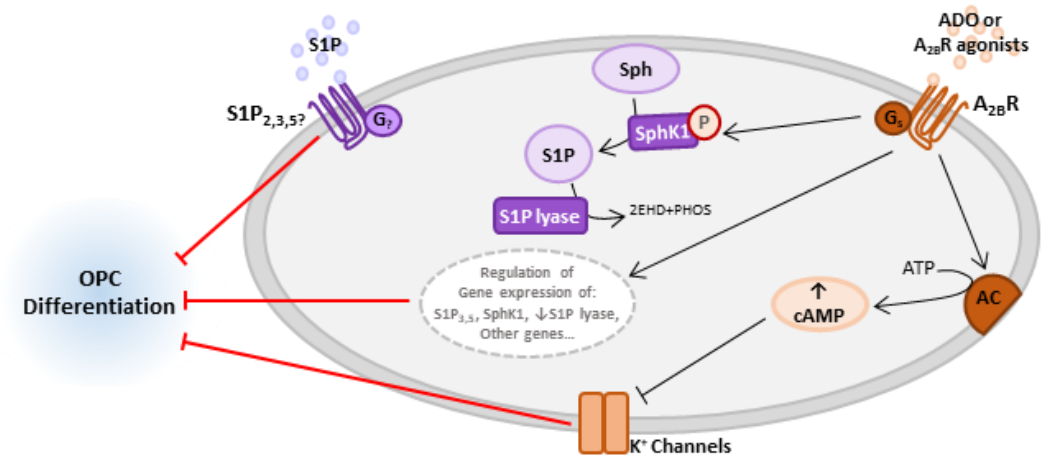

Figure 39. *Schematic representation of the results discussed in this section.*

Aim III - *Adenosine A3 receptor activation inhibits pronociceptive N-type Ca^{2+} currents and cell excitability in dorsal root ganglion neurons.*

The following results are recently published in:

Coppi, E., Cherchi, F., Fusco, I., Failli, P., Vona, A., Dettori, I., Gaviano, L., Lucarini, E., Jacobson, K.A., Tosh, D.K., et al. (2019). ***Adenosine A3 receptor activation inhibits pronociceptive N-type Ca^{2+} currents and cell excitability in dorsal root ganglion neurons***.

Pain 160, 1103–1118.

3.1. Selective A_3R activation inhibits Ca^{2+} currents in cultured rat dorsal root ganglion neurons

Because no data are available up to now concerning the electrophysiological effect/s of A_3R on DRG neurons, we first tested the prototypical A_3R agonist Cl-IB-MECA under "similar physiological conditions," i.e., we applied a voltage-ramp protocol (from +65 to -135 mV, 800-ms duration: see inset of Fig. A) in K^+-containing solutions before, during, and after the superfusion of this compound. As shown in figure 40A, the application of 100 nM Cl-IB-MECA decreased overall outward currents evoked by the voltage ramp: the effect peaked within 5 minutes and was partially reversed after drug washout. Figure 40B shows that the net Cl-IB-MECA–inhibited current was an outward current activated at potentials positive to -45 mV. Ramp current inhibition measured at +65 mV in the presence of Cl-IB-MECA was statistically significant in 14 cells investigated (Fig. 40C, D: from 799.0 ± 111.9 pA/pF in control to 617.2 ± 92.3 pA/pF in 100 nM Cl-IB-MECA, $P < 0.001$, the paired Student t-test), whereas no changes in inward ramp currents at 2135 mV were detected (Fig. 40C, D: from -46.6 ± 10.7 pA/pF in control to -42.8 ± 7.5 pA/pF in 100 nM Cl-IB-MECA, $P = 0.3734$, the paired Student t-test). The Cl-IB-MECA effect was observed in all cells tested, in agreement with high A_3R levels expression in DRG homogenate as revealed by RT-PCR (Fig. 40E) and immunocytochemical analysis (Fig. 40F, G). Our data are in line with previous

work in the literature demonstrating the expression of this receptor subtype on rat DRG neurons, even if species-specific differences have been found (Ray et al., 2018; Usoskin et al., 2015). The effect was concentration dependent (Fig. 40H), with an EC_{50} of 2.0 nM (confidence limits: from 1.2 to 3.2 nM; Fig. 40I), and prevented by 2 different A3AR antagonists: VUF5574 (100 nM) andMRS1523 (100 nM) (Fig. 40 J, K).

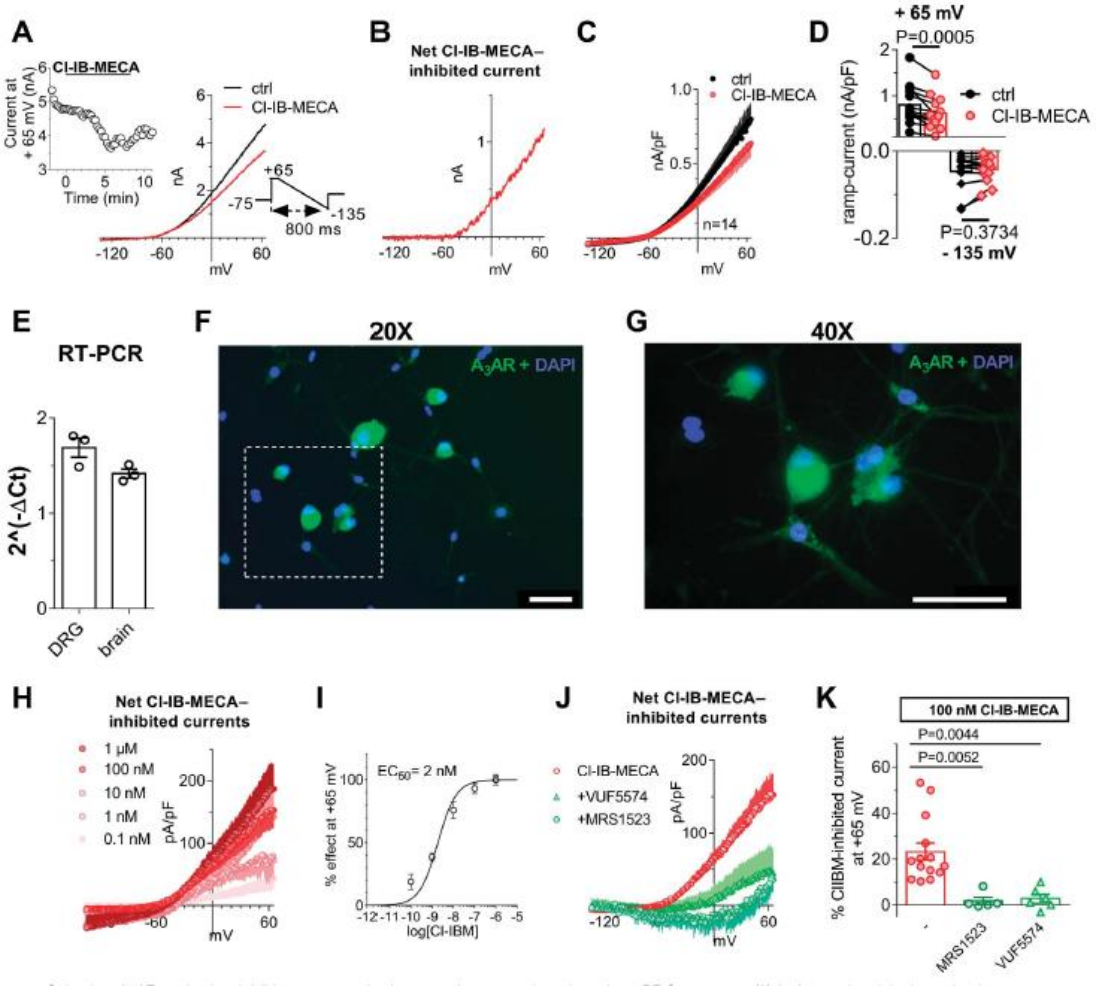

Figure 40. ***Selective A_3R activation inhibits ramp-evoked outward currents in cultured rat DRG neurons.*** **A.** Left panel: original patch-clamp current traces recorded in a representative cell where a voltage-ramp protocol (165/2135 mV, 800 ms: lower inset) was applied before (ctrl), during, and after Cl-IB-MECA (100 nM) superfusion. Upper inset: time course of ramp-evoked currents at 165 mV in the same cell. **B.** Net Cl-IB-MECA–inhibited current, obtained by subtraction of the ramp recorded in Cl-IB-MECA from the control ramp, in the same cell. **C, D.** Averaged ramp traces (**C**) and pooled data at +65 and -135mV (**D**) of ramp-evoked currents measured in the absence or presence of Cl-IB-MECA in 14 cells investigated. P = 0.0005 at +65 mV; P = 0.3734 at −135 mV; the paired Student t test, n = 14. **E.** Real-time polymerase chain reaction experiments demonstrated that A_3R-coding mRNA is present in rat DRG homogenates. Data were normalized to A3 receptor expression as a fraction of the house-keeping gene GADPH (glyceraldehyde-3-phosphate dehydrogenase) and have been obtained in 3 independent experiments performed in triplicate. A brain tissue homogenate was taken as the positive control. **F, G.** 20× (**F**) and 40× (**G**) magnification of A_3R immunofluorescent labelling (green) of DRG cultures. Cells nuclei were marked with DAPI (blue). Scale bar: 50 µm. **H**. Averaged Cl-IB-MECA–inhibited currents at different agonist concentrations (0.1–1000 nM; at least n = 4 in each experimental condition). **I.** Concentration-response curve of Cl-IB-MECA effect on ramp currents measured at +65 mV (confidence limit: from 1.2 to 3.2 nM). **J, K.** Net 100 nM Cl-IB-MECA–inhibited currents (**J**) and respective pooled data at +65 mV (**K**) recorded in the absence or presence of 2 different A_3R antagonists: MRS1523 (100 nM; n = 5) and VUF5574 (100 nM; n = 6). One-way ANOVA, Bonferroni post-test.

Another highly selective A_3R agonist was tested: MRS5980, whose EC_{50} is described in the sub nanomolar range (EC_{50} = 0.7 ± 0.1 nM; (D. Tosh et al., 2014)). This compound also concentration dependently inhibited total outward currents evoked by the ramp protocol at +65 mV in 8 cells investigated (Fig. 41A–C), and the effect was prevented by MRS1523 (inset in Fig. 41A). The effect of both A_3R agonists was shared by the endogenous ligand adenosine (30 µM: Fig. 41D), which significantly decreased ramp currents at + 65 mV in 5 cells tested without modifying the inward component (Fig. 41E). Notably, the adenosine effect was significantly inhibited by VUF5574 (100 nM; n = 6: Fig. 41F; **P < 0.01, the unpaired Student t-test).

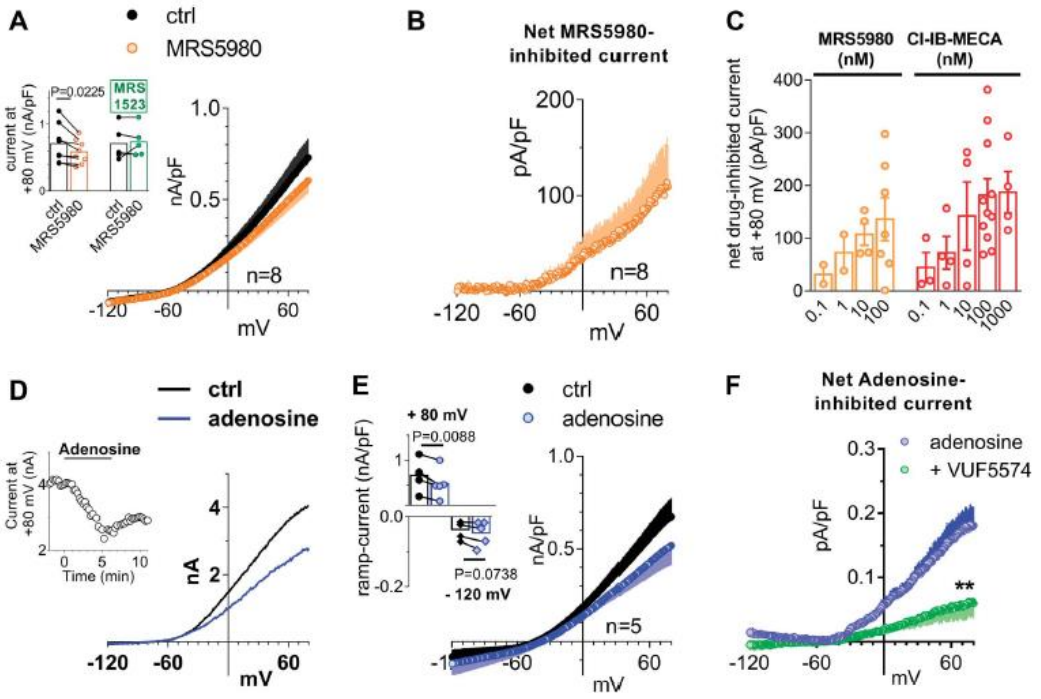

Figure 41. ***The newly synthetized, highly selective, A_3R agonist MRS5980 and the endogenous ligand adenosine mimic Cl-IB-MECA effect in inhibiting ramp-evoked outward currents in isolated rat DRG neurons.*** **A.** Averaged traces of ramp-evoked currents measured before or after MRS5980 application (100 nM) in 8 cells investigated. Inset: pooled data or ramp-evoked current at +65 mV in the presence of MRS5980 alone or during coapplication with the A_3R antagonist MRS1523 (100 nM; n = 5). The paired Student t-test. **B.** Net MRS5980-inhibited current in 8 cells tested. **C.** Comparison between net Cl-IB-MECA–or MRS5980-inhibited ramp currents measured at +65 mV at different agonists concentrations. **D.** Original ramp current traces recorded in a representative cell before (ctrl), during, or after adenosine (30 µM) superfusion. Inset: time course of ramp-evoked currents at +65 mV in the same cell. **E.** Pooled data of ramp-evoked currents at +65 mV or −135 mV before or after the application of adenosine in 5 cells investigated. P = 0.0088 at +65 mV; P = 0.0738 at −135 mV, the paired Student t-test, n = 5. **F.** Averaged adenosine-inhibited currents, obtained by subtraction of the adenosine ramp from the control ramp, recorded in the absence (n = 5) or presence of A_3R antagonist VUF5574 (100 nM, n = 6). **P < 0.01 at + 65 mV, the unpaired Student t test.

To define A_3R -responding DRG neurons as nociceptors, cells were tested for their responsiveness to the TRPA1 agonist AITC and the TRPV1 agonist capsaicin. At least 5 minutes after Cl-IB-MECA removal, cells were voltage clamped at −75 mV and the 2 TRP agonists were applied consecutively. As shown in a typical cell in figure 42A, both compounds activated an inward current in the vast majority of cells investigated (Fig. 42B): 8 of 33 cells tested for TRP response were insensitive to 1 of the 2 TRP agonists, and 1 cell was insensitive to both compounds but still sensitive to Cl-IB-MECA. In figure 42C, we pooled cell capacitance values measured in those 33 TRP-sensitive cells vs capacitance values measured in the residual cells analyzed in the present research but not tested for TRP responses (TRP not tested: n = 112). Of note, cell capacitance, as a measure of a spherical-approximated cell soma, was not statistically different in TRP-sensitive (25.1 ± 1.7 pF; n = 33, corresponding to a cell diameter of 28.3 µm: see Methods) vs TRP not tested (25.3 ± 1.2 pF; n = 112, corresponding to a cell diameter of 28.4 µm; the unpaired Student t test, P = 0.9825; Fig. 42C) neurons. Our results thus indicate that both groups of cells were composed of neurons with a 25-µm diameter, therefore adhering to the definition of small- to medium-sized DRG neurons defined as "nociceptors" (Harper and Lawson, 1985; Scroggs and Fox, 1992).

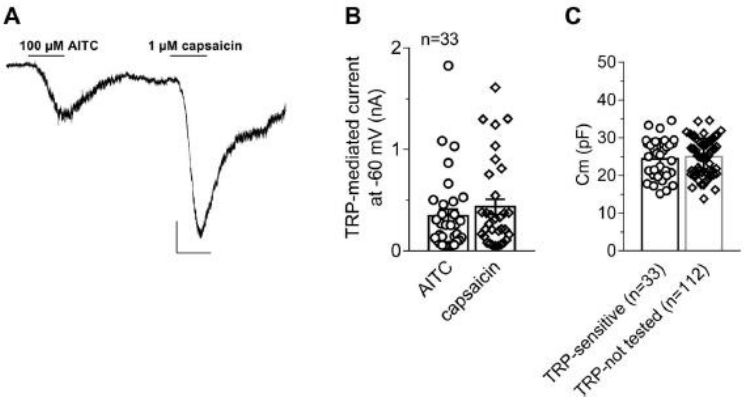

Figure 42. ***Dorsal root ganglion (DRG) neurons responding to Cl-IB-MECA are nociceptors sensitive to the TRPV1 and TRPA1 agonists capsaicin and allyl isothiocyanate.*** **A.** Original current trace recorded in a −75 mV-clamped cell after 10-minute washout of a previous Cl-IB-MECA application. Scale bars: 200 pA; 1 minute. **B.** Pooled data of AITC- and capsaicin-activated currents in 33 cells investigated. **C.** Pooled data of cell capacitance measured in AITC- and capsaicin-sensitive cells ("TRP-sensitive" neurons: n = 33) or in cells not exposed to capsaicin or AITC challenge ("TRP non-tested" neurons, n = 112). P = 0.8045, the unpaired Student t test. AITC, allyl isothiocyanate.

Data in the literature demonstrate that adenosine and its analogues inhibit Ca_Vs in rat DRG neurons (A. C. Dolphin et al., 1986; MacDonald et al., 1986) with no obvious distinction between A_1- vs A3-mediated effects provided to date. For this reason, we tested the hypothesis that the decreased total outward currents observed in the present work by A_3R activation might depend on a decrease of Ca^{2+} entry from Ca_Vs and, thus, reduced activation of Ca^{2+}-activated K^+ conductances (KCa). Therefore, we applied Cl-IB-MECA in the presence of the nonselective Ca_V blocker Cd^{2+}. First of all, by using our voltage-ramp protocol, we confirmed the activation of KCa channels in DRG neurons by applying extracellular Cd^{2+} that, *per se*, induced a 34.0 ± 13.3% inhibition of total outward currents evoked by the ramp protocol (from +245.7 ± 15.6 pA/pF in ctrl to 167.2 ± 26.3 pA/pF in 100-µM Cd^{2+} at +65 mV, n = 4, P < 0.05; the paired Student t test; Fig. 43C: 34.0 ± 8.7% current inhibition). The effect of Cd^{2+} was not different when applied at 100 µM, 500 µM, or 1 mM concentrations (Fig. 43A–C).

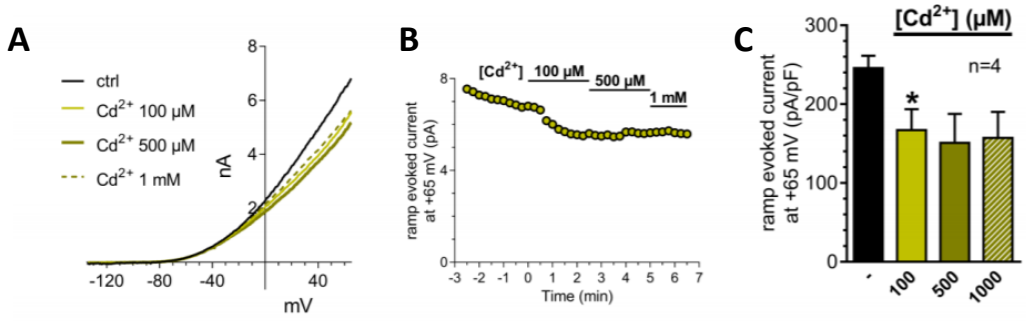

Figure 43. ***Extracellular Cd^{2+} inhibits outward K^+ currents evoked by the voltage ramp protocol.*** **A.** Original ramp current traces recorded before (control: ctrl) and after the application of different concentrations of Cd^{2+} in a representative DRG neuron. **B.** Time course of ramp-evoked currents at +65 mV in the same cell. **C.** Pooled data of ramp-evoked currents at +65 mV before or after the application of different Cd^{2+} concentrations. *P=0.0339 vs ctrl, paired Student's t-test, n=4.

Thus, we applied Cl-IB-MECA in the presence of Cd^{2+} to test whether the A_3R agonist effect was prevented in conditions of Ca^{2+} entry block. As shown in Figure 44A–C, Cd^{2+} completely prevented Cl-IB-MECA–induced decrease of outward ramp currents. Data were confirmed by applying 2 selective blockers of KCa channels: apamin (100 nM), which selectively blocks small-

conductance KCa (SK channels), and TEA at low concentrations (200 µM), which selectively inhibits big-conductance KCa (BK channels). Alone or in combination, both compounds significantly or completely prevented Cl-IB-MECA–mediated inhibition of ramp-evoked outward currents (Fig. 44D, E). The above data demonstrate that BK and SK channel activation was necessary for the A_3R-mediated ramp-current inhibition in rat DRG neurons.

Two possibilities exist to explain this phenomenon: (i) A_3R activation directly inhibits SK and BK channels; or (2) A_3Rs activation inhibits Ca^{2+} entry from Ca_V, which, in turn, decreases SK and BK channel opening. To test the latter hypothesis, we blocked all K^+ currents by replacing intracellular and extracellular K^+ ions with equimolar Cs^+. In these experimental conditions, an inward component arose in the ramp protocol peaking around 0 mV (Fig. 44F). This current was identified as a Ca^{2+} current because it was abolished by extracellular Cd^{2+} (Fig. 44F, G). When applying Cl-IB-MECA in Cs^+-replacement conditions, a significant decrease in inward peak current was observed (Fig. 44H: from −64.3 ± 14.8 pA/pF in control to −41.1 ± 11.4 pA/pF in Cl-IB-MECA, *P < 0.05, the paired Student t-test; n = 5), thus demonstrating that A_3R activation directly inhibited Ca^{2+}currents.

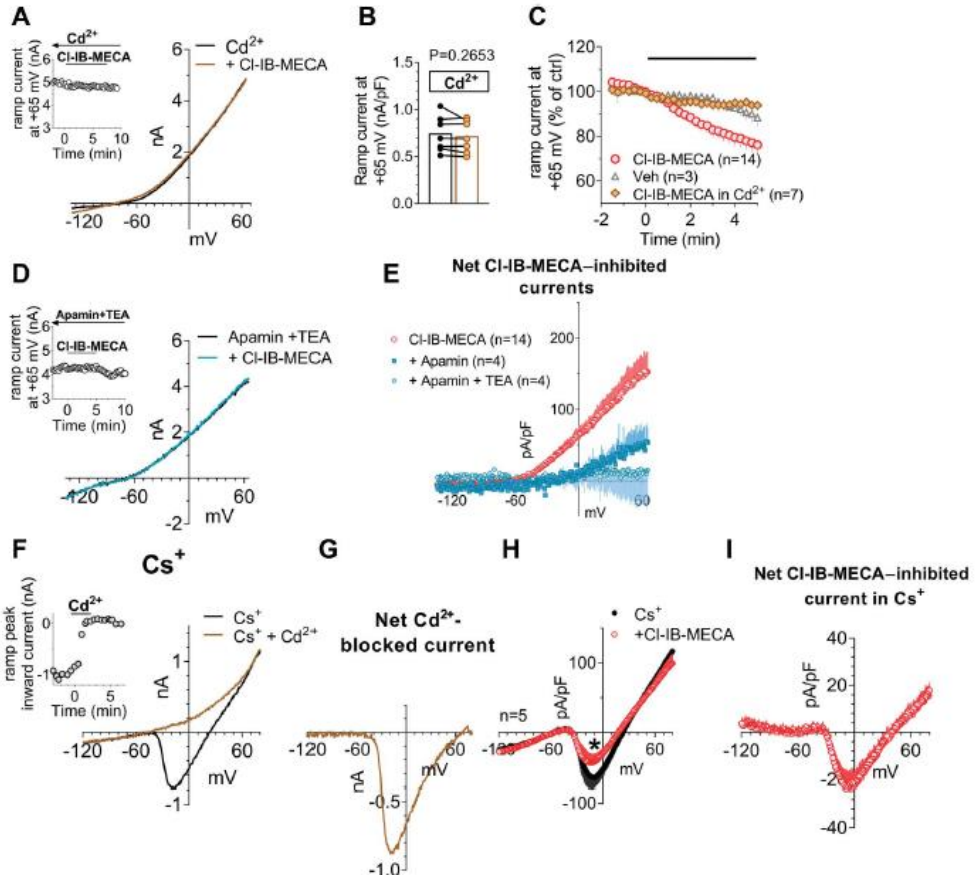

Figure 44. ***A_3R activation in DRG neurons inhibits Ca^{2+}-activated K^+ currents by reducing Ca^{2+} influx from voltage-dependent Ca^{2+} channels.*** **A.** Original ramp current traces recorded in 1 mM Cd^{2+}containing extracellular solution before (ctrl) or during Cl-IB-MECA (100 nM) application in a representative cell. Inset: time course of ramp-evoked currents at +65 mV in the same cell. **B.** Pooled data of ramp-evoked currents measured at +65 mV in the absence or presence of Cl-IB-MECA in Cd^{2+}-containing extracellular solution in 7 cells investigated. P = 0.2653, the paired Student t-test. **C.** Averaged time course of ramp-evoked currents at +65 mV in the presence of Cl-IB-MECA (n = 14), its vehicle (Veh: 0.1% DMSO: n = 3), or Cl-IB-MECA in Cd^{2+} (n = 7). **D.** Original ramp current traces recorded in apamin (100 nM) with tetraethylammonium (TEA, 200 µM) before (apamin + TEA) or during Cl-IB-MECA (100 nM) application in a representative cell. Inset: time course of ramp-evoked currents at +65 mV in the same cell. **E.** Averaged Cl-IB-MECA–inhibited currents in the absence (n = 14) or presence of apamin alone (n = 4) or during co-application with TEA (n = 4). **F.** Original ramp current traces recorded before (ctrl) and during 1-mM Cd^{2+} application in a representative cell where extracellular and intracellular K^+ were replaced by equimolar Cs^+. Note that in these experimental conditions, a Cd^{2+}-sensitive inward current appears, which presents an I–V relationship typical of Ca^{2+} currents. Inset: time course of ramp-evoked current measured at the inward peak in the same cell. **G.** Net Cd^{2+}-blocked Ca^{2+} current evoked by the ramp protocol in the same cell. **H.** Averaged ramp-evoked currents recorded in Cs^+-replacement conditions before (ctrl) or during Cl-IB-MECA (100 nM) application in 5 cells tested. *P < 0.05, the paired Student t test. **I.** Averaged Cl-IB-MECA–inhibited Ca^{2+} currents in Cs^+-replacement experiments.

Dorsal root ganglion neurons express different subtypes of Ca^{2+} currents (Scroggs and Fox, 1992, 1991; Wilson et al., 2000). To identify which of them are inhibited by the A_3R, we further isolated Ca_V-mediated currents by adding the $Na_v1.1$, 1.2, 1.3, 1.4, 1.6, and 1.7 blocker TTX (1 mM) plus the $Na_v1.8$ inhibitor A887826 (200 nM, to block this TTX-resistant Na^+ channel) to the Cs^+-containing extracellular solution. $Na_v1.8$ is known to be expressed at high levels in DRG neurons (Dib-Hajj et al., 2009), which we confirmed, because in the presence of 1 μM extracellular TTX, 200 nM A887826 completely blocked residual, TTX-resistant, Na^+ currents (Fig. 45A, B). As shown in figure 45C, under these experimental conditions, we successfully isolated Ca^{2+} currents activated by a 0 mV voltage step depolarization (200 ms duration), which were completely blocked by 100 μM Cd^{2+} (Fig. 45C–E). Such Ca^{2+} currents were predominantly N-type currents because application of selective N-type blocker PD173212 (500 nM: Fig. 45F, G) achieved a >80% block (Hu et al., 1999; Theis et al., 2018). Residual, PD173212-insensitive (up to 1 μM: Fig. 45H) Ca^{2+} currents in our experimental conditions were blocked by Cd^{2+} (Fig. 45H) and were attributed to Cd^{2+}-sensitive L-type and, eventually, R- and/or P/Q-type Ca_Vs, consistently with a previous report (Wilson et al., 2000). Current-to-voltage (I–V plot) relationship of Ca^{2+} currents activated by a series of depolarizing voltage steps (from -50 to +50 mV, 10 mV increment, 200 ms duration, Vh = -65 mV: inset in Fig. 45I) was consistent with Cd^{2+}-blocked (Fig. 45I) and PD173212-sensitive (Fig. 45J) N-type Ca_V activation.

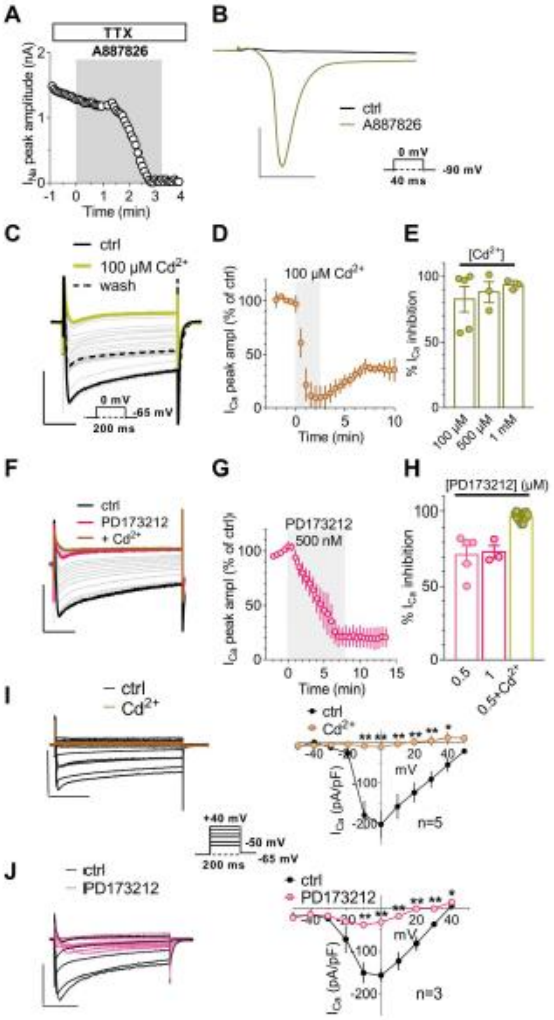

Figure 45. ***The major component of Ca^{2+} currents recorded in DRG neurons is carried by N-type Ca_V opening.*** **A.** Time course of Na^+ currents recorded in Cs^+-replacement conditions in the presence of extracellular TTX (1 µM), Cd^{2+} (500 µM), and Ni^{2+} (100 µM) and activated every 5 seconds by a 0 mV step depolarization (40 ms duration, Vh = −90 mV: lower inset in **B**) before or during the application of Nav1.8 blocker A887826 (200 nM). **B.** Original current traces recorded before and after 3 minute A887826 application. Scale bars: 3 nA; 10 ms. **C.** Original current traces evoked in a typical DRG neuron by a 0 mV step depolarization (200 ms; Vh = −65 mV: lower inset) in the presence of extracellular TTX (1 µM), Ni^{2+} (100 µM), and A887826 (200 nM) before (ctrl) or during the application of 100 µM Cd^{2+}. Scale bars: 1 nA; 50 ms. **D.** Averaged time courses of Ca^{2+} currents, measured at the inward peak, before and during the application of the nonselective Ca_V blocker 100 µM Cd^{2+} (n = 4). **E.** Pooled data of Ca^{2+} current inhibition in the presence of 100 µM, 500 µM, or 1 mM Cd^{2+}, n = 4. **F.** Original current traces evoked in a typical DRG neuron by a 0 mV step depolarization (200 ms; Vh = −65 mV) in the presence of extracellular TTX (1 µM), Ni^{2+} (100 µM), and A887826 (200 nM) before (ctrl) or during the application of PD173212 (0.5 µM) and, subsequently, 500 µM Cd^{2+}. Scale bars: 1 nA; 50 ms. **G.** Averaged time courses of Ca^{2+} currents before and during the application of selective N-type Ca^{2+} channel blocker PD173212 (500 nM, n = 4). **H.** Pooled data of Ca^{2+} current inhibition in the presence of 0.5 µM PD173212, 1 µM PD173212, or 0.5 µM PD173212 + 500 µM Cd^{2+}. **I, J.** Original current traces (left panels), and respective averaged I–V plots (right panels), of Ca^{2+} currents evoked by a series of 10 depolarizing voltage steps (from −50 to + 50 mV, 200 ms duration, Vh = −65 mV: see lower inset) before or during 500 µM Cd^{2+} (**I**) or 0.5 µM PD173212 (**J**) application. Scale bars: 1 nA; 50 ms. DRG, dorsal root ganglion; Ca_V, voltage-dependent Ca^{2+} channel. *P < 0.05; **P < 0.01; ***P < 0.001, paired Student t-test.

When Cl-IB-MECA was applied in these experimental conditions, a reversible decrease in total Ca^{2+} currents (both in the peak and steady-state component) was observed within 5 minutes of drug application (Fig. 46A). The I–V plot of such Ca^{2+} conductance (Fig. 46C) demonstrated that the A_3R agonist significantly inhibited Ca_Vs from 0 to +20 mV (the paired Student t-test, n = 5). The Cl-IB-MECA effect was significant in 8 cells tested (Fig. 46B), either as peak current amplitude (arrow in the right panel of Fig. 46A or Fig. 46B) or at the steady state (arrowhead in the right panel of Fig. 46A: from 57.4 ± 14.5 to 39.8 ± 10.2 pA/pF; $P < 0.05$, the paired Student t-test). However, the A_3R agonist apparently did not change the Ca^{2+} current kinetics because the time to peak was unaffected (from 15.1 ± 2.2 to 15.7 ± 3.0 ms; $P = 0.5553$, the paired Student t-test, data not shown). Cl-IB-MECA–mediated inhibition of Ca_Vs was concentration dependent with a maximal effect observed at 30 nM (Fig. 46E), in accordance with ramp experiments, and completely prevented by the A_3R antagonist MRS1523 (100 nM) and by the selective N-type channel blocker PD173212 (500 nM) but not by the selective, at least at 1 μM concentration (De Paoli et al., 2002), L-type blocker lacidipine (1 μM: Fig. 46D, E). The above data demonstrate that A_3R activation selectively inhibits N-type Ca^{2+} currents in rat DRG neurons. In the attempt to compare A_3R- vs A_1R-mediated effects on Ca_Vs, we applied the A_1R-selective agonist CPA. As shown in figures 46E and 42F, CPA-inhibited Ca^{2+} currents by 24.8 ± 3.2% (n = 9) and by 24.1 ± 3.0% (n = 7) at 1 and 10 μM concentrations, respectively. Of note, Ca^{2+} current inhibition measured in the presence of 1 μM CPA was significantly smaller compared with the Cl-IB-MECA–mediated effect (44.1 ± 5.6% inhibition in the presence of 30-nM ;Cl-IB-MECA vs 24.8 ± 3.2% inhibition in the presence of 1-μM CPA, $P < 0.05$, One-way ANOVA, Bonferroni post-test; fig. 46E).

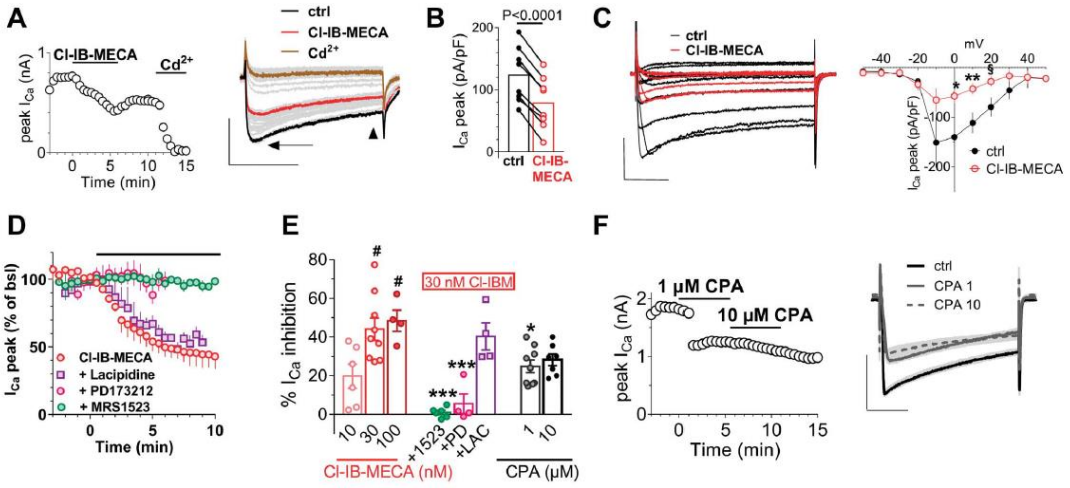

Figure 46. ***Cl-IB-MECA inhibits N-type Ca^{2+} currents in DRG neurons.*** ***A.*** *Left panel*: time course of peak Ca^{2+} currents (ICa) evoked by a 0 mV step depolarization in a typical DRG neuron. Note that Cl-IB-MECA (30 nM) inhibits Ca^{2+} currents that were completely abolished by a subsequent 500 μM Cd^{2+} application. *Right panel*: original current traces recorded in the same cell at significant time points. Scale bars: 0.5 nA, 100 ms. Arrow indicates peak Ca^{2+} currents, and arrowhead indicates steady-state Ca^{2+} currents. **B.** Pooled data of peak ICa measured in the absence or presence of Cl-IB-MECA in 8 cells investigated. $P < 0.0001$, the paired Student t-test. **C.** *Left panel*: original Ca^{2+} current traces evoked by a series of depolarizing voltage steps (inset) before (ctrl) or after Cl-IB-MECA (30 nM) application in a representative cell. *Right panel*: averaged I–V plot of Ca^{2+} currents measured at the peak in 5 cells tested. *$P < 0.05$; **$P = 0.01$; §$P = 0.0105$, the paired Student t test. Scale bars: 0.5 nA, 50 ms. **D.** Averaged time courses of peak Ca^{2+} current, expressed as % of baseline values, measured before or after the application of Cl-IB-MECA in different experimental groups. **E.** Pooled data of Cl-IB-MECA– or CPA-inhibited peak Ca^{2+} currents at different agonist concentrations, or in 30 nM Cl-IB-MECA during co-application with the A_3R antagonist MRS1523 (1523, 100 nM) or with the selective N-type and L-type Ca^{2+} channels blockers PD173212 (PD, 0.5 μM) and lacidipine (LAC, 1 μM), respectively. *$P < 0.05$; ***$P < 0.0001$ vs 30 nM Cl-IB-MECA; #$P < 0.05$ vs 10-nM Cl-IB-MECA, One-way ANOVA, Bonferroni post-test. **F.** *Left panel*: time course of peak ICa evoked by a 0 mV step depolarization in a typical DRG neuron in the absence or presence of N^6-cyclopentyladenosine (CPA: 1-10 μM). *Right panel*: original current traces recorded in the same cell at significant time points. Scale bars: 1 nA, 100 ms.

The newly synthetized A_3R agonist MRS5980 mimicked the Cl-IB-MECA effect in inhibiting Ca^{2+} currents (Fig. 47A, C) but with higher efficacy, showing a maximal Ca_V inhibition at 3 nM concentration (Fig. 47B) compared with 30 nM for Cl-IB-MECA. Furthermore, the MRS5980-mediated effect was prevented in the presence of A_3R antagonist MRS1523 (100 nM; Fig. 47B).

To explore the contribution of A_3R-mediated inhibition of Ca_Vs when the endogenous agonist is present in the extracellular space, we applied adenosine (30 μM) in the absence or presence of a selective A_1R or A_3R antagonist,

DPCPX or MRS1523, respectively. As expected from published data (A. C. Dolphin et al., 1986; MacDonald et al., 1986), adenosine inhibited Cd^{2+}-sensitive Ca^{2+} currents with a maximal effect observed at 30 µM (Fig. 47E). Of note, the effect induced by 30 µM adenosine was blocked by 39.1 ± 9.0% in the presence of DPCPX (500 nM) and by 56.6 ± 9.0% in the presence of MRS1523 (100 nM; Fig. 47E, F). No significant difference was found between DPCPX- and MRS1523-mediated inhibition of adenosine effects (One-way ANOVA, Bonferroni post-test).

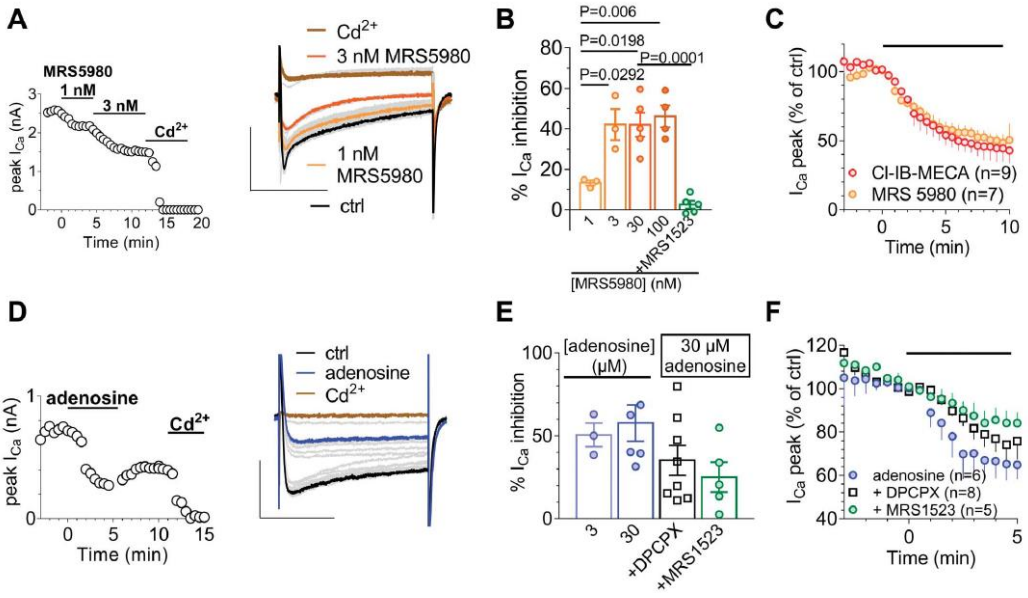

Figure 47. ***The inhibitory effect of Cl-IB-MECA on N-type Ca^{2+} currents in DRG neurons is mimicked by the newly synthetized A_3R agonist MRS5980 and by adenosine.*** **A.** *Left panel*: time course of peak ICa in a typical DRG neuron before and after MRS5980 (30 nM) and Cd^{2+} (500 µM) application. *Right panel*: original current traces recorded in the same cell at significant time points. Scale bars: 2 nA; 100 ms. **B.** Pooled data of MRS5980-inhibited peak Ca^{2+} current at different agonist concentrations or in the presence of 30 nM MRS5980 + 100 nM MRS15253. One-way ANOVA; Bonferroni post-test. **C.** Averaged time courses of peak ICa before or during Cl-IB-MECA (30 nM) or MRS5980 (3 nM) application. **D.** *Left panel*: time course of peak ICa in a typical DRG neuron before and after adenosine (30 nM) and Cd^{2+} (500 µM) application. *Right panel*: original current traces recorded in the same cell at significant time points. **E.** Pooled data of adenosine-inhibited peak Ca^{2+} currents at different agonist concentrations or in the presence of 30 µM adenosine + the A_3R antagonist MRS15253 (100 nM) or the A_1R antagonist DPCPX (500 nM). No significant difference was found between any of the experimental groups (One-way ANOVA, Bonferroni post-test). **F.** Averaged time courses of peak Ca^{2+} current amplitude before or after adenosine (30 µM) application alone or in the presence of DPCPX (500 nM) or MRS1523 (100 nM).

Finally, we evaluated the impact of selective A_3R activation on neuronal excitability. We induced AP firing by injecting a depolarizing ramp current from the resting membrane potential. As shown in figure 48A, this protocol induced repetitive firing in DRG neurons, which was markedly reduced in the presence of Cl-IBMECA (Fig. 48A, B). The effect was statistically significant in 6 cells tested (Fig. 48C) and prevented in the presence of A_3R antagonist MRS1523 (100 nM; Fig. 48D–F) but not by the N-type Ca_V blocker PD173212 (1 mM; Fig. 48G–I). Of note, a two-way ANOVA comparison between the effect of Cl-IB-MECA when applied alone (Fig. 48J, left column: "in ctrl") or applied in the presence of PD173212 (Fig. 48J, right column: "in PD173212") highlighted that: (i) a statistical difference was found between the number of APs recorded in control conditions or in the presence of PD173212 alone (Fig. 48J, black circles: before Cl-IB-MECA: 6.5 ± 1.3 APs in ctrl, n = 6, vs 19.1 ± 3.4 APs in PD173212, n = 7; $P < 0.01$), indicating that N-type Ca_V block exerts a pro-excitatory effect on cells firing; and (ii) no difference was found in the inhibitory effect of Cl-IB-MECA when applied in the absence or presence of PD173212 (gray circles: after Cl-IB-MECA: 3.3 ± 1.9 APs in Cl-IB-MECA, n = 6, vs 5.6 ± 1.1 APs in Cl-IB-MECA + PD173212; $P = 0.7109$), indicating that Cl-IB-MECA effect on firing is not occluded by N-type Ca_V.

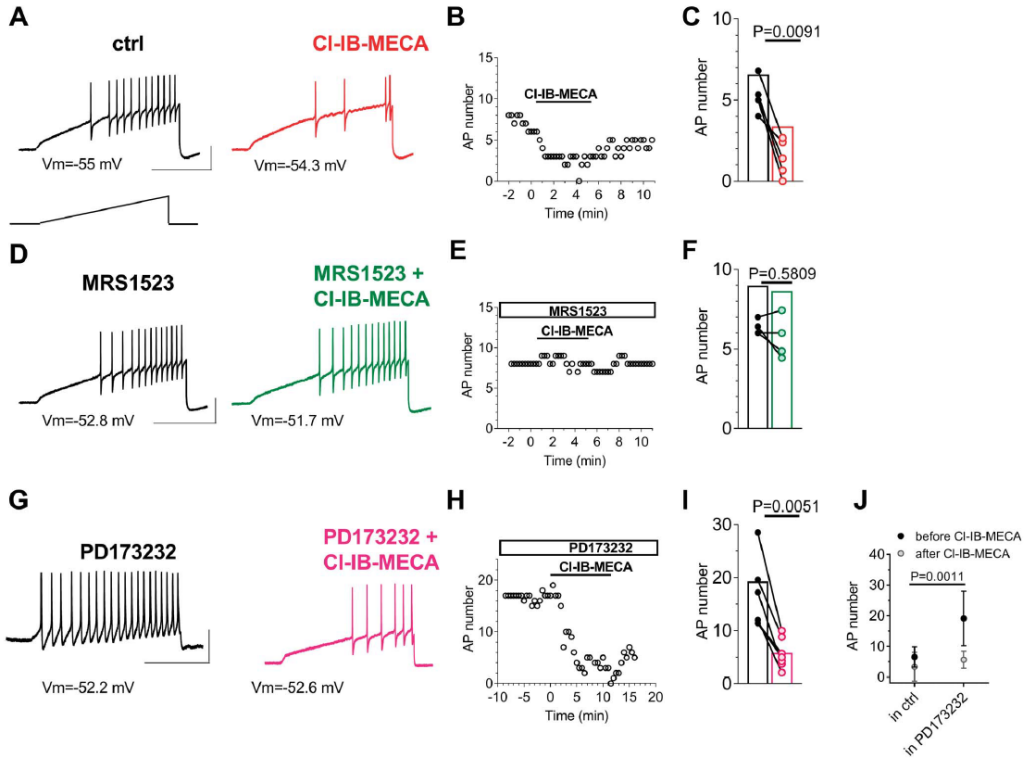

Figure 48. ***Cl-IB-MECA inhibits AP firing in DRG neurons.*** **A.** Original AP traces evoked in a typical DRG neuron by a 1 second depolarizing ramp current injection (lower inset) recorded before (black trace) or after (red trace) 5 minute Cl-IB-MECA (100 nM) application. **B.** Time course of AP number in the same cell. **C.** Pooled data of AP number measured before or after 5 minute Cl-IB-MECA application in 6 cells tested. $P < 0.01$, the paired Student t-test. **D.** Original AP traces evoked by a 1 second depolarizing ramp current injection recorded before (black trace) or after (green trace) 5 minute Cl-IB-MECA (100 nM) application in the presence of MRS1523 (100 nM). **E.** Time course of AP number in the same cell. **F.** Pooled data of AP number measured before or after 5 minute Cl-IB-MECA application in the presence of MRS1523 in 5 cells tested. $P = 0.5809$, the paired Student t-test. **G.** Original AP traces evoked by a 1 second depolarizing ramp current injection recorded before (black trace) or after (purple trace) 5 minute Cl-IB-MECA (100 nM) application in the presence of PD173212 (1 µM). **H.** Time course of AP number in the same cell. **I.** Pooled data of AP number measured before or after 5 minute Cl-IB-MECA application in the presence of PD173212 in 6 cells tested. The paired Student t-test. Scale bars: 50 mV; 500 ms. **J.** Comparison between the effect of Cl-IB-MECA on AP firing when applied alone ("in ctrl," n = 6) or when applied in the presence of 1 µM PD173212 ("in PD173212," n = 7). Treatment (Cl-IB-MECA): $F_{(1,22)} = 11.46$, $P < 0.01$; time (before/after): $F_{(1,22)} = 14.27$, $P < 0.001$; interaction: $F_{(1,22)} = 5.416$, $P < 0.01$; 2-way ANOVA, Bonferroni post-test. Note that there is a statistical difference (**$P < 0.001$) between the AP number recorded before Cl-IB-MECA application in the ctrl group ("in ctrl") or in the PD173212 group ("in PD173212") but not between the AP number recorded after Cl-IB-MECA application in the ctrl group or in the PD173212 group ($P = 0.7109$).

To corroborate the proexcitatory effect of N-type Ca_V block, we applied PD173212 alone in a separate group of cells, and we observed a significant increase in AP firing (Fig. 49) accompanied by a significant cell depolarization (Fig. 49B, C and Table 5: from −63.6 ± 2.9 mV in control to −59.7 ± 3.6 mV in 1-μM PD173212; $P < 0.05$, the paired Student t-test, n = 7) and lowering of AP threshold (Table 5: from −12.7 ± 1.9 mV in control to −14.1 ± 1.51 mV in 1-μM PD173212; $P < 0.05$, the paired Student t-test, n = 7). Furthermore, in accordance with KCa inhibition and in particular with BK channel block, we measured a significant increase in AP duration (from 3.9 ± 0.7 ms in control to 4.5 ± 0.6 ms in 1 μM PD173212; $P < 0.01$, the paired Student t-test, n = 7) and a reduction in fast afterhyperpolarization (from 46.0 ± 2.1 mV in control to 34.8 ± 4.4 mV in 1 μM PD173212; $P < 0.05$, the paired Student t test, n = 7) on PD173212 superfusion (see Table 5). Other AP parameters (reported in Table 5) were not modified by any treatment.

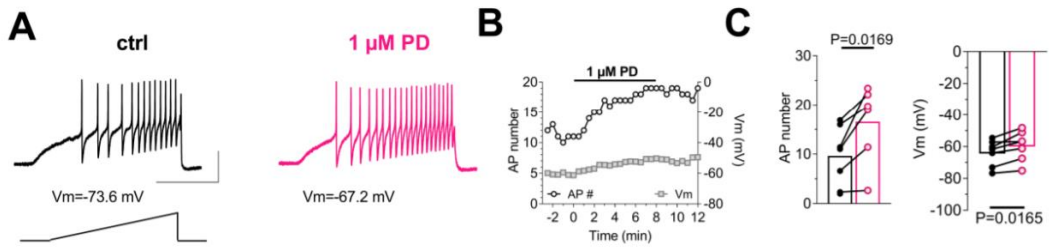

Figure 49. ***The N-type Ca^{2+} channel blocker PD173212 increases AP firing in DRG neurons*****. A.** Original AP traces evoked in a typical DRG neuron by a 1 s depolarizing ramp current injection (lower inset) recorded before (black trace) or after (purple trace) 5 min PD173212 (1 μM) application. **B.** Time course of AP number (open black circles, left y axis) and resting membrane potential (open grey circles, right y axis) in the same cell. **C.** Pooled data of AP number (left panel) and resting membrane potential (Vm: right panel) measured before or after 5 min PD173212 application in 8 cells tested. Paired Student's t-test.

In the attempt to identify the mechanism by which A_3R inhibits cell firing, we tested the effect of Cl-IB-MECA on Na^+ currents with no obvious differences detected in its presence (Fig. 50A, B), either on current amplitude (Fig. 50C) or time to peak (Fig. 50D).

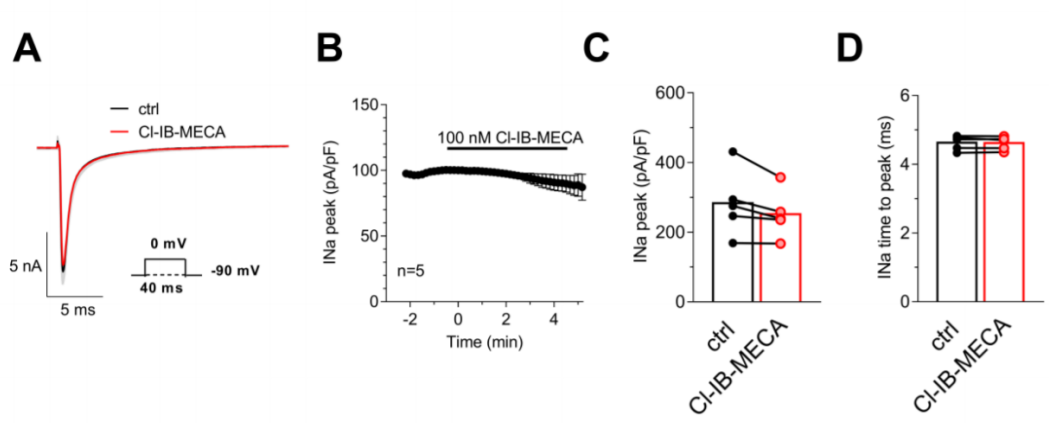

Figure 50. ***Cl-IB-MECA does not affect Na⁺ currents in DRG neurons.*** **A.** Original Na^+ current traces evoked by a 0 mV depolarization (40 ms duration, Ih = -90 mV: see lower inset) recorded in a typical DRG neuron before (black trace) or after (red trace) the application of Cl-IB-MECA (100 nM; 5 min). **B.** Averaged time course of peak INa amplitude in 5 cells investigated. **C.** Pooled data of Na^+ current peak amplitude measured before or after 5 min application of Cl-IB-MECA in 5 cells investigated. P=0.0642, paired Student's t-test. **D.** Pooled data of Na^+ current time to peak measured before or after 5 min application of Cl-IB-MECA in 5 cells investigated. P=0.5288, paired Student's t-test.

3.2. *Intracellular Ca^{2+} measurements confirmed that A_3R activation inhibits electrical field stimulation–evoked Ca^{2+} transients in isolated dorsal root ganglion neurons*

Fura-2–loaded DRG neurons analysed by transmitted light and fluorescence showed a round morphology with an average diameter of 27.6 ± 0.3 µm (n = 318). In control conditions (standard extracellular solution), 60% (40 of 68) of the DRG neurons presented electrically evoked Ca^{2+} transients on 0.1-Hz field stimulation. These cells were defined as "spiking" cells. The dynamic of cytosolic Ca^{2+} increase presented a rapid onset and a return to basal Ca^{2+} levels following a monoexponential kinetic. Figure 51A shows typical Ca^{2+} transient traces in control conditions, in the absence of extracellular Ca^{2+} ($0[Ca^{2+}]_{out}$), in the presence of TTX + A887826, or in the presence of verapamil + PD173212.

In $0[Ca^{2+}]_{out}$, only 4 of 37 (10.8%, Fig. 51B) analysed DRG neurons responded to electrical field stimulation ($P < 0.01$ vs control, the χ^2 test, Table 8). Indeed, as shown in a typical trace in figure 51A (dotted line), the majority of analysed cells did not show Ca^{2+} transients in $0[Ca^{2+}]_{out}$. Figure 51B depicts Ca^{2+} transients in 1 of the 4 spiking cells in $0[Ca^{2+}]_{out}$. In those 4 spiking cells, the

ΔF/F was slightly reduced, whereas the monoexponential decay phase was significantly reduced (Table 8). We supposed that in the 4 of 37 cells oscillating in 0$[Ca^{2+}]_{out}$, the electrical field stimulation could induce a Ca^{2+} release from intracellular stores, as already shown (Scarlett et al., 2009), or, alternatively, that incomplete Ca^{2+} buffering was achieved. In the presence of TTX + A887826, only 12 of 55 (21.8%; Fig. 51B) DRG neurons were spiking ($P < 0.05$ vs control, the χ^2 test), and in the majority of cells, we did not observe any Ca^{2+} increase (Fig. 51A). Figure 51B displays the trace of 1 of 12 responder cells in TTX + A887826. Among them, either ΔF/F or tau was slightly (but not significantly) reduced (Table 8). In finding an explanation to the observation that 12 of 55 cells still oscillated in the presence of TTX plus A887826, we have to consider that A887826 block of TTX-resistant Na^+ currents is dependent on Nav1.8 channels being in the open state (Zhang et al., 2010). In fact, A887826 potently (IC_{50} = 8 nM) inhibits TTX-resistant Na^+ currents in rat DRG neurons in a voltage-dependent way, being about 8-fold less potent at relatively hyperpolarized (Vm <−60 mV) membrane voltages in comparison with −40 mV-clamped cells (Zhang et al., 2010). Alternatively, we can envisage that in those 12 spiking cells, field depolarization was sufficient to activate Ca_Vs, in line with previous observation (MacDonald et al., 1986). The block of L- and N-type Ca_Vs by verapamil (1 μM) + PD173212 (500 nM) induced a significant reduction in ΔF/F (Table 8, $P < 0.01$, ANOVA followed by the Bonferroni test) without a significant decrease in tau. The number of spiking cells under these experimental conditions was 17 of 37 cells investigated (45.9%, not significant vs control: $P = 0.658$, the χ^2 test). Preincubation with Cl-IB-MECA significantly decreased the number of spiking cells (17 of 64: 23%; $P < 0.05$, the χ^2 test) as compared to control (Fig. 51C). However, Ca^{2+} parameters of spiking cells were not modified by this treatment (Table 8).

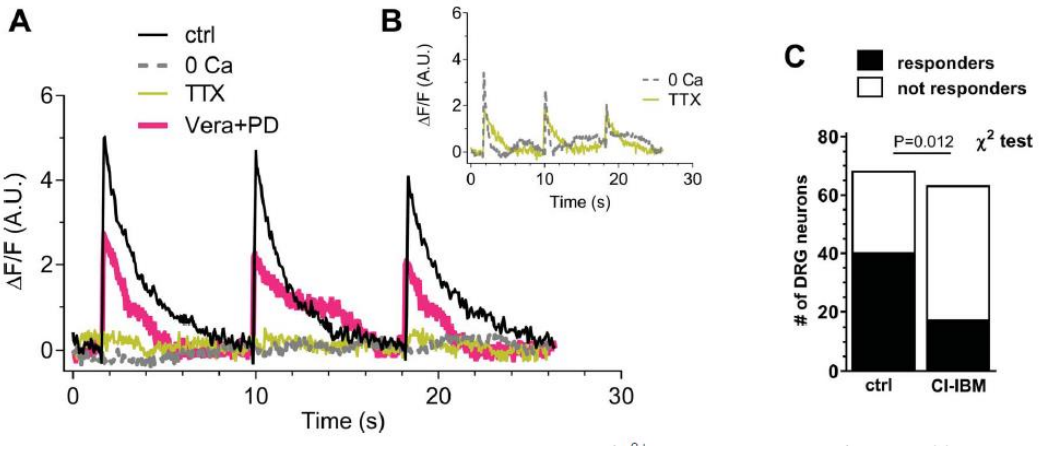

Figure 51. ***A_3R stimulation reduces electrically evoked and TTX-sensitive intracellular Ca^{2+} transients in isolated DRG neurons.*** **A.** Typical time courses of Ca^{2+} transient induce in DRG neurons by 0.1 Hz electrical field stimulation in control condition (ctrl: black trace), extracellular free-Ca^{2+} solution (0$[Ca^{2+}]_{out}$: dotted trace), 1 μM tetrodotoxin + 200 nM A887826 (TTX: yellow trace), or verapamil (VERA; 1 μM) + PD173212 (PD; 500 nM). **B.** Time courses of spiking cells recorded in 0$[Ca^{2+}]_{out}$ (dotted trace) or in TTX + A887826 (gray trace). **C.** Numbers of spiking or not spiking DRG neurons in control conditions or after preincubation with 30 nM Cl-IB-MECA. Statistical analysis was performed using the χ^2 test.

Treatment	No. of spiking cells out of analyzed cells	ΔF/F (A.U.) (spiking)	τ (decay time) (s) (spiking)
Control	40 out of 68	3.8 ± 0.47	1.24 ± 0.087
0$[Ca^{2+}]_{OUT}$	4 out of 37	2.2 ± 0.81	0.51 ± 0.082*
TTX + A887826	12 out of 55	1.6 ± 0.50	0.98 ± 0.159
VERAPAMIL + PD173212	17 out of 37	1.6 ± 0.38†	0.96 ± 0.101
CI-IB-MECA	17 out of 64	5.6 ± 0.77	1.33 ± 0.106‡

Table 9. ΔF/F and decay time (τ) measured in spiking DRG neurons during electrical field stimulation, according to treatments. The decay time (tau, τ) was calculated according to the following equation: $Y=y0+A\times e(-X/\tau)$. One-way ANOVA followed by the Bonferroni post-test. *P = 0.006 vs control. †P = 0.03. ‡P = 0.004 vs 0$[Ca^{2+}]$.

3.3. Discussion

In the present work, we investigated the expression and electrophysiological effects of A_3R in primary sensory neurons. We report evidence of A_3R mRNA expression in the rat DRG, and that A_3R activation inhibits both pronociceptive N-type Ca_V activation and AP firing in isolated DRG neurons. The bulk of evidence in studies of in vivo animal models indicates that adenosine is a powerful antihyperalgesic compound (Dickenson et al., 2000), with a crucial role recognized for A_1R activation. Of note, the A_3R has recently gained attention because its activation provides pain relief without adverse side effects (Janes et al., 2016).

In this study, we demonstrated by RT-PCR that A_3R mRNA is abundant in DRG homogenate and by immunocytochemistry that A_3R protein is present on both neurons and glia. It should be noted that although it is generally accepted that A_3Rs are expressed either by rat or human DRG neurons, a debate exists concerning their presence in the mouse. Based on mRNA sequencing, it appears that mouse DRG neurons do not express A_3R (Ray et al., 2018; Usoskin et al., 2015).

We then explored the A_3R functional role in DRG neurons by performing patch-clamp recording in the absence or presence of 2 different receptor agonists: the commercially available Cl-IB-MECA and the new highly selective A_3R agonist MRS5980 (Fang et al., 2015; D. K. Tosh et al., 2014). Our first approach was to investigate the effects of A_3R under basal (non-pharmacologically manipulated) conditions by using a voltage-ramp protocol to activate a wide range of voltage-dependent conductances. We found that the prototypical A_3R agonist Cl-IB-MECA reduced total outward K^+ currents evoked by the ramp. It is worth stressing that when tested for TRP responses, the vast majority of neurons responding to Cl-IB-MECA were also sensitive to TRPA1 and/or TRPV1 agonists, AITC and capsaicin, respectively, and presented an average cell diameter of 25 μm, thus being considered as "nociceptors".

When analyzed in detail, the Cl-IB-MECA effect on ramp K^+ currents was found to be dependent on Ca^{2+} channel opening because it was prevented by the nonselective Ca_V blocker Cd^{2+}. Indeed, in accordance with previous works (Mongan et al., 2005; Pagadala et al., 2013), we demonstrated that DRG neurons express Ca^{2+}-activated K^+ channels (KCa) as indicated by the observation that extracellular Cd^{2+} inhibits 34.0% of total outward currents evoked by the ramp. At variance, Cl-IB-MECA, that indirectly reduces Ca^{2+} currents through A_3R activation, inhibits 23.3% of total ramp-evoked outward currents. Among KCa, SK and BK channels are involved in the Cl-IB-MECA effect, as demonstrated by the fact that apamin plus TEA (200 μM) prevented ramp current inhibition.

Different Ca_V types in DRG neurons have been described: P/Q and N types, encoded by Cav2.1 and Cav2.2, respectively, which are mainly involved in neurotransmitter release, and R, L, and T types, encoded by Cav2.3, Cav1.1 to 1.4, and Cav3.1 to 3.3, respectively (Scroggs and Fox, 1992, 1991; Wilson et al., 2000). When Ca_V-mediated currents were studied in isolation, A_3R activation selectively inhibited N-type Ca^{2+} channels because the Cl-IB-MECA effect was prevented by the ω-CTX analogue PD173212 but not by the L-type blocker lacidipine. We conclude that A_3R activation directly inhibits Ca^{2+} entry by Ca_V on ramp depolarization and consequently reduces BK and SK channel opening (Fig.52).

It is known that A_1Rs also inhibit Ca_Vs in DRG neurons (A. C. Dolphin et al., 1986). Consistently, we observed a 24.8 ± 3.2% Ca^{2+} current decrease in the presence of CPA. When testing the endogenous agonist effects, adenosine-mediated inhibition of Ca^{2+} currents was either sensitive to the A_3R blocker MRS1523 or to the A_1R antagonist DPCPX, demonstrating that these two adenosine receptor subtypes are major mediators of adenosine effects in these cells. Of note, the CPA-mediated Ca^{2+} current inhibition (24.8 ± 3.2%) was significantly smaller compared with Cl-IB-MECA effect (44.1 ± 5.6%) indicating a prominent functional role of A_3R vs A_1R in this cell type.

G_i-coupled receptors, eg, A_3Rs and A_1Rs, as well as μ-opioid receptors, can inhibit Ca_V activation, and the mechanism may occur through the Gβ,γ subunit binding directly to the channel protein (Zamponi et al., 2015). Of note, the A_3R has also been found to activate secondarily G_q proteins (Jacobson et al., 2018) which could also modulate Ca_Vs (Heneghan et al., 2009). Here, we describe A_3R-induced inhibition of Ca_Vs for the first time in DRG neurons, but we have not determined the G-protein pathway involved. Furthermore, N-type channels are known to promote nociception by providing more than 60% of the neurotransmitter release by DRG neurons to lamina I dorsal horn neurons (Harding et al., 1999; Heinke et al., 2004). Previous observations demonstrate that N-type Ca_Vs blockers result in analgesia in a range of pain models (Cheong et al., 2013; Gandini et al., 2015; Vink and Alewood, 2012), and ziconotide, the first-choice compound among ω-CTX analogues, is in clinical use as an intrathecal medication for chronic pain in the United States (Adler and Lotz, 2017; Brookes et al., 2016). Of note, a direct block of N-type Ca^{2+} channels, as that achieved by ziconotide or ω-CTXs, is associated with serious side effects (psychological and neuropsychiatric symptoms including depression, cognitive impairment, and hallucinations; anxiety; panic attacks; ataxia; asthenia; headache; and dysesthesia; (Lynch et al., 2006)). Interestingly, an "indirect" Ca_V modulation as that accomplished by A_3R activation could represent a suitable approach to pain control without adverse side effects.

Beyond Ca_V inhibition, we also demonstrated that Cl-IB-MECA decreases the number of APs elicited by a depolarizing ramp current injection in isolated DRG neurons. This effect, also shared by μ-opioid agonists (Cai et al., 2014; Song et al., 2002; Valdez-Morales et al., 2013), could be a further crucial mechanism by which the A_3R exerts pain relief. The Cl-IB-MECA effect was blocked by the A_3R antagonist MRS1523 but was insensitive to the N-type Ca^{2+} channel blocker PD173212, demonstrating that A_3R-induced inhibition of cell excitability is not mediated by N-type Ca_V inhibition. Indeed, we demonstrated here that a direct block of N-type Ca^{2+} channels by PD173212 induces an opposite effect on cell firing, i.e., it increases the number of evoked

APs, depolarizes cell membrane, and reduces voltage threshold. This indicates that a reduced Ca^{2+} influx through N-type Ca_Vs is proexcitatory at a somatic level. Such an effect could be secondary to a reduced activation of KCa channels as indicated by previous data showing that either BK or SK channel inhibition increases DRG excitability (Li et al., 2007; Pagadala et al., 2013; Zhang et al., 2012). In light of this information, it appears that A_3R signalling in sensory neurons is complex and could lead to contradictory effects: Ca_V inhibition induces, on one hand, a reduction in neurotransmitter release at the presynaptic level, thus providing pain control; on the other hand, it decreases KCa opening at the somatic level, thus increasing neuronal excitability and producing a possible proalgesic effect. Indeed, multiple studies demonstrate that A_3R agonists, applied either centrally (Little et al., 2015; Wahlman et al., 2018; Yoon et al., 2005) or peripherally (Ford et al., 2015; Janes et al., 2014; Paoletta et al., 2013) are potent antihyperalgesic compounds (Janes et al., 2016). This observation supports the notion that the inhibitory effect of Cl-IB-MECA on Ca_Vs at a presynaptic level prevails over the potentially proalgesic A_3R effect at a somatic level. Furthermore, the potentially proalgesic effect of Cl-IB-MECA at a somatic level is masked by another, still unexplored, inhibitory A_3R effect on cell firing, which could provide a therapeutic advantage of an A_3R agonist over a direct Ca^{2+} channel blocker. This effect remains unexplained and will be addressed in our future work; our preliminary experiments revealed no obvious differences in Na^+ currents evoked in the absence or presence of Cl-IB-MECA.

Importantly, when we measured the intracellular Ca^{2+} rise after electrical field stimulation, we observed an overall reduction in the excitability of the DRG neuronal population in the presence of the A_3R agonist. Thus, Cl-IB-MECA significantly reduced the number of cells responding to 0.1 Hz stimulation, even if it did not change the dynamics of the Ca^{2+} rise ($\Delta F/F$ or tau) once Ca^{2+} spikes were triggered (Fig. 52).

It must be pointed out that the above-mentioned effects may not be the only mechanism by which A_3R agonists exert antihyperalgesia. Research studies have described a peripheral A_3R effect on cytokine release during chemotherapeutic-induced neuropathic pain (Janes et al., 2014; Wahlman et al., 2018). Additional A3AR-mediated modulation of nociception could possibly arise from receptor stimulation at a central level, i.e., in thalamic nuclei.

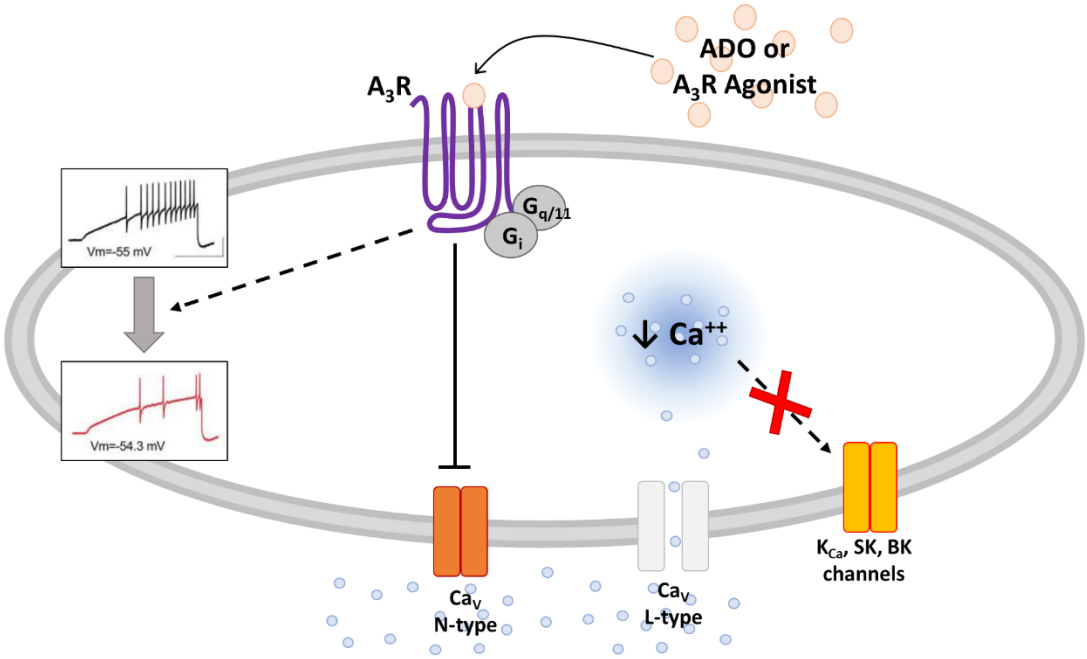

Figure 52. *Schematic representation of the results discussed in this section.*

Conclusions.

In conclusion, in the present thesis we first characterized the electrical activity of developing hfNBMs and functional modulation of their voltage-gated channels by cholinergic ligands. We found that hfNBMs spontaneously release Ach that activates either nicotinic or muscarinic receptors. Furthermore, we demonstrated that the stimulation of G_i-coupled muscarinic receptors (likely M2/M4) increases IK whereas G_q-coupled muscarinic receptors, by PLC activation (likely M1/M3/M5), inhibit INa. We disclosed the presence of an oscillatory activity of membrane voltage upon cell depolarization which is dependent on BK and Kir channels opening. Hence, our findings describe functional and electrophysiological features of human neuroblasts committed to NBM cholinergic neurons. This characterization is of relevance in view of elucidating the role of Ach as an autocrine trophic-like factor in brain development and of the involvement of BK channels in hfNBM electrophysiological behaviour. Increasing our knowledge about the biology of human NBM neurons may help to understand their role in different CNS pathologies and to develop new therapeutic strategies, including cell-based regenerative medicine, to combat brain diseases linked to deficits of cholinergic neurotransmission.

Afterwards, we demonstrated for the first time that adenosine A_{2B}Rs inhibit IK and IA currents in cultured OPCs and decrease oligodendroglial differentiation. Furthermore, by stimulating SphK1 phosphorylation, they positively modulate S1P synthesis leading to an increase in S1P intracellular levels. The increased concentration of S1P in its turn would account for an anti-differentiating effect. Results suggest the possibility that antagonism of A_{2B}Rs represents a strategy to improve remyelination processes.

Finally, we found that the selective adenosine A_3R stimulation inhibits N-type Ca_V opening, leading to a reduction in neurotransmitter release, and reduces electrically evoked excitation in isolated rat DRG neurons. Both these effects, as independent mechanisms, may be important in accounting for A_3R's pain-relieving effect and support the notion that an A_3R-based therapy may represent an important strategy to alleviate pain in different pathologies.

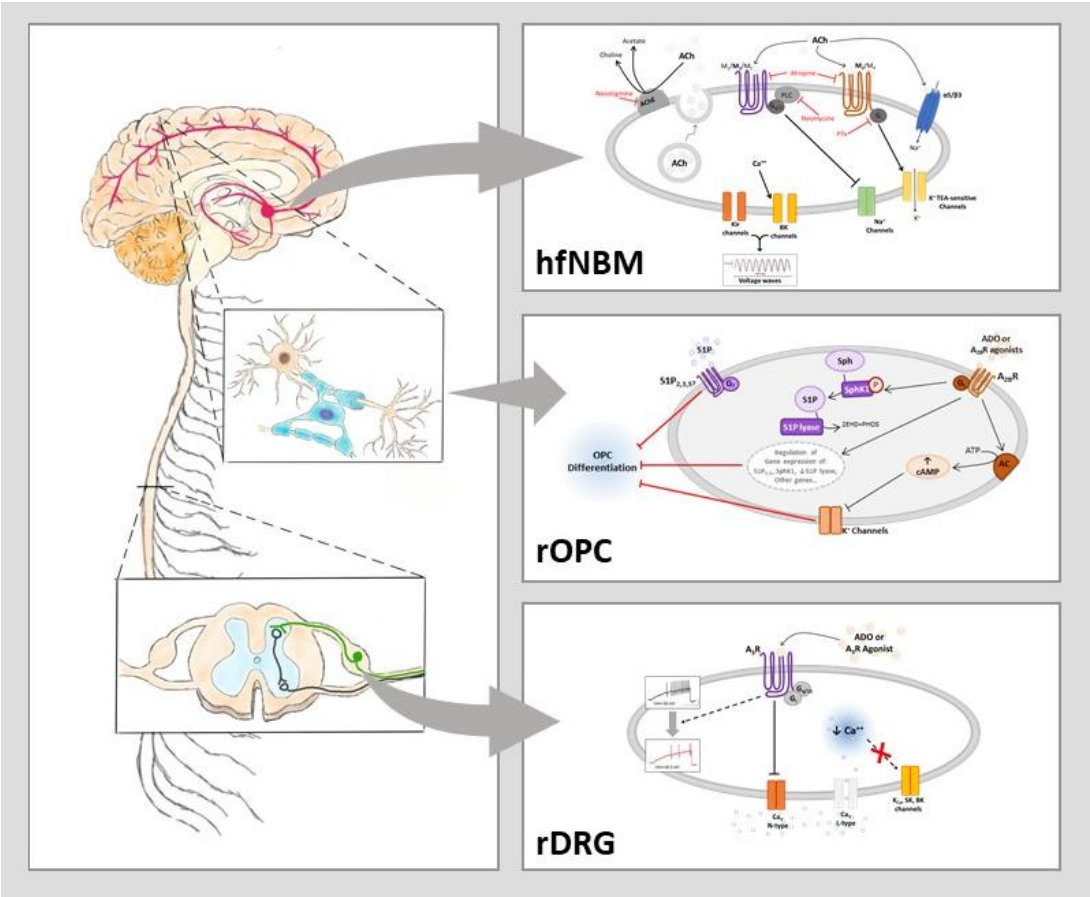

Figure 53. *Schematic representation of results obtained in different experimental models discussed in this thesis*

.

Publications.

Publications in international Journals

1. Fusco I., Ugolini F., Lana D., Coppi E., Dettori I., Gaviano L., Nosi D., **Cherchi F.**, Pedata F., Giovannini M.G., Pugliese A.M.
   The selective antagonism of adenosine A2B receptors reduces the synaptic failure and neuronal death induced by oxygen and glucose deprivation in rat CA1 hippocampus in vitro
   Front Pharmacol. 2018 Apr 24; 9:399.
2. Coppi E., Lana D., **Cherchi F.**, Fusco I., Buonvicino D., Urru M., Ranieri G., Muzzi M., Iovino L., Giovannini M.G., Pugliese A.M., Chiarugi A.
   Dexpramipexole enhances hippocampal synaptic plasticity and memory in the rat
   Neuropharmacology. 2018 Oct 3; 143:306-316.
3. Coppi E., **Cherchi F.**, Fusco I., Failli P., Vona A., Dettori I., Gaviano L., Lucarini E., Jacobson K.A., Tosh D.K., Salvemini D., Ghelardini C., Pedata F., Mannelli L.D.C., Pugliese A.M.
   Adenosine A3 receptor activation inhibits pro-nociceptive N-type Ca2+ currents and cell excitability in dorsal root ganglion neurons
   Pain. 2019 May; 160(5):1103-1118.
4. Fusco I., **Cherchi F.**, Catarzi D., Colotta V., Varano F., Pedata F., Pugliese A.M., Coppi E.
   Functional characterization of two novel adenosine A2B receptor agonists, P453 and P517, by paired pulse facilitation at Schaffer collateral-CA1 synapses
   Brain Research Bullettin. 2019 May 24; S0361-9230(18)30680-4.
5. Coppi E., **Cherchi F.**, Fusco I., Dettori I., Gaviano L., Magni G., Catarzi D., Colotta V., Varano F., Rossi F., Bernacchioni C., Donati C., Bruni P., Pedata F., Cencetti F.*, Pugliese A.M.*
   Adenosine A2B receptors inhibit K+ currents and cell differentiation in cultured oligodendrocyte precursor cells and modulate sphingosine-1-phosphate signaling pathway
   Biochemical Pharmacology. 2020 July; 177:113956.
6. Lucarini E., Coppi E., Micheli L., Parisio C., Vona A., **Cherchi F.**, Pugliese A.M., Pedata F., Failli P., Palomino S., Wahl J., Largent-Milnes T.M., Vanderah T.W., Tosh D.K., Jacobson K.A., Salvemini D., Ghelardini C., Di Cesare Mannelli L.
   Acute visceral pain relief mediated by A3AR agonists in rats: involvement of N-type voltage-gated calcium channels
   Pain. 2020 May 4.
7. Coppi E., **Cherchi F.**, Sarchielli E., Fusco I., Guarnieri G., Gallina P., Corradetti R., Pedata F., Vannelli G.B., Pugliese A.M. and Morelli A.
   Acetylcholine modulates K^+ and Na^+ currents in human basal forebrain cholinergic neuroblasts through an autocrine/paracrine mechanism
   Journal of Neurochemistry. 2020 October 8.

8. Magni G., Banchelli M., **Cherchi F.**, Coppi E., Fraccalvieri M., Rossi M., Tatini F., Pugliese A.M., Rossi Degl'Innocenti D., Alfieri D., Matteini P., Pini R., Pavone F.S., Rossi F.
   Experimental Study on Blue Light Interaction with Human Keloid-Derived Fibroblasts
   Biomedicines. 2020 December 6; 8(12):573.
9. Coppi E., Dettori I., **Cherchi F.**, Bulli I., Venturini M., Lana D., Giovannini M.G., Pedata F., Pugliese A.M.
   A2B Adenosine Receptors: When Outsiders May Become an Attractive Target to Treat Brain Ischemia or Demyelinations
   International Journal of Molecular Sciences. 2020 December 18; 21(24):9697.
10. Rossi F., Magni G., Tatini F., Banchelli M., **Cherchi F.**, Rossi M., Coppi E., Pugliese A.M., Rossi Degl'Innocenti D., Alfieri D., Pavone F.S., Pini R., Matteini P.
    Photobiomodulation of human fibroblasts and keratinocytes with blue light: implications in wound healing
    Biomedicines. 2021 January 5; 9(1):41.
11. **Cherchi F.**, Pugliese A.M., Coppi E.
    Oligodendrocyte precursor cell maturation: role of adenosine receptors
    Neural Regeneration Research. 2021 January 25; 16(9):1686-1692.
12. Coppi E., Buonvicino D., Ranieri G., **Cherchi F.**, Venturini M., Pugliese A.M., Chiarugi A.
    Dexpramipexole enhances K+ currents and inhibits cell excitability in the rat hippocampus in vitro
    Molecular Neurobiology. 2021 Feb 10.
13. Coppi E., Dettori I., **Cherchi F.**, Bulli I., Venturini M., Pedata F., Pugliese A.M.
    New insight into the role of adenosine in demyelination, stroke and neuropathic pain
    Frontiers in Pharmacology. 2021 Jan 29; 11:625662.
14. Durante D.*, Squillace S.*, Lauro F.*, Giancotti L.A., Coppi E., **Cherchi F.**, Mannelli L.D.C., Ghelardini C., Kolar G., Wahlman C., Opejin A., Xiao C., Reitman M.L., Tosh D.K., Hawiger D., Jacobson K.A., Salvemini D.
    Adenosine A3 agonists reverse neuropathic pain via T cell IL-10
    Journal of Clinical Investigation.
    (accepted)
15. Dettori I., Fusco I., Bulli I., Gaviano L., Coppi E., **Cherchi F.**, Venturini M., Mannelli L.D.C., Ghelardini C., Nocentini A., Supuran C.T., Pugliese A.M., Pedata F.
    Protective effects of carbonic anhydrase inhibition in in vitro and in vivo brain ischemia models Frontiers in Pharmacology
    (submitted)

Publications in book chapter

1. Pugliese A.M., Coppi E., **Cherchi F.**, Pepeu G.
   Cardiovascular adverse effects of psychotropic drugs
   In: Govoni S., Politi P., Vanoli E. (eds) *Brain and Heart Dynamics*. Springer, Cham, 2019
   doi: https://doi.org/10.1007/978-3-319-90305-7_45-1

Proceedings paper

1. Magni G., Rossi F., Tatini F., Pini R., Coppi E., **Cherchi F.**, Fusco I., Pugliese A.M., Pedata F., Fraccalvieri M., Gasperini S., Pavone F.S., Tripodi C., Alfieri D., Targetti L.
   Blue light-irradiated human keloid fibroblasts: an in vitro study
   Proc. SPIE 10477, Mechanisms of Photobiomodulation Therapy XIII, 104770A
   doi: 10.1117/12.2289928
   8 February 2018
2. Magni G., **Cherchi F.**, Coppi E., Fraccalvieri M., Tatini F., Fusco I., Pini R., Pugliese A.M., Pedata F., Mangia A., Gasperini S., Pavone F.S., Rossi Degl'Innocenti D., Tripodi C., Alfieri D., Targetti L., Rossi F.
   Blue light effects in human keloid fibroblasts
   Proc. SPIE 10861, Mechanisms of Photobiomodulation Therapy XIV, 1086107
   doi: 10.1117/12.2509504
   7 March 2019
3. Magni G., Banchelli M., **Cherchi F.**, Coppi E., Fraccalvieri M., Pugliese A.M., Pedata F., Mangia A., Gasperini S., Pavone F.S., Rossi Degl'Innocenti D., Targetti L., Pini R., Matteini P., Rossi F.
   Human keloid cultured fibroblasts irradiated with blue LED light: evidence from an in vitro study
   Proc. SPIE 11079, Medical Laser Applications and Laser-Tissue Interactions IX, 110790V
   doi: 10.1117/12.2527084
   22 July 2019

Abstracts at international meetings

1. Al-Hosni R., **Cherchi F.**, Cai X., Lei W., Coppi E., Huang Z. and Gibb A.J.
   Adenosine A2A - D2 dopamine receptor modulation of NMDA responses in rat substantia nigra dopaminergic neurones.
   Society for Neuroscience 2017 Annual Meeting, Washington D.C., United States.
   11–15 November 2017.
2. Magni G., Rossi F., Tatini F., Pini R., Coppi E., **Cherchi F.**, Fusco I., Pugliese A.M., Pedata F., Fraccalvieri M., Gasperini S., Pavone F.S., Tripodi C., Alfieri D., Targetti L.
   Blue light-irradiated human keloid fibroblasts: an in vitro study.
   SPIE Photonics West, The Moscone Center, San Francisco, California, United States.
   30 January - 1 February 2018.
3. Magni G., Rossi F., Tatini F., Pini R., **Cherchi F.**, Fusco I., Pugliese A.M., Alfieri D., Tripodi C., Targetti L. and Pavone F.S.
   Primary human keloid fibroblasts react to blue LED light irradiation with metabolic change.
   28th Conference of the European Wound Management Association EWMA, Krakow, Poland
   9-11 May 2018
4. Coppi E., Fusco I., **Cherchi F.**, Dettori I., Mannelli L., Lucarini E., Ghelardini C., Jacobson K.A., Tosh D.K., Salvemini D., Pedata F. and Pugliese A.M.
   Adenosine A3 receptor stimulation inhibits pro-nociceptive voltage dependent Ca2+ currents in rat dorsal root ganglion neurons.
   Purines 2018 International - Basic and Translational Science on Purinergic Signaling and its Components for a Healthy and Better World, Foz de Iguazu, Brasil.
   19-22 June 2018.
5. Al-Hosni R., **Cherchi F.**, Cai X., Lei W., Huang Z., Coppi E., Gibb A.J.
   Investigation of NMDA receptor modulation by adenosine A2A and D2 dopamine receptor activation in rat substantia nigra dopaminergic neurons.
   Europhysiology 2018 – The QEII Center, London, UK
   14-16 September 2018
6. Magni G., **Cherchi F.**, Coppi E., Fraccalvieri M., Tatini F., Fusco I., Pini R., Pugliese A.M., Pedata F., Mangia A., Gasperini S., Pavone F.S., Rossi Degl'Innocenti D., Tripodi C., Alfieri D., Targetti L., Rossi F.
   Blue light effects in human keloid fibroblasts.
   SPIE BiOS 2019 - The Moscone Center San Francisco, California, United States
   2-7 February 2019
7. Coppi E., **Cherchi F.**, Fusco I., Failli P., Vona A., Dettori I., Gaviano L., Lucarini E., Jacobson K.A., Tosh D.K., Salvemini D., Ghelardini C., Pedata F., Di Cesare Mannelli L., Pugliese A.M.
   Molecular mechanisms for A3 adenosine receptor mediated pain control: an in vitro study on dorsal root ganglion neuron excitability.
   1st European Purine Meeting – Santiago de Compostela, Spain
   4-6 September 2019

8. **Cherchi F.**, Coppi E., Fusco I., Scortichini M., Jacobson K.A., Pedata F., Pugliese A.M.
   The selective stimulation of adenosine A3 receptor inhibits N-type Ca2+ currents in rat dorsal root ganglion neurons.
   1st European Purine Meeting – Santiago de Compostela, Spain
   4-6 September 2019
9. Coppi E., Fusco I., **Cherchi F.***, Dettori I., Cencetti F., Gaviano L., Colotta V., Catarzi D., Bruni P., Pedata F., Pugliese A.M.
   Adenosine A_{2B} receptors and sphingosine kinase/sphingosine- 1-phosphate signalling axis control maturation of oligodendrocyte precursor cells in vitro
   1st European Purine Meeting – Santiago de Compostela, Spain
   4-6 September 2019 (*oral communication presented by* *)
10. **Cherchi F.**, Coppi E., Fusco I., Sarchielli E., Guarnieri G., Vannelli G., Pedata F., Morelli A. and Pugliese A.M.
    Cholinergic modulation of ionic currents and a novel oscillatory activity in human fetal cholinergic neurons from the nucleus basalis of Meynert.
    Society for Neuroscience 2019 Annual Meeting, Chicago, IL, United States.
    19–23 October 2019.
11. **Cherchi F.**, Sarchielli E., Guarnieri G., Vannelli G., Pedata F., Morelli A., Pugliese A.M. and Coppi E.
    Electrophysiological characterization of human foetal cholinergic neurons from the nucleus basalis of Meynert.
    12th FENS – Virtual Forum of Neuroscience
    11–15 July 2020.

Abstracts at national meetings

1. Coppi E., Fusco I., **Cherchi F.**, Pedata F. and Pugliese A.M.
   Purinergic signalling modulates in vitro ischemic damage and oligodendrocyte progenitor cell differentiation.
   XVI Congresso Nazionale SINS, Ischia (NA)
   01-04 Ottobre, 2017.
2. Coppi E., Fusco I., **Cherchi F.**, Pedata F. and Pugliese A.M.
   Molecular basis of adenosine A3 receptor-mediated analgesic effect: an in vitro electrophysiological study on isolated rat dorsal root ganglion neurons.
   38° Congresso Nazionale della Società Italiana di Farmacologia, Rimini
   25-28 October 2017.
3. Gaviano L., Dettori I., Coppi E., **Cherchi F.**, Cencetti F. Catarzi D., Pedata F. and Pugliese A.M.
   Adenosine A2B receptor and sphingosine 1-phosphate receptors regulate K+ currents and maturation of oligodendrocyte precursor cells.
   National Meeting of PhD Students in Neuroscience – "New Perspectives in Neuroscience: Research Results of Young Italian Neuroscientists", Naples
   23 February 2018.
4. Magni G., Rossi F., Tatini F., Pini R., **Cherchi F.**, Coppi E., Pugliese A.M., Fraccalvieri M., e Pavone F.S.

A new possible treatment for skin fibrosis with blue light: an in vitro study.
Fotonica 2018 AEIT – 20° Edizione, Covegno Italiano delle Tecnologie Fotoniche, Lecce
23-25 May 2018.

5. **Cherchi F.**, Fusco I., Dettori I., Cencetti F., Gaviano L., Pedata F., Coppi E., Pugliese A.M.
Adenosine A2B receptors and sphingosine kinase/sphingosine-1-phosphate signalling axis control maturation of oligodendrocyte precursor cells in vitro.
BraYn 2018 - Brainstorming Research Assembly For Young Neuroscientists, Genoa
29-30 June 2018.
6. Fusco I., Ugolini F., Lana D., Dettori I., Gaviano L., **Cherchi F.**, Catarzi D., Colotta V., Pedata F., Nosi D., Giovannini M.G., Coppi E., Pugliese A.M.
Role of adenosine A2B receptor under normoxic and oxygen and glucose deprivation at Schaffer collateral-CA1 synapses.
Italian Purine Club Meeting, Florence, Italy
18 January 2019
7. **Cherchi F.**, Coppi E., Fusco I., Vannelli G., Morelli A., Pedata F., Pugliese A.M.
Human foetal cholinergic neurons isolated from nucleus basalis of Meynert express functional cholinergic receptors whose activation modulates neuronal excitability.
National Meeting of PhD Students in Neuroscience – "New Perspectives in Neuroscience: Research Results of Young Italian Neuroscientists", Naples, Italy
1 March 2019.
8. **Cherchi F.**, Fusco I., Cencetti F., Dettori I., Gaviano L., Pedata F., Colotta V., Catarzi V., Coppi E., Pugliese A.M.
Adenosine A2B receptors and sphingosine kinase/sphingosine-1-phosphate signalling axis control maturation of oligodendrocyte precursor cells in vitro.
18th National Congress of the Italian Society for Neuroscience (SINS), Perugia, Italy
26-29 September 2019.
9. **Cherchi F.**, Coppi E., Fusco I., Scortichini M., Jacobson K.A., Pedata F., Pugliese A.M.
An irreversible A3 adenosine receptor selective agonist ICBM inhibits N-type Ca2+ currents in rat dorsal root ganglion neurons.
39° Congresso Nazionale della Società Italiana di Farmacologia, Firenze, Italy
20-23 Novembre 2019.
10. Magni G., **Cherchi F.**, Coppi E., Fraccalvieri M., Pedata F., Pini R., Pugliese A.M. Pavone F.S., Rossi F.
Investigation into Blue LED light effects on cell metabolism, proliferation rate and ionic currents in cultured human keloid fibroblasts: a possible involvement of adenosine A2A receptors.
39° Congresso Nazionale della Società Italiana di Farmacologia, Firenze, Italy
20-23 Novembre 2019.
11. **Cherchi F.***, Coppi E., Scortichini M., Jacobson K.A., Pedata F., Pugliese A.M.

Selective stimulation of adenosine A3 receptor activation inhibits pro-nociceptive N-type Ca2+ currents in dorsal root ganglion neurons
Italian Purine Club Meeting, Ferrara, Italy
27 January 2020 (*oral communication presented by* *)

12. **Cherchi F.***, Fusco I., Cencetti F., Dettori I., Gaviano L., Venturini M., Pedata F., Colotta V., Catarzi D., Coppi E., Pugliese A.M.
Adenosine A_{2B} receptors and sphingosine kinase/sphingosine-1-phosphate signalling axis are involved in the maturation of oligodendrocyte precursor cells in vitro
National Meeting of PhD students in Neuroscience, Webinar
29-30 September 2020 (*oral communication presented by* *)

References.

Abbracchio, M.P., Burnstock, G., 1994. Purinoceptors: Are there families of P2X and P2Y purinoceptors? Pharmacol. Ther. https://doi.org/10.1016/0163-7258(94)00048-4

Abo-Salem, O.M., Hayallah, A.M., Bilkei-Gorzo, A., Filipek, B., Zimmer, A., Müller, C.E., 2004. Antinociceptive Effects of Novel A2B Adenosine Receptor Antagonists. J. Pharmacol. Exp. Ther. 308, 358–366. https://doi.org/10.1124/jpet.103.056036

Abreu-Villaça, Y., Filgueiras, C.C., Manhães, A.C., 2011. Developmental aspects of the cholinergic system. Behav. Brain Res. https://doi.org/10.1016/j.bbr.2009.12.049

Adachi, K., Kohara, T., Nakao, N., Arita, M., Chiba, K., Mishina, T., Sasaki, S., Fujita, T., 1995. Design, synthesis, and structure-activity relationships of 2-substituted-2-amino-1,3-propanediols: Discovery of a novel immunosuppressant, FTY720. Bioorganic Med. Chem. Lett. 5, 853–856. https://doi.org/10.1016/0960-894X(95)00127-F

Adler, J.A., Lotz, N.M., 2017. Intrathecal pain management: A team-based approach. J. Pain Res. https://doi.org/10.2147/JPR.S142147

Ahlijanian, M.K., Westenbroek, R.E., Catterall, W.A., 1990. Subunit structure and localization of dihydropyridine-sensitive calcium channels in mammalian brain, spinal cord, and retina. Neuron 4, 819–832. https://doi.org/10.1016/0896-6273(90)90135-3

Akopian, A.N., Souslova, V., England, S., Okuse, K., Ogata, N., Ure, J., Smith, A., Kerr, B.J., McMahon, S.B., Boyce, S., Hill, R., Stanfa, L.C., Dickenson, A.H., Wood, J.N., 1999. The tetrodotoxin-resistant sodium channel SNS has a specialized function in pain pathways. Nat. Neurosci. 2, 541–548. https://doi.org/10.1038/9195

Akundi, R.S., Rivkees, S.A., 2009. Hypoxia alters cell cycle regulatory protein expression and induces premature maturation of oligodendrocyte precursor cells. PLoS One 4. https://doi.org/10.1371/journal.pone.0004739

Alam, M., Sanghera, M.K., Schwabe, K., Lütjens, G., Jin, X., Song, J., von Wrangel, C., Stewart, R.M., Jankovic, J., Grossman, R.G., Darbin, O., Krauss, J.K., 2016. Globus pallidus internus neuronal activity: a comparative study of linear and non-linear features in patients with dystonia or Parkinson's disease. J. Neural Transm. 123, 231–240. https://doi.org/10.1007/s00702-015-1484-3

Aldskogius, H., Elfvin, L.G., Andersson Forsman, C., 1986. Primary sensory afferents in the inferior mesenteric ganglion and related nerves of the guinea pig. An experimental study with anterogradely transported wheat germ agglutinin-horseradish peroxidase conjugate. J. Auton. Nerv. Syst. 15, 179–190. https://doi.org/10.1016/0165-1838(86)90013-5

Aldskogius, H., Kozlova, E.N., 1998. Central neuron-glial and glial-glial interactions following axon injury. Prog. Neurobiol. 55, 1–26. https://doi.org/10.1016/S0301-0082(97)00093-2

Alemany, R., Van Koppen, C.J., Danneberg, K., Ter Braak, M., Meyer Zu Heringdorf, D., 2007. Regulation and functional roles of sphingosine kinases. Naunyn. Schmiedebergs. Arch. Pharmacol. https://doi.org/10.1007/s00210-007-0132-3

Allen, T.G.J., Brown, D.A., 1996. Detection and modulation of acetylcholine release from neuntes of rat basal forebrain cells in culture. J. Physiol. 492, 453–466. https://doi.org/10.1113/jphysiol.1996.sp021321

Almeida, T., Rodrigues, R.J., De Mendonça, A., Ribeiro, J.A., Cunha, R.A., 2003. Purinergic P2 receptors trigger adenosine release leading to adenosine A2A receptor activation and facilitation of long-term potentiation in rat hippocampal slices. Neuroscience 122, 111–121. https://doi.org/10.1016/S0306-4522(03)00523-2

Amir, R., Argoff, C.E., Bennett, G.J., Cummins, T.R., Durieux, M.E., Gerner, P., Gold, M.S., Porreca, F., Strichartz, G.R., 2006. The Role of Sodium Channels in Chronic Inflammatory and Neuropathic Pain. J. Pain 7. https://doi.org/10.1016/j.jpain.2006.01.444

Andoh, T., Kobayashi, N., Uta, D., Kuraishi, Y., 2017. Prophylactic topical paeoniflorin prevents mechanical allodynia caused by paclitaxel in mice through adenosine A1 receptors. Phytomedicine 25, 1–7. https://doi.org/10.1016/j.phymed.2016.12.010

Annunziato, L., Boscia, F., Pignataro, G., 2013. Ionic transporter activity in astrocytes, microglia, and oligodendrocytes during brain ischemia. J. Cereb. Blood Flow Metab. https://doi.org/10.1038/jcbfm.2013.44

Antonioli, L., Blandizzi, C., Pacher, P., Haskó, G., 2019. The purinergic system as a pharmacological target for the treatment of immune-mediated inflammatory diseases.

Pharmacol. Rev. 71, 345–382. https://doi.org/10.1124/pr.117.014878
Antonioli, L., Blandizzi, C., Pacher, P., Haskó, G., 2013. Immunity, inflammation and cancer: A leading role for adenosine. Nat. Rev. Cancer. https://doi.org/10.1038/nrc3613
Antonioli, L., Csóka, B., Fornai, M., Colucci, R., Kókai, E., Blandizzi, C., Haskó, G., 2014. Adenosine and inflammation: What's new on the horizon? Drug Discov. Today. https://doi.org/10.1016/j.drudis.2014.02.010
Araque, A., Clarac, F., Buno, W., 1994. P-type Ca2+ channels mediate excitatory and inhibitory synaptic transmitter release in crayfish muscle. Proc. Natl. Acad. Sci. U. S. A. 91, 4224–4228. https://doi.org/10.1073/pnas.91.10.4224
Arnsten, A.F.T., 2006. Stimulants: Therapeutic actions in ADHD. Neuropsychopharmacology. https://doi.org/10.1038/sj.npp.1301164
Asghari, A.A., Azarnia, M., Mirnajafi-Zadeh, J., Javan, M., 2013. Adenosine A1 receptor agonist, N6-cyclohexyladenosine, protects myelin and induces remyelination in an experimental model of rat optic chiasm demyelination; electrophysiological and histopathological studies. J. Neurol. Sci. 325, 22–28. https://doi.org/10.1016/j.jns.2012.11.008
Atluri, P., Fleck, M.W., Shen, Q., Mah, S.J., Stadfelt, D., Barnes, W., Goderie, S.K., Temple, S., Schneider, A.S., 2001. Functional nicotinic acetylcholine receptor expression in stem and progenitor cells of the early embryonic mouse cerebral cortex. Dev. Biol. 240, 143–156. https://doi.org/10.1006/dbio.2001.0453
Attali, B., Wang, N., Kolot, A., Sobko, A., Cherepanov, V., Soliven, B., 1997. Characterization of delayed rectifier Kv channels in oligodendrocytes and progenitor cells. J. Neurosci. 17, 8234–8245. https://doi.org/10.1523/jneurosci.17-21-08234.1997
Back, S.A., Luo, N.L., Borenstein, N.S., Levine, J.M., Volpe, J.J., Kinney, H.C., 2001. Late oligodendrocyte progenitors coincide with the developmental window of vulnerability for human perinatal white matter injury. J. Neurosci. 21, 1302–1312. https://doi.org/10.1523/jneurosci.21-04-01302.2001
Backx, P.H., Yue, D.T., Lawrence, J.H., Marban, E., Tomaselli, G.F., 1992. Molecular localization of an ion-binding site within the pore of mammalian sodium channels. Science (80-.). 257, 248–251. https://doi.org/10.1126/science.1321496
Bagal, S.K., Marron, B.E., Owen, R.M., Storer, R.I., Swain, N.A., 2015. Voltage gated sodium channels as drug discovery targets. Channels. https://doi.org/10.1080/19336950.2015.1079674
Balatoni, B., Storch, M.K., Swoboda, E.M., Schönborn, V., Koziel, A., Lambrou, G.N., Hiestand, P.C., Weissert, R., Foster, C.A., 2007. FTY720 sustains and restores neuronal function in the DA rat model of MOG-induced experimental autoimmune encephalomyelitis. Brain Res. Bull. 74, 307–316. https://doi.org/10.1016/j.brainresbull.2007.06.023
Baldwin, S.A., Mackey, J.R., Cass, C.E., Young, J.D., 1999. Nucleoside transporters: Molecular biology and implications for therapeutic development. Mol. Med. Today. https://doi.org/10.1016/S1357-4310(99)01459-8
Bandhuvula, P., Tam, Y.Y., Oskouian, B., Saba, J.D., 2005. The immune modulator FTY720 inhibits sphingosine-1-phosphate lyase activity. J. Biol. Chem. 280, 33697–33700. https://doi.org/10.1074/jbc.C500294200
Baraldi, P.G., Borea, P.A., 2000. New potent and selective human adenosine A3 receptor antagonists. Trends Pharmacol. Sci. https://doi.org/10.1016/S0165-6147(00)01581-9
Barateiro, A., Fernandes, A., 2014. Temporal oligodendrocyte lineage progression: In vitro models of proliferation, differentiation and myelination. Biochim. Biophys. Acta - Mol. Cell Res. https://doi.org/10.1016/j.bbamcr.2014.04.018
Barres, B.A., Koroshetz, W.J., Swartz, K.J., Chun, L.L.Y., Corey, D.P., 1990. Ion channel expression by white matter glia: The O-2A glial progenitor cell. Neuron 4, 507–524. https://doi.org/10.1016/0896-6273(90)90109-S
Bassi, R., Anelli, V., Giussani, P., Tettamanti, G., Viani, P., Riboni, L., 2006. Sphingosine-1-phosphate is released by cerebellar astrocytes in response to bFGF and induces astrocyte proliferation through Gi-protein-coupled receptors. Glia 53, 621–630. https://doi.org/10.1002/glia.20324
Bayliss, D.A., Barrett, P.Q., 2008. Emerging roles for two-pore-domain potassium channels

and their potential therapeutic impact. Trends Pharmacol. Sci. https://doi.org/10.1016/j.tips.2008.07.013

Becchetti, A., Aracri, P., Meneghini, S., Brusco, S., Amadeo, A., 2015. The role of nicotinic acetylcholine receptors in autosomal dominant nocturnal frontal lobe epilepsy. Front. Physiol. https://doi.org/10.3389/fphys.2015.00022

Benzing, W.C., Mufson, E.J., 1995. Increased number of NADPH-d-positive neurons within the substantia innominata in Alzheimer's disease. Brain Res. 670, 351–355. https://doi.org/10.1016/0006-8993(94)01362-L

Berne, R.M., 1963. Cardiac nucleotides in hypoxia: possible role in regulation of coronary blood flow. Am. J. Physiol. 204, 317–322. https://doi.org/10.1152/ajplegacy.1963.204.2.317

Besnard, F., Perraud, F., Sensenbrenner, M., Labourdette, G., 1989. Effects of acidic and basic fibroblast growth factors on proliferation and maturation of cultured rat oligodendrocytes. Int. J. Dev. Neurosci. 7, 401–409. https://doi.org/10.1016/0736-5748(89)90061-0

Betti, M., Catarzi, D., Varano, F., Falsini, M., Varani, K., Vincenzi, F., Dal Ben, D., Lambertucci, C., Colotta, V., 2018. The aminopyridine-3,5-dicarbonitrile core for the design of new non-nucleoside-like agonists of the human adenosine A2B receptor. Eur. J. Med. Chem. 150, 127–139. https://doi.org/10.1016/j.ejmech.2018.02.081

Beukers, M.W., Den Dulk, H., Van Tilburg, E.W., Brouwer, J., Ijzerman, A.P., 2000. Why are A(2B) receptors low-affinity adenosine receptors? Mutation of Asn273 to Tyr increases affinity of human A(2B) receptor for 2-(1-hexynyl)adenosine. Mol. Pharmacol. https://doi.org/10.1124/mol.58.6.1349

Beukers, M.W., Van Oppenraaij, J., Van Der Hoorn, P.P.W., Blad, C.C., Den Dulk, H., Brouwer, J., Ijzerman, A.P., 2004. Random Mutagenesis of the Human Adenosine A2B Receptor Followed by Growth Selection in Yeast. Identification of Constitutively Active and Gain of Function Mutations. Mol. Pharmacol. 65, 702–710. https://doi.org/10.1124/mol.65.3.702

Biber, K., Fiebich, B., Gebicke-Harter, P., Calker, D. van, 1999. Carbamazepine-induced upregulation of adenosine A(1)-receptors in astrocyte cultures affects coupling to the phosphoinositol signaling pathway. Neuropsychopharmacology 20, 271–278.

Bilici, D., Akpinar, E., Gürsan, N., Dengiz, G.Ö., Bilici, S., Altaş, S., 2001. Protective effect of T-type calcium channel blocker in histamine-induced paw inflammation in rat. Pharmacol. Res. 44, 527–531. https://doi.org/10.1006/phrs.2001.0877

Billich, A., Bornancin, F., Dévay, P., Mechtcheriakova, D., Urtz, N., Baumruker, T., 2003. Phosphorylation of the Immunomodulatory Drug FTY720 by Sphingosine Kinases. J. Biol. Chem. 278, 47408–47415. https://doi.org/10.1074/jbc.M307687200

Binder, B.Y.K., Williams, P.A., Silva, E.A., Leach, J.K., 2015. Lysophosphatidic Acid and Sphingosine-1-Phosphate: A Concise Review of Biological Function and Applications for Tissue Engineering. Tissue Eng. - Part B Rev. https://doi.org/10.1089/ten.teb.2015.0107

Bissonnette, C.J., Lyass, L., Bhattacharyya, B.J., Belmadani, A., Miller, R.J., Kessler, J.A., 2011. The controlled generation of functional basal forebrain cholinergic neurons from human embryonic stem cells. Stem Cells 29, 802–811. https://doi.org/10.1002/stem.626

Blanc, C.A., Grist, J.J., Rosen, H., Sears-Kraxberger, I., Steward, O., Lane, T.E., 2015. Sphingosine-1-Phosphate Receptor Antagonism Enhances Proliferation and Migration of Engrafted Neural Progenitor Cells in a Model of Viral-Induced Demyelination. Am. J. Pathol. 185, 2819–2832. https://doi.org/10.1016/j.ajpath.2015.06.009

Bond, C.T., Maylie, J., Adelman, J.P., 2005. SK channels in excitability, pacemaking and synaptic integration. Curr. Opin. Neurobiol. https://doi.org/10.1016/j.conb.2005.05.001

Borea, P.A., Gessi, S., Merighi, S., Vincenzi, F., Varani, K., 2018. Pharmacology of adenosine receptors: The state of the art. Physiol. Rev. https://doi.org/10.1152/physrev.00049.2017

Borea, P.A., Varani, K., Vincenzi, F., Baraldi, P.G., Tabrizi, M.A., Merighi, S., Gessi, S., 2015. The a3 adenosine receptor: History and perspectives. Pharmacol. Rev. 67, 74–102. https://doi.org/10.1124/pr.113.008540

Bosch, D.A., 1978. Atlas for stereotaxy of the human brain. Clin. Neurol. Neurosurg. 80, 299.

https://doi.org/10.1016/s0303-8467(78)80027-4
Brady, N.R., Elmore, S.P., Van Beek, J.J.H.G.M., Krab, K., Courtoy, P.J., Hue, L., Westerhoff, H. V., 2004. Coordinated behavior of mitochondria in both space and time: A reactive oxygen species-activated wave of mitochondrial depolarization. Biophys. J. 87, 2022–2034. https://doi.org/10.1529/biophysj.103.035097
Brand, A., Vissiennon, Z., Eschke, D., Nieber, K., 2001. Adenosine A1 and A3 receptors mediate inhibition of synaptic transmission in rat cortical neurons. Neuropharmacology 40, 85–95. https://doi.org/10.1016/S0028-3908(00)00117-9
Breustedt, J., Vogt, K.E., Miller, R.J., Nicoll, R.A., Schmitz, D., 2003. α1E-Containing Ca2+ channels are involved in synaptic plasticity. Proc. Natl. Acad. Sci. U. S. A. 100, 12450–12455. https://doi.org/10.1073/pnas.2035117100
Brigo, F., Igwe, S.C., 2017. Ethosuximide, sodium valproate or lamotrigine for absence seizures in children and adolescents. Cochrane Database Syst. Rev. https://doi.org/10.1002/14651858.CD003032.pub3
Brinkmann, V., 2007. Sphingosine 1-phosphate receptors in health and disease: Mechanistic insights from gene deletion studies and reverse pharmacology. Pharmacol. Ther. https://doi.org/10.1016/j.pharmthera.2007.04.006
Brinkmann, V., Cyster, J.G., Hla, T., 2004. FTY720: Sphingosine 1-phosphate receptor-1 in the control of lymphocyte egress and endothelial barrier function. Am. J. Transplant. https://doi.org/10.1111/j.1600-6143.2004.00476.x
Brinkmann, V., Davis, M.D., Heise, C.E., Albert, R., Cottens, S., Hof, R., Bruns, C., Prieschl, E., Baumruker, T., Hiestand, P., Foster, C.A., Zollinger, M., Lynch, K.R., 2002. The immune modulator FTY720 targets sphingosine 1-phosphate receptors. J. Biol. Chem. 277, 21453–21457. https://doi.org/10.1074/jbc.C200176200
Brookes, M.E., Eldabe, S., Batterham, A., 2016. Ziconotide Monotherapy: A Systematic Review of Randomised Controlled Trials. Curr. Neuropharmacol. 15, 217–231. https://doi.org/10.2174/1570159x14666160210142056
Brown, D.A., 2018. Regulation of neural ion channels by muscarinic receptors. Neuropharmacology. https://doi.org/10.1016/j.neuropharm.2017.11.024
Bruel-Jungerman, E., Lucassen, P.J., Francis, F., 2011. Cholinergic influences on cortical development and adult neurogenesis. Behav. Brain Res. https://doi.org/10.1016/j.bbr.2011.01.021
Brunet, N., Bosman, C.A., Roberts, M., Oostenveld, R., Womelsdorf, T., De Weerd, P., Fries, P., 2015. Visual cortical gamma-band activity during free viewing of natural images. Cereb. Cortex 25, 918–926. https://doi.org/10.1093/cercor/bht280
Brunkhorst, R., Vutukuri, R., Pfeilschifter, W., 2014. Fingolimod for the treatment of neurological diseases—state of play and future perspectives3. Front. Cell. Neurosci. https://doi.org/10.3389/fncel.2014.00283
Bruno, G., Cencetti, F., Bernacchioni, C., Donati, C., Blankenbach, K.V., Thomas, D., Meyer zu Heringdorf, D., Bruni, P., 2018. Bradykinin mediates myogenic differentiation in murine myoblasts through the involvement of SK1/Spns2/S1P 2 axis. Cell. Signal. 45, 110–121. https://doi.org/10.1016/j.cellsig.2018.02.001
Bruns, R.F., Fergus, J.H., 1990. Allosteric enhancement of adenosine A1 receptor binding and function by 2-amino-3-benzoylthiophenes. Mol. Pharmacol. 38.
Bura, S.A., Nadal, X., Ledent, C., Maldonado, R., Valverde, O., 2008. A2A adenosine receptor regulates glia proliferation and pain after peripheral nerve injury. Pain 140, 95–103. https://doi.org/10.1016/j.pain.2008.07.012
Burnstock, G., B. Fredholm, B., Verkhratsky, A., 2011. Adenosine and ATP Receptors in the Brain. Curr. Top. Med. Chem. 11, 973–1011. https://doi.org/10.2174/156802611795347627
Burnstock, G., Cocks, T., Crowe, R., 1978. Evidence for purinergic innervation of the anococcygeus muscle. Br. J. Pharmacol. 64, 13–20. https://doi.org/10.1111/j.1476-5381.1978.tb08635.x
Cai, Q., Qiu, C.Y., Qiu, F., Liu, T.T., Qu, Z.W., Liu, Y.M., Hu, W.P., 2014. Morphine inhibits acid-sensing ion channel currents in rat dorsal root ganglion neurons. Brain Res. 1554, 12–20. https://doi.org/10.1016/j.brainres.2014.01.042

Cain, S.M., Snutch, T.P., 2011. Voltage-gated calcium channels and disease. BioFactors. https://doi.org/10.1002/biof.158

Calabrese, M., Magliozzi, R., Ciccarelli, O., Geurts, J.J.G., Reynolds, R., Martin, R., 2015. Exploring the origins of grey matter damage in multiple sclerosis. Nat. Rev. Neurosci. https://doi.org/10.1038/nrn3900

Candy, J.M., Perry, R.H., Perry, E.K., Irving, D., Blessed, G., Fairbairn, A.F., Tomlinson, B.E., 1983. Pathological changes in the nucleus of meynert in Alzheimer's and Parkinson's diseases. J. Neurol. Sci. 59, 277–289. https://doi.org/10.1016/0022-510X(83)90045-X

Cantrell, A.R., Catterall, W.A., 2001. Neuromodulation of Na+ channels: An unexpected form of cellular plasticity. Nat. Rev. Neurosci. https://doi.org/10.1038/35077553

Cantrell, A.R., Ma, J.Y., Scheuer, T., Catterall, W.A., 1996. Muscarinic modulation of sodium current by activation of protein kinase C in rat hippocampal neurons. Neuron 16, 1019–1026. https://doi.org/10.1016/S0896-6273(00)80125-7

Cao, T., Ma, T., Xu, Y., Tian, Y., Cai, Q., Li, B., Li, H., 2019. Caffeine treatment promotes differentiation and maturation of hypoxic oligodendrocytes via counterbalancing adenosine 1 adenosine receptor-induced calcium overload. Med. Sci. Monit. 25, 1729–1739. https://doi.org/10.12659/MSM.915147

Cao, X., Zhao, S., Liu, D., Wang, Z., Niu, L., Hou, L., Wang, C., 2011. ROS-Ca2+ is associated with mitochondria permeability transition pore involved in surfactin-induced MCF-7 cells apoptosis. Chem. Biol. Interact. 190, 16–27. https://doi.org/10.1016/j.cbi.2011.01.010

Casanova, M.F., Walker, L.C., Whitehouse, P.J., Price, D.L., 1985. Abnormalities of the nucleus basalis in Down's syndrome. Ann. Neurol. 18, 310–313. https://doi.org/10.1002/ana.410180306

Casida, J.E., Durkin, K.A., 2013. Anticholinesterase insecticide retrospective, in: Chemico-Biological Interactions. NIH Public Access, pp. 221–225. https://doi.org/10.1016/j.cbi.2012.08.002

Catacuzzeno, L., Franciolini, F., 2018. Role of KCa3.1 channels in modulating ca2+ oscillations during glioblastoma cell migration and invasion. Int. J. Mol. Sci. https://doi.org/10.3390/ijms19102970

Catterall, W.A., 2017. Forty Years of Sodium Channels: Structure, Function, Pharmacology, and Epilepsy. Neurochem. Res. 42, 2495–2504. https://doi.org/10.1007/s11064-017-2314-9

Catterall, W.A., 2000. From ionic currents to molecular mechanisms: The structure and function of voltage-gated sodium channels. Neuron. https://doi.org/10.1016/S0896-6273(00)81133-2

Catterall, W.A., 1987. Common modes of drug action on Na+ channels: local anesthetics, antiarrhythmics and anticonvulsants. Trends Pharmacol. Sci. https://doi.org/10.1016/0165-6147(87)90011-3

Catterall, W.A., Dib-Hajj, S., Meisler, M.H., Pietrobon, D., 2008. Inherited neuronal ion channelopathies: New windows on complex neurological diseases, in: Journal of Neuroscience. Society for Neuroscience, pp. 11768–11777. https://doi.org/10.1523/JNEUROSCI.3901-08.2008

Catterall, W.A., Perez-Reyes, E., Snutch, T.P., Striessnig, J., 2005. International Union of Pharmacology. XLVIII. Nomenclature and structure-function relationships of voltage-gated calcium channels. Pharmacol. Rev. https://doi.org/10.1124/pr.57.4.5

Cencetti, F., Bernacchioni, C., Nincheri, P., Donati, C., Bruni, P., 2010. Transforming growth factor-β1 induces transdifferentiation of myoblasts into myofibroblasts via up-regulation of sphingosine kinase-1/S1P3 axis. Mol. Biol. Cell 21, 1111–1124. https://doi.org/10.1091/mbc.E09-09-0812

Cencetti, F., Bernacchioni, C., Tonelli, F., Roberts, E., Donati, C., Bruni, P., 2013. TGFβ1 evokes myoblast apoptotic response *via* a novel signaling pathway involving S1P $_4$ transactivation upstream of Rho-kinase-2 activation. FASEB J. 27, 4532–4546. https://doi.org/10.1096/fj.13-228528

Chang, A., Nishiyama, A., Peterson, J., Prineas, J., Trapp, B.D., 2000. NG2-positive oligodendrocyte progenitor cells in adult human brain and multiple sclerosis lesions. J.

Neurosci. 20, 6404–6412. https://doi.org/10.1523/JNEUROSCI.20-17-06404.2000
Changeux, J.P., Devillers-Thiéry, A., Chemouilli, P., 1984. Acetylcholine receptor: An allosteric protein. Science (80-.). 225, 1335–1345. https://doi.org/10.1126/science.6382611
Chen, D., Yu, S.P., Wei, L., 2014. Ion Channels in Regulation of Neuronal Regenerative Activities. Transl. Stroke Res. 5, 156–162. https://doi.org/10.1007/s12975-013-0320-z
Chen, S.-R., Cai, Y.-Q., Pan, H.-L., 2009. Plasticity and emerging role of BK $_{Ca}$ channels in nociceptive control in neuropathic pain. J. Neurochem. 110, 352–362. https://doi.org/10.1111/j.1471-4159.2009.06138.x
Chen, S., Ren, Y.Q., Bing, R., Hillman, D.E., 2000. Alpha 1E subunit of the R-type calcium channel is associated with myelinogenesis. J. Neurocytol. 29, 719–728. https://doi.org/10.1023/A:1010986303924
Chen, X., Yuan, L.L., Zhao, C., Birnbaum, S.G., Frick, A., Jung, W.E., Schwarz, T.L., Sweatt, J.D., Johnston, D., 2006. Deletion of Kv4.2 gene eliminates dendritic A-type K+ current and enhances induction of long-term potentiation in hippocampal CA1 pyramidal neurons. J. Neurosci. 26, 12143–12151. https://doi.org/10.1523/JNEUROSCI.2667-06.2006
Chen, Y., Zhang, Z.X., Zheng, L.P., Wang, L., Liu, Y.F., Yin, W.Y., Chen, Y.Y., Wang, X.S., Hou, S.T., Chen, J.F., Zheng, R.Y., 2019. The adenosine A2A receptor antagonist SCH58261 reduces macrophage/microglia activation and protects against experimental autoimmune encephalomyelitis in mice. Neurochem. Int. 129, 104490. https://doi.org/10.1016/j.neuint.2019.104490
Chen, Z., Janes, K., Chen, C., Doyle, T., Bryant, L., Tosh, D.K., Jacobson, K.A., Salvemini, D., 2012. Controlling murine and rat chronic pain through A $_3$ adenosine receptor activation. FASEB J. 26, 1855–1865. https://doi.org/10.1096/fj.11-201541
Cheong, S.L., Federico, S., Venkatesan, G., Mandel, A.L., Shao, Y.-M., Moro, S., Spalluto, G., Pastorin, G., 2013. The A $_3$ adenosine receptor as multifaceted therapeutic target: pharmacology, medicinal chemistry, and in silico approaches. Med. Res. Rev. 33, 235–335. https://doi.org/10.1002/med.20254
Cherkas, P.S., Huang, T.Y., Pannicke, T., Tal, M., Reichenbach, A., Hanani, M., 2004. The effects of axotomy on neurons and satellite glial cells in mouse trigeminal ganglion. Pain 110, 290–298. https://doi.org/10.1016/j.pain.2004.04.007
Chittajallu, R., Aguirre, A.A., Gallo, V., 2005. Downregulation of platelet-derived growth factor-α receptor-mediated tyrosine kinase activity as a cellular mechanism for K+-channel regulation during oligodendrocyte development in situ. J. Neurosci. 25, 8601–8610. https://doi.org/10.1523/JNEUROSCI.2122-05.2005
Cho, C.K., Sung, T.Y., Choi, S.J., Choi, H.R., Kim, Y.B., Lee, J.U., Yang, H.S., 2018. The effect of magnesium sulfate concentration on the effective concentration of rocuronium, and sugammadex-mediated reversal, in isolated left phrenic nerve hemidiaphragm preparations from the rat. Korean J. Anesthesiol. 71, 401–406. https://doi.org/10.4097/kja.d.17.27150
Choi, J.W., Gardell, S.E., Herr, D.R., Rivera, R., Lee, C.W., Noguchi, K., Teo, S.T., Yung, Y.C., Lu, M., Kennedy, G., Chun, J., 2011. FTY720 (fingolimod) efficacy in an animal model of multiple sclerosis requires astrocyte sphingosine 1-phosphate receptor 1 (S1P1) modulation. Proc. Natl. Acad. Sci. U. S. A. 108, 751–756. https://doi.org/10.1073/pnas.1014154108
Chun, J., Brinkmann, V., 2011. A mechanistically novel, first oral therapy for multiple sclerosis: the development of fingolimod (FTY720, Gilenya). Discov. Med.
Cieślik, M., Czapski, G.A., Strosznajder, J.B., 2015. The Molecular Mechanism of Amyloid β42 Peptide Toxicity: The Role of Sphingosine Kinase-1 and Mitochondrial Sirtuins. PLoS One 10, e0137193. https://doi.org/10.1371/journal.pone.0137193
Ciruela, F., Ferré, S., Casadó, V., Cortés, A., Cunha, R.A., Lluis, C., Franco, R., 2006. Heterodimeric adenosine receptors: A device to regulate neurotransmitter release. Cell. Mol. Life Sci. https://doi.org/10.1007/s00018-006-6216-2
Clapham, D.E., 2007. Calcium Signaling. Cell. https://doi.org/10.1016/j.cell.2007.11.028
Clarke, L.E., Young, K.M., Hamilton, N.B., Li, H., Richardson, W.D., Attwell, D., 2012. Properties and fate of oligodendrocyte progenitor cells in the corpus callosum, motor

cortex, and piriform cortex of the mouse. J. Neurosci. 32, 8173–8185. https://doi.org/10.1523/JNEUROSCI.0928-12.2012

Coelho, R.P., Payne, S.G., Bittman, R., Spiegel, S., Sato-Bigbee, C., 2007. The immunomodulator FTY720 has a direct cytoprotective effect in oligodendrocyte progenitors. J. Pharmacol. Exp. Ther. 323, 626–635. https://doi.org/10.1124/jpet.107.123927

Cohen, J.A., Barkhof, F., Comi, G., Hartung, H.P., Khatri, B.O., Montalban, X., Pelletier, J., Capra, R., Gallo, P., Izquierdo, G., Tiel-Wilck, K., De Vera, A., Jin, J., Stites, T., Wu, S., Aradhye, S., Kappos, L., 2010. Oral fingolimod or intramuscular interferon for relapsing multiple sclerosis. N. Engl. J. Med. 362, 402–415. https://doi.org/10.1056/NEJMoa0907839

Colotta, V., Lenzi, O., Catarzi, D., Varano, F., Squarcialupi, L., Costagli, C., Galli, A., Ghelardini, C., Pugliese, A.M., Maraula, G., Coppi, E., Pellegrini-Giampietro, D.E., Pedata, F., Sabbadin, D., Moro, S., 2012. 3-Hydroxy-1H-quinazoline-2,4-dione derivatives as new antagonists at ionotropic glutamate receptors: Molecular modeling and pharmacological studies. Eur. J. Med. Chem. 54, 470–482. https://doi.org/10.1016/j.ejmech.2012.05.036

Comi, G., Radaelli, M., Soelberg Sørensen, P., 2017. Evolving concepts in the treatment of relapsing multiple sclerosis. Lancet. https://doi.org/10.1016/S0140-6736(16)32388-1

Compston, A., Coles, A., 2002. Multiple sclerosis, in: Lancet. Elsevier Limited, pp. 1221–1231. https://doi.org/10.1016/S0140-6736(02)08220-X

Cooper, E., Couturier, S., Ballivet, M., 1991. Pentameric structure and subunit stoichiometry of a neuronal nicotinic acetylcholine receptor. Nature 350, 235–238. https://doi.org/10.1038/350235a0

Coppi, E., Cellai, L., Maraula, G., Dettori, I., Melani, A., Pugliese, A.M., Pedata, F., 2015. Role of adenosine in oligodendrocyte precursor maturation. Front. Cell. Neurosci. 9. https://doi.org/10.3389/fncel.2015.00155

Coppi, E., Cellai, L., Maraula, G., Pugliese, A.M., Pedata, F., 2013a. Adenosine A2A receptors inhibit delayed rectifier potassium currents and cell differentiation in primary purified oligodendrocyte cultures. Neuropharmacology 73, 301–310. https://doi.org/10.1016/j.neuropharm.2013.05.035

Coppi, E., Maraula, G., Fumagalli, M., Failli, P., Cellai, L., Bonfanti, E., Mazzoni, L., Coppini, R., Abbracchio, M.P., Pedata, F., Pugliese, A.M., 2013b. UDP-glucose enhances outward K^+ currents necessary for cell differentiation and stimulates cell migration by activating the GPR17 receptor in oligodendrocyte precursors. Glia 61, 1155–1171. https://doi.org/10.1002/glia.22506

Coppi, E., Pedata, F., Gibb, A.J., 2012. P2Y1 receptor modulation of Ca2+-activated K+ currents in medium-sized neurons from neonatal rat striatal slices. J. Neurophysiol. 107, 1009–21. https://doi.org/10.1152/jn.00816.2009

Corradetti, R., Lo Conte, G., Moroni, F., Beatrice Passani, M., Pepeu, G., 1984. Adenosine decreases aspartate and glutamate release from rat hippocampal slices. Eur. J. Pharmacol. 104, 19–26. https://doi.org/10.1016/0014-2999(84)90364-9

Corsi, C., Melani, A., Bianchi, L., Pedata, F., 2000. Striatal A2(A) adenosine receptor antagonism differentially modifies striatal glutamate outflow in vivo in young and aged rats. Neuroreport 11, 2591–2595. https://doi.org/10.1097/00001756-200008030-00048

Corsi, C., Melani, A., Bianchi, L., Pepeu, G., Pedata, F., 1999. Striatal A(2A) adenosine receptors differentially regulate spontaneous and K+-evoked glutamate release in vivo in young and aged rats. Neuroreport 10, 687–691. https://doi.org/10.1097/00001756-199903170-00005

Corti, F., Cellai, L., Melani, A., Donati, C., Bruni, P., Pedata, F., 2013. Adenosine is present in rat brain synaptic vesicles. Neuroreport 24, 982–987. https://doi.org/10.1097/WNR.0000000000000033

Costa, M.R.C., Catterall, W.A., 1984. Cyclic AMP-dependent phosphorylation of the α subunit of the sodium channel in synaptic nerve ending particles. J. Biol. Chem. 259, 8210–8218.

Costenla, A.R., Lopes, L. V., De Mendonça, A., Ribeiro, J.A., 2001. A functional role for adenosine A3 receptors: Modulation of synaptic plasticity in the rat hippocampus.

Neurosci. Lett. 302, 53–57. https://doi.org/10.1016/S0304-3940(01)01633-0
Couttas, T.A., Kain, N., Daniels, B., Lim, X.Y., Shepherd, C., Kril, J., Pickford, R., Li, H., Garner, B., Don, A.S., 2014. Loss of the neuroprotective factor Sphingosine 1-phosphate early in Alzheimer's disease pathogenesis. Acta Neuropathol. Commun. 2, 9. https://doi.org/10.1186/2051-5960-2-9
Covarrubias, M., Bhattacharji, A., De Santiago-Castillo, J.A., Dougherty, K., Kaulin, Y.A., Na-Phuket, T.R., Wang, G., 2008. The neuronal Kv4 channel complex. Neurochem. Res. https://doi.org/10.1007/s11064-008-9650-8
Cristalli, G., Lambertucci, C., Marucci, G., Volpini, R., Ben, D., 2008. A2A Adenosine Receptor and its Modulators: Overview on a Druggable GPCR and on Structure-Activity Relationship Analysis and Binding Requirements of Agonists and Antagonists. Curr. Pharm. Des. 14, 1525–1552. https://doi.org/10.2174/138161208784480081
Cruzblanca, H., 2006. An M 2-like muscarinic receptor enhances a delayed rectifier K + current in rat sympathetic neurones. Br. J. Pharmacol. 149, 441–449. https://doi.org/10.1038/sj.bjp.0706874
Cummings, J.L., Benson, D.F., 1987. The role of the nucleus basalis of Meynert in dementia: review and reconsideration. Alzheimer Dis. Assoc. Disord. https://doi.org/10.1097/00002093-198701030-00003
Cunha, R.A., Johansson, B., Fredholm, B.B., Alexandre Ribeiro, J., Sebastião, A.M., 1995. Adenosine A2A receptors stimulate acetylcholine release from nerve terminals of the rat hippocampus. Neurosci. Lett. 196, 41–44. https://doi.org/10.1016/0304-3940(95)11833-I
D'Alcantara, P., Ledent, C., Swillens, S., Schiffmann, S.N., 2001. Inactivation of adenosine A2A receptor impairs long term potentiation in the accumbens nucleus without altering basal synaptic transmission. Neuroscience 107, 455–464. https://doi.org/10.1016/S0306-4522(01)00372-4
Dale, H.H., Dudley, H.W., 1929. The presence of histamine and acetylcholine in the spleen of the ox and the horse. J. Physiol. 68, 97–123. https://doi.org/10.1113/jphysiol.1929.sp002598
Dascal, N., Kahanovitch, U., 2015. The Roles of Gβγ and Gα in Gating and Regulation of GIRK Channels, in: International Review of Neurobiology. Academic Press Inc., pp. 27–85. https://doi.org/10.1016/bs.irn.2015.06.001
Dawson, M.R.L., Polito, A., Levine, J.M., Reynolds, R., 2003. NG2-expressing glial progenitor cells: An abundant and widespread population of cycling cells in the adult rat CNS. Mol. Cell. Neurosci. 24, 476–488. https://doi.org/10.1016/S1044-7431(03)00210-0
Day, M., Carr, D.B., Ulrich, S., Ilijic, E., Tkatch, T., Surmeier, D.J., 2005. Dendritic excitability of mouse frontal cortex pyramidal neurons is shaped by the interaction among HCN, Kir2, and Kleak channels. J. Neurosci. 25, 8776–8787. https://doi.org/10.1523/JNEUROSCI.2650-05.2005
De Castro, F., Bribián, A., 2005. The molecular orchestra of the migration of oligodendrocyte precursors during development. Brain Res. Rev. https://doi.org/10.1016/j.brainresrev.2004.12.034
De Nuccio, C., Bernardo, A., Ferrante, A., Pepponi, R., Martire, A., Falchi, M., Visentin, S., Popoli, P., Minghetti, L., 2019. Adenosine A2A receptor stimulation restores cell functions and differentiation in Niemann-Pick type C-like oligodendrocytes. Sci. Rep. 9, 1–10. https://doi.org/10.1038/s41598-019-46268-8
De Paoli, P., Cerbai, E., Koidl, B., Kirchengast, M., Sartiani, L., Mugelli, A., 2002. Selectivity of different calcium antagonists on T- and L-type calcium currents in guinea-pig ventricular myocytes. Pharmacol. Res. 46. https://doi.org/10.1016/S1043661802002360
De Stefano, N., Silva, D.G., Barnett, M.H., 2017. Effect of Fingolimod on Brain Volume Loss in Patients with Multiple Sclerosis. CNS Drugs. https://doi.org/10.1007/s40263-017-0415-2
Deckert, J., Jorgensen, M.B., 1988. Evidence for pre- and postsynaptic localization of adenosine A1 receptors in the CA1 region of rat hippocampus: a quantitative autoradiographic study. Brain Res. 446, 161–164. https://doi.org/10.1016/0006-8993(88)91308-X
DeLuca, G.C., Yates, R.L., Beale, H., Morrow, S.A., 2015. Cognitive Impairment in Multiple

Sclerosis: Clinical, Radiologic and Pathologic Insights. Brain Pathol. 25, 79–98. https://doi.org/10.1111/bpa.12220

Dennis, D., Picketts, D., Slack, R.S., Schuurmans, C., 2016. Forebrain neurogenesis: From embryo to adult. Trends Dev. Biol. 9, 77–90.

Dettori, I., Gaviano, L., Ugolini, F., Lana, D., Bulli, I., Magni, G., Rossi, F., Giovannini, M.G., Pedata, F., 2020. Protective effect of adenosine A2B receptor agonist, BAY60-6583, against transient focal brain ischemia in rat. Front. Pharmacol. 11, 1639. https://doi.org/10.3389/FPHAR.2020.588757

Dev, K.K., Mullershausen, F., Mattes, H., Kuhn, R.R., Bilbe, G., Hoyer, D., Mir, A., 2008. Brain sphingosine-1-phosphate receptors: Implication for FTY720 in the treatment of multiple sclerosis. Pharmacol. Ther. https://doi.org/10.1016/j.pharmthera.2007.08.005

Devor, M., Govrin-Lippmann, R., Angelides, K., 1993. Na+ channel immunolocalization in peripheral mammalian axons and changes following nerve injury and neuroma formation. J. Neurosci. 13, 1976–1992. https://doi.org/10.1523/jneurosci.13-05-01976.1993

Di Cesare Mannelli, L., Zanardelli, M., Landini, I., Pacini, A., Ghelardini, C., Mini, E., Bencini, A., Valtancoli, B., Failli, P., 2016. Effect of the SOD mimetic MnL4 on in vitro and in vivo oxaliplatin toxicity: Possible aid in chemotherapy induced neuropathy. Free Radic. Biol. Med. 93, 67–76. https://doi.org/10.1016/j.freeradbiomed.2016.01.023

Di Filippo, M., Tozzi, A., Costa, C., Belcastro, V., Tantucci, M., Picconi, B., Calabresi, P., 2008. Plasticity and repair in the post-ischemic brain. Neuropharmacology 55, 353–362. https://doi.org/10.1016/j.neuropharm.2008.01.012

Dib-Hajj, S.D., Black, J.A., Waxman, S.G., 2009. Voltage-Gated Sodium Channels: Therapeutic Targets for Pain. Pain Med. 10, 1260–1269. https://doi.org/10.1111/j.1526-4637.2009.00719.x

Dickenson, A., Suzuki, R., Reeve, A., 2000. Adenosine as a potential analgesic target in inflammatory and neuropathic pains. CNS DRUGS , 13 77 - 85. .

Dietrich, D., Kirschstein, T., Kukley, M., Pereverzev, A., Von Der Brelie, C., Schneider, T., Beck, H., 2003. Functional specialization of presynaptic Cav2.3 Ca2+ channels. Neuron 39, 483–496. https://doi.org/10.1016/S0896-6273(03)00430-6

Dixon, A.K., Gubitz, A.K., Sirinathsinghji, D.J.S., Richardson, P.J., Freeman, T.C., 1996. Tissue distribution of adenosine receptor mRNAs in the rat. Br. J. Pharmacol. 118, 1461–1468. https://doi.org/10.1111/j.1476-5381.1996.tb15561.x

Dobolyi, Á., Reichart, A., Szikra, T., Nyitrai, G., Kékesi, K.A., Juhász, G., 2000. Sustained depolarisation induces changes in the extracellular concentrations of purine and pyrimidine nucleosides in the rat thalamus. Neurochem. Int. 37, 71–79. https://doi.org/10.1016/S0197-0186(99)00162-X

Dolphin, A.C., Forda, S.R., Scott, R.H., 1986. Calcium-dependent currents in cultured rat dorsal root ganglion neurones are inhibited by an adenosine analogue. J. Physiol. 373, 47–61.

Dolphin, B.Y.A.C., Forda, S.R., Scott, R.H., 1986. St. George's 47–61.

Donati, C., Cencetti, F., Bruni, P., 2013. New insights into the role of sphingosine 1-phosphate and lysophosphatidic acid in the regulation of skeletal muscle cell biology. Biochim. Biophys. Acta - Mol. Cell Biol. Lipids. https://doi.org/10.1016/j.bbalip.2012.06.013

Donati, C., Cencetti, F., Nincheri, P., Bernacchioni, C., Brunelli, S., Clementi, E., Cossu, G., Bruni, P., 2007. Sphingosine 1-Phosphate Mediates Proliferation and Survival of Mesoangioblasts. Stem Cells 25, 1713–1719. https://doi.org/10.1634/stemcells.2006-0725

Donati, C., Meacci, E., Nuti, F., Becciolini, L., Farnararo, M., Bruni, P., 2005. Sphingosine 1-phosphate regulates myogenic differentiation: a major role for S1P $_2$ receptor. FASEB J. 19, 1–22. https://doi.org/10.1096/fj.04-1780fje

Dong, X.P., Xu, T. Le, 2002. Radix paeoniae rubra suppression of sodium current in acutely dissociated rat hippocampal CA1 neurons. Brain Res. 940, 1–9. https://doi.org/10.1016/S0006-8993(02)02555-6

Dong, X.W., Goregoaker, S., Engler, H., Zhou, X., Mark, L., Crona, J., Terry, R., Hunter, J., Priestley, T., 2007. Small interfering RNA-mediated selective knockdown of NaV1.8

tetrodotoxin-resistant sodium channel reverses mechanical allodynia in neuropathic rats. Neuroscience 146, 812–821. https://doi.org/10.1016/j.neuroscience.2007.01.054

Doyle, D.A., Cabral, J.M., Pfuetzner, R.A., Kuo, A., Gulbis, J.M., Cohen, S.L., Chait, B.T., MacKinnon, R., 1998. The structure of the potassium channel: Molecular basis of K+ conduction and selectivity. Science (80-.). 280, 69–77. https://doi.org/10.1126/science.280.5360.69

Drury, A.N., Szent-Györgyi, A., 1929. The physiological activity of adenine compounds with especial reference to their action upon the mammalian heart. J. Physiol. 68, 213–237. https://doi.org/10.1113/jphysiol.1929.sp002608

Dukala, D.E., Soliven, B., 2016. *S1P* $_1$ deletion in oligodendroglial lineage cells: Effect on differentiation and myelination. Glia 64, 570–582. https://doi.org/10.1002/glia.22949

Dunwiddie, T.V., Fredholm, B.B., 1997. Adenosine neuromodulation J. KA, and J. MF, eds. (New York, NY: Wiley-Liss), in: KA, J., MF, J. (Eds.), Purinergics Approaches in Experimental Therapeutics. Wiley-Liss, New York, pp. 359–382.

Dunwiddie, T. V., 1985. The Physiological Role of Adenosine In The Central Nervous System. Int. Rev. Neurobiol. 27, 63–139. https://doi.org/10.1016/S0074-7742(08)60556-5

Dunwiddie, T. V., Hoffer, B.J., 1980. Adenine nucleotides and synaptic transmission in the in vitro rat hippocampus. Br. J. Pharmacol. 69, 59–68. https://doi.org/10.1111/j.1476-5381.1980.tb10883.x

Eckle, T., Faigle, M., Grenz, A., Laucher, S., Thompson, L.F., Eltzschig, H.K., 2008. A2B adenosine receptor dampens hypoxia-induced vascular leak. Blood 111, 2024–2035. https://doi.org/10.1182/blood-2007-10-117044

Ekberg, J., Jayamanne, A., Vaughan, C.W., Aslan, S., Thomas, L., Mould, J., Drinkwater, R., Baker, M.D., Abrahamsen, B., Wood, J.N., Adams, D.J., Christie, M.J., Lewis, R.J., 2006. μO-conotoxin MrVIB selectively blocks NaV1.8 sensory neuron specific sodium channels and chronic pain behavior without motor deficits. Proc. Natl. Acad. Sci. U. S. A. 103, 17030–17035. https://doi.org/10.1073/pnas.0601819103

Emery, B., 2010. Regulation of oligodendrocyte differentiation and myelination. Science (80-.). https://doi.org/10.1126/science.1190927

Englert, M., Quitterer, U., Klotz, K.N., 2002. Effector coupling of stably transfected human A3 adenosine receptors in CHO cells. Biochem. Pharmacol. 64, 61–65. https://doi.org/10.1016/S0006-2952(02)01071-7

English, C., Aloi, J.J., 2015. New FDA-approved disease-modifying therapies for multiple sclerosis. Clin. Ther. https://doi.org/10.1016/j.clinthera.2015.03.001

Ewins, A.J., 1914. Acetylcholine, a New Active Principle of Ergot. Biochem. J. 8, 44–49. https://doi.org/10.1042/bj0080044

Falk, L., Nordberg, A., Seiger, Å., Kjældgaard, A., Hellström-Lindahl, E., 2002. The α7 nicotinic receptors in human fetal brain and spinal cord. J. Neurochem. 80, 457–465. https://doi.org/10.1046/j.0022-3042.2001.00714.x

Fang, Z.-Z., Tosh, D.K., Tanaka, N., Wang, H., Krausz, K.W., O'Connor, R., Jacobson, K.A., Gonzalez, F.J., 2015. Metabolic mapping of A3 adenosine receptor agonist MRS5980. Biochem. Pharmacol. 97, 215–23. https://doi.org/10.1016/j.bcp.2015.07.007

Fda, Cder, 2020. Zeposia - Highlights of prescribing information.

Fda, Cder, 2019. Mayzent - Highlights of prescribing information.

Feldberg, W., Vogt, M., 1948. Acetylcholine synthesis in different regions of the central nervous system. J. Physiol. 107, 372–381. https://doi.org/10.1113/jphysiol.1948.sp004282

Felder, C.C., Albrecht, F., Eisner, G.M., Jose, P.A., 1990. The signal transducer for the dopamine-1 regulated sodium transport in renal cortical brush border membrane vesicles, in: American Journal of Hypertension. Am J Hypertens. https://doi.org/10.1093/ajh/3.6.47s

Ferre, S., Von Euler, G., Johansson, B., Fredholm, B.B., Fuxe, K., 1991. Stimulation of high-affinity adenosine A2 receptors decreases the affinity of dopamine D2 receptors in rat striatal membranes. Proc. Natl. Acad. Sci. U. S. A. 88, 7238–7241. https://doi.org/10.1073/pnas.88.16.7238

Ferreira-Vieira, T.H., Guimaraes, I.M., Silva, F.R., Ribeiro, F.M., 2016. Alzheimer's disease:

Targeting the Cholinergic System. Curr. Neuropharmacol. 14, 101–115. https://doi.org/10.2174/1570159x13666150716165726

Fiebich, B.L., Biber, K., Lieb, K., Van Calker, D., Berger, M., Bauer, J., Gebicke-Haerter, P.J., 1996. Cyclooxygenase-2 expression in rat microglia is induced by adenosine A2a-receptors. Glia 18, 152–180. https://doi.org/10.1002/(sici)1098-1136(199610)18:2<152::aid-glia7>3.0.co;2-2

Field, M.J., Li, Z., Schwarz, J.B., 2007. Ca2+ channel α2-δ ligands for the treatment of neuropathic pain. J. Med. Chem. https://doi.org/10.1021/jm060650z

Fields, R.D., 2004. Volume transmission in activity-dependent regulation of myelinating glia. Neurochem. Int. 45, 503–509. https://doi.org/10.1016/j.neuint.2003.11.015

Fields, R.D., Burnstock, G., 2006. Purinergic signalling in neuron-glia interactions. Nat. Rev. Neurosci. https://doi.org/10.1038/nrn1928

Figueroa, K.P., Minassian, N.A., Stevanin, G., Waters, M., Garibyan, V., Forlani, S., Strzelczyk, A., Bürk, K., Brice, A., Dürr, A., Papazian, D.M., Pulst, S.M., 2010. KCNC3: phenotype, mutations, channel biophysics-a study of 260 familial ataxia patients. Hum. Mutat. 31, 191–196. https://doi.org/10.1002/humu.21165

Filippi, M., Rocca, M.A., Barkhof, F., Brück, W., Chen, J.T., Comi, G., DeLuca, G., De Stefano, N., Erickson, B.J., Evangelou, N., Fazekas, F., Geurts, J.J.G., Lucchinetti, C., Miller, D.H., Pelletier, D., Popescu, B.F.G., Lassmann, H., 2012. Association between pathological and MRI findings in multiple sclerosis. Lancet Neurol. https://doi.org/10.1016/S1474-4422(12)70003-0

Flajolet, M., Wang, Z., Futter, M., Shen, W., Nuangchamnong, N., Bendor, J., Wallach, I., Nairn, A.C., Surmeier, D.J., Greengard, P., 2008. FGF acts as a co-transmitter through adenosine A2A receptor to regulate synaptic plasticity. Nat. Neurosci. 11, 1402–1409. https://doi.org/10.1038/nn.2216

Fontenas, L., Welsh, T.G., Piller, M., Coughenour, P., Gandhi, A. V., Prober, D.A., Kucenas, S., 2019. The Neuromodulator Adenosine Regulates Oligodendrocyte Migration at Motor Exit Point Transition Zones. Cell Rep. 27, 115-128.e5. https://doi.org/10.1016/j.celrep.2019.03.013

Ford, A., Castonguay, A., Cottet, M., Little, J.W., Chen, Z., Symons-Liguori, A.M., Doyle, T., Egan, T.M., Vanderah, T.W., De Koninck, Y., Tosh, D.K., Jacobson, K.A., Salvemini, D., 2015. Engagement of the GABA to KCC2 Signaling Pathway Contributes to the Analgesic Effects of A $_3$ AR Agonists in Neuropathic Pain. J. Neurosci. 35, 6057–6067. https://doi.org/10.1523/JNEUROSCI.4495-14.2015

Franco, R., Canela, E.I., Bozal, J., 1986. Heterogeneous localization of some purine enzymes in subcellular fractions of rat brain and cerebellum. Neurochem. Res. 11, 423–435. https://doi.org/10.1007/BF00965016

Fredholm, B.B., 1995. Purinoceptors in the Nervous System. Pharmacol. Toxicol. 76, 228–239. https://doi.org/10.1111/j.1600-0773.1995.tb00135.x

Fredholm, B.B., Arslan, G., Halldner, L., Kull, B., Schulte, G., Wasserman, W., 2000. Structure and function of adenosine receptors and their genes. Naunyn. Schmiedebergs. Arch. Pharmacol. https://doi.org/10.1007/s002100000313

Fredholm, B.B., Ijzerman, A.P., Jacobson, K.A., Klotz, K.N., Linden, J., 2001. International Union of Pharmacology. XXV. Nomenclature and classification of adenosine receptors. Pharmacol. Rev.

Fredholm, B.B., Lindgren, E., LindstrÖm, K., Nordstedt, C., 1987. α-Adrenoceptor stimulation, but not muscarinic stimulation, increases cyclic AMP accumulation in brain slices due to protein kinase C mediated enhancement of adenosine receptor effects. Acta Physiol. Scand. 131, 543–551. https://doi.org/10.1111/j.1748-1716.1987.tb08274.x

Fredholm, B.B., Svenningsson, P., 2003. Adenosine-dopamine interactions: Development of a concept and some comments on therapeutic possibilities. Neurology. https://doi.org/10.1212/01.wnl.0000095204.89871.ff

Frenguelli, B.G., Wigmore, G., Llaudet, E., Dale, N., 2007. Temporal and mechanistic dissociation of ATP and adenosine release during ischaemia in the mammalian hippocampus. J. Neurochem. 101, 1400–1413. https://doi.org/10.1111/j.1471-4159.2006.04425.x

Fries, P., 2015. Rhythms for Cognition: Communication through Coherence. Neuron. https://doi.org/10.1016/j.neuron.2015.09.034

Fries, P., 2009. Neuronal Gamma-Band Synchronization as a Fundamental Process in Cortical Computation. Annu. Rev. Neurosci. 32, 209–224. https://doi.org/10.1146/annurev.neuro.051508.135603

Fujita, T., Hirose, R., Yoneta, M., Sasaki, S., Inoue, K., Kiuchi, M., Hirase, S., Chiba, K., Sakamoto, H., Arita, M., 1996. Potent immunosuppressants, 2-alkyl-2-aminopropane-1,3-diols. J. Med. Chem. 39, 4451–4459. https://doi.org/10.1021/jm9603911

Fumagalli, M., Daniele, S., Lecca, D., Lee, P.R., Parravicini, C., Douglas Fields, R., Rosa, P., Antonucci, F., Verderio, C., Letizia Trincavelli, M., Bramanti, P., Martini, C., Abbracchio, M.P., 2011. Phenotypic changes, signaling pathway, and functional correlates of GPR17-expressing neural precursor cells during oligodendrocyte differentiation. J. Biol. Chem. 286, 10593–10604. https://doi.org/10.1074/jbc.M110.162867

Fusco, I., Cherchi, F., Catarzi, D., Colotta, V., Varano, F., Pedata, F., Pugliese, A.M., Coppi, E., 2019. Functional characterization of a novel adenosine A2B receptor agonist on short-term plasticity and synaptic inhibition during oxygen and glucose deprivation in the rat CA1 hippocampus. Brain Res. Bull. 151, 174–180. https://doi.org/10.1016/j.brainresbull.2019.05.018

Fusco, I., Ugolini, F., Lana, D., Coppi, E., Dettori, I., Gaviano, L., Nosi, D., Cherchi, F., Pedata, F., Giovannini, M.G., Pugliese, A.M., 2018. The selective antagonism of adenosine A2B receptors reduces the synaptic failure and neuronal death induced by oxygen and glucose deprivation in rat CA1 hippocampus in vitro. Front. Pharmacol. 9. https://doi.org/10.3389/fphar.2018.00399

Fusi, C., Materazzi, S., Benemei, S., Coppi, E., Trevisan, G., Marone, I.M., Minocci, D., De Logu, F., Tuccinardi, T., Di Tommaso, M.R., Susini, T., Moneti, G., Pieraccini, G., Geppetti, P., Nassini, R., 2014. Steroidal and non-steroidal third-generation aromatase inhibitors induce pain-like symptoms via TRPA1. Nat. Commun. 5, 5736. https://doi.org/10.1038/ncomms6736

Gallina, P., Paganini, M., Lombardini, L., Saccardi, R., Marini, M., De Cristofaro, M.T., Pinzani, P., Salvianti, F., Crescioli, C., Di Rita, A., Bucciantini, S., Mechi, C., Sarchielli, E., Moretti, M., Piacentini, S., Gritti, G., Bosi, A., Sorbi, S., Orlandini, G., Vannelli, G.B., Di Lorenzo, N., 2008. Development of human striatal anlagen after transplantation in a patient with Huntington's disease. Exp. Neurol. 213, 241–244. https://doi.org/10.1016/j.expneurol.2008.06.003

Gallo, V., Wright, P., McKinnon, R.D., 1994. Expression and regulation of a glutamate receptor subunit by bFGF in oligodendrocyte progenitors. Glia 10, 149–153. https://doi.org/10.1002/glia.440100209

Gallo, V., Zhou, J.M., McBain, C.J., Wright, P., Knutson, P.L., Armstrong, R.C., 1996. Oligodendrocyte progenitor cell proliferation and lineage progression are regulated by glutamate receptor-mediated K+ channel block. J. Neurosci. 16, 2659–2670. https://doi.org/10.1523/jneurosci.16-08-02659.1996

Gandini, M., Sandoval, A., Felix, R., 2015. Toxins Targeting Voltage-Activated Ca^{2+} Channels and their Potential Biomedical Applications. Curr. Top. Med. Chem. 15, 604–616. https://doi.org/10.2174/1568026615666150225112605

Gao, T., Yatani, A., Dell'Acqua, M.L., Sako, H., Green, S.A., Dascal, N., Scott, J.D., Hosey, M.M., 1997. cAMP-dependent regulation of cardiac L-type Ca2+ channels requires membrane targeting of PKA and phosphorylation of channel subunits. Neuron 19, 185–196. https://doi.org/10.1016/S0896-6273(00)80358-X

Gao, Z.-G., Balasubramanian, R., Kiselev, E., Wei, Q., Jacobson, K.A., 2014. Probing biased/partial agonism at the G protein-coupled A2B adenosine receptor. Biochem. Pharmacol. 90, 297–306. https://doi.org/10.1016/j.bcp.2014.05.008

Gao, Z., Chen, T., Weber, M.J., Linden, J., 1999. A(2B) adenosine and P2Y2 receptors stimulate mitogen-activated protein kinase in human embryonic kidney-293 cells: Cross-talk between cyclic AMP and protein kinase C pathways. J. Biol. Chem. 274, 5972–5980. https://doi.org/10.1074/jbc.274.9.5972

Gard, A.L., Pfeiffer, S.E., 1990. Two proliferative stages of the oligodendrocyte lineage

(A2B5+O4- and O4+GaIC-) under different mitogenic control. Neuron 5, 615–625. https://doi.org/10.1016/0896-6273(90)90216-3

Gassowska, M., Cieslik, M., Wilkaniec, A., Strosznajder, J.B., 2014. Sphingosine kinases/sphingosine-1-phosphate and death signalling in APP-transfected cells. Neurochem. Res. 39, 645–652. https://doi.org/10.1007/s11064-014-1240-3

Gautier, H.O.B., Evans, K.A., Volbracht, K., James, R., Sitnikov, S., Lundgaard, I., James, F., Lao-Peregrin, C., Reynolds, R., Franklin, R.J.M., Káradóttir, R.T., 2015. Neuronal activity regulates remyelination via glutamate signalling to oligodendrocyte progenitors. Nat. Commun. 6, 1–15. https://doi.org/10.1038/ncomms9518

Gelderd, J.B., Chopin, S.F., 1977. The vertebral level of origin of spinal nerves in the rat. Anat. Rec. 188, 45–47. https://doi.org/10.1002/ar.1091880106

Gemes, G., Koopmeiners, A., Rigaud, M., Lirk, P., Sapunar, D., Bangaru, M.L., Vilceanu, D., Garrison, S.R., Ljubkovic, M., Mueller, S.J., Stucky, C.L., Hogan, Q.H., 2013. Failure of action potential propagation in sensory neurons: Mechanisms and loss of afferent filtering in C-type units after painful nerve injury. J. Physiol. 591, 1111–1131. https://doi.org/10.1113/jphysiol.2012.242750

Giocomo, L.M., Hasselmo, M.E., 2007. Neuromodulation by glutamate and acetylcholine can change circuit dynamics by regulating the relative influence of afferent input and excitatory feedback. Mol. Neurobiol. https://doi.org/10.1007/s12035-007-0032-z

Glickman, M., Malek, R.L., Kwitek-Black, A.E., Jacob, H.J., Lee, N.H., 1999. Molecular cloning, tissue-specific expression, and chromosomal localization of a novel nerve growth factor-regulated G-protein-coupled receptor, nrg-1. Mol. Cell. Neurosci. 14, 141–152. https://doi.org/10.1006/mcne.1999.0776

Gold, M.S., Weinreich, D., Kim, C.S., Wang, R., Treanor, J., Porreca, F., Lai, J., 2003. Redistribution of Nav1.8 in uninjured axons enables neuropathic pain. J. Neurosci. 23, 158–166. https://doi.org/10.1523/jneurosci.23-01-00158.2003

Goldberg, D.S., McGee, S.J., 2011. Pain as a global public health priority. BMC Public Health 11, 770. https://doi.org/10.1186/1471-2458-11-770

Goldin, A.L., 2001. Resurgence of sodium channel research. Annu. Rev. Physiol. https://doi.org/10.1146/annurev.physiol.63.1.871

Gomes, C., Ferreira, R., George, J., Sanches, R., Rodrigues, D.I., Gonçalves, N., Cunha, R.A., 2013. Activation of microglial cells triggers a release of brain-derived neurotrophic factor (BDNF) inducing their proliferation in an adenosine A2A receptor-dependent manner: A2A receptor blockade prevents BDNF release and proliferation of microglia. J. Neuroinflammation 10, 780. https://doi.org/10.1186/1742-2094-10-16

Gonçalves, F.Q., Pires, J., Pliassova, A., Beleza, R., Lemos, C., Marques, J.M., Rodrigues, R.J., Canas, P.M., Köfalvi, A., Cunha, R.A., Rial, D., 2015. Adenosine A(2b) receptors control A(1) receptor-mediated inhibition of synaptic transmission in the mouse hippocampus. Eur. J. Neurosci. 41. https://doi.org/10.1111/ejn.12851

Gonçalves, M.L., Cunha, R.A., Ribeiro, J.A., 1997. Adenosine A(2A) receptors facilitate 45Ca2+ uptake through class A calcium channels in rat hippocampal CA3 but not CA1 synaptosomes. Neurosci. Lett. 238, 73–77. https://doi.org/10.1016/S0304-3940(97)00803-3

Gonda, K., Okamoto, H., Takuwa, N., Yatomi, Y., Okazaki, H., Sakurai, T., Kimura, S., Sillard, R., Harii, K., Takuwa, Y., 1999. The novel sphingosine 1-phosphate receptor AGR16 is coupled via pertussis toxin-sensitive and -insensitive G-proteins to multiple signalling pathways. Biochem. J. 337, 67–75. https://doi.org/10.1042/0264-6021:3370067

González-Fernández, E., Sánchez-Gómez, M.V., Pérez-Samartín, A., Arellano, R.O., Matute, C., 2014. A3 Adenosine receptors mediate oligodendrocyte death and ischemic damage to optic nerve. Glia 62, 199–216. https://doi.org/10.1002/glia.22599

González, C., Baez-Nieto, D., Valencia, I., Oyarzún, I., Rojas, P., Naranjo, D., Latorre, R., 2012. K+ channels: Function-structural overview. Compr. Physiol. 2, 2087–2149. https://doi.org/10.1002/cphy.c110047

Gorry, J.D., 1963. Studies on the comparative anatomy of the ganglion basale of Meynert. Acta Anat. (Basel). 55, 51–104. https://doi.org/10.1159/000142464

Gräler, M.H., Bernhardt, G., Lipp, M., 1998. EDG6, a novel G-protein-coupled receptor related

to receptors for bioactive lysophospholipids, is specifically expressed in lymphoid tissue. Genomics 53, 164–169. https://doi.org/10.1006/geno.1998.5491

Grassi, S., Giussani, P., Prioni, S., Button, D., Cao, J., Hakimi, I., Sarmiere, P., Srinivas, M., Cabitta, L., Sonnino, S., Prinetti, A., 2019. Human Remyelination Promoting Antibody Stimulates Astrocytes Proliferation Through Modulation of the Sphingolipid Rheostat in Primary Rat Mixed Glial Cultures. Neurochem. Res. 44, 1460–1474. https://doi.org/10.1007/s11064-018-2701-x

Gratwicke, J., Kahan, J., Zrinzo, L., Hariz, M., Limousin, P., Foltynie, T., Jahanshahi, M., 2013. The nucleus basalis of Meynert: A new target for deep brain stimulation in dementia? Neurosci. Biobehav. Rev. https://doi.org/10.1016/j.neubiorev.2013.09.003

Greene, R.W., Haas, H.L., 1991. The electrophysiology of adenosine in the mammalian central nervous system. Prog. Neurobiol. https://doi.org/10.1016/0301-0082(91)90005-L

Gremo, F., Palomba, M., Marchisio, A.M., Marcello, C., Mulas, M.L., Torelli, S., 1987. Heterogeneity of muscarinic cholinergic receptors in the developing human fetal brain: regional distribution and characterization. Early Hum. Dev. 15, 165–177. https://doi.org/10.1016/0378-3782(87)90004-1

Grissmer, S., Nguyen, A.N., Aiyar, J., Hanson, D.C., Mather, R.J., Gutman, G.A., Karmilowicz, M.J., Auperin, D.D., Chandy, K.G., 1994. Pharmacological characterization of five cloned voltage-gated K+ channels, types Kv1.1, 1.2, 1.3, 1.5, and 3.1, stably expressed in mammalian cell lines. Mol. Pharmacol. 45.

Gritti, I., Mainville, L., Jones, B.E., 1994. Projections of GABAergic and cholinergic basal forebrain and GABAergic preoptic-anterior hypothalamic neurons to the posterior lateral hypothalamus of the rat. J. Comp. Neurol. 339, 251–268. https://doi.org/10.1002/cne.903390206

Gross, R.A., Macdonald, R.L., Ryan-Jastrow, T., 1989. 2-Chloroadenosine reduces the N calcium current of cultured mouse sensory neurones in a pertussis toxin-sensitive manner. J. Physiol. 411, 585–95.

Grothe, M.J., Barthel, H., Sepulcre, J., Dyrba, M., Sabri, O., Teipel, S.J., 2017. In vivo staging of regional amyloid deposition. Neurology 89, 2031–2038. https://doi.org/10.1212/WNL.0000000000004643

Guarnieri, G., Sarchielli, E., Vannelli, G., Morelli, A., 2018. Cell-based therapy in Alzheimer's disease: Can human fetal cholinergic neurons "untangle the skein"? Neural Regen. Res. 13, 2105. https://doi.org/10.4103/1673-5374.241459

Gubitz, A.K., Widdowson, L., Kurokawa, M., Kirkpatrick, K.A., Richardson, P.J., 1996. Dual signalling by the adenosine A2a receptor involves activation of both N- and P-type calcium channels by different G proteins and protein kinases in the same striatal nerve terminals. J. Neurochem. 67, 374–381. https://doi.org/10.1046/j.1471-4159.1996.67010374.x

Gulledge, A.T., Park, S.B., Kawaguchi, Y., Stuart, G.J., 2007. Heterogeneity of phasic cholinergic signaling in neocortical neurons. J. Neurophysiol. 97, 2215–2229. https://doi.org/10.1152/jn.00493.2006

Gutman, G.A., Chandy, K.G., Grissmer, S., Lazdunski, M., Mckinnon, D., Pardo, L.A., Robertson, G.A., Rudy, B., Sanguinetti, M.C., Stühmer, W., Wang, X., 2005. International Union of Pharmacology. LIII. Nomenclature and Molecular Relationships of Voltage-Gated Potassium Channels. Pharmacol. Rev. 57, 473–508. https://doi.org/10.1124/pr.57.4.10

Hait, N.C., Bellamy, A., Milstien, S., Kordula, T., Spiegel, S., 2007. Sphingosine kinase type 2 activation by ERK-mediated phosphorylation. J. Biol. Chem. 282, 12058–12065. https://doi.org/10.1074/jbc.M609559200

Hall, D.D., Davare, M.A., Shi, M., Allen, M.L., Weisenhaus, M., McKnight, G.S., Hell, J.W., 2007. Critical role of cAMP-dependent protein kinase anchoring to the L-type calcium channel Cav1.2 via A-kinase anchor protein 150 in neurons. Biochemistry 46, 1635–1646. https://doi.org/10.1021/bi062217x

Hammond, C., 2008. Celular and Molecular Neurophisiology, Culture.

Hampel, H., Mesulam, M.M., Cuello, A.C., Farlow, M.R., Giacobini, E., Grossberg, G.T., Khachaturian, A.S., Vergallo, A., Cavedo, E., Snyder, P.J., Khachaturian, Z.S., 2018. The

cholinergic system in the pathophysiology and treatment of Alzheimer's disease. Brain. https://doi.org/10.1093/brain/awy132

Hannon, H.E., Atchison, W.D., 2013. Omega-conotoxins as experimental tools and therapeutics in pain management. Mar. Drugs 11, 680–699. https://doi.org/10.3390/md11030680

Harada, J., Foley, M., Moskowitz, M.A., Waeber, C., 2004. Sphingosine-1-phosphate induces proliferation and morphological changes of neural progenitor cells. J. Neurochem. 88, 1026–1039. https://doi.org/10.1046/j.1471-4159.2003.02219.x

Harata, N., Tateishi, N., Akaike, N., 1991. Acetylcholine receptors in dissociated nucleus basalis of Meynert neurons of the rat. Neurosci. Lett. 130, 153–156. https://doi.org/10.1016/0304-3940(91)90385-7

Hardenacke, K., Shubina, E., Bührle, C.P., Zapf, A., Lenartz, D., Klosterkötter, J., Visser-Vandewalle, V., Kuhn, J., 2013. Deep brain stimulation as a tool for improving cognitive functioning in Alzheimer's dementia: A systematic review. Front. Psychiatry. https://doi.org/10.3389/fpsyt.2013.00159

Harding, L.M., Beadle, D.J., Bermudez, I., 1999. Voltage-dependent calcium channel subtypes controlling somatic substance P release in the peripheral nervous system. Prog. Neuro-Psychopharmacology Biol. Psychiatry 23, 1103–1112. https://doi.org/10.1016/S0278-5846(99)00049-4

Harms, H.H., Wardeh, G., Mulder, A.H., 1979. Effects of adenosine on depolarization-induced release of various radiolabelled neurotransmitters from slices of rat corpus striatum. Neuropharmacology 18, 577–580. https://doi.org/10.1016/0028-3908(79)90107-2

Harms, H.H., Wardeh, G., Mulder, A.H., 1978. Adenosine modulates depolarization-induced release of 3H-noradrenaline from slices of rat brain neocortex. Eur. J. Pharmacol. 49, 305–308. https://doi.org/10.1016/0014-2999(78)90107-3

Harper, A.A., Lawson, S.N., 1985. Conduction velocity is related to morphological cell type in rat dorsal root ganglion neurones. J. Physiol. 359, 31–46. https://doi.org/10.1113/jphysiol.1985.sp015573

Hart, M.L., Jacobi, B., Schittenhelm, J., Henn, M., Eltzschig, H.K., 2009. Cutting Edge: A2B Adenosine Receptor Signaling Provides Potent Protection during Intestinal Ischemia/Reperfusion Injury. J. Immunol. 182, 3965–3968. https://doi.org/10.4049/jimmunol.0802193

Hasegawa, T., An, H.S., Haughton, V.M., 1993. Imaging anatomy of the lateral lumbar spinal canal. Semin. Ultrasound, CT, MRI 14, 404–413. https://doi.org/10.1016/S0887-2171(05)80034-4

Hasegawa, T., Mikawa, Y., Watanabe, R., An, H.S., 1996. Morphometric analysis of the lumbosacral nerve roots and dorsal root ganglia by magnetic resonance imaging. Spine (Phila. Pa. 1976). 21, 1005–1009. https://doi.org/10.1097/00007632-199605010-00001

Haskó, G., Csóka, B., Németh, Z.H., Vizi, E.S., Pacher, P., 2009. A2B adenosine receptors in immunity and inflammation. Trends Immunol. https://doi.org/10.1016/j.it.2009.04.001

Haskó, G., Linden, J., Cronstein, B., Pacher, P., 2008. Adenosine receptors: Therapeutic aspects for inflammatory and immune diseases. Nat. Rev. Drug Discov. https://doi.org/10.1038/nrd2638

Haydon, P.G., 2001. Glia: Listening and talking to the synapse. Nat. Rev. Neurosci. 2, 185–193. https://doi.org/10.1038/35058528

He, X., Huang, Y., Li, B., Gong, C.X., Schuchman, E.H., 2010. Deregulation of sphingolipid metabolism in Alzheimer's disease. Neurobiol. Aging 31, 398–408. https://doi.org/10.1016/j.neurobiolaging.2008.05.010

Heath, C.J., Picciotto, M.R., 2009. Nicotine-induced plasticity during development: Modulation of the cholinergic system and long-term consequences for circuits involved in attention and sensory processing. Neuropharmacology. https://doi.org/10.1016/j.neuropharm.2008.07.020

Hedrick, T., Waters, J., 2010. Physiological Properties of Cholinergic and Non-Cholinergic Magnocellular Neurons in Acute Slices from Adult Mouse Nucleus Basalis. PLoS One 5, e11046. https://doi.org/10.1371/journal.pone.0011046

Heinemann, S.H., Terlau, H., Imoto, K., 1992a. Molecular basis for pharmacological

differences between brain and cardiac sodium channels. Pflügers Arch. Eur. J. Physiol. 422, 90–92. https://doi.org/10.1007/BF00381519

Heinemann, S.H., Terlau, H., Stühmer, W., Imoto, K., Numa, S., 1992b. Calcium channel characteristics conferred on the sodium channel by single mutations. Nature 356, 441–443. https://doi.org/10.1038/356441a0

Heinke, B., Balzer, E., Sandkühler, J., 2004. Pre- and postsynaptic contributions of voltage-dependent Ca2+ channels to nociceptive transmission in rat spinal lamina I neurons. Eur. J. Neurosci. 19, 103–11.

Hellström-Lindahl, E., Gorbounova, O., Seiger, Å., Mousavi, M., Nordberg, A., 1998. Regional distribution of nicotinic receptors during prenatal development of human brain and spinal cord. Dev. Brain Res. 108, 147–160. https://doi.org/10.1016/S0165-3806(98)00046-7

Heneghan, J.F., Mitra-Ganguli, T., Stanish, L.F., Liu, L., Zhao, R., Rittenhouse, A.R., 2009. The Ca2+ channel β subunit determines whether stimulation of Gq-coupled receptors enhances or inhibits N current. J. Gen. Physiol. 134, 369–384. https://doi.org/10.1085/jgp.200910203

Hettinger, B.D., Lee, A., Linden, J., Rosin, D.L., 2001. Ultrastructural localization of adenosine A2A receptors suggests multiple cellular sites for modulation of GABAergic neurons in rat striatum. J. Comp. Neurol. 431, 331–346. https://doi.org/10.1002/1096-9861(20010312)431:3<331::AID-CNE1074>3.0.CO;2-W

Hibino, H., Fujita, A., Iwai, K., Yamada, M., Kurachi, Y., 2004. Differential assembly of inwardly rectifying K+ channel subunits, Kir4.1 and Kir5.1, in brain astrocytes. J. Biol. Chem. 279, 44065–44073. https://doi.org/10.1074/jbc.M405985200

Hibino, H., Inanobe, A., Furutani, K., Murakami, S., Findlay, I., Kurachi, Y., 2010. Inwardly rectifying potassium channels: Their structure, function, and physiological roles. Physiol. Rev. https://doi.org/10.1152/physrev.00021.2009

Hodgkin, A.L., Huxley, A.F., 1952a. A quantitative description of membrane current and its application to conduction and excitation in nerve. J. Physiol. 117, 500–544. https://doi.org/10.1113/jphysiol.1952.sp004764

Hodgkin, A.L., Huxley, A.F., 1952b. Currents carried by sodium and potassium ions through the membrane of the giant axon of Loligo. J. Physiol. 116, 449–472. https://doi.org/10.1113/jphysiol.1952.sp004717

Hoffman, D.A., Magee, J.C., Colbert, C.M., Johnston, D., 1997. K+ channel regulation of signal propagation in dendrites of hippocampal pyramidal neurons. Nature 387, 869–875. https://doi.org/10.1038/43119

Hofmann, F., Biel, M., Flockerzi, V., 1994. Molecular basis for Ca2+ channel diversity. Annu. Rev. Neurosci. https://doi.org/10.1146/annurev.ne.17.030194.002151

Hogan, Q., Lirk, P., Poroli, M., Rigaud, M., Fuchs, A., Fillip, P., Ljubkovic, M., Gemes, G., Sapunar, D., 2008. Restoration of calcium influx corrects membrane hyperexcitability in injured rat dorsal root ganglion neurons. Anesth. Analg. 107, 1045–1051. https://doi.org/10.1213/ane.0b013e31817bd1f0

Hollingsworth, E.B., Mcneal, E.T., Burton, J.L., Williams, R.J., Daly, J.W., Creveling, C.R., 1985. Biochemical characterization of a filtered synaptoneurosome preparation from guinea pig cerebral cortex: Cyclic adenosine 3′:5′-monophosphate-generating systems, receptors, and enzymes. J. Neurosci. 5, 2240–2253. https://doi.org/10.1523/jneurosci.05-08-02240.1985

Holz IV, G.G., Dunlap, K., Kream, R.M., 1988. Characterization of the electrically evoked release of substance P from dorsal root ganglion neurons: Methods and dihydropyridine sensitivity. J. Neurosci. 8, 463–471. https://doi.org/10.1523/jneurosci.08-02-00463.1988

Honoré, E., 2007. The neuronal background K2P channels: Focus on TREK1. Nat. Rev. Neurosci. https://doi.org/10.1038/nrn2117

Horst, N.K., Heath, C.J., Neugebauer, N.M., Kimchi, E.Y., Laubach, M., Picciotto, M.R., 2012. Impaired auditory discrimination learning following perinatal nicotine exposure or β2 nicotinic acetylcholine receptor subunit deletion. Behav. Brain Res. 231, 170–180. https://doi.org/10.1016/j.bbr.2012.03.002

Howe, C.L., Bieber, A.J., Warrington, A.E., Pease, L.R., Rodriguez, M., 2004. Antiapoptotic

signaling by a remyelination-promoting human antimyelin antibody. Neurobiol. Dis. 15, 120–131. https://doi.org/10.1016/j.nbd.2003.09.002

Hsieh, C.Y., Leslie, F.M., Metherate, R., 2002. Nicotine exposure during a postnatal critical period alters NR2A and NR2B mRNA expression in rat auditory forebrain. Dev. Brain Res. 133, 19–25. https://doi.org/10.1016/S0165-3806(01)00314-5

Hu, H., Shao, L.R., Chavoshy, S., Gu, N., Trieb, M., Behrens, R., Laake, P., Pongs, O., Knaus, H.G., Ottersen, O.P., Storm, J.F., 2001. Presynaptic Ca2+-activated K+channels in glutamatergic hippocampal terminals and their role in spike repolarization and regulation of transmitter release. J. Neurosci. 21, 9585–9597. https://doi.org/10.1523/jneurosci.21-24-09585.2001

Hu, L.Y., Ryder, T.R., Rafferty, M.F., Dooley, D.J., Geer, J.J., Lotarski, S.M., Miljanich, G.P., Millerman, E., Rock, D.M., Stoehr, S.J., Szoke, B.G., Taylor, C.P., Vartanian, M.G., 1999. Structure-activity relationship of N-methyl-N-aralkylpeptidylamines as novel N-type calcium channel blockers. Bioorganic Med. Chem. Lett. 9, 2151–2156. https://doi.org/10.1016/S0960-894X(99)00359-5

Hu, X., Adebiyi, M.G., Luo, J., Sun, K., Le, T.T.T., Zhang, Y., Wu, H., Zhao, S., Karmouty-Quintana, H., Liu, H., Huang, A., Wen, Y.E., Zaika, O.L., Mamenko, M., Pochynyuk, O.M., Kellems, R.E., Eltzschig, H.K., Blackburn, M.R., Walters, E.T., Huang, D., Hu, H., Xia, Y., 2016. Sustained Elevated Adenosine via ADORA2B Promotes Chronic Pain through Neuro-immune Interaction. Cell Rep. 16, 106–119. https://doi.org/10.1016/j.celrep.2016.05.080

Huang, C.L., Feng, S., Hilgemann, D.W., 1998. Direct activation of inward rectifier potassium channels by PIP2 and its stabilization by Gβγ. Nature 391, 803–806. https://doi.org/10.1038/35882

Hutchison, A.J., Webb, R.L., Oei, H.H., Ghai, G.R., Zimmerman, M.B., Williams, M., 1989. CGS 21680C, an A2 selective adenosine receptor agonist with preferential hypotensive activity. J. Pharmacol. Exp. Ther. 251.

Ibrahim, N., Bosch, M.A., Smart, J.L., Qiu, J., Rubinstein, M., Rønnekleiv, O.K., Low, M.J., Kelly, M.J., 2003. Hypothalamic Proopiomelanocortin Neurons Are Glucose Responsive and Express K $_{ATP}$ Channels. Endocrinology 144, 1331–1340. https://doi.org/10.1210/en.2002-221033

Ilyaskina, O.S., Lemoine, H., Bünemann, M., 2018. Lifetime of muscarinic receptor–G-protein complexes determines coupling efficiency and G-protein subtype selectivity. Proc. Natl. Acad. Sci. U. S. A. 115, 5016–5021. https://doi.org/10.1073/pnas.1715751115

Im, D.S., Ungar, A.R., Lynch, K.R., 2000. Characterization of a zebrafish (Danio rerio) sphingosine 1-phosphate receptor expressed in the embryonic brain. Biochem. Biophys. Res. Commun. 279, 139–143. https://doi.org/10.1006/bbrc.2000.3933

Imeri, F., Schwalm, S., Lyck, R., Zivkovic, A., Stark, H., Engelhardt, B., Pfeilschifter, J., Huwiler, A., 2016. Sphingosine kinase 2 deficient mice exhibit reduced experimental autoimmune encephalomyelitis: Resistance to FTY720 but not ST-968 treatments. Neuropharmacology 105, 341–350. https://doi.org/10.1016/j.neuropharm.2016.01.031

Ingwersen, J., Wingerath, B., Graf, J., Lepka, K., Hofrichter, M., Schröter, F., Wedekind, F., Bauer, A., Schrader, J., Hartung, H.P., Prozorovski, T., Aktas, O., 2016. Dual roles of the adenosine A2a receptor in autoimmune neuroinflammation. J. Neuroinflammation 13, 48. https://doi.org/10.1186/s12974-016-0512-z

Ishikawa, K., Tanaka, M., Black, J.A., Waxman, S.G., 1999. Changes in expression of voltage-gated potassium channels in dorsal root ganglion neurons following axotomy. Muscle and Nerve 22, 502–507. https://doi.org/10.1002/(SICI)1097-4598(199904)22:4<502::AID-MUS12>3.0.CO;2-K

Jacobson, K., Chemistry, M.J.-E.J. of M., 1997, U., 1997. Purinergic approaches in experimental therapeutics. Eur. J. Med. Chem. 32, 842. https://doi.org/10.1016/s0223-5234(97)82766-3

Jacobson, K.A., Merighi, S., Varani, K., Borea, P.A., Baraldi, S., Aghazadeh Tabrizi, M., Romagnoli, R., Baraldi, P.G., Ciancetta, A., Tosh, D.K., Gao, Z.G., Gessi, S., 2018. A3 Adenosine Receptors as Modulators of Inflammation: From Medicinal Chemistry to Therapy. Med. Res. Rev. https://doi.org/10.1002/med.21456

Jaillard, C., Harrison, S., Stankoff, B., Aigrot, M.S., Calver, A.R., Duddy, G., Walsh, F.S., Pangalos, M.N., Arimura, N., Kaibuchi, K., Zalc, B., Lubetzki, C., 2005. Edg8/S1P5: An oligodendroglial receptor with dual function on process retraction and cell survival. J. Neurosci. 25, 1459–1469. https://doi.org/10.1523/JNEUROSCI.4645-04.2005

Jain, K.K., 2000. An evaluation of intrathecal ziconotide for the treatment of chronic pain. Expert Opin. Investig. Drugs 9, 2403–2410. https://doi.org/10.1517/13543784.9.10.2403

Janes, K., Esposito, E., Doyle, T., Cuzzocrea, S., Tosh, D.K., Jacobson, K.A., Salvemini, D., 2014. A3 adenosine receptor agonist prevents the development of paclitaxel-induced neuropathic pain by modulating spinal glial-restricted redox-dependent signaling pathways. Pain 155, 2560–2567. https://doi.org/10.1016/j.pain.2014.09.016

Janes, K., Symons-Liguori, A.M., Jacobson, K.A., Salvemini, D., 2016. Identification of A3 adenosine receptor agonists as novel non-narcotic analgesics. Br. J. Pharmacol. 173, 1253–67. https://doi.org/10.1111/bph.13446

Janes, K., Wahlman, C., Little, J.W., Doyle, T., Tosh, D.K., Jacobson, K.A., Salvemini, D., 2015. Spinal neuroimmune activation is independent of T-cell infiltration and attenuated by A3 adenosine receptor agonists in a model of oxaliplatin-induced peripheral neuropathy. Brain. Behav. Immun. 44, 91–99. https://doi.org/10.1016/j.bbi.2014.08.010

Jarvis, M.F., Schulz, R., Hutchison, A.J., Do, U.H., Sills, M.A., Williams, M., 1989. [3H]CGS 21680, a selective A2 adenosine receptor agonist directly labels A2 receptors in rat brain. J. Pharmacol. Exp. Ther. 251, 888–893.

Jelacic, T.M., Kennedy, M.E., Wickman, K., Clapham, D.E., 2000. Functional and biochemical evidence for G-protein-gated inwardly rectifying K+ (GIRK) channels composed of GIRK2 and GIRK3. J. Biol. Chem. 275, 36211–36216. https://doi.org/10.1074/jbc.M007087200

Jensen, B.S., Hertz, M., Christophersen, P., Madsen, L.S., 2002. The Ca2+-activated K+ channel of intermediate conductance: A possible target for immune suppression. Expert Opin. Ther. Targets. https://doi.org/10.1517/14728222.6.6.623

Jeong, L.S., Jin, D.Z., Kim, H.O., Shin, D.H., Moon, H.R., Gunaga, P., Chun, M.W., Kim, Y.C., Melman, N., Gao, Z.G., Jacobson, K.A., 2003. N6-substituted D-4′-thioadenosine-5′-methyluronamides: Potent and selective agonists at the human A3 adenosine receptor. J. Med. Chem. 46, 3775–3777. https://doi.org/10.1021/jm034098e

Ji, X.-D., Lubitz, D. Von, Olah, M.E., Stiles, G.L., Jacobson, K.A., 1994. Species differences in ligand affinity at central A3-adenosine receptors. Drug Dev. Res. 33, 51–59. https://doi.org/10.1002/ddr.430330109

Ji, X.D., Kim, Y.C., Ahern, D.G., Linden, J., Jacobson, K.A., 2001. [3H]MRS 1754, a selective antagonist radioligand for A2B adenosine receptors. Biochem. Pharmacol. 61, 657–663. https://doi.org/10.1016/S0006-2952(01)00531-7

John, S.A., Weiss, J.N., Xie, L.H., Ribalet, B., 2003. Molecular mechanism for ATP-dependent closure of the K+ channel Kir6.2. J. Physiol. 552, 23–34. https://doi.org/10.1113/jphysiol.2003.048843

Jones, C.K., Byun, N., Bubser, M., 2012. Muscarinic and nicotinic acetylcholine receptor agonists and allosteric modulators for the treatment of schizophrenia. Neuropsychopharmacology. https://doi.org/10.1038/npp.2011.199

Joshi, S.K., Mikusa, J.P., Hernandez, G., Baker, S., Shieh, C.C., Neelands, T., Zhang, X.F., Niforatos, W., Kage, K., Han, P., Krafte, D., Faltynek, C., Sullivan, J.P., Jarvis, M.F., Honore, P., 2006. Involvement of the TTX-resistant sodium channel Nav 1.8 in inflammatory and neuropathic, but not post-operative, pain states. Pain 123, 75–82. https://doi.org/10.1016/j.pain.2006.02.011

Jung, C.G., Kim, H.J., Miron, V.E., Cook, S., Kennedy, T.E., Foster, C.A., Antel, J.P., Soliven, B., 2007. Functional consequences of S1P receptor modulation in rat oligodendroglial lineage cells. Glia 55, 1656–1667. https://doi.org/10.1002/glia.20576

Jung, M., Sommer, I., Schachner, M., Nave, K.A., 1996. Monoclonal antibody O10 defines a conformationally sensitive cell- surface epitope of proteolipid protein (PLP): Evidence that PLP misfolding underlies dysmyelination in mutant mice. J. Neurosci. 16, 7920–7929. https://doi.org/10.1523/jneurosci.16-24-07920.1996

Jurewicz, A., Matysiak, M., Andrzejak, S., Selmaj, K., 2006. TRAIL-induced death of human

adult oligodendrocytes is mediated by JNK pathway. Glia 53, 158–166. https://doi.org/10.1002/glia.20249

Kajander, K.C., Wakisaka, S., Bennett, G.J., 1992. Spontaneous discharge originates in the dorsal root ganglion at the onset of a painful peripheral neuropathy in the rat. Neurosci. Lett. 138, 225–228. https://doi.org/10.1016/0304-3940(92)90920-3

Kalla, R. V., Zablocki, J., 2009. Progress in the discovery of selective, high affinity A2B adenosine receptor antagonists as clinical candidates. Purinergic Signal. https://doi.org/10.1007/s11302-008-9119-x

Kamiya, H., Zhang, W., Sima, A.A., 2006. Degeneration of the Golgi and neuronal loss in dorsal root ganglia in diabetic BioBreeding/Worcester rats. Diabetologia 49, 2763–2774. https://doi.org/10.1007/s00125-006-0379-0

Kamp, T.J., Hell, J.W., 2000. Regulation of cardiac L-type calcium channels by protein kinase A and protein kinase C. Circ. Res. https://doi.org/10.1161/01.RES.87.12.1095

Kan, H.W., Chang, C.H., Lin, C.L., Lee, Y.C., Hsieh, S.T., Hsieh, Y.L., 2018. Downregulation of adenosine and adenosine A1 receptor contributes to neuropathic pain in resiniferatoxin neuropathy. Pain 159, 1580–1591. https://doi.org/10.1097/j.pain.0000000000001246

Kanjhan, R., Coulson, E.J., Adams, D.J., Bellingham, M.C., 2005. Tertiapin-Q blocks recombinant and native large conductance K+ channels in a use-dependent manner. J. Pharmacol. Exp. Ther. 314, 1353–1361. https://doi.org/10.1124/jpet.105.085928

Kaplan, M.R., Cho, M.H., Ullian, E.M., Isom, L.L., Levinson, S.R., Barres, B.A., 2001. Differential control of clustering of the sodium channels Nav1.2 and Nav1.6 at developing CNS nodes of Ranvier. Neuron 30, 105–119. https://doi.org/10.1016/S0896-6273(01)00266-5

Káradóttir, R., Hamilton, N.B., Bakiri, Y., Attwell, D., 2008. Spiking and nonspiking classes of oligodendrocyte precursor glia in CNS white matter. Nat. Neurosci. 11, 450–456. https://doi.org/10.1038/nn2060

Kataoka, H., Sugahara, K., Shimano, K., Teshima, K., Koyama, M., Fukunari, A., Chiba, K., 2005. FTY720, Sphingosine 1-Phosphate Receptor Modulator, Ameliorates Experimental Autoimmune Encephalomyelitis by Inhibition of T Cell Infiltration, Cellular & Molecular Immunology.

Kawano, T., Zoga, V., McCallum, J.B., Wu, H.E., Gemes, G., Liang, M.Y., Abram, S., Kwok, W.M., Hogan, Q.H., Sarantopoulos, C.D., 2009. ATP-sensitive potassium currents in rat primary afferent neurons: biophysical, pharmacological properties, and alterations by painful nerve injury. Neuroscience 162, 431–443. https://doi.org/10.1016/j.neuroscience.2009.04.076

Kessey, K., Mogul, D.J., 1997. NMDA-independent LTP by adenosine A2 receptor-mediated postsynaptic AMPA potentiation in hippocampus. J. Neurophysiol. 78, 1965–1972. https://doi.org/10.1152/jn.1997.78.4.1965

Kettenmann, H., Blankenfeld, G. V., Trotter, J., 1991. Physiological Properties of Oligodendrocytes during Development. Ann. N. Y. Acad. Sci. 633, 64–77. https://doi.org/10.1111/j.1749-6632.1991.tb15596.x

Keynes, R.D., Greeff, N.G., Forster, I.C., 1992. Activation, inactivation and recovery in the sodium channels of the squid giant axon dialysed with different solutions. Philos. Trans. R. Soc. London. Ser. B Biol. Sci. 337, 471–484. https://doi.org/10.1098/rstb.1992.0122

Khateb, A., Fort, P., Williams, S., Serafin, M., Jones, B.E., Mühlethaler, M., 1997. Modulation of cholinergic nucleus basalis neurons by acetylcholine and n-methyl-d-aspartate. Neuroscience 81, 47–55. https://doi.org/10.1016/S0306-4522(97)00167-X

Kihara, Y., Maceyka, M., Spiegel, S., Chun, J., 2014. Lysophospholipid receptor nomenclature review: IUPHAR Review 8. Br. J. Pharmacol. https://doi.org/10.1111/bph.12678

Kilimann, I., Grothe, M., Heinsen, H., Alho, E.J.L., Grinberg, L., Amaro, E., Dos Santos, G.A.B., Da Silva, R.E., Mitchell, A.J., Frisoni, G.B., Bokde, A.L.W., Fellgiebel, A., Filippi, M., Hampel, H., Klöppel, S., Teipel, S.J., 2014. Subregional basal forebrain atrophy in alzheimer's disease: A multicenter study. J. Alzheimer's Dis. 40, 687–700. https://doi.org/10.3233/JAD-132345

Kim, C.S., Johnston, D., 2015. A1 adenosine receptor-mediated GIRK channels contribute to the resting conductance of CA1 neurons in the dorsal hippocampus. J. Neurophysiol.

113, 2511–2523. https://doi.org/10.1152/jn.00951.2014
Kim, H.J., Miron, V.E., Dukala, D., Proia, R.L., Ludwin, S.K., Traka, M., Antel, J.P., Soliven, B., 2011. Neurobiological effects of sphingosine 1-phosphate receptor modulation in the cuprizone model. FASEB J. 25, 1509–1518. https://doi.org/10.1096/fj.10-173203
Kim, Y.C., Ji, X.D., Melman, N., Linden, J., Jacobson, K.A., 2000. Anilide derivatives of an 8-phenylxanthine carboxylic congener are highly potent and selective antagonists at human A(2B) adenosine receptors. J. Med. Chem. 43, 1165–1172. https://doi.org/10.1021/jm990421v
Knutson, P., Ghiani, C.A., Zhou, J.M., Gallo, V., McBain, C.J., 1997. K+ channel expression and cell proliferation are regulated by intracellular sodium and membrane depolarization in oligodendrocyte progenitor cells. J. Neurosci. 17, 2669–2682. https://doi.org/10.1523/JNEUROSCI.17-08-02669.1997
Kodachi, T., Matsumoto, S., Mizuguchi, M., Osaka, H., Kanai, N., Nanba, E., Ohno, K., Yamagata, T., 2017. Severe demyelination in a patient with a late infantile form of Niemann-Pick disease type C. Neuropathology 37, 426–430. https://doi.org/10.1111/neup.12380
Kolachala, V., Asamoah, V., Wang, L., Obertone, T.S., Ziegler, T.R., Merlin, D., Sitaraman, S. V., 2005. TNF-α upregulates adenosine 2b (A2b) receptor expression and signaling in intestinal epithelial cells: A basis for A2bR overexpression in colitis. Cell. Mol. Life Sci. 62, 2647–2657. https://doi.org/10.1007/s00018-005-5328-4
Kolachala, V.L., Ruble, B.K., Vijay-Kumar, M., Wang, L., Mwangi, S., Figler, H.E., Figler, R.A., Srinivasan, S., Gewirtz, A.T., Linden, J., Merlin, D., Sitaraman, S. V, 2008. Blockade of adenosine A 2B receptors ameliorates murine colitis. Br. J. Pharmacol. 155, 127–137. https://doi.org/10.1038/bjp.2008.227
Kolliker, A., von Ebner, V., 1903. A Koelliker's Handbuch der Gewebelehre des Menschen. Nature 68, 414–414. https://doi.org/10.1038/068414a0
Kong, T., Westerman, K.A., Faigle, M., Eltzschig, H.K., Colgan, S.P., 2006. HIF-dependent induction of adenosine A2B receptor in hypoxia. FASEB J. 20, 2242–2250. https://doi.org/10.1096/fj.06-6419com
Kostopoulos, G.K., Limacher, J.J., Phillis, J.W., 1975. Action of various adenine derivatives on cerebellar Purkinje cells. Brain Res. 88, 162–165. https://doi.org/10.1016/0006-8993(75)90966-X
Kostović, I., 1986. Prenatal development of nucleus basalis complex and related fiber systems in man: A histochemical study. Neuroscience 17, 1047–1063. https://doi.org/10.1016/0306-4522(86)90077-1
Koulousakis, P., Andrade, P., Visser-Vandewalle, V., Sesia, T., 2019. The nucleus basalis of meynert and its role in deep brain stimulation for cognitive disorders: A historical perspective. J. Alzheimer's Dis. https://doi.org/10.3233/JAD-180133
Krames, E.S., 2015. The Dorsal Root Ganglion in Chronic Pain and as a Target for Neuromodulation: A Review. Neuromodulation Technol. Neural Interface 18, 24–32. https://doi.org/10.1111/ner.12247
Kull, B., Arslan, G., Nilsson, C., Owman, C., Lorenzen, A., Schwabe, U., Fredholm, B.B., 1999. Differences in the order of potency for agonists but not antagonists at human and rat adenosine A(2A) receptors. Biochem. Pharmacol. 57, 65–75. https://doi.org/10.1016/S0006-2952(98)00298-6
Kumar, R., Kumar, A., Långström, B., Darreh-Shori, T., 2017. Discovery of novel choline acetyltransferase inhibitors using structure-based virtual screening. Sci. Rep. 7, 1–17. https://doi.org/10.1038/s41598-017-16033-w
Kurachi, Y., Nakajima, T., Sugimoto, T.N., 1986. On the mechanism of activation of muscarinic K+ channels by adenosine in isolated atrial cells: involvement of GTP-binding proteins. Pflügers Arch. Eur. J. Physiol. 407, 264–274. https://doi.org/10.1007/BF00585301
Kwilasz, A.J., Ellis, A., Wieseler, J., Loram, L., Favret, J., McFadden, A., Springer, K., Falci, S., Rieger, J., Maier, S.F., Watkins, L.R., 2018. Sustained reversal of central neuropathic pain induced by a single intrathecal injection of adenosine A 2A receptor agonists. Brain. Behav. Immun. 69, 470–479. https://doi.org/10.1016/j.bbi.2018.01.005
Kwilasz, A.J., Green Fulgham, S.M., Ellis, A., Patel, H.P., Duran-Malle, J.C., Favret, J., Harvey,

L.O., Rieger, J., Maier, S.F., Watkins, L.R., 2019. A single peri-sciatic nerve administration of the adenosine 2A receptor agonist ATL313 produces long-lasting anti-allodynia and anti-inflammatory effects in male rats. Brain. Behav. Immun. 76, 116–125. https://doi.org/10.1016/j.bbi.2018.11.011

Lampert, A., Eberhardt, M., Waxman, S.G., 2014. Altered sodium channel gating as molecular basis for pain: Contribution of activation, inactivation, and resurgent currents. Handb. Exp. Pharmacol. 221, 91–110. https://doi.org/10.1007/978-3-642-41588-3_5

Latini, S., Bordoni, F., Pedata, F., Corradetti, R., 1999. Extracellular adenosine concentrations during *in vitro* ischaemia in rat hippocampal slices. Br. J. Pharmacol. 127, 729–739. https://doi.org/10.1038/sj.bjp.0702591

Latini, S., Pazzagli, M., Pepeu, G., Pedata, F., 1996. A2 adenosine receptors: Their presence and neuromodulatory role in the central nervous system. Gen. Pharmacol. https://doi.org/10.1016/0306-3623(96)00044-4

Latini, S., Pedata, F., 2001. Adenosine in the central nervous system: Release mechanisms and extracellular concentrations. J. Neurochem. https://doi.org/10.1046/j.1471-4159.2001.00607.x

Lecca, D., Trincavelli, M.L., Gelosa, P., Sironi, L., Ciana, P., Fumagalli, M., Villa, G., Verderio, C., Grumelli, C., Guerrini, U., Tremoli, E., Rosa, P., Cuboni, S., Martini, C., Buffo, A., Cimino, M., Abbracchio, M.P., 2008. The recently identified P2Y-like receptor GPR17 is a sensor of brain damage and a new target for brain repair. PLoS One 3. https://doi.org/10.1371/journal.pone.0003579

Lee, C., Ruben, P., 2009. Adaptive Tetrodotoxin-Resistance in Garter Snake Sodium Channels. undefined.

Lee, D.J., Milosevic, L., Gramer, R., Sasikumar, S., Al-Ozzi, T.M., De Vloo, P., Dallapiazza, R.F., Elias, G.J.B., Cohn, M., Kalia, S.K., Hutchison, W.D., Fasano, A., Lozano, A.M., 2020. Nucleus basalis of Meynert neuronal activity in Parkinson's disease. J. Neurosurg. 132, 574–582. https://doi.org/10.3171/2018.11.JNS182386

Lee, M., Martin-Ruiz, C., Graham, A., Court, J., Jaros, E., Perry, R., Iversen, P., Bauman, M., Perry, E., 2002. Nicotinic receptor abnormalities in the cerebellar cortex in autism. Brain 125, 1483–1495. https://doi.org/10.1093/brain/awf160

Lee, U.S., Cui, J., 2009. β subunit-specific modulations of BK channel function by a mutation associated with epilepsy and dyskinesia. J. Physiol. 587, 1481–1498. https://doi.org/10.1113/jphysiol.2009.169243

Lee, Y.-C., Chien, C.-L., Sun, C.-N., Huang, C.-L., Huang, N.-K., Chiang, M.-C., Lai, H.-L., Lin, Y.-S., Chou, S.-Y., Wang, C.-K.L., Tai, M.-H., Liao, W.-L., Lin, T.-N., Liu, F.-C., Chern, Y., 2003. Characterization of the rat A2A adenosine receptor gene: a 4.8-kb promoter-proximal DNA fragment confers selective expression in the central nervous system. Eur. J. Neurosci. 18, 1786–1796. https://doi.org/10.1046/j.1460-9568.2003.02907.x

Lehmann-Horn, F., Jurkat-Rott, K., 1999. Voltage-gated ion channels and hereditary disease. Physiol. Rev. https://doi.org/10.1152/physrev.1999.79.4.1317

Lepski, G., Maciaczyk, J., Jannes, C.E., Maciaczyk, D., Bischofberger, J., Nikkhah, G., 2011. Delayed functional maturation of human neuronal progenitor cells in vitro. Mol. Cell. Neurosci. 47, 36–44. https://doi.org/10.1016/j.mcn.2011.02.011

Levi, G., Gallo, V., Ciotti, M.T., 1986. Bipotential precursors of putative fibrous astrocytes and oligodendrocytes in rat cerebellar cultures express distinct surface features and "neuron-like" γ-aminobutyric acid transport. Proc. Natl. Acad. Sci. U. S. A. 83, 1504–1508. https://doi.org/10.1073/pnas.83.5.1504

Levine, E.S., Dreyfus, C.F., Black, I.B., Plummer, M.R., 1995. Differential effects of NGF and BDNF on voltage-gated calcium currents in embryonic basal forebrain neurons. J. Neurosci. 15, 3084–3091. https://doi.org/10.1523/jneurosci.15-04-03084.1995

Levine, J.M., Reynolds, R., Fawcett, J.W., 2001. The oligodendrocyte precursor cell in health and disease. Trends Neurosci. https://doi.org/10.1016/S0166-2236(00)01691-X

Li, M., West, J.W., Lai, Y., Scheuer, T., Catterall, W.A., 1992. Functional modulation of brain sodium channels by cAMP-dependent phosphorylation. Neuron 8, 1151–1159. https://doi.org/10.1016/0896-6273(92)90135-Z

Li, P., Zhu, S., 2011. Molecular design of new sodium channel blockers. Biochem. Biophys.

Res. Commun. 414, 321–325. https://doi.org/10.1016/j.bbrc.2011.09.052
Li, W., Gao, S.B., Lv, C.X., Wu, Y., Guo, Z.H., Ding, J.P., Xu, T., 2007. Characterization of voltage- and Ca2+-activated K+ channels in rat dorsal root ganglion neurons. J. Cell. Physiol. 212, 348–357. https://doi.org/10.1002/jcp.21007
Liao, Y., Kristiansen, A.M., Oksvold, C.P., Tuvnes, F.A., Gu, N., Rundén-Pran, E., Ruth, P., Sausbier, M., Storm, J.F., 2010. Neuronal Ca2+ - activated K+ channels limit brain infarction and promote survival. PLoS One 5. https://doi.org/10.1371/journal.pone.0015601
Lichter-Konecki, U., Mangin, J.M., Gordish-Dressman, H., Hoffman, E.P., Gallo, V., 2008. Gene expression profiling of astrocytes from hyperammonemic mice reveals altered pathways for water and potassium homeostasis in vivo. Glia 56, 365–377. https://doi.org/10.1002/glia.20624
Ligon, K.L., Kesari, S., Kitada, M., Sun, T., Arnett, H.A., Alberta, J.A., Anderson, D.J., Stiles, C.D., Rowitch, D.H., 2006. Development of NG2 neural progenitor cells requires Olig gene function. Proc. Natl. Acad. Sci. U. S. A. 103, 7853–7858. https://doi.org/10.1073/pnas.0511001103
Lin, D.H., Sterling, H., Lerea, K.M., Giebisch, G., Wang, W.H., 2002. Protein kinase C (PKC)-induced phosphorylation of ROMK1 is essential for the surface expression of ROMK1 channels. J. Biol. Chem. 277, 44278–44284. https://doi.org/10.1074/jbc.M203702200
Linden, J., Taylor, H.E., Robeva, A.S., Tucker, A.L., Stehle, J.H., Rivkees, S.A., Fink, J.S., Reppert, S.M., 1993. Molecular cloning and functional expression of a sheep A3 adenosine receptor with widespread tissue distribution. Mol. Pharmacol. 44.
Linden, J., Thai, T., Figler, H., Jin, X., Robeva, A.S., 1999. Characterization of Human A2B Adenosine Receptors: Radioligand Binding, Western Blotting, and Coupling to Gqin Human Embryonic Kidney 293 Cells and HMC-1 Mast Cells | Molecular Pharmacology. Mol. Pharmacol. 56, 705–713.
Lipscombe, D., Helton, T.D., Xu, W., 2004. L-type calcium channels: The low down. J. Neurophysiol. https://doi.org/10.1152/jn.00486.2004
Lirk, P., Poroli, M., Rigaud, M., Fuchs, A., Fillip, P., Huang, C.Y., Ljubkovic, M., Sapunar, D., Hogan, Q., 2008. Modulators of calcium influx regulate membrane excitability in rat dorsal root ganglion neurons. Anesth. Analg. 107, 673–685. https://doi.org/10.1213/ane.0b013e31817b7a73
Little, J.W., Ford, A., Symons-Liguori, A.M., Chen, Z., Janes, K., Doyle, T., Xie, J., Luongo, L., Tosh, D.K., Maione, S., Bannister, K., Dickenson, A.H., Vanderah, T.W., Porreca, F., Jacobson, K.A., Salvemini, D., 2015. Endogenous adenosine A3 receptor activation selectively alleviates persistent pain states. Brain 138, 28–35. https://doi.org/10.1093/brain/awu330
Liu, A.K.L., Chang, R.C.C., Pearce, R.K.B., Gentleman, S.M., 2015. Nucleus basalis of Meynert revisited: anatomy, history and differential involvement in Alzheimer's and Parkinson's disease. Acta Neuropathol. https://doi.org/10.1007/s00401-015-1392-5
Liu, G., Zhang, W., Guo, J., Kong, F., Zhou, S., Chen, S., Wang, Z., Zang, D., 2018. Adenosine binds predominantly to adenosine receptor A1 subtype in astrocytes and mediates an immunosuppressive effect. Brain Res. 1700, 47–55. https://doi.org/10.1016/j.brainres.2018.06.021
Liu, M.L., Zang, T., Zou, Y., Chang, J.C., Gibson, J.R., Huber, K.M., Zhang, C.L., 2013. Small molecules enable neurogenin 2 to efficiently convert human fibroblasts into cholinergic neurons. Nat. Commun. 4, 2183. https://doi.org/10.1038/ncomms3183
Liu, R., Lin, G., Xu, H., 2013. An Efficient Method for Dorsal Root Ganglia Neurons Purification with a One-Time Anti-Mitotic Reagent Treatment. PLoS One 8, 3–9. https://doi.org/10.1371/journal.pone.0060558
Liu, Y., Alahiri, M., Ulloa, B., Xie, B., Sadiq, S.A., 2018. Adenosine A2A receptor agonist ameliorates EAE and correlates with Th1 cytokine-induced blood brain barrier dysfunction via suppression of MLCK signaling pathway: Immun. Inflamm. Dis. 6, 72–80. https://doi.org/10.1002/iid3.187
Liu, Y.B., Guo, J.Z., Chiappinelli, V.A., 2007. Nicotinic receptor-mediated biphasic effect on neuronal excitability in chick lateral spiriform neurons. Neuroscience 148, 1004–1014.

https://doi.org/10.1016/j.neuroscience.2007.07.009
Liu, Z., Neff, R.A., Berg, D.K., 2006. Sequential interplay of nicotinic and GABAergic siqnaling guides neuronal development. Science (80-.). 314, 1610–1613. https://doi.org/10.1126/science.1134246
Long, S.B., Campbell, E.B., MacKinnon, R., 2005. Voltage sensor of Kv1.2: Structural basis of electromechanical coupling. Science (80-.). 309, 903–908. https://doi.org/10.1126/science.1116270
Lopatin, A.N., Makhina, E.N., Nichols, C.G., 1994. Potassium channel block by cytoplasmic polyamines as the mechanism of intrinsic rectification. Nature 372, 366–369. https://doi.org/10.1038/372366a0
Lopes, L. V., Rebola, N., Pinheiro, P.C., Richardson, P.J., Oliveira, C.R., Cunha, R.A., 2003. Adenosine A3 receptors are located in neurons of the rat hip... : NeuroReport. Neuroreport 14, 1645–1648.
Loram, L.C., Taylor, F.R., Strand, K.A., Harrison, J.A., RzasaLynn, R., Sholar, P., Rieger, J., Maier, S.F., Watkins, L.R., 2013. Intrathecal injection of adenosine 2A receptor agonists reversed neuropathic allodynia through protein kinase (PK)A/PKC signaling. Brain. Behav. Immun. 33, 112–122. https://doi.org/10.1016/j.bbi.2013.06.004
Lorenzon, N.M., Foehring, R.C., 1992. Relationship between repetitive firing and afterhyperpolarizations in human neocortical neurons. J. Neurophysiol. 67, 350–363. https://doi.org/10.1152/jn.1992.67.2.350
Lory, P., Nicole, S., Monteil, A., 2020. Neuronal Cav3 channelopathies: recent progress and perspectives. Pflugers Arch. Eur. J. Physiol. https://doi.org/10.1007/s00424-020-02429-7
Lozada, A.F., Wang, X., Gounko, N. V., Massey, K.A., Duan, J., Liu, Z., Berg, D.K., 2012. Glutamatergic synapse formation is promoted by α7-containing nicotinic acetylcholine receptors. J. Neurosci. 32, 7651–7661. https://doi.org/10.1523/JNEUROSCI.6246-11.2012
Lu, S.G., Zhang, X.L., Luo, Z.D., Gold, M.S., 2010. Persistent inflammation alters the density and distribution of voltage-activated calcium channels in subpopulations of rat cutaneous DRG neurons. Pain 151, 633–643. https://doi.org/10.1016/j.pain.2010.08.030
Lundgaard, I., Luzhynskaya, A., Stockley, J.H., Wang, Z., Evans, K.A., Swire, M., Volbracht, K., Gautier, H.O.B., Franklin, R.J.M., ffrench-Constant, C., Attwell, D., Káradóttir, R.T., 2013. Neuregulin and BDNF Induce a Switch to NMDA Receptor-Dependent Myelination by Oligodendrocytes. PLoS Biol. 11, e1001743. https://doi.org/10.1371/journal.pbio.1001743
Luongo, L., Petrelli, R., Gatta, L., Giordano, C., Guida, F., Vita, P., Franchetti, P., Grifantini, M., De Novellis, V., Cappellacci, L., Maione, S., 2012. 5′-Chloro-5′-deoxy-(±)-ENBA, a potent and selective adenosine A1 receptor agonist, alleviates neuropathic pain in mice through functional glial and microglial changes without affecting motor or cardiovascular functions. Molecules 17, 13712–13726. https://doi.org/10.3390/molecules171213712
Lynch, S.S., Cheng, C.M., Yee, J.L., 2006. Formulary Forum: Intrathecal Ziconotide for Refractory Chronic Pain. Ann. Pharmacother. 40, 1293–1300. https://doi.org/10.1345/aph.1G584
Ma, H., Cohen, S., Li, B., Tsien, R.W., 2013. Exploring the dominant role of Cav1 channels in signalling to the nucleus. Biosci. Rep. https://doi.org/10.1042/BSR20120099
MacDonald, R.L., Skerritt, J.H., Werz, M.A., 1986. Adenosine agonists reduce voltage-dependent calcium conductance of mouse sensory neurones in cell culture. J. Physiol. 370, 75–90.
Maenhaut, C., Van Sande, J., Libert, F., Abramowicz, M., Parmentier, M., Vanderhaegen, J.J., Dumont, J.E., Vassart, G., Schiffmann, S., 1990. RDC8 codes for an adenosine A2 receptor with physiological constitutive activity. Biochem. Biophys. Res. Commun. 173, 1169–1178. https://doi.org/10.1016/S0006-291X(05)80909-X
Malcangio, M., Clark, A.K., Old, E.A., 2013. Neuropathic pain and cytokines: current perspectives. J. Pain Res. 6, 803. https://doi.org/10.2147/JPR.S53660
Malek, R.L., Toman, R.E., Edsall, L.C., Wong, S., Chiu, J., Letterle, C.A., Van Brocklyn, J.R.,

Milstien, S., Spiegel, S., Lee, N.H., 2001. Nrg-1 Belongs to the Endothelial Differentiation Gene Family of G Protein-coupled Sphingosine-1-phosphate Receptors. J. Biol. Chem. 276, 5692–5699. https://doi.org/10.1074/jbc.M003964200

Malenka, R.C., 2009. Intercellular Communication in the Nervous System. Elsevier, Amsterdam.

Malerba, F., Paoletti, F., Ercole, B.B., Materazzi, S., Nassini, R., Coppi, E., Patacchini, R., Capsoni, S., Lamba, D., Cattaneo, A., 2015. Functional characterization of human ProNGF and NGF mutants: Identification of NGF P61SR100E as a "Painless" lead investigational candidate for therapeutic applications. PLoS One 10. https://doi.org/10.1371/journal.pone.0136425

Maloy, C., Janes, K., Bryant, L., Tosh, D., Jacobson, K., Salvemini, D., 2014. (336) A3 adenosine receptor agonists reverse established oxaliplatin-induced neuropathic pain through an IL-10 mediated mechanism of action in spinal cord. J. Pain 15, S60. https://doi.org/10.1016/j.jpain.2014.01.246

Mandala, S., Hajdu, R., Bergstrom, J., Quackenbush, E., Xie, J., Milligan, J., Thornton, R., Shei, G.J., Card, D., Keohane, C.A., Rosenbach, M., Hale, J., Lynch, C.L., Rupprecht, K., Parsons, W., Rosen, H., 2002. Alteration of lymphocyte trafficking by sphingosine-1-phosphate receptor agonists. Science (80-.). 296, 346–349. https://doi.org/10.1126/science.1070238

Manns, I.D., Mainville, L., Jones, B.E., 2001. Evidence for glutamate, in addition to acetylcholine and GABA, neurotransmitter synthesis in basal forebrain neurons projecting to the entorhinal cortex. Neuroscience 107, 249–263. https://doi.org/10.1016/S0306-4522(01)00302-5

Marques, S., van Bruggen, D., Vanichkina, D.P., Floriddia, E.M., Munguba, H., Väremo, L., Giacomello, S., Falcão, A.M., Meijer, M., Björklund, Å.K., Hjerling-Leffler, J., Taft, R.J., Castelo-Branco, G., 2018. Transcriptional Convergence of Oligodendrocyte Lineage Progenitors during Development. Dev. Cell 46, 504-517.e7. https://doi.org/10.1016/j.devcel.2018.07.005

Martinez-Rubio, C., Paulk, A.C., McDonald, E.J., Widge, A.S., Eskandar, E.N., 2018. Multimodal encoding of novelty, reward, and learning in the primate nucleus basalis of meynert. J. Neurosci. 38, 1942–1958. https://doi.org/10.1523/JNEUROSCI.2021-17.2017

Martire, A., Calamandrei, G., Felici, F., Scattoni, M.L., Lastoria, G., Domenici, M.R., Tebano, M.T., Popoli, P., 2007. Opposite effects of the A2A receptor agonist CGS21680 in the striatum of Huntington's disease versus wild-type mice. Neurosci. Lett. 417, 78–83. https://doi.org/10.1016/j.neulet.2007.02.034

Masino, S., Boison, D., 2013. Adenosine: A key link between metabolism and brain activity, Adenosine: A Key Link between Metabolism and Brain Activity. https://doi.org/10.1007/978-1-4614-3903-5

Matloubian, M., Lo, C.G., Cinamon, G., Lesneski, M.J., Xu, Y., Brinkmann, V., Allende, M.L., Proia, R.L., Cyster, J.G., 2004. Lymphocyte egress from thymus and peripheral lymphoid organs is dependent on S1P receptor 1. Nature 427, 355–360. https://doi.org/10.1038/nature02284

Matsuda, H., Saigusa, A., Irisawa, H., 1987. Ohmic conductance through the inwardly rectifying K channel and blocking by internal Mg2+. Nature 325, 156–159. https://doi.org/10.1038/325156a0

McCallum, J.B., Kwok, W.M., Mynlieff, M., Bosnjak, Z.J., Hogan, Q.H., 2003. Loss of T-type calcium current in sensory neurons of rats with neuropathic pain. Anesthesiology 98, 209–216. https://doi.org/10.1097/00000542-200301000-00032

McCallum, J.B., Kwok, W.M., Sapunar, D., Fuchs, A., Hogan, Q.H., 2006. Painful peripheral nerve injury decreases calcium current in axotomized sensory neurons. Anesthesiology 105, 160–168. https://doi.org/10.1097/00000542-200607000-00026

McCool, B.A., Farroni, J.S., 2001. A1 adenosine receptors inhibit multiple voltage-gated Ca2+ channel subtypes in acutely isolated rat basolateral amygdala neurons. Br. J. Pharmacol. 132, 879–888. https://doi.org/10.1038/sj.bjp.0703884

McDonough, S.I., Mintz, I.M., Bean, B.P., 1997. Alteration of P-type calcium channel gating by the spider toxin ω-Aga- IVA. Biophys. J. 72, 2117–2128. https://doi.org/10.1016/S0006-

3495(97)78854-4
McDowell, G.C., Pope, J.E., 2016. Intrathecal Ziconotide: Dosing and Administration Strategies in Patients With Refractory Chronic Pain. Neuromodulation. https://doi.org/10.1111/ner.12392
McGaughy, J., Dalley, J.W., Morrison, C.H., Everitt, B.J., Robbins, T.W., 2002. Selective behavioral and neurochemical effects of cholinergic lesions produced by intrabasalis infusions of 192 IgG-saporin on attentional performance in a five-choice serial reaction time task. J. Neurosci. 22, 1905–1913. https://doi.org/10.1523/jneurosci.22-05-01905.2002
Melani, A., Cipriani, S., Vannucchi, M.G., Nosi, D., Donati, C., Bruni, P., Giovannini, M.G., Pedata, F., 2009. Selective adenosine A2a receptor antagonism reduces JNK activation in oligodendrocytes after cerebral ischaemia. Brain 132, 1480–1495. https://doi.org/10.1093/brain/awp076
Melani, A., Corti, F., Stephan, H., Müller, C.E., Donati, C., Bruni, P., Vannucchi, M.G., Pedata, F., 2012. Ecto-ATPase inhibition: ATP and adenosine release under physiological and ischemic in vivo conditions in the rat striatum. Exp. Neurol. 233, 193–204. https://doi.org/10.1016/j.expneurol.2011.09.036
Ment, L.R., Schwartz, M., Makuch, R.W., Stewart, W.B., 1998. Association of chronic sublethal hypoxia with ventriculomegaly in the developing rat brain. Dev. Brain Res. 111, 197–203. https://doi.org/10.1016/S0165-3806(98)00139-4
Merighi, S., Bencivenni, S., Vincenzi, F., Varani, K., Borea, P.A., Gessi, S., 2017. A2B adenosine receptors stimulate IL-6 production in primary murine microglia through p38 MAPK kinase pathway. Pharmacol. Res. 117, 9–19. https://doi.org/10.1016/j.phrs.2016.11.024
Mesulam, M., 2013. Afasia Progressiva Primária: Uma Demência Da Rede De Linguagem. Dement. e Neuropsychol. https://doi.org/10.1590/S1980-57642013DN70100002
Mesulam, M. -M, Geula, C., 1988. Nucleus basalis (Ch4) and cortical cholinergic innervation in the human brain: Observations based on the distribution of acetylcholinesterase and choline acetyltransferase. J. Comp. Neurol. 275, 216–240. https://doi.org/10.1002/cne.902750205
Mesulam, M. -Marsel, Mufson, E.J., Levey, A.I., Wainer, B.H., 1983. Cholinergic innervation of cortex by the basal forebrain: Cytochemistry and cortical connections of the septal area, diagonal band nuclei, nucleus basalis (Substantia innominata), and hypothalamus in the rhesus monkey. J. Comp. Neurol. 214, 170–197. https://doi.org/10.1002/cne.902140206
Mesulam, M.M., 2013. Cholinergic circuitry of the human nucleus basalis and its fate in Alzheimer's disease. J. Comp. Neurol. https://doi.org/10.1002/cne.23415
Meyerhof, W., Müller-Brechlin, R., Richter, D., 1991. Molecular cloning of a novel putative G-protein coupled receptor expressed during rat spermiogenesis. FEBS Lett. 284, 155–160. https://doi.org/10.1016/0014-5793(91)80674-R
Mi, H., Deerinck, T.J., Jones, M., Ellisman, M.H., Schwarz, T.L., 1996. Inwardly rectifying K+ channels that may participate in K+ buffering are localized in microvilli of Schwann cells. J. Neurosci. 16, 2421–2429. https://doi.org/10.1523/jneurosci.16-08-02421.1996
Michaelis, M.L., Michaelis, E.K., Myers, S.L., 1979. Adenosine modulation of synaptosomal dopamine release. Life Sci. 24, 2083–2092. https://doi.org/10.1016/0024-3205(79)90082-1
Miki, T., Liss, B., Minami, K., Shiuchi, T., Saraya, A., Kashima, Y., Horiuchi, M., Ashcroft, F., Minokoshi, Y., Roeper, J., Seino, S., 2001. ATP-sensitive K+ channels in the hypothalamus are essential for the maintenance of glucose homeostasis. Nat. Neurosci. 4, 507–512. https://doi.org/10.1038/87455
Miledi, R., Molinoff, P., Potter, L.T., 1971. Biological sciences: Isolation of the cholinergic receptor protein of Torpedo electric tissue. Nature 229, 554–557. https://doi.org/10.1038/229554a0
Mills, J.H., Alabanza, L.M., Mahamed, D.A., Bynoe, M.S., 2012. Extracellular adenosine signaling induces CX3CL1 expression in the brain to promote experimental autoimmune encephalomyelitis. J. Neuroinflammation 9. https://doi.org/10.1186/1742-2094-9-193
Mirabet, M., Mallol, J., Lluis, C., Franco, R., 1997. Calcium mobilization in Jurkat cells via A(2b) adenosine receptors. Br. J. Pharmacol. 122, 1075–1082.

https://doi.org/10.1038/sj.bjp.0701495
Miron, V.E., Schubart, A., Antel, J.P., 2008. Central nervous system-directed effects of FTY720 (fingolimod). J. Neurol. Sci. 274, 13–17. https://doi.org/10.1016/j.jns.2008.06.031
Mizugishi, K., Yamashita, T., Olivera, A., Miller, G.F., Spiegel, S., Proia, R.L., 2005. Essential Role for Sphingosine Kinases in Neural and Vascular Development. Mol. Cell. Biol. 25, 11113–11121. https://doi.org/10.1128/mcb.25.24.11113-11121.2005
Mlinar, B., Biagi, B.A., Enyeart, J.J., 1995. Losartan-sensitive AII receptors linked to depolarization-dependent cortisol secretion through a novel signaling pathway. J. Biol. Chem. 270, 20942–20951. https://doi.org/10.1074/jbc.270.36.20942
Mo, Z., Moore, A.R., Filipovic, R., Ogawa, Y., Kazuhiro, I., Antic, S.D., Zecevic, N., 2007. Human cortical neurons originate from radial glia and neuron-restricted progenitors. J. Neurosci. 27, 4132–4145. https://doi.org/10.1523/JNEUROSCI.0111-07.2007
Mogul, D.J., Adams, M.E., Fox, A.P., 1993. Differential activation of adenosine receptors decreases N-type but potentiates P-type Ca2+ current in hippocampal CA3 neurons. Neuron 10, 327–334. https://doi.org/10.1016/0896-6273(93)90322-I
Mongan, L.C., Hill, M.J., Chen, M.X., Tate, S.N., Collins, S.D., Buckby, L., Grubb, B.D., 2005. The distribution of small and intermediate conductance calcium-activated potassium channels in the rat sensory nervous system. Neuroscience 131, 161–175. https://doi.org/10.1016/j.neuroscience.2004.09.062
Moreau, J.L., Huber, G., 1999. Central adenosine A(2A) receptors: An overview. Brain Res. Rev. https://doi.org/10.1016/S0165-0173(99)00059-4
Morelli, A., Sarchielli, E., Guarnieri, G., Coppi, E., Pantano, D., Comeglio, P., Nardiello, P., Pugliese, A.M., Ballerini, L., Matucci, R., Ambrosini, S., Castronovo, G., Valente, R., Mazzanti, B., Bucciantini, S., Maggi, M., Casamenti, F., Gallina, P., Vannelli, G.B., 2017. Young human cholinergic neurons respond to physiological regulators and improve cognitive symptoms in an animal model of Alzheimer's disease. Front. Cell. Neurosci. 11. https://doi.org/10.3389/fncel.2017.00339
Morishita, H., Miwa, J.M., Heintz, N., Hensch, T.K., 2010. Lynx1, a cholinergic brake, limits plasticity in adult visual cortex. Science (80-.). 330, 1238–1240. https://doi.org/10.1126/science.1195320
Mtui, E., 2016. Clinical neuroanatomy and neuroscience, 7th ed. ed. Elsevier, Philadelphia PA. https://doi.org/10.1128/AAC.03728-14
Mufson, E.J., Deecher, D.C., Basile, M., Izenwasse, S., Mash, D.C., 2000. Galanin receptor plasticity within the nucleus basalis in early and late Alzheimer's disease: An in vitro autoradiographic analysis. Neuropharmacology 39, 1404–1412. https://doi.org/10.1016/S0028-3908(00)00011-3
Muneoka, K., Ogawa, T., Kamei, K., Mimura, Y., Kato, H., Takigawa, M., 2001. Nicotine exposure during pregnancy is a factor which influences serotonin transporter density in the rat brain. Eur. J. Pharmacol. 411, 279–282. https://doi.org/10.1016/S0014-2999(00)00925-0
Myat, L.O., Thangada, S., Wu, M.T., Liu, C.H., Macdonald, T.L., Lynch, K.R., Lin, C.Y., Hla, T., 2007. Immunosuppressive and anti-angiogenic sphingosine 1-phosphate receptor-1 agonists induce ubiquitinylation and proteasomal degradation of the receptor. J. Biol. Chem. 282, 9082–9089. https://doi.org/10.1074/jbc.M610318200
Nakajima, Y., Nakajima, S., Obata, K., Carlson, C.G., Yamaguchi, K., 1985. Dissociated cell culture of cholinergic neurons from nucleus basalis of Meynert and other basal forebrain nuclei. Proc. Natl. Acad. Sci. U. S. A. 82, 6325–6329. https://doi.org/10.1073/pnas.82.18.6325
Nassini, R., Fusi, C., Materazzi, S., Coppi, E., Tuccinardi, T., Marone, I.M., De Logu, F., Preti, D., Tonello, R., Chiarugi, A., Patacchini, R., Geppetti, P., Benemei, S., 2015. The TRPA1 channel mediates the analgesic action of dipyrone and pyrazolone derivatives. Br. J. Pharmacol. 172, 3397–3411. https://doi.org/10.1111/bph.13129
Nerbonne, J.M., Kass, R.S., 2005. Molecular physiology of cardiac repolarization. Physiol. Rev. https://doi.org/10.1152/physrev.00002.2005
Nestler, E., Hyman, S., Malenka, R.C., 2002. Molecular Neuropharmacology: A foundation for clinical neuroscience, Trends in Pharmacological Sciences.

https://doi.org/10.1016/S0165-6147(02)01903-X
Neubert, J.K., Maidment, N.T., Matsuka, Y., Adelson, D.W., Kruger, L., Spigelman, I., 2000. Inflammation-induced changes in primary afferent-evoked release of substance P within trigeminal ganglia in vivo. Brain Res. 871, 181–191. https://doi.org/10.1016/S0006-8993(00)02440-9
Newby, A.C., 1984. Adenosine and the concept of "retaliatory metabolites." Trends Biochem. Sci. https://doi.org/10.1016/0968-0004(84)90176-2
Newcomb, R., Szoke, B., Palma, A., Wang, G., Chen, X.H., Hopkins, W., Cong, R., Miller, J., Urge, L., Tarczy-Hornoch, K., Loo, J.A., Dooley, D.J., Nadasdi, L., Tsien, R.W., Lemos, J., Miljanich, G., 1998. Selective peptide antagonist of the class E calcium channel from the venom of the tarantula Hysterocrates gigas. Biochemistry 37, 15353–15362. https://doi.org/10.1021/bi981255g
Newman, E.A., 2003. New roles for astrocytes: Regulation of synaptic transmission. Trends Neurosci. https://doi.org/10.1016/S0166-2236(03)00237-6
Newman, E.A., 1984. Regional specialization of retinal glial cell membrane. Nature 309, 155–157. https://doi.org/10.1038/309155a0
Nguyen, M.J., Angkawaijawa, S., Hashitani, H., Lang, R.J., 2013. Nicotinic receptor activation on primary sensory afferents modulates autorhythmicity in the mouse renal pelvis. Br. J. Pharmacol. 170, 1221–1232. https://doi.org/10.1111/bph.12395
Nishiyama, A., Watanabe, M., Yang, Z., Bu, J., 2002. Identity, distribution, and development of polydendrocytes: NG2-expressing glial cells. J. Neurocytol. https://doi.org/10.1023/A:1025783412651
Noble, D., 1965. Electrical properties of cardiac muscle attributable to inward going (anomalous) rectification. J. Cell. Comp. Physiol. 66, 127–135. https://doi.org/10.1002/jcp.1030660520
Novgorodov, A.S., El-Awani, M., Bielawski, J., Obeid, L.M., Gudz, T.I., 2007. Activation of sphingosine-1-phosphate receptor S1P5 inhibits oligodendrocyte progenitor migration. FASEB J. 21, 1503–1514. https://doi.org/10.1096/fj.06-7420com
Numann, R., Catterall, W.A., Scheuer, T., 1991. Functional modulation of brain sodium channels by protein kinase C phosphorylation. Science (80-.). 254, 115–118. https://doi.org/10.1126/science.1656525
O'Sullivan, C., Schubart, A., Mir, A.K., Dev, K.K., 2016. The dual S1PR1/S1PR5 drug BAF312 (Siponimod) attenuates demyelination in organotypic slice cultures. J. Neuroinflammation 13, 31. https://doi.org/10.1186/s12974-016-0494-x
O'Sullivan, S., Dev, K.K., 2017. Sphingosine-1-phosphate receptor therapies: Advances in clinical trials for CNS-related diseases. Neuropharmacology. https://doi.org/10.1016/j.neuropharm.2016.11.006
Oades, R.D., 2007. Role of the serotonin system in ADHD. Expert Rev. Neurother. 7, 1357–1374.
Okasa, Y., Ozawa, S., 1980. Inhibitory action of adenosine on synaptic transmission in the hippocampus of the guinea pig in vitro. Eur. J. Pharmacol. 68, 483–492. https://doi.org/10.1016/0014-2999(80)90424-0
Olsen, R.W., Meunier, J.C., Changeux, J.P., 1972. Progress in the purification of the cholinergic receptor protein from Electrophorus electricus by affinity chromatography. FEBS Lett. 28, 96–100. https://doi.org/10.1016/0014-5793(72)80686-0
Ontaneda, D., Thompson, A.J., Fox, R.J., Cohen, J.A., 2017. Progressive multiple sclerosis: prospects for disease therapy, repair, and restoration of function. Lancet. https://doi.org/10.1016/S0140-6736(16)31320-4
Othman, T., Yan, H., Rivkees, S.A., 2003. Oligodendrocytes Express Functional A1 Adenosine Receptors That Stimulate Cellular Migration. Glia 44, 166–172. https://doi.org/10.1002/glia.10281
Pagadala, P., Park, C.K., Bang, S., Xu, Z.Z., Xie, R.G., Liu, T., Han, B.X., Daniel Tracey, J., Wang, F., Ji, R.R., 2013. Loss of NR1 subunit of NMDARs in primary sensory neurons leads to hyperexcitability and pain hypersensitivity: Involvement of Ca2+-activated small conductance potassium channels. J. Neurosci. 33, 13425–13430. https://doi.org/10.1523/JNEUROSCI.0454-13.2013

Pan, S., Gray, N.S., Gao, W., Mi, Y., Fan, Y., Wang, X., Tuntland, T., Che, J., Lefebvre, S., Chen, Y., Chu, A., Hinterding, K., Gardin, A., End, P., Heining, P., Bruns, C., Cooke, N.G., Nuesslein-Hildesheim, B., 2013. Discovery of BAF312 (Siponimod), a potent and selective S1P receptor modulator. ACS Med. Chem. Lett. 4, 333–337. https://doi.org/10.1021/ml300396r

Panjehpour, M., Castro, M., Klotz, K.N., 2005. Human breast cancer cell line MDA-MB-231 expresses endogenous A 2B adenosine receptors mediating a Ca 2+ signal. Br. J. Pharmacol. 145, 211–218. https://doi.org/10.1038/sj.bjp.0706180

Paoletta, S., Tosh, D.K., Finley, A., Gizewski, E.T., Moss, S.M., Gao, Z.G., Auchampach, J.A., Salvemini, D., Jacobson, K.A., 2013. Rational design of sulfonated A3 adenosine receptor-selective nucleosides as pharmacological tools to study chronic neuropathic pain. J. Med. Chem. 56, 5949–5963. https://doi.org/10.1021/jm4007966

Paraoanu, L.E., Layer, P.G., 2008. Acetylcholinesterase in cell adhesion, neurite growth and network formation. FEBS J. 275, 618–624. https://doi.org/10.1111/j.1742-4658.2007.06237.x

Park, S.M., Angel, C.E., McIntosh, J.D., Brooks, A.E.S., Middleditch, M., Chen, C.-J.J., Ruggiero, K., Cebon, J., Rod Dunbar, P., 2014. Sphingosine-1-phosphate lyase is expressed by CD68 + cells on the parenchymal side of marginal reticular cells in human lymph nodes. Eur. J. Immunol. 44, 2425–2436. https://doi.org/10.1002/eji.201344158

Parmar, M., 2018. Towards stem cell based therapies for parkinson's disease. Dev. 145. https://doi.org/10.1242/dev.156117

Pazzagli, M., Pedata, F., Pepeu, G., 1993. Effect of K+ depolarization, tetrodotoxin, and NMDA receptor inhibition on extracellular adenosine levels in rat striatum. Eur. J. Pharmacol. 234, 61–65. https://doi.org/10.1016/0014-2999(93)90706-N

Pchejetski, D., Bohler, T., Brizuela, L., Sauer, L., Doumerc, N., Golzio, M., Salunkhe, V., Teissié, J., Malavaud, B., Waxman, J., Cuvillier, O., 2010. FTY720 (fingolimod) sensitizes prostate cancer cells to radiotherapy by inhibition of sphingosine kinase-1. Cancer Res. 70, 8651–8661. https://doi.org/10.1158/0008-5472.CAN-10-1388

Peakman, M.-C., Hill, S.J., 1994. Adenosine A2B-receptor-mediated cyclic AMP accumulation in primary rat astrocytes. Br. J. Pharmacol. 111, 191–198. https://doi.org/10.1111/j.1476-5381.1994.tb14043.x

Pedata, F., Corsi, C., Melani, A., Bordoni, F., Latini, S., 2001. Adenosine extracellular brain concentrations and role of A2A receptors in ischemia, in: Annals of the New York Academy of Sciences. New York Academy of Sciences, pp. 74–84. https://doi.org/10.1111/j.1749-6632.2001.tb03614.x

Pedata, F., Dettori, I., Coppi, E., Melani, A., Fusco, I., Corradetti, R., Pugliese, A.M., 2016. Purinergic signalling in brain ischemia. Neuropharmacology. https://doi.org/10.1016/j.neuropharm.2015.11.007

Pedata, F., Latini, S., Pugliese, A.M., Pepeu, G., 1993. Investigations into the Adenosine Outflow from Hippocampal Slices Evoked by Ischemia-Like Conditions. J. Neurochem. 61, 284–289. https://doi.org/10.1111/j.1471-4159.1993.tb03566.x

Pedata, F., Melani, A., Pugliese, A.M., Coppi, E., Cipriani, S., Traini, C., 2007. The role of ATP and adenosine in the brain under normoxic and ischemic conditions. Purinergic Signal. 3, 299–310. https://doi.org/10.1007/s11302-007-9085-8

Pedata, F., Pazzagli, M., Tilli, S., Pepeu, G., 1990. Regional differences in the electrically stimulated release of endogenous and radioactive adenosine and purine derivatives from rat brain slices. Naunyn. Schmiedebergs. Arch. Pharmacol. 342, 447–453. https://doi.org/10.1007/BF00169463

Pedata, F., Pepeu, G., Spignoli, G., 1984. Biphasic effect of methylxanthines on acetylcholine release from electrically-stimulated brain slices. Br. J. Pharmacol. 83, 69–73. https://doi.org/10.1111/j.1476-5381.1984.tb10120.x

Pedata, F., Pugliese, A.M., Coppi, E., Dettori, I., Maraula, G., Cellai, L., Melani, A., 2014. Adenosine A 2A receptors modulate acute injury and neuroinflammation in brain ischemia. Mediators Inflamm. https://doi.org/10.1155/2014/805198

Perez-Reyes, E., 2003. Molecular physiology of low-voltage-activated T-type calcium channels. Physiol. Rev. https://doi.org/10.1152/physrev.00018.2002

Phillis, J.W., 2004. Adenosine and adenine nucleotides as regulators of cerebral blood flow: Roles of acidosis, cell swelling, and KATP channels. Crit. Rev. Neurobiol. https://doi.org/10.1615/CritRevNeurobiol.v16.i4.20

Phillis, J.W., Edstrom, J.P., Kostopoulos, G.K., Kirkpatrick, J.R., 1979. Effects of adenosine and adenine nucleotides on synaptic transmission in the cerebral cortex. Can. J. Physiol. Pharmacol. 57, 1289–1312. https://doi.org/10.1139/y79-194

Phillis, J.W., O'Regan, M.H., Perkins, L.M., 1993. Effect of adenosine receptor agonists on spontaneous and K+-evoked acetylcholine release from the in vivo rat cerebral cortex. Brain Res. 605, 293–297. https://doi.org/10.1016/0006-8993(93)91753-F

Pitson, S.M., Moretti, P.A.B., Zebol, J.R., Lynn, H.E., Xia, P., Vadas, M.A., Wattenberg, B.W., 2003. Activation of sphingosine kinase 1 by ERK1/2-mediated phosphorylation. EMBO J. 22, 5491–5500. https://doi.org/10.1093/emboj/cdg540

Pizzo, P.A., Clark, N.M., 2012. Alleviating Suffering 101 — Pain Relief in the United States. N. Engl. J. Med. 366, 197–199. https://doi.org/10.1056/NEJMp1109084

Popoli, P., Betto, P., Reggio, R., Ricciarello, G., 1995. Adenosine A2A receptor stimulation enhances striatal extracellular glutamate levels in rats. Eur. J. Pharmacol. 287, 215–217. https://doi.org/10.1016/0014-2999(95)00679-6

Posadas, I., Lopez-Hernandez, B., Cena, V., 2013. Nicotinic Receptors in Neurodegeneration. Curr. Neuropharmacol. 11, 298–314. https://doi.org/10.2174/1570159x11311030005

Poucher, S.M., Keddie, J.R., Singh, P., Stoggall, S.M., Caulkett, P.W.R., Jones, G., Collis, M.G., 1995. The in vitro pharmacology of ZM 241385, a potent, non-xanthine, A2a selective adenosine receptor antagonist. Br. J. Pharmacol. 115, 1096–1102. https://doi.org/10.1111/j.1476-5381.1995.tb15923.x

Powell, K.L., Cain, S.M., Ng, C., Sirdesai, S., David, L.S., Kyi, M., Garcia, E., Tyson, J.R., Reid, C.A., Bahlo, M., Foote, S.J., Snutch, T.P., O'Brien, T.J., 2009. A Cav3.2 T-type calcium channel point mutation has splice-variant-specific effects on function and segregates with seizure expression in a polygenic rat model of absence epilepsy. J. Neurosci. 29, 371–380. https://doi.org/10.1523/JNEUROSCI.5295-08.2009

Prè, D., Nestor, M.W., Sproul, A.A., Jacob, S., Koppensteiner, P., Chinchalongporn, V., Zimmer, M., Yamamoto, A., Noggle, S.A., Arancio, O., 2014. A Time Course Analysis of the Electrophysiological Properties of Neurons Differentiated from Human Induced Pluripotent Stem Cells (iPSCs). PLoS One 9, e103418. https://doi.org/10.1371/journal.pone.0103418

Pringle, N.P., Mudhar, H.S., Collarini, E.J., Richardson, W.D., 1992. PDGF receptors in the rat CNS: during late neurogenesis, PDGF alpha-receptor expression appears to be restricted to glial cells of the oligodendrocyte lineage. Development 115.

Prior, C., Marshall, I.G., Parsons, S.M., 1992. The pharmacology of vesamicol: An inhibitor of the vesicular acetylcholine transporter. Gen. Pharmacol. https://doi.org/10.1016/0306-3623(92)90280-W

Pugliese, A.M., Coppi, E., Volpini, R., Cristalli, G., Corradetti, R., Jeong, L.S., Jacobson, K.A., Pedata, F., 2007. Role of adenosine A3 receptors on CA1 hippocampal neurotransmission during oxygen-glucose deprivation episodes of different duration. Biochem. Pharmacol. 74, 768–779. https://doi.org/10.1016/j.bcp.2007.06.003

Pugliese, A.M., Latini, S., Corradetti, R., Pedata, F., 2003. Brief, repeated, oxygen-glucose deprivation episodes protect neurotransmission from a longer ischemic episode in the *in vitro* hippocampus: role of adenosine receptors. Br. J. Pharmacol. 140, 305–314. https://doi.org/10.1038/sj.bjp.0705442

Putnam, J., 1873. The anatomy of the mammal brain by Prof. Meynert. J.B. Lippincott & Co., New York.

Raffaelli, G., Saviane, C., Mohajerani, M.H., Pedarzani, P., Cherubini, E., 2004. BK potassium channels control transmitter release at CA3-CA3 synapses in the rat hippocampus. J. Physiol. 557, 147–157. https://doi.org/10.1113/jphysiol.2004.062661

Rafii, M.S., Baumann, T.L., Bakay, R.A.E., Ostrove, J.M., Siffert, J., Fleisher, A.S., Herzog, C.D., Barba, D., Pay, M., Salmon, D.P., Chu, Y., Kordower, J.H., Bishop, K., Keator, D., Potkin, S., Bartus, R.T., 2014. A phase1 study of stereotactic gene delivery of AAV2-NGF for Alzheimer's disease. Alzheimers. Dement. 10, 571–581.

https://doi.org/10.1016/j.jalz.2013.09.004
Raja, S.N., Carr, D.B., Cohen, M., Finnerup, N.B., Flor, H., Gibson, S., Keefe, F.J., Mogil, J.S., Ringkamp, M., Sluka, K.A., Song, X.-J., Stevens, B., Sullivan, M.D., Tutelman, P.R., Ushida, T., Vader, K., 2020. The revised International Association for the Study of Pain definition of pain: concepts, challenges, and compromises. Pain 161, 1976–1982. https://doi.org/10.1097/j.pain.0000000000001939
Rajasundaram, S., 2018. Adenosine A2A receptor signaling in the immunopathogenesis of experimental autoimmune encephalomyelitis. Front. Immunol. https://doi.org/10.3389/fimmu.2018.00402
Rao, V.R., Perez-Neut, M., Kaja, S., Gentile, S., 2015. Voltage-gated ion channels in cancer cell proliferation. Cancers (Basel). https://doi.org/10.3390/cancers7020813
Rasband, M.N., Park, E.W., Vanderah, T.W., Lai, J., Porreca, F., Trimmer, J.S., 2001. Distinct potassium channels on pain-sensing neurons. Proc. Natl. Acad. Sci. U. S. A. 98, 13373–13378. https://doi.org/10.1073/pnas.231376298
Ray, P., Torck, A., Quigley, L., Wangzhou, A., Neiman, M., Rao, C., Lam, T., Kim, J.Y., Kim, T.H., Zhang, M.Q., Dussor, G., Price, T.J., 2018. Comparative transcriptome profiling of the human and mouse dorsal root ganglia: An RNA-seq-based resource for pain and sensory neuroscience research. Pain 159, 1325–1345. https://doi.org/10.1097/j.pain.0000000000001217
Rebola, N., Pinheiro, P.C., Oliveira, C.R., Malva, J.O., Cunha, R.A., 2003. Subcellular localization of adenosine A1 receptors in nerve terminals and synapses of the rat hippocampus. Brain Res. 987, 49–58. https://doi.org/10.1016/S0006-8993(03)03247-5
Resende, R.R., Adhikari, A., 2009. Cholinergic receptor pathways involved in apoptosis, cell proliferation and neuronal differentiation. Cell Commun. Signal. https://doi.org/10.1186/1478-811X-7-20
Resende, R.R., Alves, A.S., Britto, L.R.G., Ulrich, H., 2008. Role of acetylcholine receptors in proliferation and differentiation of P19 embryonal carcinoma cells. Exp. Cell Res. 314, 1429–1443. https://doi.org/10.1016/j.yexcr.2008.01.003
Ribary, U., Lichtensteiger, W., 1989. Effects of acute and chronic prenatal nicotine treatment on central catecholamine systems of male and female rat fetuses and offspring. J. Pharmacol. Exp. Ther. 248.
Ribeiro, J.A., 1995. Purinergic Inhibition of Neurotransmitter Release in the Central Nervous System. Pharmacol. Toxicol. 77, 299–305. https://doi.org/10.1111/j.1600-0773.1995.tb01031.x
Richardson, R.T., DeLong, M.R., 1991. Electrophysiological studies of the functions of the nucleus basalis in primates. Adv. Exp. Med. Biol. https://doi.org/10.1007/978-1-4757-0145-6_12
Riddy, D.M., Stamp, C., Sykes, D.A., Charlton, S.J., Dowling, M.R., 2012. Reassessment of the pharmacology of Sphingosine-1-phosphate S1P3 receptor ligands using the DiscoveRx PathHunter™ and Ca2+ release functional assays. Br. J. Pharmacol. 167, 868–880. https://doi.org/10.1111/j.1476-5381.2012.02032.x
Rieger, J.M., Brown, M.L., Sullivan, G.W., Linden, J., Macdonald, T.L., 2001. Design, synthesis, and evaluation of novel A2A adenosine receptor agonists. J. Med. Chem. 44, 531–539. https://doi.org/10.1021/jm0003642
Rissanen, E., Virta, J.R., Paavilainen, T., Tuisku, J., Helin, S., Luoto, P., Parkkola, R., Rinne, J.O., Airas, L., 2013. Adenosine A2A receptors in secondary progressive multiple sclerosis: A [11 C]TMSX brain PET study. J. Cereb. Blood Flow Metab. 33, 1394–1401. https://doi.org/10.1038/jcbfm.2013.85
Rivkees, S.A., Price, S.L., Zhou, F.C., 1995. Immunohistochemical detection of A1 adenosine receptors in rat brain with emphasis on localization in the hippocampal formation, cerebral cortex, cerebellum, and basal ganglia. Brain Res. 677, 193–203. https://doi.org/10.1016/0006-8993(95)00062-U
Rivkees, S.A., Wendler, C.C., 2011. Adverse and protective influences of adenosine on the newborn and embryo: Implications for preterm white matter injury and embryo protection. Pediatr. Res. https://doi.org/10.1203/PDR.0b013e31820efbcf
Rogers, J.D., Brogan, D., Mirra, S.S., 1985. The nucleus basalis of Meynert in neurological

disease: A quantitative morphological study. Ann. Neurol. 17, 163–170. https://doi.org/10.1002/ana.410170210

Rosen, H., Gonzalez-Cabrera, P.J., Sanna, M.G., Brown, S., 2009. Sphingosine 1-phosphate receptor signaling. Annu. Rev. Biochem. https://doi.org/10.1146/annurev.biochem.78.072407.103733

Rosin, D.L., Hettinger, B.D., Lee, A., Linden, J., 2003. Anatomy of adenosine A2A receptors in brain: Morphological substrates for integration of striatal function. Neurology 61. https://doi.org/10.1212/01.wnl.0000095205.33940.99

Rosin, D.L., Talley, E.M., Lee, A., Stornetta, R.L., Gaylinn, B.D., Guyenet, P.G., Lynch, K.R., 1996. Distribution of ?2C-adrenergic receptor-like immunoreactivity in the rat central nervous system. J. Comp. Neurol. 372, 135–165. https://doi.org/10.1002/(sici)1096-9861(19960812)372:1<135::aid-cne9>3.0.co;2-4

Rossi, D.J., Oshima, T., Attwell, D., 2000. Glutamate release in severe brain ischaemia is mainly by reversed uptake. Nature 403, 316–321. https://doi.org/10.1038/35002090

Rothhammer, V., Kenison, J.E., Tjon, E., Takenaka, M.C., De Lima, K.A., Borucki, D.M., Chao, C.C., Wilz, A., Blain, M., Healy, L., Antel, J., Quintana, F.J., 2017. Sphingosine 1-phosphate receptor modulation suppresses pathogenic astrocyte activation and chronic progressive CNS inflammation. Proc. Natl. Acad. Sci. U. S. A. 114, 2012–2017. https://doi.org/10.1073/pnas.1615413114

Russchen, F.T., Amaral, D.G., Price, J.L., 1985. The afferent connections of the substantia innominata in the monkey, Macaca fascicularis. J. Comp. Neurol. 242, 1–27. https://doi.org/10.1002/cne.902420102

Sabbadini, M., Yost, C.S., 2009. Molecular Biology of Background K Channels: Insights from K2P Knockout Mice. J. Mol. Biol. 385, 1331–1344. https://doi.org/10.1016/j.jmb.2008.11.048

Sachdeva, S., Gupta, M., 2013. Adenosine and its receptors as therapeutic targets: An overview. Saudi Pharm. J. https://doi.org/10.1016/j.jsps.2012.05.011

Saegusa, H., Kurihara, T., Zong, S., Minowa, O., Kazuno, A.A., Han, W., Matsuda, Y., Yamanaka, H., Osanai, M., Noda, T., Tanabe, T., 2000. Altered pain responses in mice lacking α1E subunit of the voltage-dependent Ca2+ channel. Proc. Natl. Acad. Sci. U. S. A. 97, 6132–6137. https://doi.org/10.1073/pnas.100124197

Saeki, T., Kimura, T., Hashidume, K., Murayama, T., Yamamura, H., Ohya, S., Suzuki, Y., Nakayama, S., Imaizumi, Y., 2019. Conversion of Ca2+ oscillation into propagative electrical signals by Ca2+-activated ion channels and connexin as a reconstituted Ca2+ clock model for the pacemaker activity. Biochem. Biophys. Res. Commun. 510, 242–247. https://doi.org/10.1016/j.bbrc.2019.01.080

Sah, D.W.Y., 1995. Human fetal central neurons in culture: Voltage- and ligand-gated currents. J. Neurophysiol. 74, 1889–1899. https://doi.org/10.1152/jn.1995.74.5.1889

Saini, H.S., Coelho, R.P., Goparaju, S.K., Jolly, P.S., Maceyka, M., Spiegel, S., Sato-Bigbee, C., 2005. Novel role of sphingosine kinase 1 as a mediator of neurotrophin-3 action in oligodendrocyte progenitors. J. Neurochem. 95, 1298–1310. https://doi.org/10.1111/j.1471-4159.2005.03451.x

Salvatore, C.A., Jacobson, M.A., Taylor, H.E., Linden, J., Johnson, R.G., 1993. Molecular cloning and characterization of the human A3 adenosine receptor. Proc. Natl. Acad. Sci. U. S. A. 90, 10365–10369. https://doi.org/10.1073/pnas.90.21.10365

Satoi, H., Tomimoto, H., Ohtani, R., Kitano, T., Kondo, T., Watanabe, M., Oka, N., Akiguchi, I., Furuya, S., Hirabayashi, Y., Okazaki, T., 2005. Astroglial expression of ceramide in Alzheimer's disease brains: A role during neuronal apoptosis. Neuroscience 130, 657–666. https://doi.org/10.1016/j.neuroscience.2004.08.056

Sattin, A., Rall, T.W., 1970. The effect of adenosine and adenine nucleotides on the cyclic adenosine 3′, 5′-phosphate content of guinea pig cerebral cortex slices. Mol. Pharmacol. 6, 13–23.

Savio-Galimberti, E., Gollob, M.H., Darbar, D., 2012. Voltage-gated sodium channels: Biophysics, pharmacology, and related channelopathies. Front. Pharmacol. 3 JUL, 124. https://doi.org/10.3389/fphar.2012.00124

Sawynok, J., Reid, A.R., Fredholm, B.B., 2010. Caffeine reverses antinociception by

oxcarbazepine by inhibition of adenosine A1 receptors: Insights using knockout mice. Neurosci. Lett. 473, 178–181. https://doi.org/10.1016/j.neulet.2010.02.028

Scarlett, S.S., White, J.A., Blackmore, P.F., Schoenbach, K.H., Kolb, J.F., 2009. Regulation of intracellular calcium concentration by nanosecond pulsed electric fields. Biochim. Biophys. Acta - Biomembr. 1788, 1168–1175. https://doi.org/10.1016/j.bbamem.2009.02.006

Schlumpf, M., Palacios, J.M., Cortes, R., Lichtensteiger, W., 1991. Regional development of muscarinic cholinergic binding sites in the prenatal rat brain. Neuroscience 45, 347–357. https://doi.org/10.1016/0306-4522(91)90232-D

Schmittgen, T.D., Livak, K.J., 2008. Analyzing real-time PCR data by the comparative CT method. Nat. Protoc. 3, 1101–1108. https://doi.org/10.1038/nprot.2008.73

Schulte, G., Fredholm, B.B., 2003. Signalling from adenosine receptors to mitogen-activated protein kinases. Cell. Signal. https://doi.org/10.1016/S0898-6568(03)00058-5

Schulz, A., Ajayi, T., Specchio, N., de Los Reyes, E., Gissen, P., Ballon, D., Dyke, J.P., Cahan, H., Slasor, P., Jacoby, D., Kohlschütter, A., 2018. Study of intraventricular cerliponase alfa for CLN2 disease. N. Engl. J. Med. 378, 1898–1907. https://doi.org/10.1056/NEJMoa1712649

Schulz, J., Pagano, G., Fernández Bonfante, J.A., Wilson, H., Politis, M., 2018. Nucleus basalis of Meynert degeneration precedes and predicts cognitive impairment in Parkinson's disease. Brain 141, 1501–1516. https://doi.org/10.1093/brain/awy072

Scolding, N.J., Frith, S., Linington, C., Morgan, B.P., Campbell, A.K., Compston, D.A.S., 1989. Myelin-oligodendrocyte glycoprotein (MOG) is a surface marker of oligodendrocyte maturation. J. Neuroimmunol. 22, 169–176. https://doi.org/10.1016/0165-5728(89)90014-3

Scott, F.L., Clemons, B., Brooks, J., Brahmachary, E., Powell, R., Dedman, H., Desale, H.G., Timony, G.A., Martinborough, E., Rosen, H., Roberts, E., Boehm, M.F., Peach, R.J., 2016. Ozanimod (RPC1063) is a potent sphingosine-1-phosphate receptor-1 ($S1P_1$) and receptor-5 ($S1P_5$) agonist with autoimmune disease-modifying activity. Br. J. Pharmacol. 173, 1778–1792. https://doi.org/10.1111/bph.13476

Scroggs, R.S., Fox, A.P., 1992. Calcium current variation between acutely isolated adult rat dorsal root ganglion neurons of different size. J. Physiol. 445, 639–58.

Scroggs, R.S., Fox, A.P., 1991. Distribution of dihydropyridine and omega-conotoxin-sensitive calcium currents in acutely isolated rat and frog sensory neuron somata: diameter-dependent L channel expression in frog. J. Neurosci. 11, 1334–46.

Sebastião, A.M., Ribeiro, J.A., 1996. Adenosine A2 receptor-mediated excitatory actions on the nervous system. Prog. Neurobiol. https://doi.org/10.1016/0301-0082(95)00035-6

Sforna, L., Megaro, A., Pessia, M., Franciolini, F., Catacuzzeno, L., 2018. Structure, Gating and Basic Functions of the Ca2+-activated K Channel of Intermediate Conductance. Curr. Neuropharmacol. 16, 608–617. https://doi.org/10.2174/1570159x15666170830122402

Shida, D., Takabe, K., Kapitonov, D., Milstien, S., Spiegel, S., 2008. Targeting SphK1 as a New Strategy against Cancer. Curr. Drug Targets 9, 662–673. https://doi.org/10.2174/138945008785132402

Shneyvays, V., Leshem, D., Zinman, T., Mamedova, L.K., Jacobson, K.A., Shainberg, A., 2005. Role of adenosine A1 and A3 receptors in regulation of cardiomyocyte homeostasis after mitochondrial respiratory chain injury. Am. J. Physiol. - Hear. Circ. Physiol. 288, 2792–2801. https://doi.org/10.1152/ajpheart.01157.2004

Shneyvays, V., Zinman, T., Shainberg, A., 2004. Analysis of calcium responses mediated by the A3 adenosine receptor in cultured newborn rat cardiac myocytes. Cell Calcium 36, 387–396. https://doi.org/10.1016/j.ceca.2004.03.004

Shrager, P., Novakovic, S.D., 1995. Control of myelination, axonal growth, and synapse formation in spinal cord explants by ion channels and electrical activity. Dev. Brain Res. 88, 68–78. https://doi.org/10.1016/0165-3806(95)00081-N

Shyng, S.L., Nichols, C.G., 1997. Octameric stoichiometry of the K(ATP) channel complex. J. Gen. Physiol. 110, 655–664. https://doi.org/10.1085/jgp.110.6.655

Singer, W., 1999. Neuronal synchrony: A versatile code for the definition of relations? Neuron. https://doi.org/10.1016/S0896-6273(00)80821-1

Sitkovsky, M. V., Lukashev, D., Apasov, S., Kojima, H., Koshiba, M., Caldwell, C., Ohta, A., Thiel, M., 2004. Physiological control of immune response and inflammatory tissue damage by hypoxia-inducible factors and adenosine A2A receptors. Annu. Rev. Immunol. https://doi.org/10.1146/annurev.immunol.22.012703.104731

Sivilotti, L., Okuse, K., Akopian, A.N., Moss, S., Wood, J.N., 1997. A single serine residue confers tetrodotoxin insensitivity on the rat sensory-neuron-specific sodium channel SNS. FEBS Lett. 409, 49–52. https://doi.org/10.1016/S0014-5793(97)00479-1

Slotkin, T.A., 2004. Cholinergic systems in brain development and disruption by neurotoxicants: Nicotine, environmental tobacco smoke, organophosphates. Toxicol. Appl. Pharmacol. https://doi.org/10.1016/j.taap.2003.06.001

Slotkin, T.A., Ryde, I.T., Seidler, F.J., 2007. Separate or sequential exposure to nicotine prenatally and in adulthood: Persistent effects on acetylcholine systems in rat brain regions. Brain Res. Bull. 74, 91–103. https://doi.org/10.1016/j.brainresbull.2007.05.007

Soliven, B., Miron, V., Chun, J., 2011. The neurobiology of sphingosine 1-phosphate signaling and sphingosine 1-phosphate receptor modulators. Neurology 76, S9–S14. https://doi.org/10.1212/WNL.0b013e31820d9507

Soliven, B., Szuchet, S., Arnason, B.G.W., Nelson, D.J., 1988. Forskolin and phorbol esters decrease the same K+ conductance in cultured oligodendrocytes. J. Membr. Biol. 105, 177–186. https://doi.org/10.1007/BF02009170

Song, M., Mohamad, O., Chen, D., Yu, S.P., 2013. Coordinated development of voltage-gated Na+ and K+ currents regulates functional maturation of forebrain neurons derived from human induced pluripotent stem cells. Stem Cells Dev. 22, 1551–1563. https://doi.org/10.1089/scd.2012.0556

Song, P., Lie-Cheng, W., Wang, G. Du, Zhou, Z., Zhao, Z.Q., 2002. Interleukin-2 regulates membrane potentials and calcium channels via μ opioid receptors in rat dorsal root ganglion neurons. Neuropharmacology 43, 1324–1329. https://doi.org/10.1016/S0028-3908(02)00298-8

Sontheimer, H., Kettenmann, H., 1988. Heterogeneity of potassium currents in cultured oligodendrocytes. Glia 1, 415–420. https://doi.org/10.1002/glia.440010609

Sontheimer, H., Trotter, J., Schachner, M., Kettenmann, H., 1989. Channel expression correlates with differentiation stage during the development of Oligodendrocytes from their precursor cells in culture. Neuron 2, 1135–1145. https://doi.org/10.1016/0896-6273(89)90180-3

Sørensen, P.S., 2016. Ozanimod: A better or just another S1P receptor modulator? Lancet Neurol. https://doi.org/10.1016/S1474-4422(16)00041-7

Spignoli, G., Pedata, F., Pepeu, G., 1984. A1 and A2 adenosine receptors modulate acetylcholine release from brain slices. Eur. J. Pharmacol. 97, 341–342. https://doi.org/10.1016/0014-2999(84)90475-8

Spitzer, S.O., Sitnikov, S., Kamen, Y., De Faria, O., 2019. Oligodendrocyte Progenitor Cells Become Regionally Diverse and Heterogeneous with Age. Neuron 101, 459-471.e5. https://doi.org/10.1016/j.neuron.2018.12.020

Stanika, R.I., Villanueva, I., Kazanina, G., Brian Andrews, S., Pivovarova, N.B., 2012. Comparative impact of voltage-gated calcium channels and NMDA receptors on mitochondria-mediated neuronal injury. J. Neurosci. 32, 6642–6650. https://doi.org/10.1523/JNEUROSCI.6008-11.2012

Stellwagen, D., Malenka, R.C., 2006. Synaptic scaling mediated by glial TNF-α. Nature 440, 1054–1059. https://doi.org/10.1038/nature04671

Sterling, G.H., Doukas, P.H., Ricciardi, F.J., Biedrzycka, D.W., O'Neill, J.J., 1986. Inhibition of High-Affinity Choline Uptake and Acetylcholine Synthesis by Quinuclidinyl and Hemicholinium Derivatives. J. Neurochem. 46, 1170–1175. https://doi.org/10.1111/j.1471-4159.1986.tb00633.x

Stevens, B., Porta, S., Haak, L.L., Gallo, V., Fields, R.D., 2002. Adenosine: A neuron-glial transmitter promoting myelination in the CNS in response to action potentials. Neuron 36, 855–868. https://doi.org/10.1016/S0896-6273(02)01067-X

Striessnig, J., Ortner, N., Pinggera, A., 2015. Pharmacology of L-type Calcium Channels: Novel Drugs for Old Targets? Curr. Mol. Pharmacol. 8, 110–122.

https://doi.org/10.2174/1874467208666150507105845
Strub, G.M., Maceyka, M., Hait, N.C., Milstien, S., Spiegel, S., 2010. Extracellular and intracellular actions of sphingosine-1-phosphate. Adv. Exp. Med. Biol. 688, 141–155. https://doi.org/10.1007/978-1-4419-6741-1_10
Sukhotinsky, I., Ben-Dor, E., Raber, P., Devor, M., 2004. Key role of the dorsal root ganglion in neuropathic tactile hypersensibility. Eur. J. Pain 8, 135–143. https://doi.org/10.1016/S1090-3801(03)00086-7
Sun, K., Zhang, Y., Bogdanov, M. V., Wu, H., Song, A., Li, J., Dowhan, W., Idowu, M., Juneja, H.S., Molina, J.G., Blackburn, M.R., Kellems, R.E., Xia, Y., 2015. Elevated adenosine signaling via adenosine A2B receptor induces normal and sickle erythrocyte sphingosine kinase 1 activity. Blood 125, 1643–1652. https://doi.org/10.1182/blood-2014-08-595751
Sun, Y., Huang, P., 2016. Adenosine A2B receptor: From cell biology to human diseases. Front. Chem. https://doi.org/10.3389/fchem.2016.00037
Suzuki, S., Enosawa, S., Kakefuda, T., Li, X.K., Mitsusada, M., Takahara, S., Amemiya, H., 1996. Immunosuppressive effect of a new drug, FTY720, on lymphocyte responses in vitro and cardiac allograft survival in rats. Transpl. Immunol. 4, 252–255. https://doi.org/10.1016/S0966-3274(96)80026-8
Svenningsson, P., Hall, H., Sedvall, G., Fredholm, B.B., 1997. Distribution of adenosine receptors in the postmortem human brain: An extended autoradiographic study. Synapse 27, 322–335. https://doi.org/10.1002/(SICI)1098-2396(199712)27:4<322::AID-SYN6>3.0.CO;2-E
Swanson, T.H., Drazba, J.A., Rivkees, S.A., 1995. Adenosine A1 receptors are located predominantly on axons in the rat hippocampal formation. J. Comp. Neurol. 363, 517–531. https://doi.org/10.1002/cne.903630402
Szuchet, S., Nielsen, J.A., Lovas, G., Domowicz, M.S., de Velasco, J.M., Maric, D., Hudson, L.D., 2011. The genetic signature of perineuronal oligodendrocytes reveals their unique phenotype. Eur. J. Neurosci. 34, 1906–1922. https://doi.org/10.1111/j.1460-9568.2011.07922.x
Takigawa, T., Alzheimer, C., 2002. Phasic and tonic attenuation of EPSPs by inward rectifier K+ channels in rat hippocampal pyramidal cells. J. Physiol. 539, 67–75. https://doi.org/10.1113/jphysiol.2001.012883
Talley, E.M., Solórzano, G., Lei, Q., Kim, D., Bayliss, D.A., 2001. CNS distribution of members of the two-pore-domain (KCNK) potassium channel family. J. Neurosci. 21, 7491–7505. https://doi.org/10.1523/jneurosci.21-19-07491.2001
ten Donkelaar, H.J., 2015. Development of the Basal Ganglia and the Basal Forebrain, in: Brain Mapping: An Encyclopedic Reference. Elsevier Inc., pp. 357–365. https://doi.org/10.1016/B978-0-12-397025-1.00236-0
ten Donkelaar, H.J., Lammens, M., Cruysberg, J.R.M., Ulzen, K.K. Van, Hori, A., Shiota, K., 2014. Development and developmental disorders of the forebrain, in: Clinical Neuroembryology: Development and Developmental Disorders of the Human Central Nervous System. Springer-Verlag Berlin Heidelberg, pp. 421–521. https://doi.org/10.1007/978-3-642-54687-7_9
Terayama, R., Tabata, M., Maruhama, K., Iida, S., 2018. A 3 adenosine receptor agonist attenuates neuropathic pain by suppressing activation of microglia and convergence of nociceptive inputs in the spinal dorsal horn. Exp. Brain Res. 236, 3203–3213. https://doi.org/10.1007/s00221-018-5377-1
Thastrup, O., Cullen, P.J., Drobak, B.K., Hanley, M.R., Dawson, A.P., 1990. Thapsigargin, a tumor promoter, discharges intracellular Ca2+ stores by specific inhibition of the endoplasmic reticulum Ca2+-ATPase. Proc. Natl. Acad. Sci. U. S. A. 87, 2466–2470. https://doi.org/10.1073/pnas.87.7.2466
Theis, A.K., Rózsa, B., Katona, G., Schmitz, D., Johenning, F.W., 2018. Voltage gated calcium channel activation by backpropagating action potentials downregulates NMDAR function. Front. Cell. Neurosci. 12, 109. https://doi.org/10.3389/fncel.2018.00109
Toledo-Aral, J.J., Moss, B.L., He, Z.J., Koszowski, A.G., Whisenand, T., Levinson, S.R., Wolf, J.J., Silos-Santiago, I., Halegoua, S., Mandel, G., 1997. Identification of PN1, a predominant voltage-dependent sodium channel expressed principally in peripheral

neurons. Proc. Natl. Acad. Sci. U. S. A. 94, 1527–1532. https://doi.org/10.1073/pnas.94.4.1527

Tonelli, F., Lim, K.G., Loveridge, C., Long, J., Pitson, S.M., Tigyi, G., Bittman, R., Pyne, S., Pyne, N.J., 2010. FTY720 and (S)-FTY720 vinylphosphonate inhibit sphingosine kinase 1 and promote its proteasomal degradation in human pulmonary artery smooth muscle, breast cancer and androgen-independent prostate cancer cells. Cell. Signal. 22, 1536–1542. https://doi.org/10.1016/j.cellsig.2010.05.022

Tosh, D., Paoletta, S., … A.F.-A., 2014, U., 2014. Discovery of next generation A (3) adenosine receptor selective agonists for treatment of chronic neuropathic pain. Chem. SOC 1155 16TH ST, NW ….

Tosh, D.K., Finley, A., Paoletta, S., Moss, S.M., Gao, Z.-G., Gizewski, E.T., Auchampach, J.A., Salvemini, D., Jacobson, K.A., 2014. In Vivo Phenotypic Screening for Treating Chronic Neuropathic Pain: Modification of *C* 2-Arylethynyl Group of Conformationally Constrained A $_3$ Adenosine Receptor Agonists. J. Med. Chem. 57, 9901–9914. https://doi.org/10.1021/jm501021n

Tregellas, J.R., Wylie, K.P., 2019. Alpha7 nicotinic receptors as therapeutic targets in schizophrenia. Nicotine Tob. Res. https://doi.org/10.1093/ntr/nty034

Tsai, H.C., Han, M.H., 2016. Sphingosine-1-Phosphate (S1P) and S1P Signaling Pathway: Therapeutic Targets in Autoimmunity and Inflammation. Drugs 76, 1067–1079. https://doi.org/10.1007/s40265-016-0603-2

Tsutsui, S., Schnermann, J., Noorbakhsh, F., Henry, S., Yong, V.W., Winston, B.W., Warren, K., Power, C., 2004. A1 Adenosine Receptor Upregulation and Activation Attenuates Neuroinflammation and Demyelination in a Model of Multiple Sclerosis. J. Neurosci. 24, 1521–1529. https://doi.org/10.1523/JNEUROSCI.4271-03.2004

Turner, C.P., Seli, M., Ment, L., Stewart, W., Yan, H., Johansson, B., Fredholm, B.B., Blackburn, M., Rivkees, S.A., 2003. A1 adenosine receptors mediate hypoxia-induced ventriculomegaly. Proc. Natl. Acad. Sci. U. S. A. 100, 11718–11722. https://doi.org/10.1073/pnas.1931975100

Turner, C.P., Yan, H., Schwartz, M., Othman, T., Rivkees, S.A., 2002. A1 adenosine receptor activation induces ventriculomegaly and white matter loss. Neuroreport 13, 1199–1204. https://doi.org/10.1097/00001756-200207020-00026

Typlt, M., Mirkowski, M., Azzopardi, E., Ruettiger, L., Ruth, P., Schmid, S., 2013. Mice with Deficient BK Channel Function Show Impaired Prepulse Inhibition and Spatial Learning, but Normal Working and Spatial Reference Memory. PLoS One 8, e81270. https://doi.org/10.1371/journal.pone.0081270

Uhl, G.R., McKinney, M., Hedreen, J.C., White, C.L., Coyle, J.T., Whitehouse, P.J., Price, D.L., 1982. Dementia pugilistica: loss of basal forebrain cholinergic neurons and cholinergic cortical markers. Ann. Neurol. 12, 99.

Umana, I.C., Daniele, C.A., McGehee, D.S., 2013. Neuronal nicotinic receptors as analgesic targets: It's a winding road. Biochem. Pharmacol. https://doi.org/10.1016/j.bcp.2013.08.001

Usoskin, D., Furlan, A., Islam, S., Abdo, H., Lönnerberg, P., Lou, D., Hjerling-Leffler, J., Haeggström, J., Kharchenko, O., Kharchenko, P. V., Linnarsson, S., Ernfors, P., 2015. Unbiased classification of sensory neuron types by large-scale single-cell RNA sequencing. Nat. Neurosci. 18, 145–153. https://doi.org/10.1038/nn.3881

Valdez-Morales, E., Guerrero-Alba, R., Ochoa-Cortes, F., Benson, J., Spreadbury, I., Hurlbut, D., Miranda-Morales, M., Lomax, A.E., Vanner, S., 2013. Release of endogenous opioids during a chronic IBD model suppresses the excitability of colonic DRG neurons. Neurogastroenterol. Motil. 25. https://doi.org/10.1111/nmo.12008

Van Calker, D., Hamprecht, B., 1979. Lithium long-term treatment View project. Artic. J. Neurochem. https://doi.org/10.1111/j.1471-4159.1979.tb05236.x

Van Der Klein, P.A.M., Kourounakis, A.P., IJzerman, A.P., 1999. Allosteric modulation of the adenosine A1 receptor. Synthesis and biological evaluation of novel 2-amino-3-benzoylthiophenes as allosteric enhancers of agonist binding. J. Med. Chem. 42, 3629–3635. https://doi.org/10.1021/jm991051d

van Doorn, R., Lopes Pinheiro, M.A., Kooij, G., Lakeman, K., van het Hof, B., van der Pol,

S.M.A., Geerts, D., van Horssen, J., van der Valk, P., van der Kam, E., Ronken, E., Reijerkerk, A., de Vries, H.E., 2012. Sphingosine 1-phosphate receptor 5 mediates the immune quiescence of the human brain endothelial barrier. J. Neuroinflammation 9, 663. https://doi.org/10.1186/1742-2094-9-133

Van Muijlwijk-Koezen, J.E., Timmerman, H., Van Der Goot, H., Menge, W.M.P.B., Von Drabbe Künzel, J.F., De Groote, M., Ijzerman, A.P., 2000. Isoquinoline and quinazoline urea analogues as antagonists for the human-adenosine A3 receptor. J. Med. Chem. 43, 2227–2238. https://doi.org/10.1021/jm000002u

Vasung, L., Huang, H., Jovanov-Milošević, N., Pletikos, M., Mori, S., Kostović, I., 2010. Development of axonal pathways in the human fetal fronto-limbic brain: Histochemical characterization and diffusion tensor imaging. J. Anat. 217, 400–417. https://doi.org/10.1111/j.1469-7580.2010.01260.x

Verkhratsky, A.N., Trotter, J., Kettenmann, H., 1990. Cultured glial precursor cells from mouse cortex express two types of calcium currents. Neurosci. Lett. 112, 194–198. https://doi.org/10.1016/0304-3940(90)90202-K

Vessey, D.A., Kelley, M., Zhang, J., Li, L., Tao, R., Karliner, J.S., 2007. Dimethylsphingosine and FTY720 inhibit the SK1 form but activate the SK2 form of sphingosine kinase from rat heart. J. Biochem. Mol. Toxicol. 21, 273–279. https://doi.org/10.1002/jbt.20193

Vincenzi, F., Targa, M., Romagnoli, R., Merighi, S., Gessi, S., Baraldi, P.G., Borea, P.A., Varani, K., 2014. TRR469, a potent A1 adenosine receptor allosteric modulator, exhibits anti-nociceptive properties in acute and neuropathic pain models in mice. Neuropharmacology 81, 6–14. https://doi.org/10.1016/j.neuropharm.2014.01.028

Vink, S., Alewood, P.F., 2012. Targeting voltage-gated calcium channels: Developments in peptide and small-molecule inhibitors for the treatment of neuropathic pain. Br. J. Pharmacol. https://doi.org/10.1111/j.1476-5381.2012.02082.x

von Lubitz, D.K., 1999. Adenosine and cerebral ischemia: Therapeutic future or death of a brave concept? Eur. J. Pharmacol. 365, 9–25. https://doi.org/10.1016/S0014-2999(98)00788-2

Wadel, K., Neher, E., Sakaba, T., 2007. The Coupling between Synaptic Vesicles and Ca2+ Channels Determines Fast Neurotransmitter Release. Neuron 53, 563–575. https://doi.org/10.1016/j.neuron.2007.01.021

Wahl-Schott, C., Fenske, S., Biel, M., 2014. HCN channels: New roles in sinoatrial node function. Curr. Opin. Pharmacol. https://doi.org/10.1016/j.coph.2013.12.005

Wahlman, C., Doyle, T.M., Little, J.W., Luongo, L., Janes, K., Chen, Z., Esposito, E., Tosh, D.K., Cuzzocre, S., Jacobson, K.A., Salvemini, D., 2018. Chemotherapy-induced pain is promoted by enhanced spinal adenosine kinase levels through astrocyte-dependent mechanisms. Pain 159, 1025–1034. https://doi.org/10.1097/j.pain.0000000000001177

Wall, P.D., Devor, M., 1983. Sensory afferent impulses originate from dorsal root ganglia as well as from the periphery in normal and nerve injured rats. Pain 17, 321–339. https://doi.org/10.1016/0304-3959(83)90164-1

Walterfang, M., Fahey, M., Desmond, P., Wood, A., Seal, M.L., Steward, C., Adamson, C., Kokkinos, C., Fietz, M., Velakoulis, D., 2010. White and gray matter alterations in adults with Niemann-Pick disease type C: A cross-sectional study. Neurology 75, 49–56. https://doi.org/10.1212/WNL.0b013e3181e6210e

Wang, H.S., Pan, Z., Shi, W., Brown, B.S., Wymore, R.S., Cohen, I.S., Dixon, J.E., McKinnon, D., 1998. KCNQ2 and KCNQ3 potassium channel subunits: Molecular correlates of the M-channel. Science (80-.). 282, 1890–1893. https://doi.org/10.1126/science.282.5395.1890

Wang, J., Huxley, V.H., 2006. Adenosine A2A receptor modulation of juvenile female rat skeletal muscle microvessel permeability. Am. J. Physiol. - Hear. Circ. Physiol. 291. https://doi.org/10.1152/ajpheart.00526.2006

Wang, J., Wang, Yali, Wang, Yang, Wang, R., Zhang, Y., Zhang, Q., Lu, C., 2014. Contribution of α4β2 nAChR in nicotine-induced intracellular calcium response and excitability of MSDB neurons. Brain Res. 1592, 1–10. https://doi.org/10.1016/j.brainres.2014.10.018

Wang, L., Kang, H., Li, Y., Shui, Y., Yamamoto, R., Sugai, T., Kato, N., 2015. Cognitive recovery by chronic activation of the large-conductance calcium-activated potassium channel in a

mouse model of Alzheimer's disease. Neuropharmacology 92, 8–15. https://doi.org/10.1016/j.neuropharm.2014.12.033

Warrington, A.E., Barbarese, E., Pfeiffer, S.E., 1992. Stage specific, (04+GalC-) isolated oligodendrocyte progenitors produce MBP+ myelin in vivo. Dev. Neurosci. 14, 93–97. https://doi.org/10.1159/000111652

Watkins, L.R., Maier, S.F., 2002. Beyond neurons: Evidence that immune and glial cells contribute to pathological pain states. Physiol. Rev. https://doi.org/10.1152/physrev.00011.2002

Watson, C., Long, J.S., Orange, C., Tannahill, C.L., Mallon, E., McGlynn, L.M., Pyne, S., Pyne, N.J., Edwards, J., 2010. High expression of sphingosine 1-phosphate receptors, S1P1and S1P3, sphingosine kinase 1, and extracellular signal-regulated kinase-1/2 is associated with development of tamoxifen resistance in estrogen receptor-positive breast cancer patients. Am. J. Pathol. 177, 2205–2215. https://doi.org/10.2353/ajpath.2010.100220

Waxman, S.G., Cummins, T.R., Dib-Hajj, S., Fjell, J., Black, J.A., 1999. Sodium channels, excitability of primary sensory neurons, and the molecular basis of pain. Muscle and Nerve. https://doi.org/10.1002/(SICI)1097-4598(199909)22:9<1177::AID-MUS3>3.0.CO;2-P

Wei, W., Du, C., Lv, J., Zhao, G., Li, Z., Wu, Z., Haskó, G., Xie, X., 2013. Blocking A 2B Adenosine Receptor Alleviates Pathogenesis of Experimental Autoimmune Encephalomyelitis via Inhibition of IL-6 Production and Th17 Differentiation . J. Immunol. 190, 138–146. https://doi.org/10.4049/jimmunol.1103721

Wendell, S.G., Fan, H., Zhang, C., 2020. G protein–coupled receptors in asthma therapy: Pharmacology and drug actions. Pharmacol. Rev. 72, 1–49. https://doi.org/10.1124/pr.118.016899

West, J.W., Numann, R., Murphy, B.J., Scheuer, T., Catterall, W.A., 1991. A phosphorylation site in the Na+ channel required for modulation by protein kinase C. Science (80-.). 254, 866–868. https://doi.org/10.1126/science.1658937

Westenbroek, R.E., Byers, M.R., 1999. Up-regulation of class A Ca2+ channels in trigeminal ganglion after pulp exposure. Neuroreport 10, 381–385. https://doi.org/10.1097/00001756-199902050-00031

Westenbroek, R.E., Merrick, D.K., Catterall, W.A., 1989. Differential subcellular localization of the RI and RII Na+ channel subtypes in central neurons. Neuron 3, 695–704. https://doi.org/10.1016/0896-6273(89)90238-9

Wickman, K., Clapham, D.E., 1995. Ion channel regulation by G proteins. Physiol. Rev. 75, 865–885. https://doi.org/10.1152/physrev.1995.75.4.865

Wilkerson, B.A., Argraves, K.M., 2014. The role of sphingosine-1-phosphate in endothelial barrier function. Biochim. Biophys. Acta - Mol. Cell Biol. Lipids. https://doi.org/10.1016/j.bbalip.2014.06.012

Williams, M.R., Marsh, R., Macdonald, C.D., Jain, J., Pearce, R.K.B., Hirsch, S.R., Ansorge, O., Gentleman, S.M., Maier, M., 2013. Neuropathological changes in the nucleus basalis in schizophrenia. Eur. Arch. Psychiatry Clin. Neurosci. 263, 485–495. https://doi.org/10.1007/s00406-012-0387-7

Williams, T.C., Jarvis, S.M., 1991. Multiple sodium-dependent nucleoside transport systems in bovine renal brush-border membrane vesicles. Biochem. J. 274, 27–33. https://doi.org/10.1042/bj2740027

Williamson, A. V., Compston, D.A.S., Randall, A.D., 1997. Analysis of the Ion Channel Complement of the Rat Oligodendrocyte Progenitor in a Commonly Studied In vitro Preparation . Eur. J. Neurosci. 9, 706–720. https://doi.org/10.1111/j.1460-9568.1997.tb01419.x

Wilson, S.M., Toth, P.T., Oh, S.B., Gillard, S.E., Volsen, S., Ren, D., Philipson, L.H., Lee, E.C., Fletcher, C.F., Tessarollo, L., Copeland, N.G., Jenkins, N.A., Miller, R.J., 2000. The status of voltage-dependent calcium channels in alpha 1E knock-out mice. J. Neurosci. 20, 8566–71. https://doi.org/10.1523/JNEUROSCI.20-23-08566.2000

Wollny, T., Wątek, M., Durnaś, B., Niemirowicz, K., Piktel, E., Z˙endzian-Piotrowska, M., Góźdź, S., Bucki, R., 2017. Sphingosine-1-phosphate metabolism and its role in the development of inflammatory bowel disease. Int. J. Mol. Sci.

https://doi.org/10.3390/ijms18040741

Woolf, C.J., Bennett, G.J., Doherty, M., Dubner, R., Kidd, B., Koltzenburg, M., Lipton, R., Loeser, J.D., Payne, R., Torebjork, E., 1998. Towards a mechanism-based classification of pain? Pain 77, 227–229. https://doi.org/10.1016/S0304-3959(98)00099-2

Wu, G., Ringkamp, M., Murinson, B.B., Pogatzki, E.M., Hartke, T. V., Weerahandi, H.M., Campbell, J.N., Griffin, J.W., Meyer, R.A., 2002. Degeneration of myelinated efferent fibers induces spontaneous activity in uninjured C-fiber afferents. J. Neurosci. 22, 7746–7753. https://doi.org/10.1523/jneurosci.22-17-07746.2002

Wu, W.P., Hao, J.X., Halldner, L., Lövdahl, C., DeLander, G.E., Wiesenfeld-Hallin, Z., Fredholm, B.B., Xu, X.J., 2005. Increased nociceptive response in mice lacking the adenosine A1 receptor. Pain 113, 395–404. https://doi.org/10.1016/j.pain.2004.11.020

Xaus, J., Mirabet, M., Lloberas, J., Soler, C., Lluis, C., Franco, R., Celada, A., 1999. IFN-γ Up-Regulates the A2B Adenosine Receptor Expression in Macrophages: A Mechanism of Macrophage Deactivation | The Journal of Immunology. J. Immunol. 162, 3607–3614.

Xu, K., Bastia, E., Schwarzschild, M., 2005. Therapeutic potential of adenosine A2A receptor antagonists in Parkinson's disease. Pharmacol. Ther. https://doi.org/10.1016/j.pharmthera.2004.10.007

Yaar, R., Jones, M.R., Chen, J.F., Ravid, K., 2005. Animal models for the study of adenosine receptor function. J. Cell. Physiol. https://doi.org/10.1002/jcp.20138

Yamagata, K., Tagami, M., Torii, Y., Takenaga, F., Tsumagari, S., Itoh, S., Yamori, Y., Nara, Y., 2003. Sphingosine 1-phosphate induces the production of glial cell line-derived neurotrophic factor and cellular proliferation in astrocytes. Glia 41, 199–206. https://doi.org/10.1002/glia.10180

Yamamoto, K., Ueta, Y., Wang, L., Yamamoto, R., Inoue, N., Inokuchi, K., Aiba, A., Yonekura, H., Kato, N., 2011. Suppression of a neocortical potassium channel activity by intracellular amyloid-β and its rescue with homer1a. J. Neurosci. 31, 11100–11109. https://doi.org/10.1523/JNEUROSCI.6752-10.2011

Yanagawa, Y., Masubuchi, Y., Chiba, K., 1998. FTY720, a novel immunosuppressant, induces sequestration of circulating mature lymphocytes by acceleration of lymphocyte homing in rats, III. Increase in frequency of CD62L-positive T cells in Peyer's patches by FTY720-induced lymphocyte homing. Immunology 95, 591–594. https://doi.org/10.1046/j.1365-2567.1998.00639.x

Yang, D., Zhang, Y., Nguyen, H.G., Koupenova, M., Chauhan, A.K., Makitalo, M., Jones, M.R., St. Hilaire, C., Seldin, D.C., Toselli, P., Lamperti, E., Schreiber, B.M., Gavras, H., Wagner, D.D., Ravid, K., 2006. The A2B adenosine receptor protects against inflammation and excessive vascular adhesion. J. Clin. Invest. 116, 1913–1923. https://doi.org/10.1172/JCI27933

Yang, X., Xu, B., Mulvey, B., Evans, M., Jordan, S., Wang, Y.D., Pagala, V., Peng, J., Fan, Y., Patel, A., Peng, J.C., 2019. Differentiation of human pluripotent stem cells into neurons or cortical organoids requires transcriptional co-regulation by UTX and 53BP1. Nat. Neurosci. 22, 362–373. https://doi.org/10.1038/s41593-018-0328-5

Yao, S.-Q., Li, Z.-Z., Huang, Q.-Y., Li, F., Wang, Z.-W., Augusto, E., He, J.-C., Wang, X.-T., Chen, J.-F., Zheng, R.-Y., 2012. Genetic inactivation of the adenosine A $_{2A}$ receptor exacerbates brain damage in mice with experimental autoimmune encephalomyelitis. J. Neurochem. 123, 100–112. https://doi.org/10.1111/j.1471-4159.2012.07807.x

Yao, Y., Sei, Y., Abbracchio, M.P., Jiang, J.L., Kim, Y.C., Jacobson, K.A., 1997. Adenosine A3 receptor agonists protect HL-60 and U-937 cells from apoptosis induced by A3 antagonists. Biochem. Biophys. Res. Commun. 232, 317–322. https://doi.org/10.1006/bbrc.1997.6290

Yin, K.J., Kim, G.M., Lee, J.M., He, Y.Y., Xu, J., Hsu, C.Y., 2005. JNK activation contributes to DP5 induction and apoptosis following traumatic spinal cord injury. Neurobiol. Dis. 20, 881–889. https://doi.org/10.1016/j.nbd.2005.05.026

Yoon, M.H., Bae, H.B., Choi, J. Il, 2005. Antinociception of intrathecal adenosine receptor subtype agonists in rat formalin test. Anesth. Analg. 101, 1417–1421. https://doi.org/10.1213/01.ANE.0000180994.10087.6F

Yoshii, F., Moriya, Y., Ohnuki, T., Ryo, M., Takahashi, W., 2017. Neurological safety of

fingolimod: An updated review. Clin. Exp. Neuroimmunol. 8, 233–243. https://doi.org/10.1111/cen3.12397

Young, S.H., Poo, M.M., 1983. Spontaneous release of transmitter from growth cones of embryonic neurones. Nature 305, 634–637. https://doi.org/10.1038/305634a0

Yu, F.H., Catterall, W.A., 2003. Overview of the voltage-gated sodium channel family. Genome Biol. https://doi.org/10.1186/gb-2003-4-3-207

Yu, N., Lariosa-Willingham, K.D., Lin, F.F., Webb, M., Rao, T.S., 2004. Characterization of Lysophosphatidic Acid and Sphingosine-1-Phosphate-Mediated Signal Transduction in Rat Cortical Oligodendrocytes. Glia 45, 17–27. https://doi.org/10.1002/glia.10297

Yu, W.P., Collarini, E.J., Pringle, N.P., Richardson, W.D., 1994. Embryonic expression of myelin genes: Evidence for a focal source of oligodendrocyte precursors in the ventricular zone of the neural tube. Neuron 12, 1353–1362. https://doi.org/10.1016/0896-6273(94)90450-2

Zagha, E., Manita, S., Ross, W.N., Rudy, B., 2010. Dendritic Kv3.3 potassium channels in cerebellar Purkinje cells regulate generation and spatial dynamics of dendritic Ca2+ spikes. J. Neurophysiol. 103, 3516–3525. https://doi.org/10.1152/jn.00982.2009

Zago, W.M., Massey, K.A., Berg, D.K., 2006. Nicotinic activity stabilizes convergence of nicotinic and GABAergic synapses on filopodia of hippocampal interneurons. Mol. Cell. Neurosci. 31, 549–559. https://doi.org/10.1016/j.mcn.2005.11.009

Zaki, P.A., Quinn, J.C., Price, D.J., 2003. Mouse models of telencephalic development. Curr. Opin. Genet. Dev. https://doi.org/10.1016/S0959-437X(03)00084-4

Zamponi, G.W., Striessnig, J., Koschak, A., Dolphin, A.C., 2015. The Physiology, Pathology, and Pharmacology of Voltage-Gated Calcium Channels and Their Future Therapeutic Potential. Pharmacol. Rev. 67, 821–870. https://doi.org/10.1124/pr.114.009654

Zemann, B., Kinzel, B., Müller, M., Reuschel, R., Mechtcheriakova, D., Urtz, N., Bornancin, F., Baumruker, T., Billich, A., 2006. Sphingosine kinase type 2 is essential for lymphopenia induced by the immunomodulatory drug FTY720. Blood 107, 1454–1458. https://doi.org/10.1182/blood-2005-07-2628

Zhang, M., Dai, Q., Liang, D., Li, D., Chen, Sijia, Chen, Shuangdong, Han, K., Huang, L., Wang, J., 2018. Involvement of adenosine A1 receptor in electroacupuncture-mediated inhibition of astrocyte activation during neuropathic pain. Arq. Neuropsiquiatr. 76, 736–742. https://doi.org/10.1590/0004-282x20180128

Zhang, S.C., 2001. Defining glial cells during CNS development. Nat. Rev. Neurosci. 2, 840–843. https://doi.org/10.1038/35097593

Zhang, X.F., Shieh, C.C., Chapman, M.L., Matulenko, M.A., Hakeem, A.H., Atkinson, R.N., Kort, M.E., Marron, B.E., Joshi, S., Honore, P., Faltynek, C.R., Krafte, D.S., Jarvis, M.F., 2010. A-887826 is a structurally novel, potent and voltage-dependent Nav1.8 sodium channel blocker that attenuates neuropathic tactile allodynia in rats. Neuropharmacology 59, 201–207. https://doi.org/10.1016/j.neuropharm.2010.05.009

Zhang, X.L., Mok, L.P., Lee, K.Y., Charbonnet, M., Gold, M.S., 2012. Inflammation-induced changes in BK Ca currents in cutaneous dorsal root ganglion neurons from the adult rat. Mol. Pain 8. https://doi.org/10.1186/1744-8069-8-37

Zhang, Y.-Q., Ji, Y.-P., Mei, J., 2000. Effects of cholinergic agents on spontaneous activity of nucleus basalis magnocellularis neurons in different age rats. Neurosci. Lett. 288, 91–94. https://doi.org/10.1016/S0304-3940(00)01186-1

Zhang, Y., Yu, Q., Lai, T.B., Yang, Y., Li, G., Sun, S.G., 2013. Effects of small interfering RNA targeting sphingosine kinase-1 gene on the animal model of Alzheimer's disease. J. Huazhong Univ. Sci. Technol. - Med. Sci. 33, 427–432. https://doi.org/10.1007/s11596-013-1136-5

Zhao, Z., Francis, C.E., Ravid, K., 1997. An A3-subtype adenosine receptor is highly expressed in rat vascular smooth muscle cells: Its role in attenuating adenosine-induced increase in cAMP. Microvasc. Res. 54, 243–252. https://doi.org/10.1006/mvre.1997.2044

Zheng, J.Q., Felder, M., Connor, J.A., Poo, M.M., 1994. Turning of nerve growth cones induced by neurotransmitters. Nature 368, 140–144. https://doi.org/10.1038/368140a0

Zhou, X., Gong, Z., Su, Y., Lin, J., Tang, K., 2009. Cordyceps fungi: natural products, pharmacological functions and developmental products. J. Pharm. Pharmacol. 61, 279–

291. https://doi.org/10.1211/jpp/61.03.0002
Zimmermann, H., 2000. Extracellular metabolism of ATP and other nucleotides. Naunyn. Schmiedebergs. Arch. Pharmacol. https://doi.org/10.1007/s002100000309
Zimmermann, H., Braun, N., Kegel, B., Heine, P., 1998. New insights into molecular structure and function of ecto-nucleotidases in the nervous system. Neurochem. Int. https://doi.org/10.1016/S0197-0186(97)00126-5
Zonouzi, M., Renzi, M., Farrant, M., Cull-Candy, S.G., 2011. Bidirectional plasticity of calcium-permeable AMPA receptors in oligodendrocyte lineage cells. Nat. Neurosci. 14, 1430–1438. https://doi.org/10.1038/nn.2942